

AD-A188 855

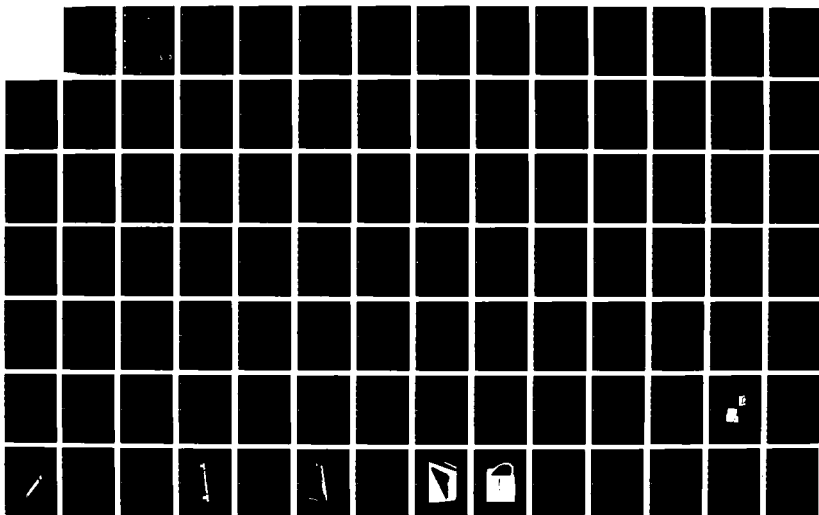
DESIGN OF AN AEROELASTIC COMPOSITE WING WIND TUNNEL
MODEL(U) AIR FORCE INST OF TECH WRIGHT-PATTERSON AFB OH
SCHOOL OF ENGINEERING W J NORTON DEC 87
AFIT/GAE/AA/87D-15

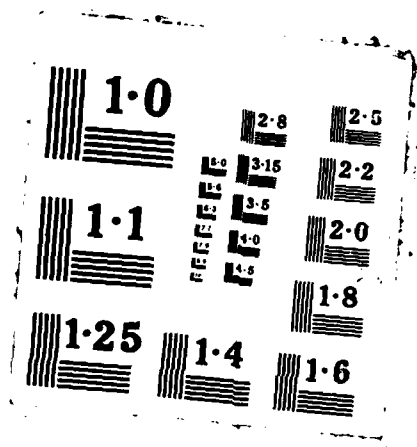
1/3

UNCLASSIFIED

F/G 1/3

NL





AD-A188 855



DTIC FILE COPY

DESIGN OF AN AEROELASTIC
COMPOSITE WING WIND TUNNEL MODEL

THESIS
William J. Norton
Captain, USAF

AFIT/GAE/AA/87D-15

DEPARTMENT OF THE AIR FORCE
AIR UNIVERSITY

AIR FORCE INSTITUTE OF TECHNOLOGY

Wright-Patterson Air Force Base, Ohio

This document has been approved
for public release and sales in
distribution is unlimited.

88 2 4 0 4 7

DTIC
ELECTE
FEB 10 1988
S E D

AFIT/GAE/AA/87D-15

DESIGN OF AN AEROELASTIC
COMPOSITE WING WIND TUNNEL MODEL

THESIS
William J. Norton
Captain, USAF

AFIT/GAE/AA/87D-15

DTIC
ELECTE
FEB 10 1988
S E D

Approved for public release; distribution unlimited

DESIGN OF AN AEROELASTIC
COMPOSITE WING WIND TUNNEL MODEL

THESIS

Presented to the Faculty of the School of Engineering
of the Air Force Institute of Technology

Air University

In Partial Fulfillment of the
Requirements for the Degree of

Masters of Science in Aeronautical Engineering



William J. Norton, B.S.
Captain, USAF

December 1987

Accession For	
NTIS GRA&I	<input checked="checked" type="checkbox"/>
DTIC TAB	<input type="checkbox"/>
Unannounced	<input type="checkbox"/>
Justification	
By _____	
Distribution/	
Availability Codes	
Dist	Avail and/or Special
A-1	

Preface

The Air Force Wright Aeronautical Laboratories (AFWAL), in cooperation with the MBB consortium of the Federal Republic of Germany, has planned to investigate the effects of composite lamina fiber orientation on control reversal for various wing/fin configurations by analytical and experimental means. While the use of fiber composites in aircraft construction has grown in the past few decades, only recently have complete wings, stabilizers, and control surfaces been fabricated from this material. Despite this, a careful parametric study of aeroelastic effects has not been undertaken. This thesis research is one element in the study, demonstrating the entire design, fabrication, and testing process for such an investigation. It includes testing a single aft swept wing planform with full and partial span aft control surfaces in a subsonic wind tunnel and comparing the results with predictions rendered from simple computer modeling. The research also includes relatively simple computer programs for designing and predicting the aeroelastic characteristics of each proposed configuration in terms of deformation, reversal, divergence, and flutter. Documentation of these programs permit them to be used as a consistent family of aeroelastic routines in operator fashion.

The author wishes to extend his appreciation for the kind and patient assistance of his research advisor, Major Lanson Hudson, and the other members of the thesis committee; Major Ronald Hinrichsen, Dr. Shankar Mall, Dr. Harold Larson, and Dr. Robert Calico. Debt is also

owed to Mr. Edmund Pendelton of AFWAL for sponsoring the project and making countless hours of time available to assist. Thanks are due to Mr. James McKiernan of the University of Dayton and Mr. Kevin Spitzer of the Flight Dynamics Laboratory for their knowledge and skill in fabricating the composite plates, and to the talented and generous craftsmen at the Air Force Institute of Technology (AFIT) model shop for the final model construction. Special thanks to Mr. Andrew Riemenschneider who operated the wind tunnel and contributed sound and timely advice.

William J. Norton

Table of Contents

	Page
Preface	iii
List of Figures	vii
List of Tables	ix
List of Symbols	x
Abstract	xvii
I. Introduction	1
II. Analytical Development - Static	5
General	5
Material Properties	7
Strain Energy	10
Governing Equations	12
Divergence	16
Aerodynamic Operator	21
Structural Operator	26
Lateral Control Reversal	30
III. Analytical Development - Dynamic	34
General	34
Modal Formulation	37
Solution Methods	38
Simplified Operator Derivations	41
IV. Computer Model	44
General	44
Optimization	46
V. Experimental Apparatus	49
Composite Plates	49
Wing Models	60
Instrumentation	66
Wind Tunnel Installation	69

VI. Experimental Procedure	74
Data Collection	74
Tunnel Corrections	74
Ground Vibration Test	75
Testing Scheme	75
VII. Results and Discussion	78
Static Analysis	78
Dynamic Analysis	89
Optimization	93
Model Fabrication	100
Instrumentation	100
Wind Tunnel Installation	101
VIII. Suggestions and Recommendations	102
Static Analysis	102
Dynamic Analysis	103
Optimization	103
Model Fabrication	104
Instrumentation	104
Wind Tunnel Installation	105
Appendix A: Aeroelastic Subroutines	106
Appendix B: Sample Statics Program	210
Appendix C: Dynamic Data	229
Ground Vibration Test Results	229
Derivation of Dynamic Parameters	243
CWINGF Results	243
Appendix D: Material Properties	246
Material Properties	246
Tensile Test Results	246
Bibliography	248
Vita	250

List of Figures

Figure	Page
1. Laminate Nomenclature	8
2. Wing Box Beam Nomenclature	14
3. Wing Panel Nomenclature	23
4. Panel Aerodynamic Nomenclature	24
5. Panel Structural Nomenclature	27
6. Wing Plate Planform	51
7. Wing Plate Static Analysis Results	54
8. Layup 1 Aileron Analysis Results	56
9. Layup 1 Flap Analysis Results	57
10. Layup 1 Flaperon Analysis Results	58
11. Layup 1 Theoretical Reversal Speeds	63
12. Control Surface Attachment Brackets and Tip Restraint	65
13. Wing Model	65
14. Test Plate Slicing Sequence	67
15. Strain Gage Balance	68
16. Model Root Mounting Fixture and Loads Balance	70
17. Tunnel Installation and Root Fairing	72
18. Lead Tape Application and Ramp	73
19. Case 3 Lift Curves - 0° AOA and 5°	79
20. Case 3 Lift Curves - 0° AOA and 10°	80
21. Case 3 Lift Curves - 5° AOA and 5°	81
22. Case 3 Lift Curves - 5° AOA and 10°	82

23. Case 1 Lift Curves - 0° AOA and 5°	83
24. Case 1 Lift Curves - 0° AOA and 10°	84
25. Case 2 Plate Flutter Mode	91
26. Theoretical Lift Effectiveness for Plain Flap	219
27. Case 1 GVT Results	230
28. Case 2 GVT Results	234
29. Case 3 GVT Results	238

List of Tables

Table	Page
I. K Parameters	21
II. Parametric Variation Examples	44
III. Test Planform Characteristics	52
IV. Analysis Layup Schedules	53
V. Wing Plate Layup Schedule	55
VI. Sensitivity Analysis Results	61
VII. Testing Schedule	76
VIII. Results Comparison	85
IX. Reversal Investigation	87
X. Example Optimization Results	94
XI. Ground Vibration Test Results	242
XII. CWINGF Flutter Results	245

List of Symbols

Symbol	Meaning
\mathcal{A}	aerodynamic operator
a_h	distance between wing or panel midchord and elastic axis
a_o	two-dimension section lift curve slope
b	wing planform semi-span
c	local structural wing chord perpendicular to reference axis
\bar{C}	Theodorsen's function
CA	wind tunnel cross-sectional area
C_f	damping coefficient
c_f/c	flap chord/section chord ratio
c_{l_α}	partial derivative of section lift coefficient wrt AOA
c_{l_δ}	partial derivative of section lift coefficient wrt control deflection
c_l^r	rigid wing section lift coefficient perpendicular to reference axis
C_{l_α}	partial derivative of wing lift coefficient wrt AOA
c_{mac}	pitching moment about the section aerodynamic center
c_{m_δ}	partial derivative of section pitching moment wrt control deflection
c_{ref}	reference chord
d	distance between wing or panel line of centers of mass and the reference axis
e	aerodynamic center and reference axis offset, positive forward
EI	bending rigidity
e_{sb}	solid blockage correction factor

E_1	modulus of elasticity along axis 1 of composite material
E_2	modulus of elasticity along axis 2 of composite material
g	torsion coupling parameter, system or structural damping
GJ	torsional rigidity
G_{12}	shear modulus
h	vertical displacement of lifting structure
h_i	panel width
h_o	magnitude of bending displacement
I_α	wing mass moment of inertia about the elastic axis
k	bending coupling parameter, reduced frequency
K	bending-torsion coupling parameter
L	lift on panel or wing
m	wing mass or mass of panel
M	bending moment
\mathcal{M}	inertia operator
N	number of composite plies
nw	distributed inertia load per unit length of wing
P	roll rate
$Pb/2V$	helix angle, aileron efficiency
P_j	lift per unit length on panel j
$p(y)$	distributed bending (upward) load
q	dynamic pressure
q_i	displacement or degree of freedom
q_o	magnitude of q_i
Q_D	dynamic forcing function
r	distance from elastic axis in streamwise direction, positive aft

r_a	radius of gyration about elastic axis in semichords
S	wing planform area
\mathcal{L}	structure operator
t	time
T	torque
t_i	i th ply thickness
T_y	pitching moment about elastic axis
$t(y)$	distributed torque
t/c	section thickness/chord ratio
u	displacement in x axis of laminate
$U(y)$	strain energy
v	displacement in y axis of laminate
v_o	spanwise stretching of box beam middle surface
V	velocity
V_D	divergence speed
V_m	model volume
V_R	reversal speed
V_z	shear force
w	displacement in z axis of laminate
x	axis perpendicular to y
\bar{x}	axis perpendicular to \bar{y}
x	distance between wing or panel center of mass and elastic axis in semichords
y	axis along reference axis of structure
\bar{y}	axis perpendicular to longitudinal axis of aircraft
z	axis perpendicular to x - y plane (box beam)

Greek

α	torsional displacement of lifting surface, angle of attack
α_c	AOA due to control surface deflection
α_o	magnitude of torsion displacement
α_r	AOA due to rigid wing incidence
α_s	AOA due to structural deformation
β_i	area moment of inertia about middle surface of box beam
γ	shear strain, system damping
Γ	slope of bending deformation
δ	control deflection
δ_i	first moment of area about middle surface of box beam
δ_o	normalized control deflection
Δ	change
ϵ	normal strain
ζ	viscous damping factor
η	normalized spanwise location parameter
θ	rotation of fiber axis relative to x-y axis
λ	taper ratio
\wedge	sweep of reference axis from y axis
μ	Poisson's ratio, mass ratio
ρ	free-stream air density
Σ	summation
σ	normal stress
τ	shear stress, nondimensional time
ψ	relative control deflection parameter
ω	frequency

ω_n	natural frequency
ω_h	wing or panel uncoupled natural frequency of bending
ω_α	wing or panel uncoupled natural frequency or torsion
Ω	eigenvalue

Subscripts

1	axis 1 of orthotropic material, laminate rotation case 1
2	axis 2 of orthotropic material, laminate rotation case 2
3	laminate rotation case 3
c	corrected
cr	critical parameter
D	divergence
i	row, index
j	column, index
r	wing root parameter
R	reversal
x	x axis parameter
y	y axis parameter
δ	control surface deflection parameter

Superscripts

(a)	antisymmetric
iv	fourth derivative wrt y
o	degrees
.	first derivative wrt time
..	second derivative wrt time

' first derivative wrt y
'' second derivative wrt y
''' third derivative wrt y

Abbreviations

ADS Automated Design Synthesis
AFIT Air Force Institute of Technology
AFWAL Air Force Wright Aeronautical Laboratories
AIC aerodynamic influence coefficient
AOA angle of attack
AR aspect ratio
deg degrees
eq equation
eqs equations
FDL Flight Dynamics Laboratory
ft feet
fwd forward
GVT ground vibration test
IO input/output
kg kilogram
mph miles per hour
NACA National Advisory Committee on Aeronautics
No. number
PA pressure altitude
psf pounds per square foot
sq squared

wrt with respect to

Other

[] matrix
{ } row or column array
[]⁻¹ matrix inverse
[] diagonal matrix
| | determinant
[a] aerodynamic matrix
[A] modal aerodynamic matrix
[A_{ij}] AIC matrix
[C_{ij}] flexibility matrix
[D] dynamical matrix
[I] identity matrix
[m] mass or inertia matrix
[M] modal mass or inertia matrix
{q} displacements or degrees of freedom
[s] stiffness matrix
[S₁] downwash matrix
[U] normalized eigenvector matrix
[w] diagonal matrix of squares of natural frequencies, modal
 stiffness matrix

Abstract

This research provides a simple and verified means for conducting parametric studies of the effects of composite lamina orientation on the aeroelastic characteristics of a swept wing. The entire design methodology for a wind tunnel model for this purpose is demonstrated. The study used beam structural analysis and aerodynamic lifting line theory for the static analysis. These methods are easy to implement and do not consume extensive computer resources. The analytical models predicted lateral control surface reversal speed, divergence speed, deformed shape, loads, and wing flutter characteristics. Computer model results for a single wing planform were compared with wind tunnel results. Three models were constructed around composite plates with identical laminate stacking schedules but with different orientations with respect to the structural reference axis. Valuable insight into fabrication of aeroelastic models for this purpose was gained.

The analytical model and symbology is based upon the work of Dr. Terrence Weissshaar (15-18). His computer codes have been modified to provide additional information for this study and to assist in the subsequent experimental effort.

DESIGN OF AN AEROELASTIC COMPOSITE WING WIND TUNNEL MODEL

I. Introduction

The Air Force Wright Aeronautical Laboratory (AFWAL) Flight Dynamics Laboratory (FDL) is undertaking a parametric study of aeroelastic effects of wings and fins constructed of composite materials. The orthotropic behavior of composite material permits "tailoring" of the structure for the aeroelastic needs of the proposed usage while maintaining light weight. The immediate task is to investigate lateral control surface reversal susceptibility of such structures, however other aeroelastic effects such as divergence and flutter must be considered when designing a wind tunnel model. This thesis research was performed as an initial effort in this project, testing both analytical and model construction methods. While actual structures of this kind would likely consist of composite laminate sheets as outer surfaces with supporting internal members (ribs, longerons, stringers, etc.), this study will concentrate on models fashioned about composite plates with aft controls surfaces consisting of a flap and an aileron, with both acting in concert to form a flaperon.

The AFWAL study entails constructing many models with varied planform and control surface configurations as a parametric analysis.

The AFWAL models will be operated at subsonic tunnel speeds. Predicted model tip deflection will be scaled to that estimated for a full scale prototype.

Lateral control reversal refers to an aeroelastic phenomena whereby wing deformation reduces the effectiveness of a roll control device to zero. The trailing edge down deflection of an aft mounted aileron or flaperon produces a leading edge down twisting moment on the wing. This causes a reduction in the effective angle-of-attack of the wing-aileron and reduces the rolling moment normally expected of a rigid wing. This twisting moment increases with airspeed until reversal speed is reached where rolling moment from the control deflection is reduced to zero. Beyond this speed aileron deflection will produce rolling moments opposite to the normal control sense. Reversal is aggravated by wing sweep which normally produces torsional structural deformation under load.

For a swept wing, structural deformation will consist of both bending and twisting components. This deformation is resisted by the restoring tendency of the wing structure. When such a wing bends, the angle of attack along the span is increased giving rise to an increase in the aerodynamic loads and thus further deformation until an equilibrium is established between the airloads and the structure's restoring tendencies. When these airloads exceed the ability of the structure to resist, the deformation will continue indefinitely or until the force/displacement relation becomes nonlinear. This effect is known as divergence, resulting in structural failure.

Flutter is the dynamic interaction of unsteady airloads with the natural vibrational characteristics of the structure. The change in the intensity and distribution of airloads with associated structural deformation and restoring motion results in a cyclic phenomena. When vibratory modes couple at a specific airspeed, undamped oscillation or flutter is likely, most often resulting in structural failure.

Several other aeroelastic phenomena are ignored in this study. Aeroservoelasticity, or the interaction of airloads and structural vibrations with the elastic behavior of actuators and hinges, has not been considered. The consequences of thermodynamic effects in structural characteristics or aerothermoelasticity was also excluded from this study.

The principle objective of this research was to investigate the control reversal characteristics of a composite wing consisting of a plate cut to the wing planform as the load-bearing structure. The challenges of constructing a wind tunnel model for such a study are manifold. The reversal speed must be predicted to occur within the range of the tunnel, requiring that the composite be tailored to this requirement. Divergence must occur beyond the reversal point and with a sufficient margin to allow for errors in the prediction methods. To demonstrate this phenomenon, divergence was sought within the speed range of the tunnel but with this constraint. Flutter must be avoided by a wide margin. A means must be found to create an airfoil shape around the plate and secured to the plate in such a way that lift forces are effectively transmitted to the laminate structure. This must be accomplished with light weight and without significantly altering the

inertial, stiffness, and geometric properties of the structure. A method must also be devised to mount the model in the tunnel in a fashion that will allow measurement of the wing loads.

II. Analytical Development - Static

General

Prior to constructing an aeroelastic wind tunnel model, analysis must be performed to predict the behavior of the model. For static characteristics, this includes structural deflection and wing divergence. The analysis will permit the model to be designed to demonstrate the effects sought as well as protect it from damage due to undesirable deformations.

The following section will summarize the assumptions and methods used to develop the relevant equations used in the static aeroelastic analysis. As much as possible, the development will produce aeroelastic operators after the fashion of Bisplinghoff and Ashley (3:chap 3). The study will proceed in steps from a straight, untapered wing to a general swept wing. The swept wing is characterized by a coupling between structural bending and twist. The upward bending of an aft swept wing results in a reduction in the angle of attack in the streamwise direction producing a negative increment of lift. However, this negative lift effectively opposes further nose up twist of the structure. Consequently, bending of a forward swept wing shifts the center of pressure of the aerodynamic loads outboard while bending of an aft swept wing gives an inboard shift. Thus, divergence of an aft swept wing is unlikely while control reversal is possible. The opposite is true for forward swept wings.

The development to follow is limited to a slender swept wing which can be treated as a slender beam wherein no warping of the transverse axis is permitted (chordwise elements will not deform). This assumption permits the introduction of an elastic axis. This is a spanwise line through the shear centers of the cross-sections of the beam. The shear center is that point in the plane of the section at which a shear force can be applied without producing a twist of the section (3:160). This assumption further allows the convenience of locating the bending reference axis (y) along the elastic axis. Bending deformation will be represented by $h(y)$, positive upward, and twisting by $\theta(y)$, positive nose up. These deflections are considered small and are therefore perturbation deformations from a slightly deformed static equilibrium state.

For the specific applications considered here, it was assumed that the bending and torsional stiffness of the wing structure is due entirely to thin, laminated composite sheets located at some distance apart (relative to their thickness) to form the surface of the constant depth box beam. The lamina sheets are assumed to be separated by rigid vertical webs. Additional stiffness produced by such other elements as shear webs are not considered. A plate for which no distance exists between beam sheets, violates none of the mathematics entailed in the development. In order to determine the equivalent bending rigidity (EI) and torsional rigidity (GJ), the Euler-Bernoulli hypothesis is utilized. This states that the strain due to bending varies linearly from the neutral surface of the box beam. This neutral or reference surface is taken as the geometric middle as is typical in laminate plate theory.

The upper and lower laminate sheets will then act as a unit to provide the stress-strain relations, assumed to be linear.

A wing with partial or full span leading or trailing edge control surfaces may not be properly considered to have the entire planform serving as primary structure. These control surfaces are usually fastened to the main wing structure with hinges and actuators which will not contribute prominently to the rigidity. Determination of the structural properties may need to be determined with a reduced planform from that used for the aerodynamic properties to which the control surfaces play a crucial role.

Material Properties

The composite lamina making up the laminate sheets are assumed to be orthotropic, that is the material properties are different in three mutually perpendicular planes of symmetry and the properties are a function of the orientation at a point in the body. Each lamina of the box beam is itself orthotropic with respect to a set of orthogonal principal axes, one of which is in the direction of the lamina fibers. The axes are labeled 1 and 2 (Figure 1) and lie in the x-y middle plane of the wing oriented at an angle θ , measured positive counterclockwise from the x-axis.

Lamina displacements are designated as u, v, and w in the x, y, and z directions, respectively, and are functions of h and α .

$$u(x,y) = z \alpha(y) \quad (1)$$

$$v(x,y) = v_0(y) - z[h' - x \alpha'] \quad (2)$$

$$w(x,y) = h(y) - x \alpha(y) \quad (3)$$

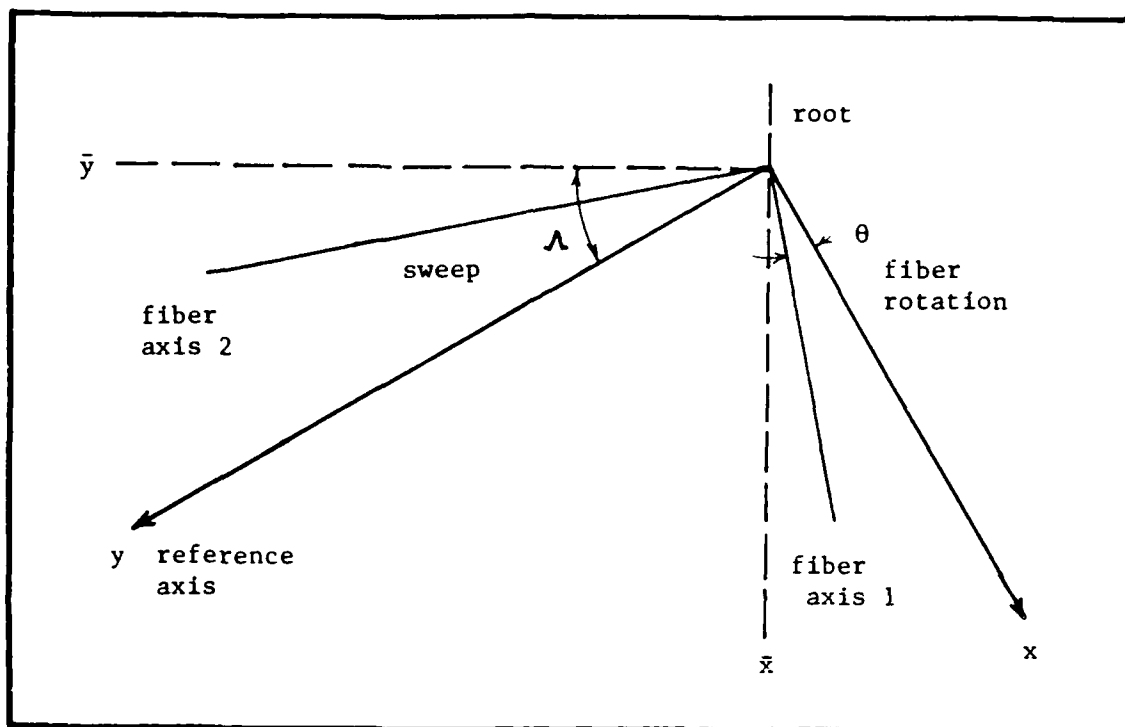


Figure 1. Laminate Nomenclature

where the ()' equates to the differential with respect to y, or d()/dy. The variable v_0 represents the spanwise stretching of the middle surface. Of the resulting strains, only two are nonzero, consistent with the Euler-Bernoulli hypothesis.

$$\epsilon_{yy} = v' = v_0' - z(h'' - x\alpha'') \quad (4)$$

$$\gamma_{xy} = u' = 2z\alpha' \quad (5)$$

The constitutive relations between the inplane or membrane stress and strain are developed by Jones (10:51) where, for an orthotropic material ($\sigma_{zz} = \tau_{yz} = \tau_{zx} = \gamma_{yz} = \gamma_{zx} = 0$), in wing reference coordinates

$$\begin{bmatrix} \sigma_{xx} \\ \sigma_{yy} \\ \tau_{xy} \end{bmatrix} = \begin{bmatrix} \bar{Q}_{11} & \bar{Q}_{12} & \bar{Q}_{16} \\ \bar{Q}_{12} & \bar{Q}_{22} & \bar{Q}_{26} \\ \bar{Q}_{16} & \bar{Q}_{26} & \bar{Q}_{66} \end{bmatrix} \begin{bmatrix} \epsilon_{xx} \\ \epsilon_{yy} \\ \gamma_{xy} \end{bmatrix} \quad (6)$$

It will be seen that σ_{xx} and τ_{xy} will play no part in the development to follow and their terms will therefore not be used. The relevant Q's are defined as

$$\bar{Q}_{22} = U_1 - U_2 \cos 2\theta + U_3 \cos 4\theta \quad (7)$$

$$\bar{Q}_{26} = .5U_2 \sin 2\theta - U_3 \sin 4\theta \quad (8)$$

$$\bar{Q}_{66} = U_5 - U_3 \cos 4\theta \quad (9)$$

where

$$U_1 = [3Q_{11} + 3Q_{22} + 2Q_{12} + 4Q_{66}]/8 \quad (10)$$

$$U_2 = [Q_{11} - Q_{22}]/2 \quad (11)$$

$$U_3 = [Q_{11} + Q_{22} - 2Q_{12} - 4Q_{66}]/8 \quad (12)$$

$$U_5 = [Q_{11} + Q_{22} - 2Q_{12} + 4Q_{66}]/8 \quad (13)$$

and

$$Q_{11} = E_1 / (1 - \mu_{12}\mu_{21}) \quad (14)$$

$$Q_{12} = \mu_{21}E_1 / (1 - \mu_{12}\mu_{21}) \quad (15)$$

$$Q_{22} = E_2 / (1 - \mu_{12}\mu_{21}) \quad (16)$$

$$Q_{66} = G_{12} \quad (17)$$

The above development is implemented in the subroutine CSTRUC (Appendix A).

Strain Energy

Strain energy is defined as the energy stored within the structure by virtue of its deformation. As a result of the Euler-Bernoulli hypothesis, a strain energy functional can be created by summing the individual strain energies of each lamina, with the middle surface of the box beam again acting as the reference plane. In addition, by assuming small deformations, linear equations result. Weisshaar (15:39) demonstrates that the strain energy functional, or strain energy density per unit volume for the composite box beam, can be written as

$$U(y) = .5EI_0(h'')^2 + .5S_0(\alpha'')^2 - K_0(h''\alpha') + .5A_{22}(v'_0)^2 + B_{33}(v'_0\alpha') - B_{22}(v'_0h'') + .5GJ_0(\alpha')^2 \quad (18)$$

Eq (18) shows how bending deformation is elastically coupled to torsional deformation by the parameter K_0 . Coupling occurs between these deformations and the middle surface stretching term $v_0(y)$. However, this latter term will be zero if the middle surface is also the neutral surface for bending. This occurs when the upper and lower

laminate sheets are symmetrical with respect to the middle surface. This condition will be enforced for this study. Neglecting the unnecessary terms then

$$EI_0 = c \left[\sum_{i=1}^N Q_{22}(i) \beta_i \right] \quad (19)$$

$$GJ_0 = c \left[\sum_{i=1}^N 4Q_{66}(i) \beta_i \right] \quad (20)$$

$$K_0 = c \left[\sum_{i=1}^N 2Q_{26}(i) \beta_i \right] \quad (21)$$

$$A_{22} = c \left[\sum_{i=1}^N Q_{22}(i) t_i \right] \quad (22)$$

$$B_{22} = c \left[\sum_{i=1}^N Q_{22}(i) \delta_i \right] \quad (23)$$

$$B_{33} = 2c \left[\sum_{i=1}^N Q_{26}(i) \delta_i \right] \quad (24)$$

where N is the total number of plies in the laminate. β_i represents the area moment of inertia about the middle surface of a strip of material of thickness t_i and unit width. This term is always positive.

δ_i is the first moment of area of the same strip about the middle surface. This term is positive if the ply area centroid is above the middle surface and negative otherwise.

$$\beta_i = \int_{z_i}^{z_{i+1}} z^2 dz = 1/3(t_i^3 + 3t_i z_i^2 + 3t_i^2 z_i) \quad (25)$$

$$\delta_i = \int_{t_i} z dz = t_i(z_{i+1} + z_i)/2 \quad (26)$$

The development of this section is implemented in the subroutine CSTRUC (Appendix A).

Governing Equations

The governing equations for a beam of uniform cross-section have been derived by Weisshaar (16:41-45) using the strain energy functional previously defined and the principle of virtual work. The equations are coupled by the parameter K . When eliminating the middle surface stretching term (v_0) one arrives at

$$p(y) = EIh^{iv} - K\alpha''' \quad (27)$$

$$t(y) = Kh''' - GJ\alpha'' \quad (28)$$

where $p(y)$ is the upward distributed load (lift) and $t(y)$ is the distributed torque. The associated boundary conditions for the cantilever wing are, at $y = 0$ (root),

$$\alpha(0) = 0 \quad (29)$$

$$h(0) = h'(0) = 0 \quad (30)$$

and at $y = b$ (tip), where b is the semi-span

$$GJ\alpha' - Kh'' = T(b) = 0 \quad (\text{torque}) \quad (31)$$

$$EIh'' - K\alpha' = M_x(b) = 0 \quad (\text{bending moment}) \quad (32)$$

$$EIh''' - K\alpha'' = V_z(b) = 0 \quad (\text{shear force}) \quad (33)$$

For the nonuniform beam (nonuniform chord and material properties along the span), these equations become

$$p(y) = [EIh'' - K\alpha']'' \quad (34)$$

$$t(y) = -[-Kh'' + GJ\alpha']' \quad (35)$$

The boundary conditions for this case are

$$h(0) = h'(0) = \alpha(0) = 0 \quad (36)$$

$$M_x(b) = EIh'' - K\alpha' = 0 \quad (37)$$

$$V_x(b) = [EIh'' - K\alpha']' = 0 \quad (38)$$

$$T(b) = GJ\alpha' - Kh'' = 0 \quad (39)$$

the bending moment, shear force, and torque, respectively, and where

$$EI = EI_0 - (B_{22})^2/A_{22} \quad (40)$$

$$GJ = GJ_0 - (B_{33})^2/A_{22} \quad (41)$$

$$K = K_0 - B_{22}B_{33}/A_{22} \quad (42)$$

These properties are computed in the subroutine CSTRUC (Appendix A).

Since eqs (40)-(42) are dependent upon the laminate stacking sequence and lamina fiber orientation, the beam may be tailored for the desired bending-torsion coupling characteristics, as they effect the aeroelastic behavior of the wing.

The deflection equations in terms of the wing geometry and other characteristics as derived from strip theory for the slender wing (see Figure 2) in which the reference axis and the elastic axis are considered as one (2:475-489 and 17:6) are

$$p(y) = cc_1^r q \cos^2 \Lambda + qca_0 \cos^2 \Lambda (\alpha - \Gamma \tan \Lambda) - nw \quad (43)$$

$$t(y) = qcec_1^r \cos^2 \Lambda + qc^2 c_{mac} \cos^2 \Lambda - nwd \\ + qcea_0 (\alpha - \Gamma \tan \Lambda) \cos^2 \Lambda \quad (44)$$

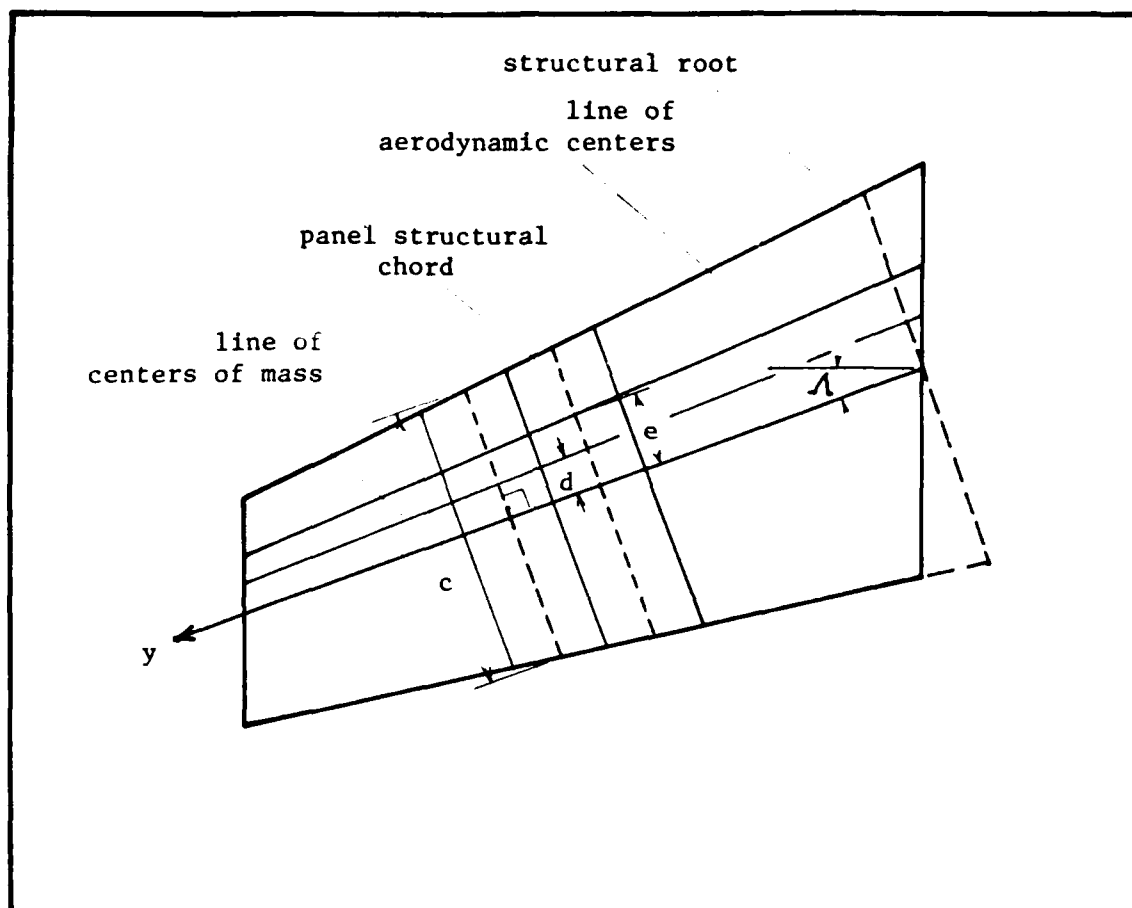


Figure 2. Wing Box Beam Nomenclature

where c_1^r is the two-dimensional lift coefficient for the wing section perpendicular to the reference axis for a rigid wing, a_0 is the two-dimensional lift-curve slope for this section, $\Gamma = h'$ is the slope of the bending deformation, nw is the distributed inertia load per unit length of the wing, with c and e as defined in Figure 2.

Weisshaar (17:7-8) details how eqs (43) and (44) can be simplified to the form

$$\alpha_e''' + a\alpha_e' - b\alpha_e = f_1' - f_2 \quad (45)$$

where

$$a = [(qcl^2 a_0 \cos^2 \Lambda) / GJ] [(1 - k \tan \Lambda) / (1 - kg)] \quad (46)$$

$$b = [(qcl^3 a_0 \cos^2 \Lambda) / EI] [(\tan \Lambda - g) / (1 - kg)] \quad (47)$$

and where

$$g = K/EI \quad (48)$$

$$k = K/GJ \quad (49)$$

the nondimensional torsion coupling parameter and bending coupling parameter, respectively, and

$$f_1 = [(1 - k \tan \Lambda) / (1 - kg)] [-1 + (cc_{mac} / ec_1^r)] \times [(qcl^2 c_1^r \cos^2 \Lambda) / GJ] + nw \bar{d} l^2 / GJ \quad (50)$$

$$f_2 = [(g - \tan \Lambda) / (1 - kg)] [(qcl^3 c_1^r \cos^2 \Lambda) / EI - nw l^3 / EI] \quad (51)$$

and where \bar{d} is the distance from the panel line of centers of mass to its reference axis, measured perpendicular to the reference axis and positive forward (see Figure 2). If the change of variables

$$\eta = 1 - y/l \quad (52)$$

is defined, where $\eta = 1$ is the root of the wing, then the boundary conditions become

$$\alpha_e(\eta = 1) = 0 \text{ (deflection)} \quad (53)$$

$$\Gamma = dh/dy(\eta = 1) = 0 \text{ (bending slope)} \quad (54)$$

$$\alpha_e'(\eta = 0) = 0 \quad (55)$$

$$\alpha_e'(0) + a\alpha_e(0) = f_1(0) \text{ (tip shear)} \quad (56)$$

For a uniform planform without twist, and for which the pitch attitude is given, the solution to eq (45) (17:8-9) is

$$\alpha_e(\eta) = f_2/b[1 - f_3(\eta)/f_3(1)] \quad (57)$$

where

$$\begin{aligned} f_3(\eta) = & [4\xi^2/(9\xi^2 + \xi^2)e^{-2\xi\eta} \\ & + e^{\xi\eta} [(5\xi^2 + \xi^2)/(9\xi^2 + \xi^2)\cos\xi\eta \\ & + [(3\xi^3 - \xi\xi^2)/(9\xi^2\xi + \xi^3)\sin\xi\eta]] \end{aligned} \quad (58)$$

and

$$\xi = -.5(c_1 + c_2) \quad (59)$$

$$\xi = 3/2(c_1 - c_2) \quad (60)$$

$$c_1 = [b/2 + (b^2/4 + a^3/27)^{1/2}]^{1/3} \quad (61)$$

$$c_2 = [b/2 - (b^2/4 + a^3/27)^{1/2}]^{1/3} \quad (62)$$

The deflection equations presented in this section must not be considered as exact. Structural modeling has been applied to simplify the formulations for ease of computation. Careful note must be made of

the assumptions made herein before any equation is used for a specific application.

Divergence

Divergence of an aerodynamic surface is an instability in which high velocities and deflections of the surface create aerodynamic forces which tend to increase the deflection. While aerodynamic forces increase with airspeed, structural restoring forces are constant. Therefore, a speed may exist in which the two forces are in balance, and beyond which divergence is possible and will likely producing catastrophic failure of the structure. This speed is referred to as the divergence speed. The extremely light structures found in World War I aeroplanes (the Fokker D-8 as an example) and the very thin wings on early supersonic aircraft were particularly susceptible to this phenomenon and wings ripping from airframes in operation was not unknown. Only moderate amounts of aft sweep are sufficient to raise the divergence speed to the extent that divergence becomes practically impossible. Forward sweep of even moderate amounts can produce divergence at relatively low airspeeds. Composite tailoring can alter these basic precepts.

The following development will assume a straight elastic axis, permitting bending and torsion to be treated separately. Diederich and Budiansky (4:10) states that movement of the elastic axis forward on an aft swept wing can raise the divergence speed for low angles of sweep but has little effect for large sweep angles. An elastic axis forward of the aerodynamic center (a supersonic condition) can diverge for only moderate to large angles of forward sweep.

In the following equations, the two dimensional lift-curve slope for zero sweep may be corrected for planform effects (4:6). That is

$$a_0 = a_0(\Lambda=0)[AR/(AR + 4\cos\Lambda)] \quad (63)$$

where AR is the wing aspect ratio.

Diederich and Budiansky (4:14-16) show the principal equations for the wing deflection which the airloads will produce.

$$p(y) = qca_0\cos^2\Lambda(\alpha - h'\tan\Lambda) \quad (64)$$

$$t(y) = qcea_0\cos^2\Lambda(\alpha - h'\tan\Lambda) \quad (65)$$

For a uniform chord wing with constant stiffness properties, the equations of equilibrium for the cantilever wing are (16:46-47 and 4:16-18)

$$EIh^{iv} - K\alpha''' = (qca_0\cos^2\Lambda)(\alpha - h'\tan\Lambda) \quad (66)$$

$$GJ\alpha'' - Kh''' = -(qcea_0\cos^2\Lambda)(\alpha - h'\tan\Lambda) \quad (67)$$

After removing the initial load of the undeflected case (3:312) and where c is measured perpendicular to the elastic axis, a critical dynamic pressure (q) at the divergence speed results.

For the more general case of a wing with uniform properties and constant chord with bending and torsional deflections permitted, Diederich and Budiansky (4:18-20; 16-18) also provides the solutions to eqs (66) and (67). Weisshaar (16:17) provides the same solution as applied to a composite wing as

$$q_D = [2.47(1 - kg)/(cl^3a_0\cos^2\Lambda)][EI/[(1 - k\tan\Lambda)/(1GJ/eEI) - 0.39(\tan\Lambda - g)]] \quad (68)$$

where g and k are as defined previously. For equation (68) to yield a negative value of q_D , the velocity must be imaginary, implying that divergence is not possible. Therefore, negative q_D is desirable. Weisshaar (16:34) also demonstrates how eq (68) can be solved for the critical sweep angle, or that which will make divergence virtually impossible.

$$\tan \Lambda_{cr} = (g + 2.56eEI/1GJ)/(1 + 2.56eg/l) \quad (69)$$

in which g can be set equal to zero for a metallic wing. Λ_{cr} is solved for in CDIVRG and MDIVRG. For a composite wing, tailoring will alter the material properties and thus permit divergence-free sweep angles, particularly forward sweep, that are not possible with conventional metal structures.

For a linearly tapered wing with geometrically similar cross-sections, Diederich and Budiansky (4:17-20) again provides the analysis with the assumption that the structural properties (EI , GJ , and K) vary as the fourth power of the chord (a distribution representative of typical wing structures). To accomplish this, the spanwise properties can be referenced to the structural root properties through the terms

$$c = fc_r \quad (70)$$

$$f = 1 - \eta(1 - \lambda) \quad (71)$$

where the subscript r refers to a root parameter and λ is the taper ratio. Therefore, the property variation is expressed as

$$EI = f^4 EI_r \quad (72)$$

$$GJ = f^4 GJ_r \quad (73)$$

$$k = f^4 K_r \quad (74)$$

This approach is used in the subroutine CSTRUC (Appendix A). For a uniform wing the order of f can be set equal to one and the same equations used. These equations are models only and entail many assumptions. Care should be taken in applying them.

The solution of the divergence problem with these new parameters yields (15:55)

$$q_D = [GJ_r / (a_0 c_r l^3 \cos^2 \Lambda)] (1/e_r) [[K_1 (1 - k_r g_r)] / [1 - k_r \tan \Lambda - K_2 (l GJ_r / e_r EI_r) (\tan \Lambda - \tau_r)]] \quad (75)$$

as implemented in the subroutine CDIVRG (Appendix A). For a metallic wing (4:8) subroutine MDIVRG (Appendix A) uses

$$q_D = GJ_r / (a_0 c_r l^3 \cos^2 \Lambda) (1/e_r c_r) [K_1 / [1 - (K_2 GJ_r l / EI_r e c_r) \tan \Lambda]] \quad (76)$$

Weisshaar (16:55) updates the values for K_1 and K_2 given by Deiderich and Budiansky (4:9) as a function of taper ratio (see Table I).

Weisshaar discusses at length some results using these equations (16:18-24, 29-30). He concludes that taper ratio has little effect on Λ_{cr} . Weisshaar also (18:5-9) discusses the optimization of V_D by the variation of other planform parameters.

TABLE I

K Parameters
(used in Equations 75 and 76)

λ	K_1	K_2
0.20	2.83	0.614
0.50	2.73	0.497
1.00	2.47	0.390
1.50	2.22	0.326

Eq (75) and (76) provide a simple one equation solution for the divergence dynamic pressure which can be performed on a hand calculator. However, they are not often used and a much more accurate method exists. The common approach to finding the divergence speed is to perform an eigenstructure decomposition on the sum of the inverted symmetric aerodynamic matrix and the flexibility matrix (see next section). The inverse of the real part of the largest eigenvalue of the matrix is the divergence dynamic pressure. It is then an easy matter to determine the divergence speed. This method, almost certainly to be performed on a computer, is used in subroutine DIVERG (Appendix A).

When eq (76) was applied to the same wing as that used in the matrix approach but using only the structural properties at the 70% span, the predicted divergence speed was 43% lower. This suggests that the single equation method is much more conservative.

Aerodynamic Operator

To determine the divergence speed of a wing the air loads acting on the wing must be known. The following analysis uses the well known lifting line theory method, which includes induced effects, to determine

these loads. The assumptions entailed in this theory tend to overestimate airloads and are less accurate at large sweep angles (15:17). The spanwise centerline of the wing box is taken as a straight line and the Euler-Bernoulli hypothesis is again enforced. The airloads are assumed to act on segments perpendicular to the structural reference axis which is taken to be at the midchord of the wing on the midplane of the laminate box beam (Figure 3). The method assumes a moderate to high aspect ratio wing with subsonic flow below the critical value.

Lifting line theory involves dividing the wing into chordwise strips and superimposing constant strength horseshoe vortices upon these strips. The vortices are assumed to be bound to the wing at the quarter chord line and influences are computed at the 3/4 chord line at the center of each panel (see Figure 4). Gray and Shenk (6:22-39) shows the development of this method and states the assumptions therein entailed: the flow is potential (boundary layer effects, separations, and compressibility are neglected), wing thickness is small, there is a stagnation point at the trailing edge, angles of attack may be considered small, the wing is free of nacelles, pylons, etc., chordwise lines are considered rigid, and the airload distribution is related to the undeformed wing. The influence of each vortex upon all others provides a set of simultaneous equations that can be solved for the incremental lift at the center of each panel, or lift per unit length p_j , where j is the panel index. The panel lift is then $p_j h_j$, where h_j is the panel width. A standard linear expression can then be formulated

$$1/q[A_{ij}]\{p_j\} = \{\alpha_i\} \quad (77)$$

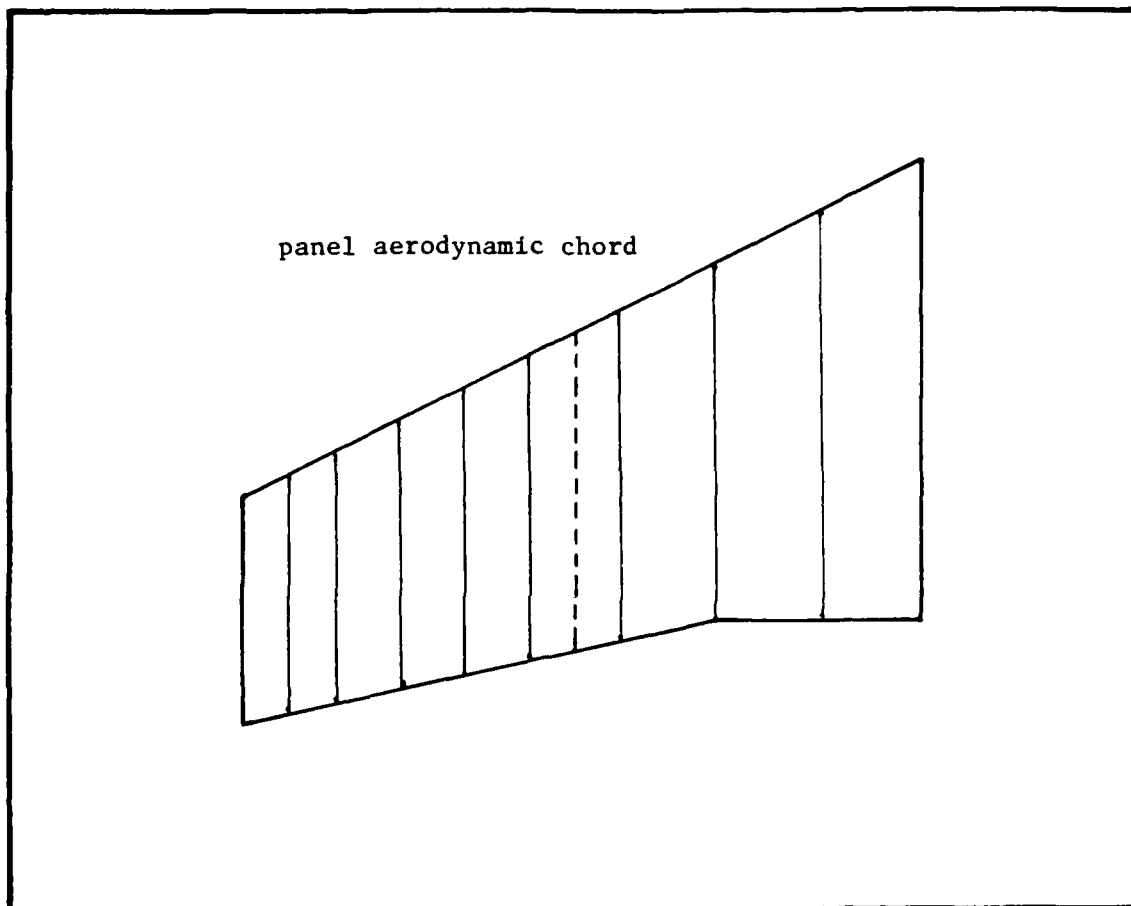


Figure 3. Wing Panel Nomenclature

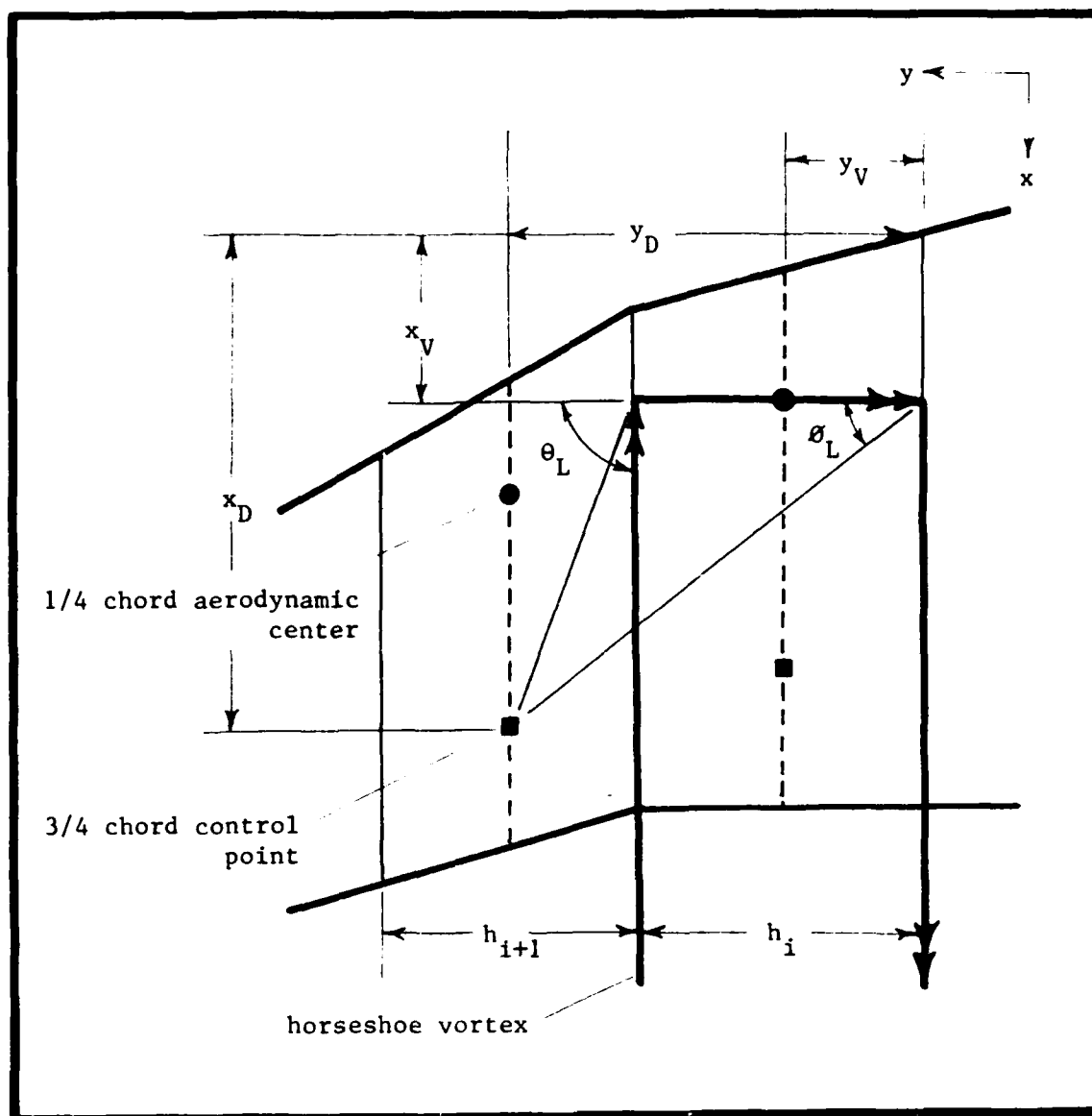


Figure 4. Panel Aerodynamic Nomenclature

where q is the dynamic pressure and α_1 is the streamwise angle of attack, positive nose up. No yaw is considered in this analysis. $[A_{ij}]$ is known as the aerodynamic influence coefficient (AIC) matrix and may be considered as simply an aerodynamic operator. It is a geometrically derived expression for the vortex influences, and can be expressed as

$$[A_{ij}] = (1/4a_0)[S_1] \quad (78)$$

The AIC matrix is typically determined for one semi-span only (left wing as used here). When a control surface such as an aileron is deflected on the wing an antisymmetrical lift distribution will result.

The downwash matrix $[S_1]$ is strictly dependent upon the geometry of the vortices as they relate to the wing planform (Figure 4) and is expressed as (6:39)

$$[S_1] = 2/c[(1 + \sin\theta_L)/\cos\theta_L - (1 + \sin\theta_L)/\cos\theta_L \pm (1 + \sin\theta_R)/\cos\theta_R \mp (1 + \sin\theta_R)/\cos\theta_R] \quad (79)$$

where the upper sign is used for the symmetrical loading condition and the bottom sign for the antisymmetrical, and where

$$\sin\theta = (x_D - x_V)/((x_D - x_V)^2 + (y_D - y_V + h)^2)^{1/2} \quad (80)$$

$$\cos\theta = (y_D - y_V + h)/((x_D - x_V)^2 + (y_D - y_V + h)^2)^{1/2} \quad (81)$$

$$\sin\theta = (x_D - x_V)/((x_D - x_V)^2 + (y_D - y_V - h)^2)^{1/2} \quad (82)$$

$$\cos\theta = (y_D - y_V - h)/((x_D - x_V)^2 + (y_D - y_V - h)^2)^{1/2} \quad (83)$$

The approach outlined in this section is implemented in the subroutine AERO1 (Appendix A).

The centers of pressure for a rigid wing and a flexible wing are calculated in subroutines RIGROL and FLEXROL, respectively (see Appendix A). As the center of pressure moves outboard an increase in the lift effectiveness is produced that promotes divergence as a consequence of the increased bending moment at the wing root (18:9-12). By tailoring the composite lamina, this center of pressure movement can be controlled to the designer's advantage.

Structural Operator

Gray and Shenk (6:10) detail how the angle of attack α_i can be broken down into

$$\{\alpha_i\} = \{\alpha_r\} + \{\alpha_s\} + \{\alpha_c\} \quad (84)$$

where α_r is the rigid body angle of attack or that which is attributed to the aircraft attitude and built-in twist of the wing, α_s is due to structural deformation of the wing, and α_c is apparent angle of attack variations resulting from such factors as wing control surface deflection and steady-state angular velocity attributed to rolling moment of the aircraft. α_s can be expressed as follows,

$$\{\alpha_s\} = [C_{ij}]\{p_j\} \quad (85)$$

for which $[C_{ij}]$ is referred to as the flexibility matrix and p_j is as defined prior to eq (77). The development for this matrix is given by Gray and Shenk (6:44-66) for a metallic wing and by Weisshaar (17:30-39) for a composite wing. The geometry parameters are the same in both developments and are shown in Figure 5. The following matrices are shared by both

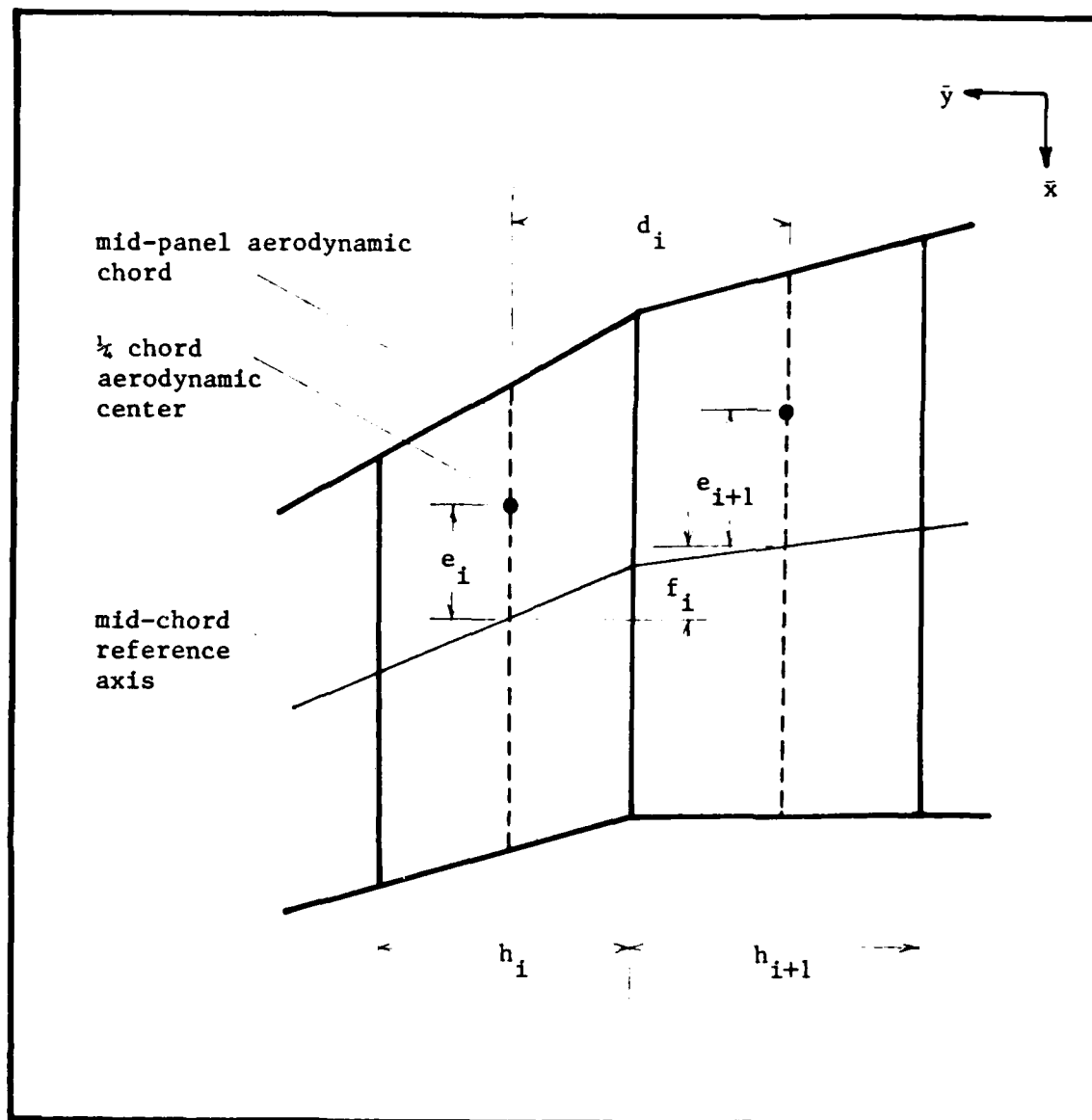


Figure 5. Panel Structural Nomenclature

$$[\cos \Lambda] = \begin{bmatrix} \cos \Lambda_1 & 0 & 0 & 0 & \dots \\ 0 & \cos \Lambda_2 & 0 & 0 & \dots \\ 0 & 0 & \cos \Lambda_3 & 0 & \dots \\ \vdots & \vdots & \vdots & \vdots & \\ \vdots & \vdots & \vdots & \vdots & \\ \vdots & \vdots & \vdots & \vdots & \end{bmatrix} \quad (86)$$

$$[\sin \Lambda] = \begin{bmatrix} \sin \Lambda_1 & 0 & 0 & 0 & \dots \\ 0 & \sin \Lambda_2 & 0 & 0 & \dots \\ 0 & 0 & \sin \Lambda_3 & 0 & \dots \\ \vdots & \vdots & \vdots & \vdots & \\ \vdots & \vdots & \vdots & \vdots & \\ \vdots & \vdots & \vdots & \vdots & \end{bmatrix} \quad (87)$$

$$[r_1] = \begin{bmatrix} \frac{h_1}{4\cos^2 \Lambda_1} - \frac{e_1 \tan \Lambda_1}{2} & 0 & 0 & \dots \\ d_1 & \frac{h_2}{4\cos^2 \Lambda_2} - \frac{e_2 \tan \Lambda_2}{2} & 0 & \dots \\ d_1+d_2 & d_2 & \frac{h_3}{4\cos^2 \Lambda_3} - \frac{e_3 \tan \Lambda_3}{2} & \dots \\ \vdots & \vdots & \vdots & \\ \vdots & \vdots & \vdots & \end{bmatrix} \quad (88)$$

$$[r_2] = \begin{bmatrix} e_1/2\tan \Lambda_1 & 0 & 0 & \dots \\ d_1 & e_2/2\tan \Lambda_2 & 0 & \dots \\ d_1+d_2 & d_2 & e_3/2\tan \Lambda_3 & \dots \\ d_1+d_2+d_3 & d_2+d_3 & d_3 & \\ \vdots & \vdots & \vdots & \\ \vdots & \vdots & \vdots & \end{bmatrix} \quad (89)$$

$$[u] = \begin{bmatrix} 0 & 0 & 0 & 0 & \dots \\ e_1 - f_1 & 0 & 0 & 0 & \dots \\ e_1 - f_1 - f_2 & e_2 - f_2 & 0 & 0 & \dots \\ e_1 - f_1 - f_1 - f_3 & e_2 - f_2 - f_3 & e_3 - f_3 & 0 & \dots \\ \vdots & \vdots & \vdots & \vdots & \vdots \\ \vdots & \vdots & \vdots & \vdots & \vdots \\ \vdots & \vdots & \vdots & \vdots & \vdots \end{bmatrix} \quad (90)$$

$$[I_0] = \begin{bmatrix} 1/2 & 1 & 1 & 1 & 1 & \dots \\ 0 & 1/2 & 1 & 1 & 1 & \dots \\ 0 & 0 & 1/2 & 1 & 1 & \dots \\ 0 & 0 & 0 & 1/2 & 1 & \dots \\ \vdots & \vdots & \vdots & \vdots & \vdots & \vdots \\ \vdots & \vdots & \vdots & \vdots & \vdots & \vdots \\ \vdots & \vdots & \vdots & \vdots & \vdots & \vdots \end{bmatrix} \quad (91)$$

For the composite wing

$$\begin{aligned} [C_{ij}] = [I_0] & [h(g - \tan \Lambda) / EI(1 - kg)] [[\cos \Lambda][r_1] - [\sin \Lambda][u]][h] \\ & + [I_0] [h(1 - k \tan \Lambda) / GJ(1 - kg)] [[\sin \Lambda][r_2] \\ & + [\cos \Lambda][u]][h] \end{aligned} \quad (92)$$

This equation is implemented in the subroutine CFLEX (Appendix A). If k and g were set equal to zero the equation becomes applicable to the metallic wing (5:65). Eq (91) is implemented in the subroutine MFLEX for the metallic wing case. The torsional deformations of eq (85) are solved for in subroutine DEFLCT (Appendix A).

By substituting eqs (77) and (85) into (84) one obtains

$$[B_{ij}]\{p_j\} = \{\alpha_r\} + \{\alpha_c\} \quad (93)$$

where

$$[B_{ij}] = (1/q[A_{ij}] - [C_{ij}]) \quad (94)$$

which relates loads to angle of attack. For a symmetrical maneuver

$$\{p_i\} = [B_{ij}]^{-1}\{\alpha_r\} \quad (95)$$

for the semi-span computations, and simply twice this for the total lift case. This permits the computation of the wing lift-curve slope (16:21)

$$C_{L_\alpha} = (2/qS)[1][B_{ij}]^{-1}\{1\} \quad (96)$$

where S is the total planform area. The subroutines RIGDROL and FLEXROL (Appendix A) apply eqs (95) and (96).

Lateral Control Reversal

Use of an aileron would require computation of the AIC matrix for the asymmetrical lift case. Weisshaar (17:22) provides the equilibrium equation for an aircraft undergoing steady-state roll.

$$\begin{aligned} 1/q[A_{ij}^{(a)}]\{p_j\} &= [C_{ij}]\{p_j\} + q[E_{ij}]\{\delta\} + \{\partial\alpha/\partial\delta\}\delta \\ &+ (Pb/2V)\{2\bar{y}_i/b\} \end{aligned} \quad (97)$$

with $[A_{ij}^{(a)}]$ as the asymmetrical AIC matrix. The first term on the right hand side of eq (97) is the angle of attack distribution due to structural flexibility. The second term involves the change in pitching moment of wing sections due to the aileron deflection producing an apparent change in angle of attack. The next term is the apparent change in angle of attack due only to the control deflection as a result of the camber change of the mean chord line. The final term in eq (97) is the damping-in-roll or the loss in lift as a result of the apparent

angle of attack change as a consequence of the rolling moment, which will tend to resist the rolling motion. This pitching moment is

$$T_y = (qc^2 c_{m_\delta}) \delta \quad (98)$$

where c_{m_δ} is the section pitching moment coefficient due to control deflection. The $[E_{ij}]$ matrix is expressed as (16:44)

$$\begin{aligned} [E_{ij}] = & [I_0] \{ [h(\sin \Lambda)(\tan \Lambda - g)] / [EI(1 - kg)] \} [I_0]^T [hc^2 c_{m_\delta}] \\ & + [I_0] \{ [h(\cos \Lambda)(1 - k \tan \Lambda)] / [GJ(1 - kg)] \} [I_0]^T [hc^2 c_{m_\delta}] \end{aligned} \quad (99)$$

where $[I_0]$ was defined previously in eq (91). These equations are applied in the subroutine CAILRN (Appendix A).

For the metallic wing (6:68), subroutine MAILRN utilizes the following form

$$\{\alpha_\delta\} = [m][2h/\cos \Lambda][1/EI]\{M\} + [t][2h/\cos \Lambda][1/GJ]\{T\} \quad (100)$$

where the following definitions apply

$$[m] = \begin{bmatrix} -\sin \Lambda_1/2 & -\sin \Lambda_2 & -\sin \Lambda_3 & -\sin \Lambda_4 & \dots \\ 0 & -\sin \Lambda_2/2 & -\sin \Lambda_3 & -\sin \Lambda_4 & \dots \\ 0 & 0 & -\sin \Lambda_3/2 & -\sin \Lambda_4 & \dots \\ 0 & 0 & 0 & -\sin \Lambda_4/2 & \dots \\ \vdots & \vdots & \vdots & \vdots & \vdots \\ \vdots & \vdots & \vdots & \vdots & \vdots \end{bmatrix} \quad (101)$$

$$[t] = \begin{bmatrix} \cos \Lambda_1/2 & \cos \Lambda_2 & \cos \Lambda_3 & \cos \Lambda_4 & \dots \\ 0 & \cos \Lambda_2/2 & \cos \Lambda_3 & \cos \Lambda_4 & \dots \\ 0 & 0 & \cos \Lambda_3/2 & \cos \Lambda_4 & \dots \\ 0 & 0 & 0 & \cos \Lambda_4/2 & \dots \\ \vdots & \vdots & \vdots & \vdots & \\ \vdots & \vdots & \vdots & \vdots & \\ \vdots & \vdots & \vdots & \vdots & \end{bmatrix} \quad (102)$$

$$\{M\} = \{[\cos \Lambda][r_1] - [\sin \Lambda][u]\}[L] \quad (103)$$

$$\{T\} = \{[\sin \Lambda][r_2] + [\cos \Lambda][u]\}[L] \quad (104)$$

$$\{L\} = \begin{Bmatrix} L_1 \\ L_2 \\ L_3 \\ \vdots \\ \vdots \\ L_n \end{Bmatrix} \quad (105)$$

where the terms of $\{L\}$ are derived from

$$L_i = p_i h_i \quad (106)$$

Solving for the $Pb/2V$ term in eq (97) permits an evaluation of the effectiveness of the aileron in producing a rolling moment. The deflection of the aileron and the flexibility of the wing result in structural deformation that effectively reduce the resultant rolling moment with increasing airspeed until an aileron deflection will produce no rolling moment. This is the control reversal speed, above which a change in control sense will occur with a control input in one direction producing a roll in the opposite direction. $Pb/2V$ can also be described as the helix angle described by the wing tip during a roll. A negative helix angle indicates a reversed control surface. Weisshaar (16:23)

provides a convenient per radian form of this equation

$$(Pb/2V)/\delta_o = \frac{-[\bar{y}_i h_i][B_{ij}^{(a)}]^{-1}\{q[E_{ij}]\{\Psi\} + \{\partial\alpha/\partial\delta\}\psi_i\}}{[\bar{y}_i h_i][B_{ij}^{(a)}]^{-1}\{2\bar{y}_i/b\}} \quad (107)$$

where

$$\{\delta_i\} = \delta_o\{\Psi\} \quad (108)$$

Ψ is used to set the relative deflections of adjacent aileron panels, permitting segmented ailerons. Therefore Ψ normalized to the deflection of the most outboard aileron panel, would be 1.0 for panels deflecting identically, or 0.5 for segment panels deflecting only half as much. This is performed in subroutine FLEXROL (Appendix A). The case of a rigid wing is dealt with in subroutine RIGROL wherein $[C_{ij}]$ and $[E_{ij}]$ are zero.

III. Analytical Development - Dynamic

General

The dynamic aeroelastic stability characteristic is known as flutter. This is a self-excited oscillatory instability in which the conservative structural forces (inertia and elasticity) extract energy from the airstream. In its most severe form, flutter becomes an oscillation of ever-increasing magnitude until catastrophic structural failure occurs. Many degrees of freedom of the structure may contribute to the instability, among them structural bending (flexure), torsion, and control surface motion. The coupling of several modes of deformation is a practical element of flutter. Although flutter may become manifest in any part of an air vehicle, wing flutter alone is of interest to this study.

In the design of the wind tunnel models described herein, it was desired that a satisfactory margin exist between the operating speeds and the predicted flutter velocity. For the parametric study upon which this project is based, a superficial flutter analysis only was required as dynamics was not an element of the investigation. Dr. Weisshaar's CWINGF program (18) was used to predict a flutter margin of greater than 100% (see Appendix D). Additionally, in an effort to provide ready-made and simple computer codes to perform quick and rudimentary flutter predictions, a series of subroutines was prepared. The supporting analysis for these codes is provided in this section.

Dynamic aeroelasticity involves the interaction of aerodynamic, structural, and inertial forces denoted by the symbols a , \mathcal{L} , and m , respectively. A forcing function may act through one or more of these components. Creating appropriate forms of the operators for these forces can become very complex. Apart from that provided in the previous section, only a simplified derivation of these operators will be provided. In dynamic analysis, the change in the system damping is primarily due to the aerodynamics. As the air velocity increases, the rate of damping of some of the modes at first increases and then may suddenly decrease rapidly (5:160). This sudden change in system damping can produce flutter with a surprisingly rapid onset.

The relationship of these fundamental operators is expressed by the equations of motion (2:43) where the operators may be integral, matrices, or any other form.

$$[\mathcal{L} - m - a]\{q\} = Q_D \quad (109)$$

where q are the generalized coordinates for the degrees of freedom used in the formulation of the operators, and Q_D are the generalized forcing function. The mass of the air may or may not (the in vacuo case) be included in the inertia operator. Only the homogeneous (unforced), linear form of this equation, will be dealt with here. The solution as a matrix equation is typically accomplished by forming the determinant (flutter determinant) and solving the resulting characteristic equation. That is,

$$|[s] - [m] - [a]| = 0 \quad (110)$$

If inertia effects are disregarded, the determinant discussed in the previous section results. For this steady formulation the unsteady aerodynamic operator may be used with evaluation at a frequency of zero. The solution of the characteristic equation then yields a series of eigenvalues, the largest of which corresponds to the inverse of the divergence dynamic pressure. Divergence, a static phenomenon, can be considered as flutter at zero frequency.

The eigenvalues of the flutter determinant will be complex, each representing a mode of deformation. The real part of the eigenvalue will indicate whether the mode it represents is stable or unstable. A negative real part is stable, with the magnitude of the value indicating the amount of damping present. Conversely, a positive real part represents an instability and implies flutter. A zero real part implies a neutrally stable condition for which a zero imaginary part represents divergence and a non-zero represents flutter (5:195).

Fung (5:205) provides some practical design considerations that are very meaningful for composites wherein torsional and flexural (bending) rigidity can be relatively easily tailored. He states that, in general, when torsional rigidity alone is increased, flutter speed also increases. However, when bending rigidity alone is varied, only a small difference in the flutter speed is seen. The minimum flutter speed will usually occur when the flexural rigidity becomes so large that the frequency of the uncoupled oscillation is equal to that of the uncoupled torsional oscillation. Further increase in this rigidity increases the flutter velocity.

Modal Formulation

Computation is much simplified by placing the operators in modal form. As described by Meirovitch (10:164), this is done by first solving for the system's natural frequencies and mode shapes (eigenvectors). Using the matrix formulation again, the system is represented by the dynamical matrix $[D]$ or

$$[D] = [m][s]^{-1} \quad (111)$$

where $[s]$ is the stiffness or the inverse of the flexibility matrix. For the application to follow, it is assumed that these operators have been formulated such that the rigid body modes (zero eigenvalues) have been removed. An eigenstructure decomposition is now performed on $[D]$. The form of the eigenvectors will describe the mode it represents. The individual eigenvalues are the inverse of the squares of the corresponding natural frequency. This solution for the natural frequencies and mode shapes is done in subroutine NFREQ (appendix A).

It is desired that the modal mass matrix $[M]$ be the identity matrix. This presents the following condition

$$[U]^{-1}[m][U] = [M] = [I] \quad (112)$$

where columns of $[U]$ are the normalized eigenvectors of the system, in ascending order, each multiplied by an unknown constant. The series of eigenvector multipliers that satisfy this condition can be easily be solved for. Applying these multipliers then produces the modal matrix, $[U]$. When operating on the stiffness matrix,

$$[U]^{-1}[s][U] = [w] \quad (113)$$

it produces a diagonal matrix of the squares of the natural frequencies $[w]$, or the modal stiffness matrix. By eliminating the rigid body modes prior to the modal operation it is ensured that $[w]$ is nonsingular. The modal aerodynamics matrix, $[A]$, is produced in a like manner but possesses no particular property. This calculation is carried out in subroutine MODAL (appendix A).

With the modal form of the aeroelastic operators, eq (109) now becomes

$$[[w] - [I] - [A]]\{q\} = Q_D \quad (114)$$

If a periodic temporal behavior is assumed

$$q_i = q_0 e^{i\Omega t} \quad (115)$$

and recognizing that the mass operator is associated with the second derivative of the displacements, the flutter determinant now takes on the more familiar eigenstructure form

$$[[w] - [A] - \Omega^2[I]] = 0 \quad (116)$$

where Ω^2 is the unknown complex eigenvalues of the complete system.

Solution Methods

By associating the eigenvalues of eq (116) with the frequency ω , the equation in the full matrix form (no external excitation) becomes

$$[[w] - [A] + \omega^2[I]]\{q\} = 0 \quad (117)$$

A structural damping term is arbitrarily applied to the structural operator.

$$[(1 + ig)[w] - [A] + \omega^2[I]]\{q\} = 0 \quad (118)$$

where g is the required structural damping for a stable system. By moving the structural operator to the right hand side and dividing through by the square of the frequency, one arrives at the form provided by Weisshaar (17:22).

$$[(1/\omega^2)[A] - [I]]\{q\} = ((1+ig)/\omega^2)[w]\{q\} \quad (119)$$

This can be solved as it is with the coefficient on the right hand side serving as the eigenvalue, or it can be cast in the more familiar determinant form by multiplying through by the inverse of the stiffness matrix and subtracting the coefficient to the left hand side.

$$|[w]^{-1}((1/\omega^2)[A] - [I]) - ((1+ig)/\omega^2)[I]| = 0 \quad (120)$$

Solutions of the flutter determinant involve solving for the component parts with a selected velocity and an assumed frequency and then performing the eigenvalue decomposition. The frequency for the mode being followed will not necessarily match that which was initially selected and an iteration must be done until a match occurs. A good practice is to start at zero velocity and use the natural frequency of the mode to be followed. This operation is repeated for increasing velocities using the final matched frequency from the last velocity as the initial guess for the next.

Velocity and frequency are often combined into one factor known as the reduced frequency or Strouhal number, k .

$$k = \omega c_{ref}/2V \quad (121)$$

where c_{ref} is a reference chord to non-dimensionalize the equation. The aerodynamic operator may be expressed as a function of k in the frequency domain. Reduced frequency characterizes the variation of flow with time, or more precisely, it represents the ratio of the characteristic length of the body to the wave length of a disturbance (5:164).

The V-g method of flutter solution entails proceeding as described above and producing a plot of velocity versus damping or a V-g plot. Each mode can be followed and the known structural damping can be represented by a line. The velocity at which the derived damping rises above this available damping for the first time for any mode is the flutter velocity. This represents a deficiency in damping. If the true available structural damping is not known then assuming zero damping will represent a conservative approximation and then the first crossing of the damping axis by any mode is the flutter velocity. This method is employed in the subroutine VGFLUTR (Appendix A). The k-method is done in the same way with k now serving as the principle variable (subroutine KFLUTR).

The inertial operator in eq (116) can be cast into the s-plane for the p-k method of flutter solution by assuming a response

$$q_i = q_0 e^{pt} \quad (122)$$

Proceeding as before, the flutter determinant now becomes

$$[W] - [A] + p^2[I] = 0 \quad (123)$$

The eigenvalue p is assumed to have the form

$$p = \gamma + i\omega \quad (124)$$

where γ in this case is the overall system damping. The solution technique is as described before but with p being plotted in the s -plane. When the real part of p enters the right-half plane flutter will occur, this representing a system instability. Again, k is the principle variable. This approach is employed in the subroutine PKFLUTR.

All of the methods outlined in this section are used in the main flutter computation program FLUTR (Appendix A).

Simplified Operator Derivations

Formulations of the aeroelastic operators can be extremely complex. Fung provides a much simplified 2-dimensional model which may be used as a typical section, normally solved at the 70% chord, or at a number of node points across the span. Camber and thickness effects are neglected and incompressible flow is assumed. With these assumptions, the section equation of motion (5:212) becomes

$$m(2V/c)^2 \ddot{h} + S(2V/c)^2 \ddot{\alpha} + m\omega_h^2 h = -M(\gamma) + p(\gamma) \quad (125)$$

$$S(2V/c)^2 \ddot{h} + I_\alpha(2V/c)^2 \ddot{\alpha} + I_\alpha \omega_\alpha^2 \alpha = T(\gamma) + t(\gamma) \quad (126)$$

where

$$S = \int r \, dm \quad (127)$$

$$I_\alpha = \int r^2 \, dm \quad (128)$$

S is the wing static moment about the elastic axis, I_α is the wing mass moment of inertia about the elastic axis, positive aft, ω_h is the uncoupled natural frequency of bending, ω_α is the uncoupled natural frequency of torsion, m is the wing mass, and γ is a nondimensionalized

time, or

$$\gamma = (2V/c)t \quad (129)$$

Again using the reduced frequency and assuming a periodic response, the unforced equations of motion reduce to

$$2M(\gamma)e^{ik\gamma}/\rho\gamma cV^2 = -k^2[(2/c)h_0 - a_h\alpha_0] + ik\alpha_0 + 2\bar{C}[\alpha_0 + i(2k/c)h_0 + ik(0.5 - a_h)\alpha_0] \quad (130)$$

$$4T(\gamma)e^{ik\gamma}/\rho\gamma c^2V^2 = 2\bar{C}(0.5 + a_h)[\alpha_0 + i(2k/c)h_0 + ik(0.5 - a_h)\alpha_0] - k^2a_h[(2/c)h_0 - a_h\alpha_0] - ik(0.5 - a_h)\alpha_0 + (k^2/8)\alpha_0 \quad (131)$$

where a_h is the distance between the midchord and the elastic axis. C is known as the Theodorsen's function given as

$$\bar{C} = H_1/(H_1 + iH_0) \quad (132)$$

(5:214) where H_1 and H_0 are Hankel functions of k . \bar{C} may be approximated for k less than 0.5 as

$$\bar{C} = 1 - 0.165/(1 - i0.0455/k) - 0.335/(1 - i0.3/k) \quad (133)$$

By employing the following definitions

$$\mathcal{M} = 4m/\rho\gamma c^2 \quad (134)$$

$$x_\alpha = 2S/mc \quad (135)$$

$$r_\alpha = (I_\alpha/mc^2)^{1/2} \quad (136)$$

where \mathcal{M} is called the mass ratio, x_α is the distance between the section center of mass and the aerodynamic chord in semi-chords, and r_α is the radius of gyration about the elastic axis in semi-chords, the

equations of motion can be simplified further and cast in matrix form as

$$[m]\{q\} = \begin{bmatrix} -M & -M x_{\alpha} \\ -M x_{\alpha} & -M r_{\alpha}^2 \end{bmatrix} \begin{Bmatrix} h_o/b \\ \alpha_o \end{Bmatrix} \quad (137)$$

$$[s] = \begin{bmatrix} M \omega_h^2 & 0 \\ 0 & M \omega_{\alpha}^2 r_{\alpha} \end{bmatrix} \quad (138)$$

$$[a] = \begin{bmatrix} -1 + i2\bar{C}/k & a_h + 2\bar{C}/k^2 + i/k + i2\bar{C}(0.5 - a_h)/k \\ a_h - i2\bar{C}(0.5 + a_h)/k & -1/8 - a_h^2 + i(0.5 - a_h)/k \\ & - i2\bar{C}(0.5 + a_h)[1 + ik(0.5 - a_h)]/k^2 \end{bmatrix} \quad (139)$$

When these operators are used for a series of sections across a span, tri-diagonal forms result. These matrices are created in subroutine FUNG (Appendix A).

IV. Computer Model

General

To provide a means for predicting the static aeroelastic characteristics of the various planform and control surface configurations to be tested, the CWINGS computer program written by Dr. Weisshaar has been adapted as the basis for the analytical models. This code provided a manageable and cost effective means for performing static aeroelastic predictions and model design. This program has been reduced to its component parts and modified to meet the particular needs of this project, with additional coding written to perform automated implementation for optimal design for the constraints of each individual testing circumstance. The listing of this revised static aeroelastic computer program, COMPSTAT (Composite Static) is provided in Appendix B and uses the many of the subroutines provided in Appendix A.

The results of a parametric analysis performed with the COMPSTAT program are provided in Table II. This table gives results for a number of alterations to the test planform and composite material described in the next section. Only one planform was used in the experimental portion of this research and so only the laminate design process will be addressed henceforth.

Optimization

As discussed in the next section, the composite plates used in the experiment were designed using standard iteration practices. To

TABLE II

Parametric Variation Examples

(Layup 1, Case 1, 1000 ft PA)

(all speeds MPH)

Condition	V_D	$\Delta\%$		V_R	$\Delta\%$
normal (ailerons)	161	-		118	-
tip aileron span reduced 1/3	161	0		127	+8
tip aileron span increased 2/3	161	0		112	-6
ailerons moved to mid-span	161	0		107	-9
ailerons moved to root	161	0		97	-18
aileron 1% of section chord	161	0		107	-9
aileron 3% of section chord	161	0		131	+11
taper ratio increased 25% *	159	-1		119	+1
taper ratio decreased 25% *	163	+1		119	+1
reference axis sweep increased 25%	144	-11		118	0
reference axis sweep decreased 25%	192	+19		118	0
reference axis sweep reversed (fwd)	106	+6		118	0
linear spanwise thickness taper	88	-46		75	-36
normal (flaperons)	161	-		109	-
reversed taper flaperons +	161	0		122	+12
straight flaperons +	161	0		114	+5

* reference axis sweep and planform area maintained constant

+ same flaperon areas

investigate the possibility of automating this design process, the ADS (Automated Design Synthesis, see Reference 14) optimization program resident on the AFIT computer system was used. It was believed that a layup schedule that better met the requirements of the experiment could be designed in this way without the strictures of the standard design practice.

A layup requiring each ply to be rotated to different orientations, as ADS would produce unless instructed to do otherwise, would significantly complicate the fabrication process and so may not be desirable in practice. Machine layup may not have this difficulty. The designer may wish to use the optimization layup as a starting point only, rounding off the orientations to the nearest 5 deg rotation and seeing how this effects the results.

Each plate stacking sequence provides different material characteristics as seen in variations in reversal, divergence, and flutter speeds for the same wing geometry. The many laminates analyzed were subject to the following criteria:

- a. Predicted reversal speed was sought below 150 miles per hour (mph), and preferably around 100 mph. This permitted 50 mph or more margin from the maximum wind tunnel velocity of 200 mph to allow for errors in the method and the unknown stiffening of the plates due to the outer shape and covering (see Section V).

- b. Divergence speed was sought at least 20% above the predicted reversal speed. If this speed was estimated to be within the range of the wind tunnel, a check of this prediction was then possible.

c. Flutter speed was to be at least 50% above the maximum tunnel speed.

d. The difference between the predicted reversal speeds for the three laminate orientations was to be at least 10 mph to ensure that instrumentation could resolve the difference. The reversal speed was to be a continuously increasing or decreasing relationship with laminate rotation rather than parabolic for the rotation range desired. This was to ensure that each reversal speed was widely different.

e. A single plate with the 90 degree plies along the reference axis was desired. It was also desired that the other laminates be less than +20 degrees off of this orientation for a more practically representative model. Automated optimization of the layup schedule would not likely produce plies oriented in this manner unless specifically instructed to do so.

Reversal within these constraints was sought for a full span flaperon. The flaperon had a cut perpendicular to the "hinge" line at 40% span creating a separate flap and aileron. If reversal of the flaperon (aileron and flap deflected equal amounts) could not be demonstrated within the speed range of the wind tunnel, reversal of either the flap or aileron alone was sought.

ADS allows the selection of strategy, optimizer, and one dimensional search methods dependent upon the constraints on the objective function to be minimized. The layup problem involves linear constraints so a sequential quadratic programming strategy was used with the method of feasible directions for constrained minimization as the optimizer, and polynomial interpolation as the one dimensional search.

ADS was run with COMPSTAT serving as the function which provided the parameter to be optimized and its constraints. The design variables for the optimization were the individual ply orientations. These were bounded by 0 and 180 deg. Reversal and divergence speeds were the results used in the objective function and constraints.

V. Experimental Apparatus

Composite Plates

The composite plates that form the structure of the wing models were fashioned from Hercules AS4-3501-6 graphite fibers in a resin matrix. This is an industry standard in carbon-carbon material. The plate layups were designed using accepted practices applied to the COMPSTAT computer code and constraints discussed in the previous section. Analysis concentrated on a 32 ply laminate as a result of AFWAL experience. The plates were designed with two identical 16 ply stacking sequences symmetric about the mid-plane of the plate. The stacking entailed the distribution of plies with the primary fiber axis oriented along the reference axis of the wing and with additional plies at 45 degrees forward and aft of the reference axis. Each model differed by the rotation of this entire stack forward or aft of this primary orientation. The ply orientations utilized are typical for such applications and were used only for this reason. Another typical practice adopted was to maintain an equal number of forward and aft 45 degree plies.

The following results were found during design iterations for the test planform and may prove helpful for future applications.

- a. Additional plies tend to stiffen the plate, increasing divergence and reversal speeds.
- b. For an aft swept wing, additional forward rotated plies tend to stiffen the plate.

c. Placing the rotated plies as outside layers of the laminate tends to increase the divergence speed.

d. Placing the rotated plies as outside layers of the laminate tends to decrease the reversal speed for laminate rotations aft of the elastic axis, and increase it for forward rotations.

e. Rotation of the laminate forward of the elastic axis tends to increase the divergence speed.

Results of this analysis for a number of typical laminates and using the material properties given in Appendix D is provided in Figure 7 for the wing plate shown in Figure 6 and characteristics specified in Table III. The stacking sequences for the laminates are provided in Table IV. A finer breakdown of plies (groups of two rather than four, or reversing signs) in the stack was found to produce results very similar to the more basic laminates shown. Based upon these results, three composite plates were fabricated with the stacking sequence and laminate orientations given in Table V. The predicted static response for each control surface for this optimum laminate is shown in Figure 8-11. This analysis was performed with manufacturer-supplied material properties which varied slightly from the values used to compare results with tunnel data. The peculiar result of the flap reversal occurring at a lower speed than the aileron reversal is intuitively incorrect, the root deflecting less by virtue of the clamped boundary condition. The implications of this result are expanded upon in a later section of the thesis.

Each plate was layed up by hand with curing and finishing by standard means. An internal stress in the plates was discovered during

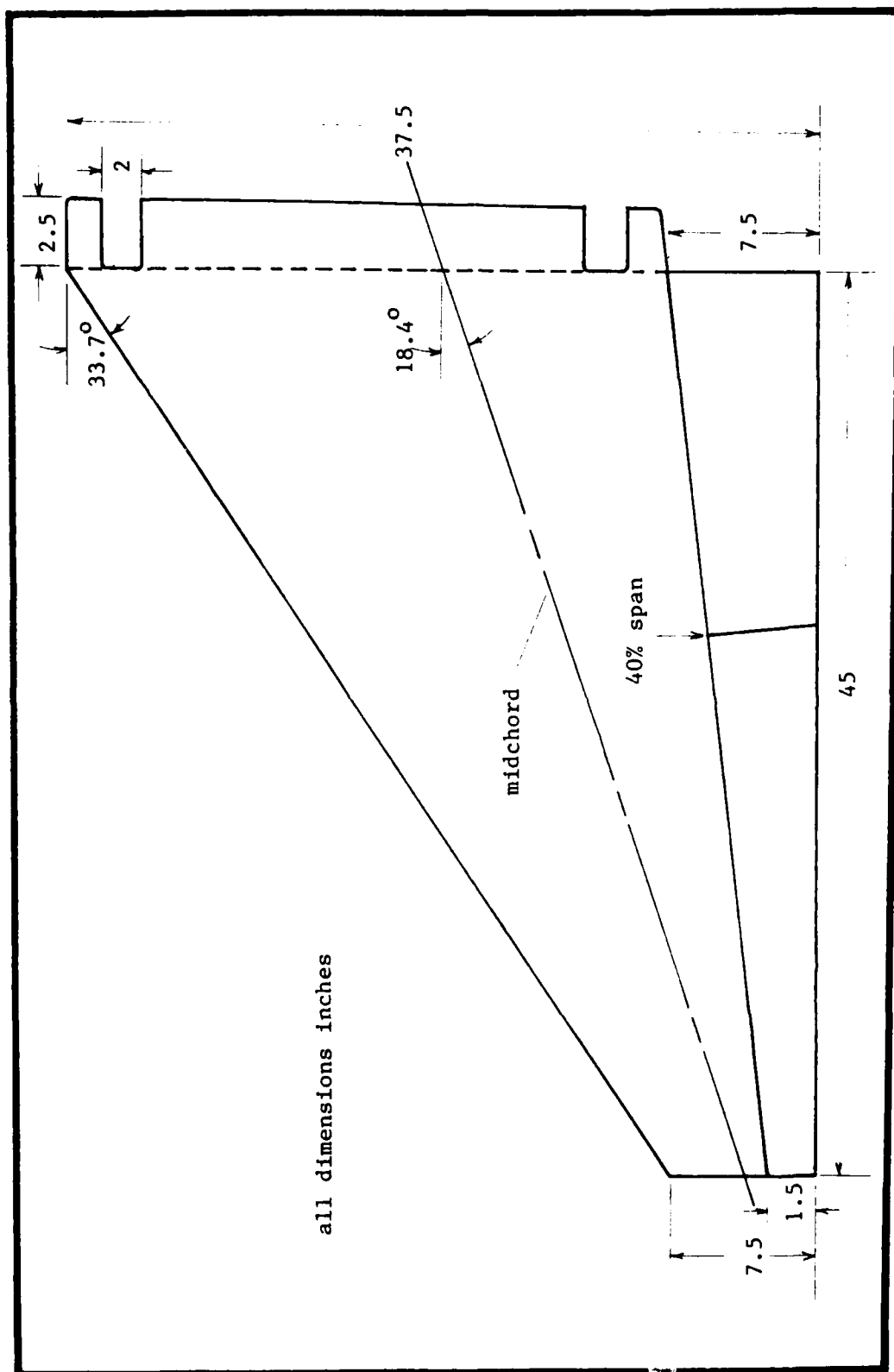


Figure 6. Wing Plate Planform

TABLE III
Test Planform Characteristics
(half-span dimensions)

section	10% thick symmetric
area	1012.5 sq inches
semi-span	45.0 inches
semi-span along reference axis	47.4 inches
reference axis at mid-chord	
aerodynamic centers at quarter-chords	
aerodynamic chord root chord	37.5 inches
structural root chord	36.13 inches
box beam structural root chord	28.25 inches
aerodynamic tip chord	7.5 inches
structural tip chord	7.25 inches
taper ratio	0.2
aspect ratio	0.4
reference axis (mid-chord) sweep	18.4 degrees
box beam reference axis sweep	21.5 degrees
leading edge sweep	33.7 degrees
trailing edge sweep	0.0 degrees
aileron/flap taper ratio	0.2
aileron/flap chord	20% of section chord

Table IV
Analysis Layup Schedules

Ply No.	Ply Orientation (deg.)					
	Layup 1	Layup 2	Layup 3	Layup 4	Layup 5	Layup 6
1	90	90	90	45	45	45
2	90	90	90	135	135	135
3	90	90	90	45	45	45
4	90	90	90	135	135	135
5	90	45	45	45	90	90
6	90	135	135	135	90	90
7	90	45	45	45	90	90
8	90	135	135	135	90	90
9	45	45	90	90	90	45
10	135	135	90	90	90	135
11	45	45	90	90	90	45
12	135	135	90	90	90	135
13	45	90	45	90	45	90
14	135	90	135	90	135	90
15	45	90	45	90	45	90
16	135	90	135	90	135	90

- mid-plane -

bottom 16 plies mirror image of top

(see Figure 1 for definition of ply orientation)

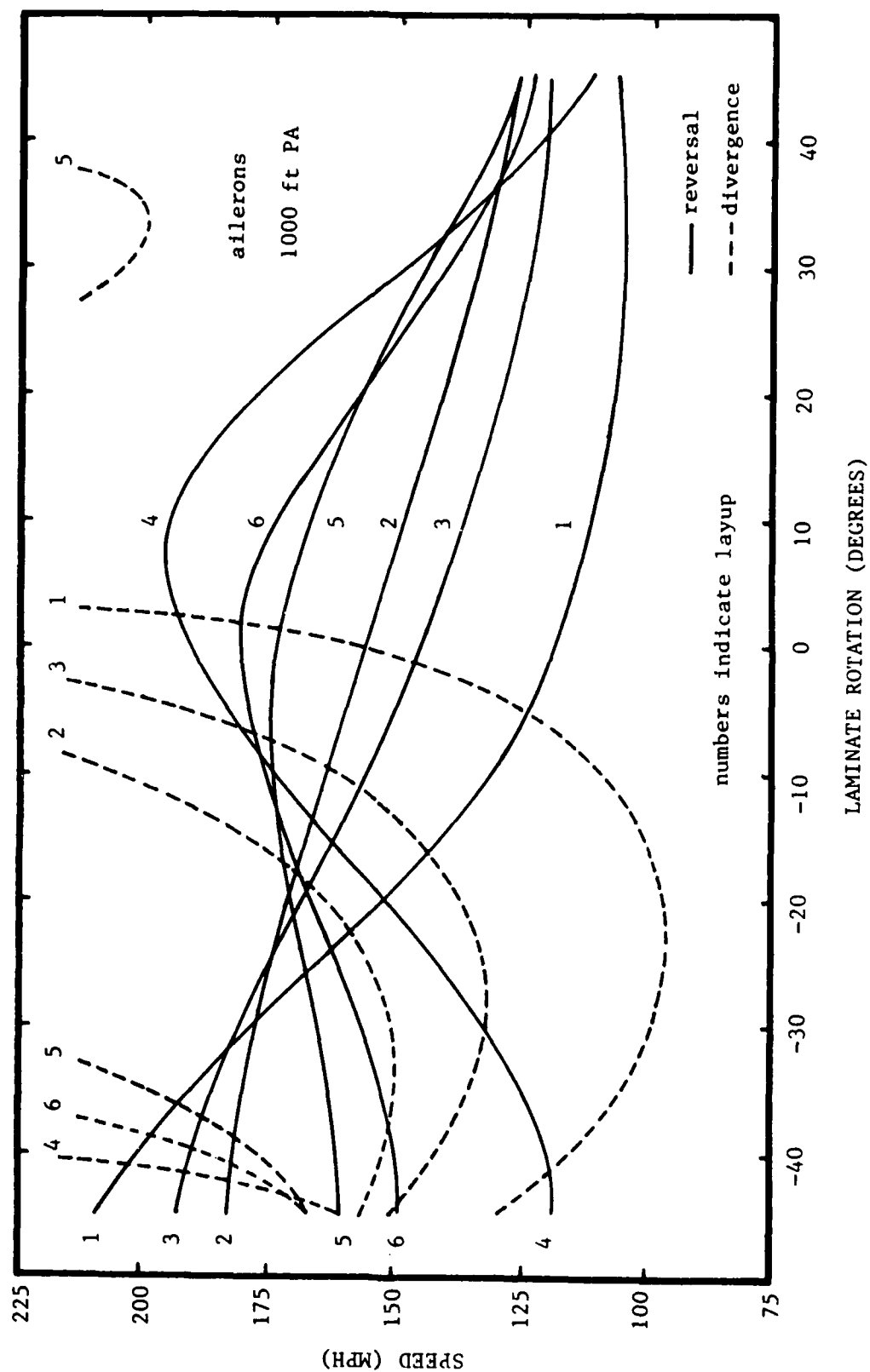


Figure 7. Wing Plate Static Analysis Results

Table V
Wing Plate Layup Schedules

Ply No.	Ply Orientation (deg.)		
	Case 1	Case 2	Case 3
1	90	100	110
2	90	100	110
3	90	100	110
4	90	100	110
5	90	100	110
6	90	100	110
7	90	100	110
8	90	100	110
9	45	35	25
10	135	145	155
11	45	35	25
12	135	145	155
13	45	35	25
14	135	145	155
15	45	35	25
16	135	145	155
- mid-plane -			

bottom 16 plies mirror image of top

(see Figure 1 for definition of ply orientation)

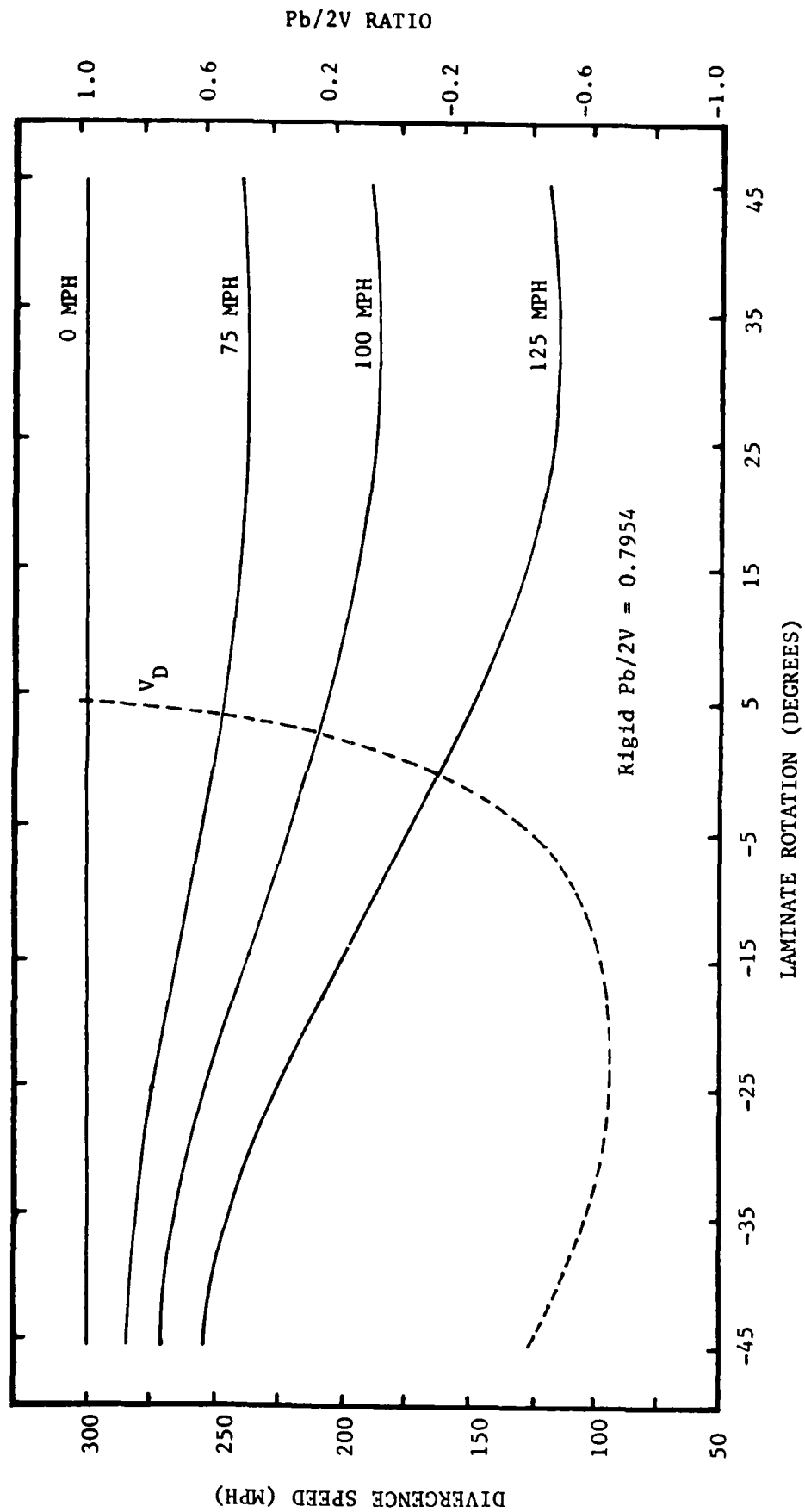


Figure 8. Layup 1 Aileron Analysis Results

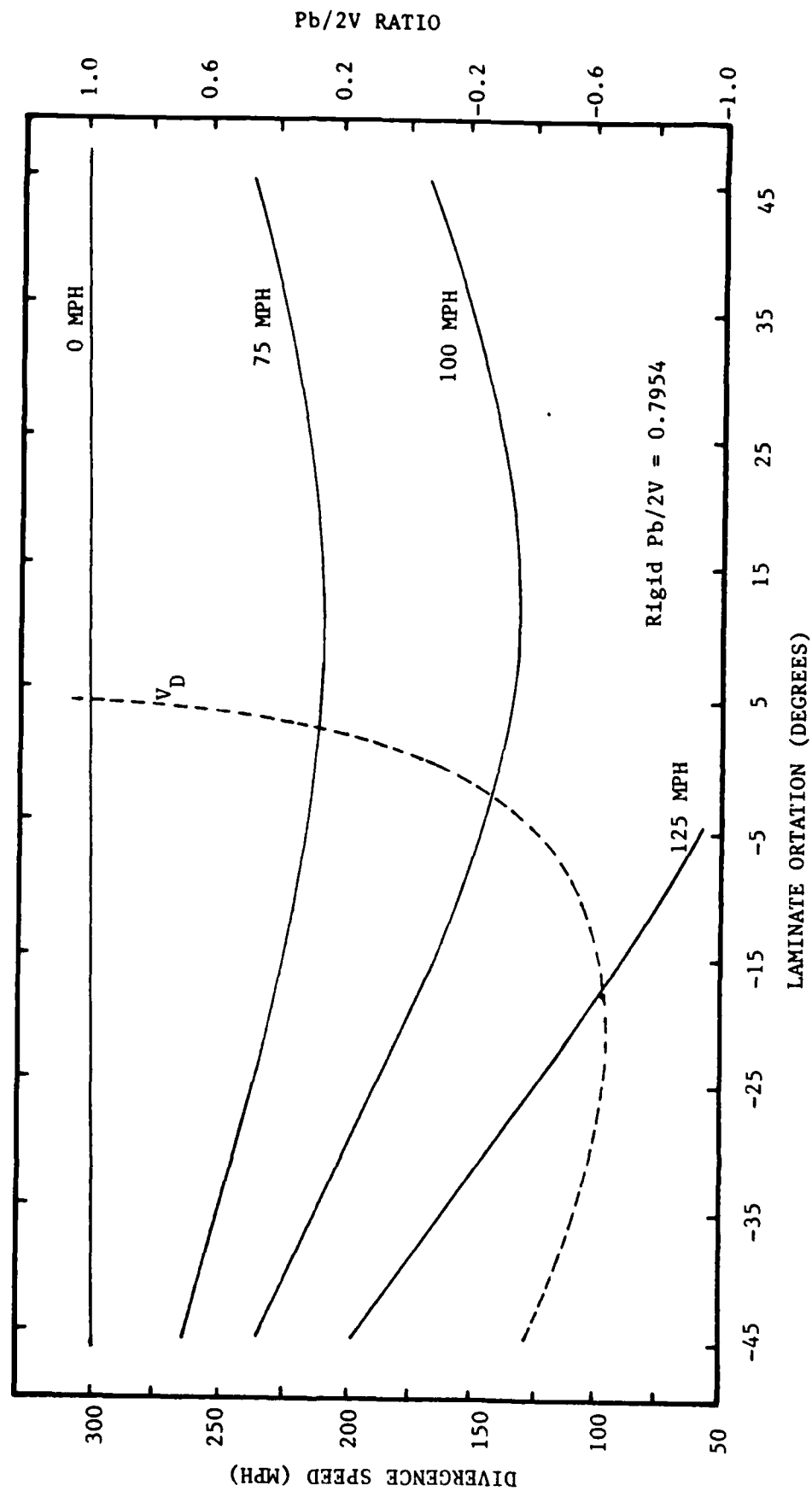


Figure 9. Layup 1 Flap Analysis Results

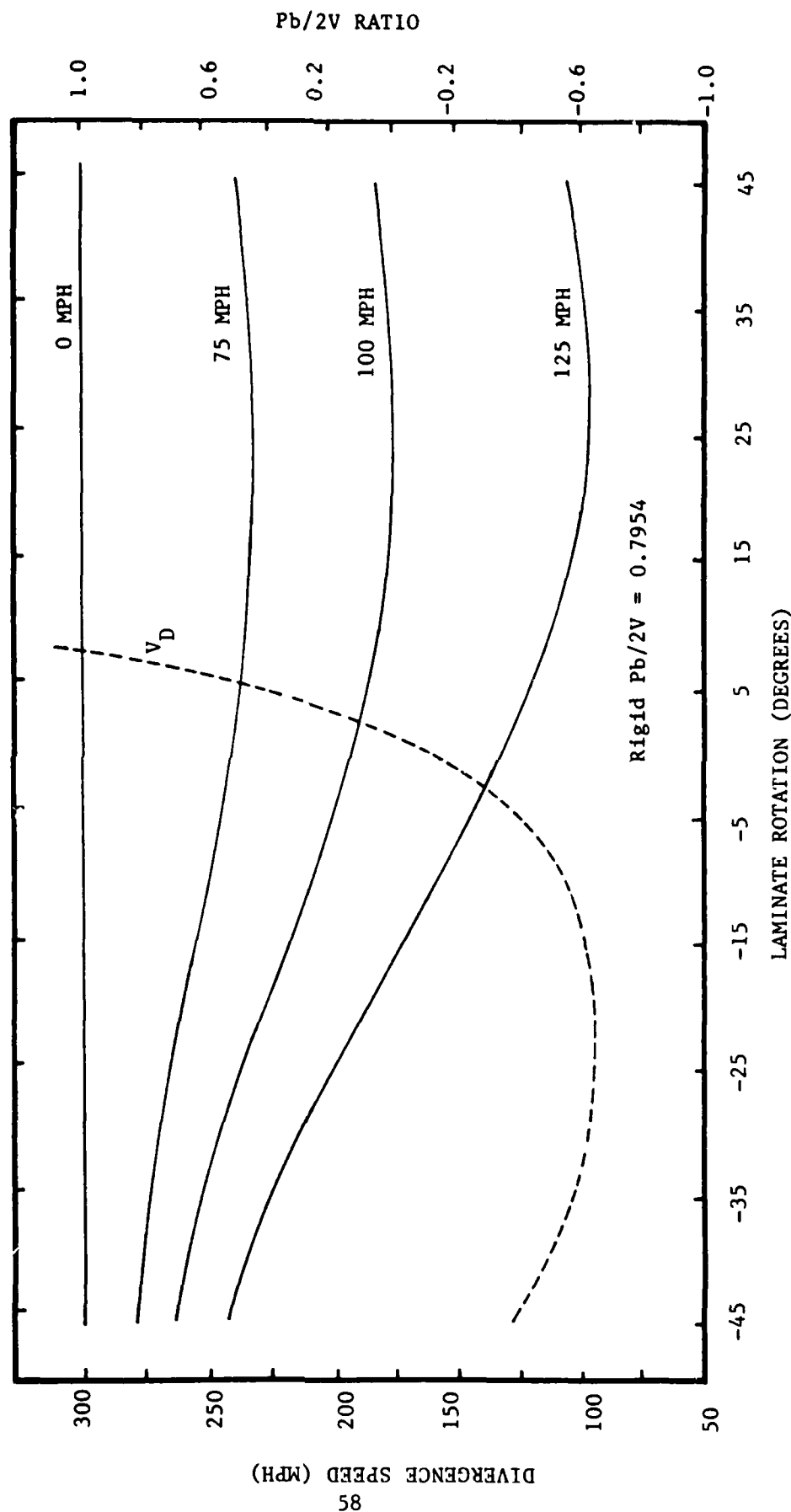


Figure 10. Layout 1 Flaperon Analysis Results

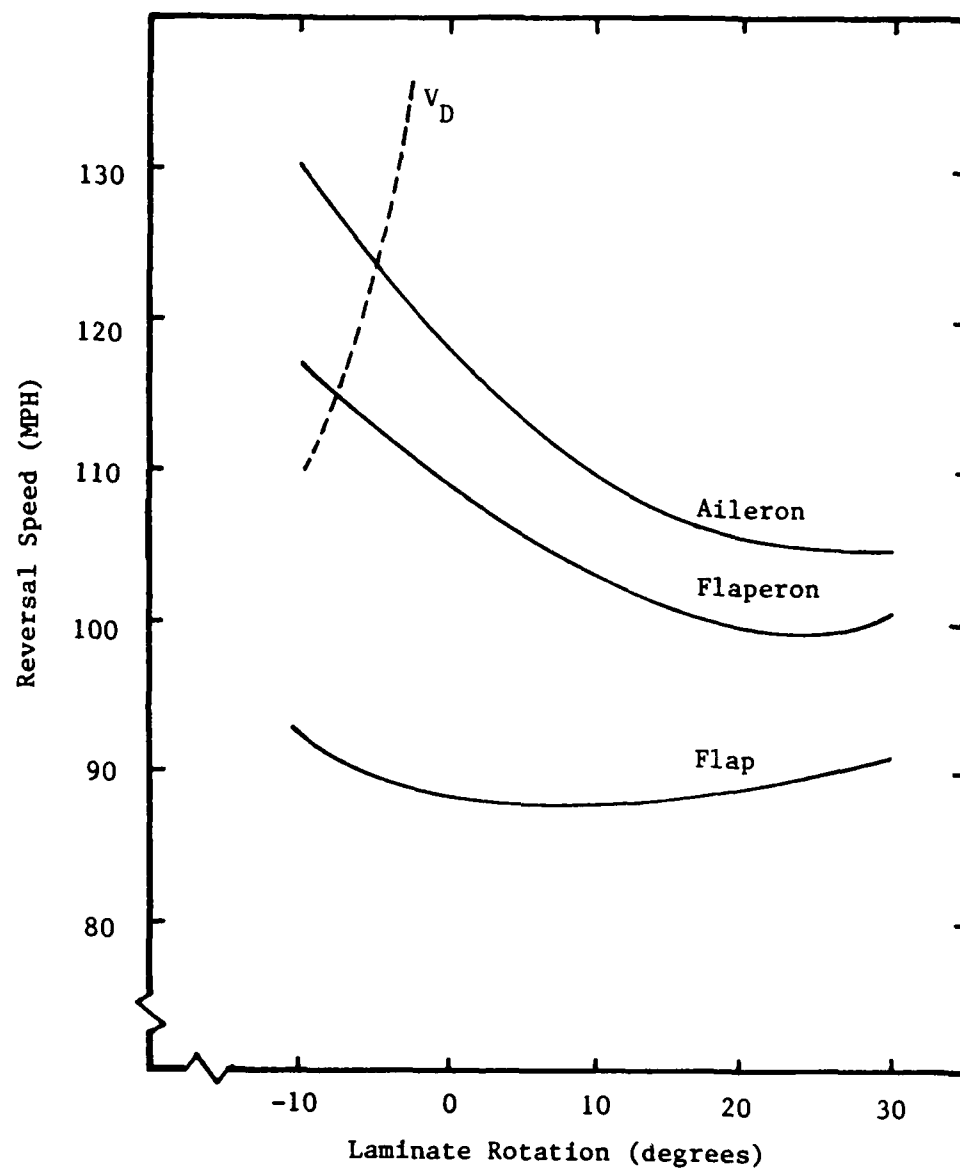


Figure 11. Layup 1 Theoretical Reversal Speeds

cutting with a rotary diamond saw. Such an internal stress is not uncommon, being produced during the cure when the carbon fibers and the epoxy matrix expand and shrink slightly, respectively. This stress could be seen in narrow samples of the plate which bowed along an axis parallel to the 90 degree plies. The final large plates, when placed in the experimental cantilever mount, showed an unloaded deformation less than the thickness of the plate for the full span. The loads to which these plates were subjected are many orders of magnitudes greater than this internal stress and so the latter was ignored. Each plate was subjected to a C-Scan to determine the extent of voids or distorted fibers within the laminate. This test indicated sound layups.

Documentation indicates that material properties for composite materials can vary various amounts even for specimens taken from the same production lot. It was found that the analytical methods used to determine the optimum laminate was highly sensitive to these minor variations, producing variations in reversal speeds of as much as 15% (see Table VI). Because of this, special specimens were produced using the same production lot composite material as that used in the wing plates. These specimens were subjected to tensile tests. An average of the results of these tests were then used to more precisely predict the aeroelastic characteristics of the models and were used in the final predictions compared with wind tunnel data. The results of these tests and are provided in Appendix D.

Wing Models

The wing planform was specified by AFWAL and represents a typical configuration planned to be used in the parametric study. The size of

TABLE VI

Sensitivity Analysis Results

(Layup 1, Case 1, 6 panel outboard aileron, 1000 ft PA)

(all speeds MPH)

Condition	V_D	$\Delta\%$		V_R	$\Delta\%$
Normal (ailerons)	161	-		118	-
E_1 increased 10%	162	+1		121	+3
decreased 10%	161	0		116	-2
E_2 increased 10%	162	+1		118	0
decreased 10%	161	0		118	0
A_{12} increased 10%	161	0		118	0
decreased 10%	162	+1		118	0
G_{12} increased 10%	169	+5		121	+3
decreased 10%	154	-4		115	-3
ply thickness increased 10%	186	+16		136	+15
decreased 10%	138	-14		101	-14
$c_{l_\delta} / c_{l_\alpha}$ increased 10%	161	0		124	+5
decreased 10%	161	0		112	-5
c_{m_δ} increased 10%	161	0		124	+5
decreased 10%	161	0		125	+6

the model was dictated by the dimensions of the 5-foot test section of the AFIT wind tunnel. Only half-span models were constructed as this was all that was necessary to illustrate the phenomena being investigated and permitted a larger model to be used in the wind tunnel.

The half-span wings had an aft-mounted flap and aileron attached to the parent plate by small, evenly spaced 3/32 inch steel brackets, two for the flap and three for the aileron (see Figure 12). A series of bent brackets were fabricated to permit orientation of the surfaces, separately or together as a flaperon, at various deflection angles. The brackets were fastened to the plates by small screws and nuts. Two brackets were used at each location, top and bottom of the plate, to avoid damage to the plate and thus provide sufficient bending strength against the control surface air loads. The depressions in the covering material required for installation and removal of the brackets were covered with tape during wind tunnel tests. By using these discrete, widely separated brackets, added bending or torsional stiffness was avoided without applying appreciable masses that could effect wing flutter. Control surface roll-up (the deflection of a portion of the control surface toward neutral under air loads at locations away from the actuator restraint) was also reduced.

The wing and control surfaces were covered with Dow 2.0 lbm/ft³ blue insulation styrofoam shaped to a NACA 0010 symmetrical airfoil. This foam was attached to the plate with a flexible rubber-like contact cement that permitted small displacement of the foam relative to the plate while still transmitting the air loads to the plate. A thin, heat-shrunk, flexible outer skin of aircraft-grade Dacron fabric with

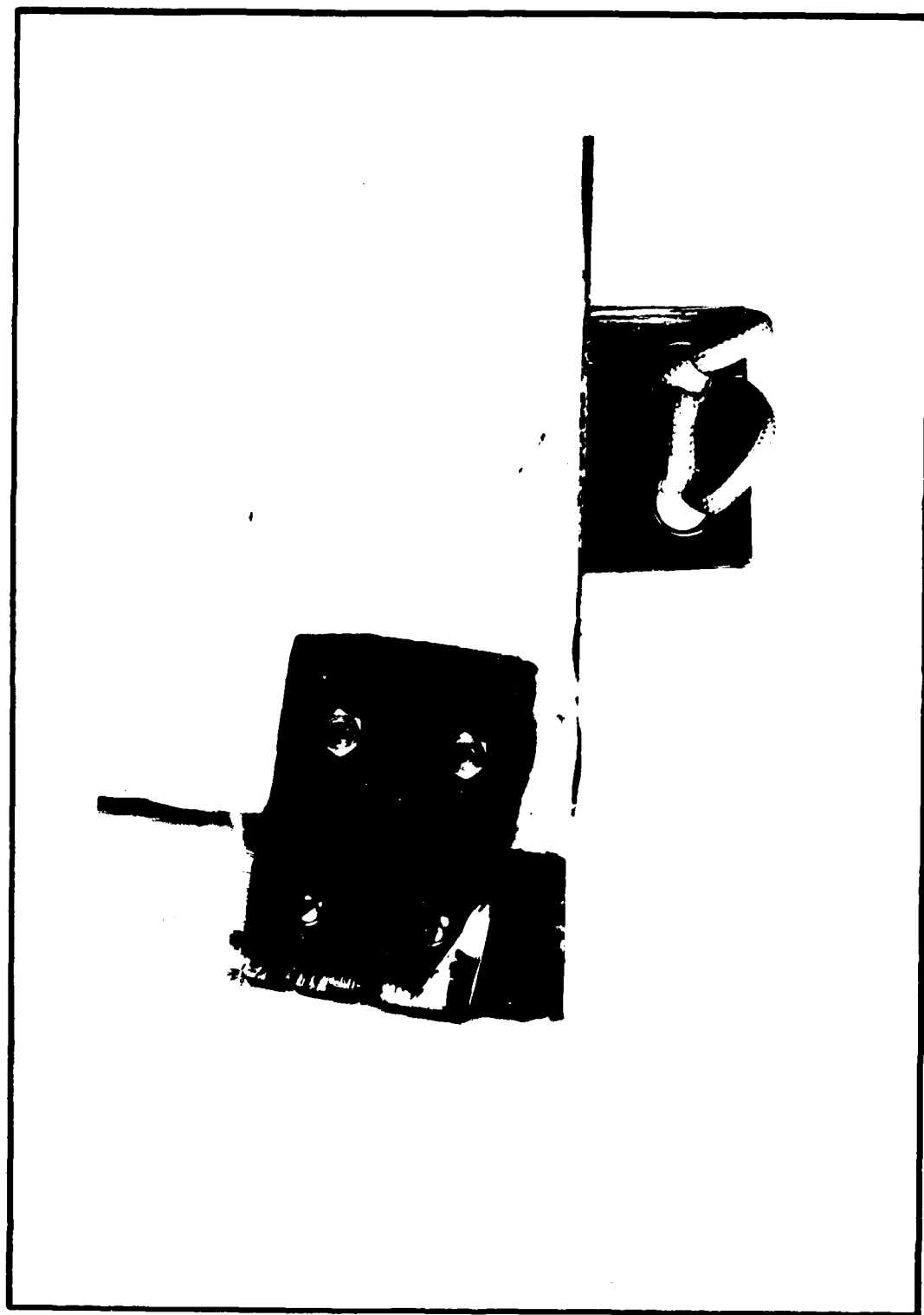


Figure 12. Control Surface Attachment Brackets and Tip Restraint

three lightly sanded coats of latex paint provided a smooth surface for the models, adhered the fabric to the foam, ensuring transmission of the airloads without fabric puckering, and protected the foam from damage (Figure 13). The models were still delicate and the surface could be easily dented. Leading and trailing edges where the plate and foam met were sealed by this outer skin. Trailing edges had balsa inserts because the styrofoam could not be worked to a point without breakage. Due to the press of time, the Case 2 plate was not covered so the wind tunnel tests proceeded with the Case 1 and Case 3 models only. An uncovered composite plate with control surfaces weighed 10.2 lbs and a final covered model 13.75 lbs.

To reduce the bending stiffness associated with the material added to the plates, five equally-spaced chordwise slices were made in both the upper and lower wing surfaces. Slices were made along the aerodynamic chords rather than structural chords (perpendicular to the elastic axis or mid-chord line) for the purpose of smooth air flow. It was not felt that this slight rotation from the optimal structural orientation would reduce the effectiveness of the slices. These slices were made down to the plate surface with an approximately 3/8 inch wide gap being created. This gap was then filled with a soft foam rubber to the surface of the wing. The Dacron fabric covered this foam rubber but was slit to allow for deformation to occur at the slices. The gap between the main wing model and the control surfaces were covered with tape.

To determine the optimum number of these slices to be made, a test specimen was prepared using scrap material from the wing composite

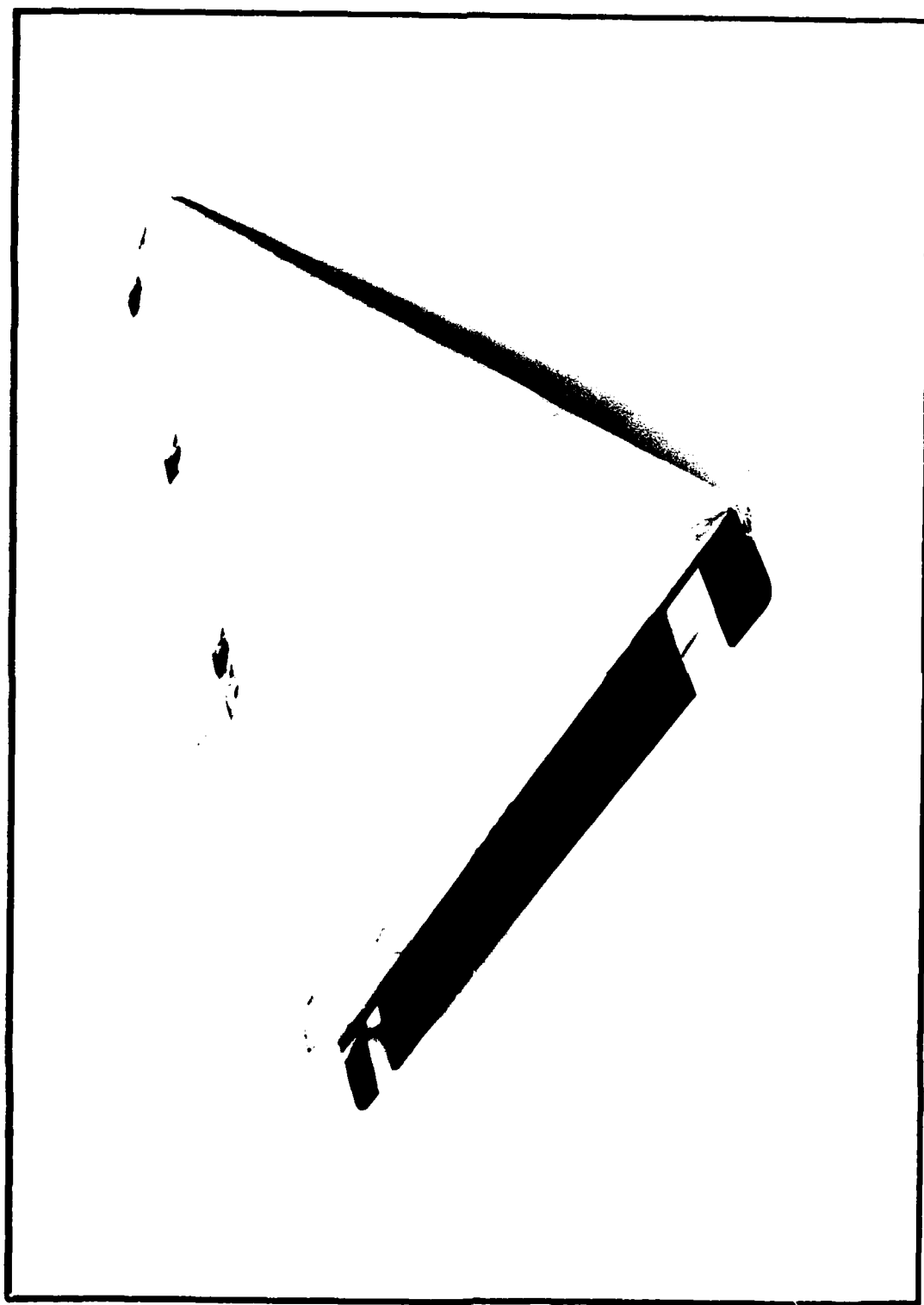


Figure 13. Wing Model

plate. This specimen was 12 inches wide and 36 inches long and had the 90 degree plies along the 36 inch dimension. This specimen was subjected to an incrementally increasing bending load of 0-10 kg applied at the tip. The plate was then covered with the an elliptical airfoil shape and covering material as used for the models. The paint treatment for the fabric was not done, this being decided upon only after the specimen testing. The loading was then repeated and the tip deflection measured. This procedure was repeated several times with more slices made in the plate each time in an attempt to find the minimum number of slices that provided a bending deflection that most closely matched that of the strip without covering (see Figure 14). Only very slight stiffening of the specimen with the addition of the covering material was seen, amounting to only 4% with considerable scatter in the deflection data as slices were introduced. In light of these results and the unknown stiffening to be added with the paint treatment, an average of 5 slices was selected for the tunnel models.

Instrumentation

A bifurcated model mount and loads balance was constructed utilizing four uniaxial strain gages, two for each side of the two mounting arms for redundancy and averaging of measured loads (see Figure 15). Thw bifurcated nature of the balance permitted a more durable mount and measurement of the resultant normal wing lift even under a twisting couple. The dimensions and material of the cantilever balance arms were dictated by the predicted maximum load on the wing. A calibration of the balance was performed by placing the mount horizontal and hanging dead weights in turn on each arm. The procedure was

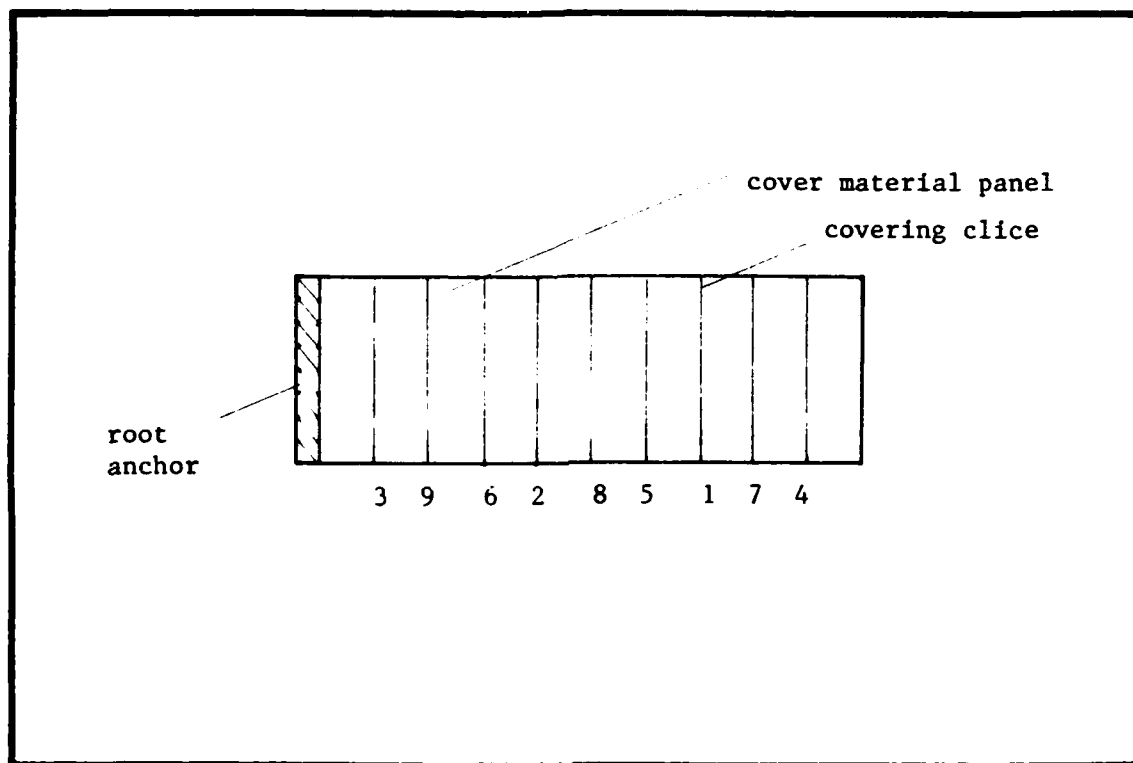


Figure 14. Test Plate Slicing Sequence

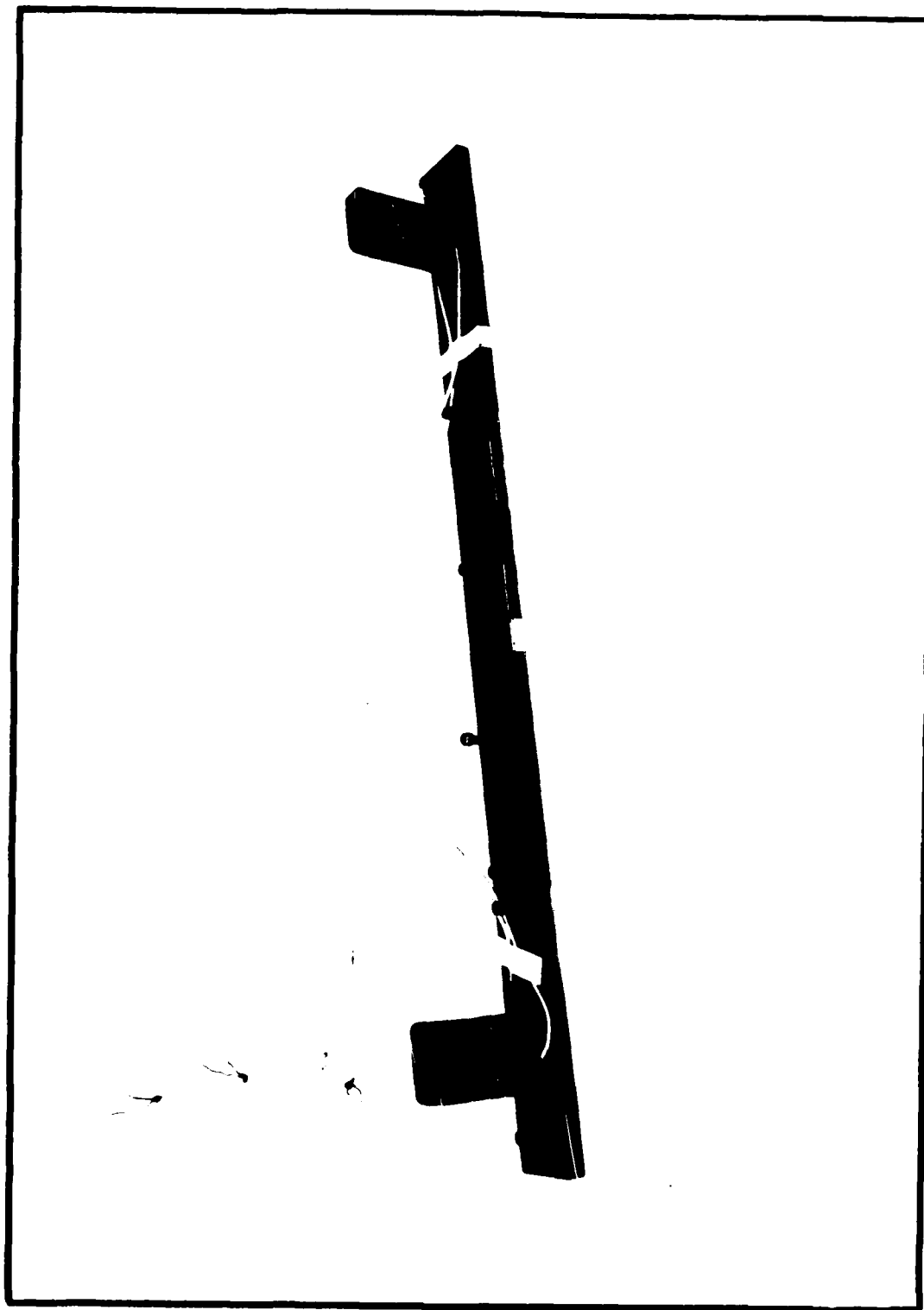


Figure 15. Strain Gage Balance

repeated with the balance reversed. The wing normal lift force was the only means of measuring control effectiveness. During the wind tunnel tests only strain was used as a measure of the lift force and the calibration used to permit an order-of-magnitude comparison with analytically predicted loads. No corrections were made to this lift, assuming all errors effected each model and configuration identically.

As a precaution in case of divergence or flutter, each wing model was tethered within the tunnel with two parachute line bungee chords attached at the wing tip and anchored to the tunnel wall, (Figure 12) and with lengths restricting the model from striking the tunnel wall.

Wind Tunnel Installation

Each model was suspended from the ceiling of the Air Force Institute of Technology (AFIT) 5-foot subsonic wind tunnel by the bifurcated strain gage balance to measure the lift force on the wing. The balance was mounted to a 1/2 inch thick aluminum plate that abutted the walls of the tunnel and the combination held in place by four bolts. The balance was secured to this plate by six bolts screwed into tapped steel bushings press-fit into the plate and installed in arcs to permit varied orientation of the balance. The bolt opposite the wing midchord axis served as a pivot, passing into a bearing assembly mounted within a tunnel hatch opposite. This balance was fastened to a flange, which was an integral part of the wing plate (Figure 13), by top and bottom metal strips that ran the full length of the root chord. These strips served to distribute root stress concentrations and avoid potential plate fracture (Figure 16). Gasket material between the plate and strips served to avoid crushing the composite plate by over-torquing of the

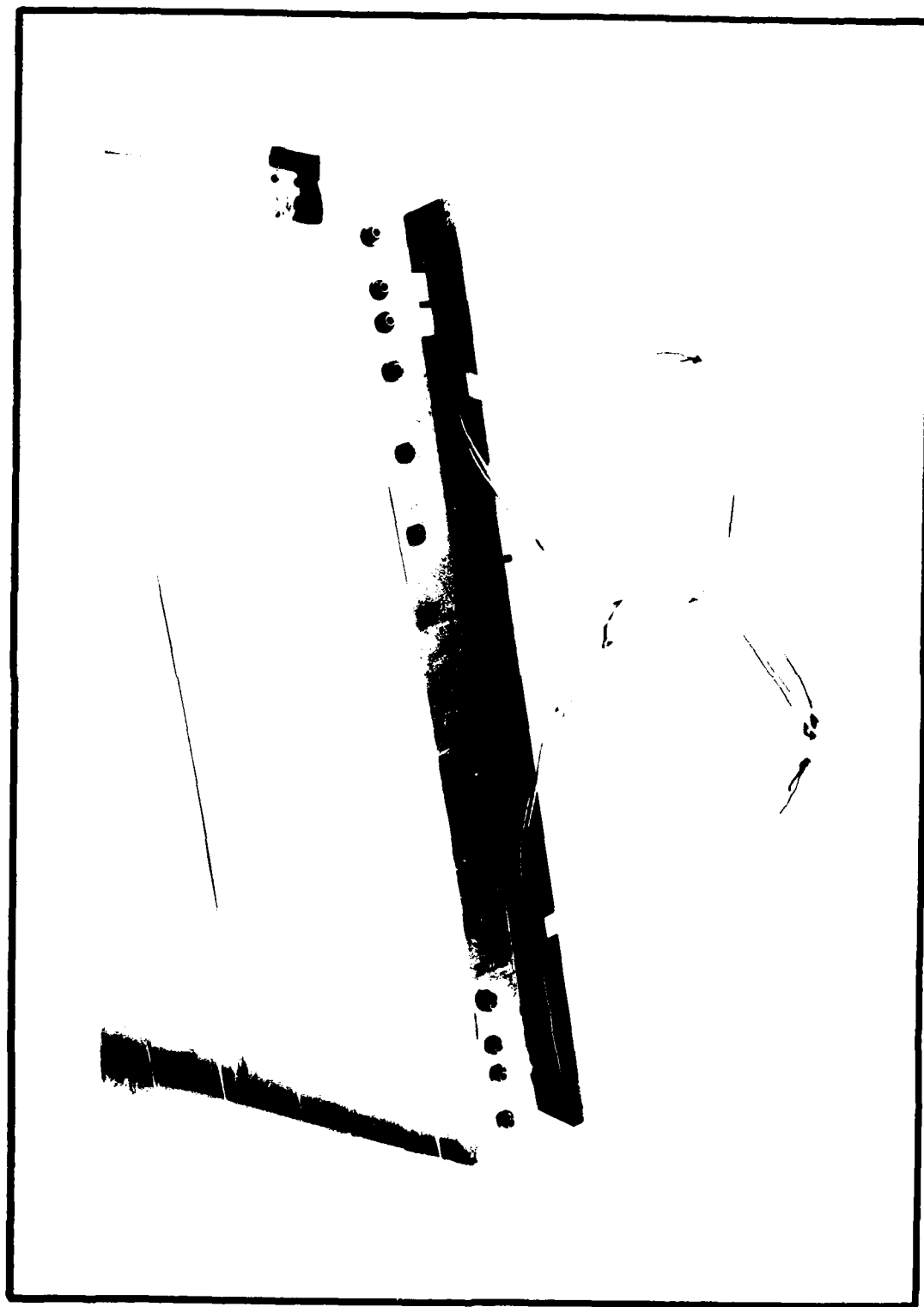


Figure 16. Model Root Mounting Fixture and Loads Balance

attachment bolts. Great rigidity was sought in the model attachment strips and the ceiling plate to ensure that as much of the lift-produced bending moment was concentrated in the balance arms as possible.

It was intended that the entire mounting assembly be covered by a foam and fiberglass fairing to avoid having it adversely influence the spanwise pressure distribution on the wing (Figure 17). However, no method could be found to simply and quickly attach this fairing to the wing with sufficient rigidity to avoid distortion or violent flapping during tunnel runs. The fairing was therefore eliminated. A ramp to improve flow around the tunnel installation was also fabricated for installation at the forward end of the ceiling plate with duct tape (Figure 18).

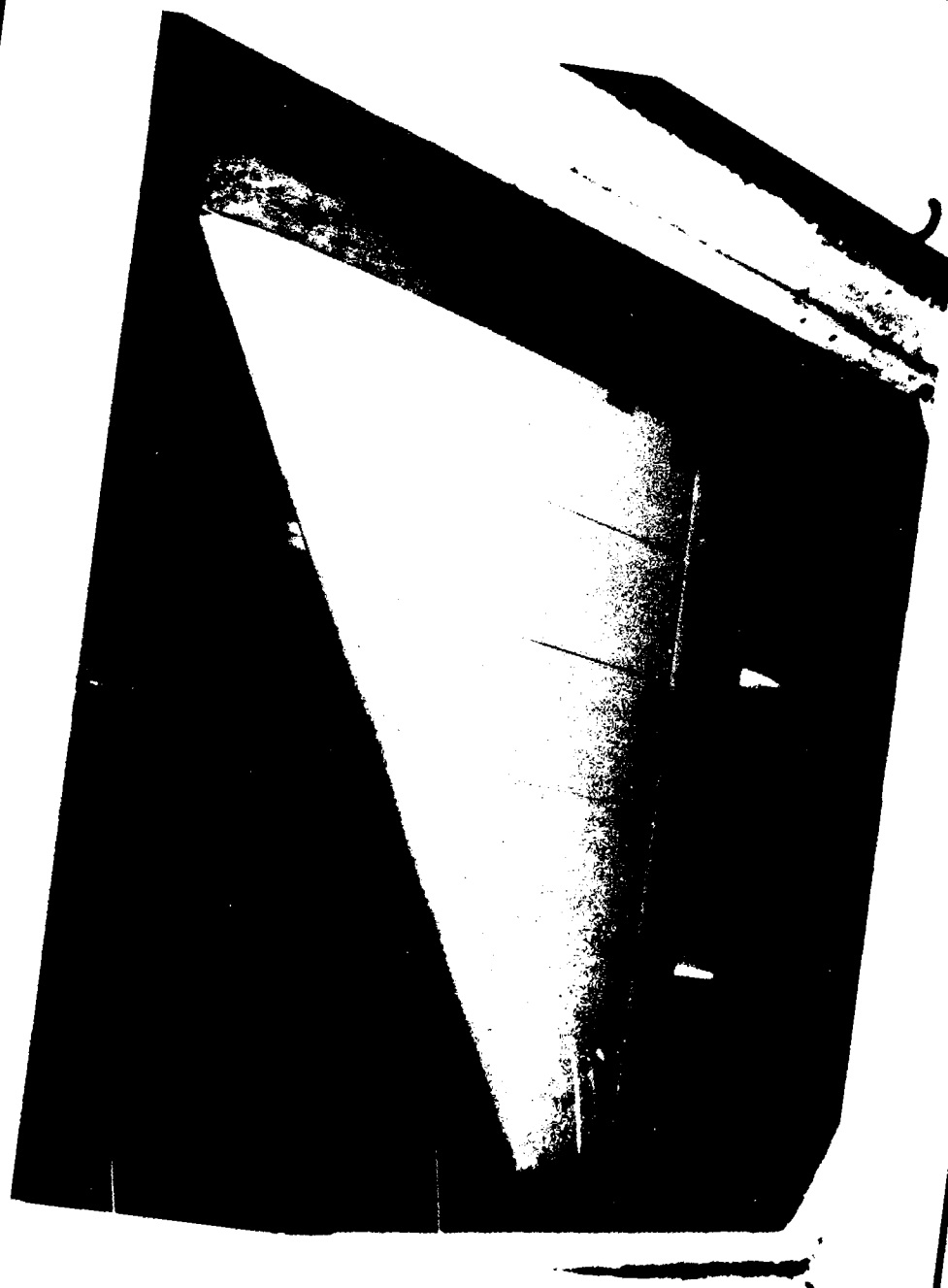


Figure 17. Tunnel Installation and Root Fairing

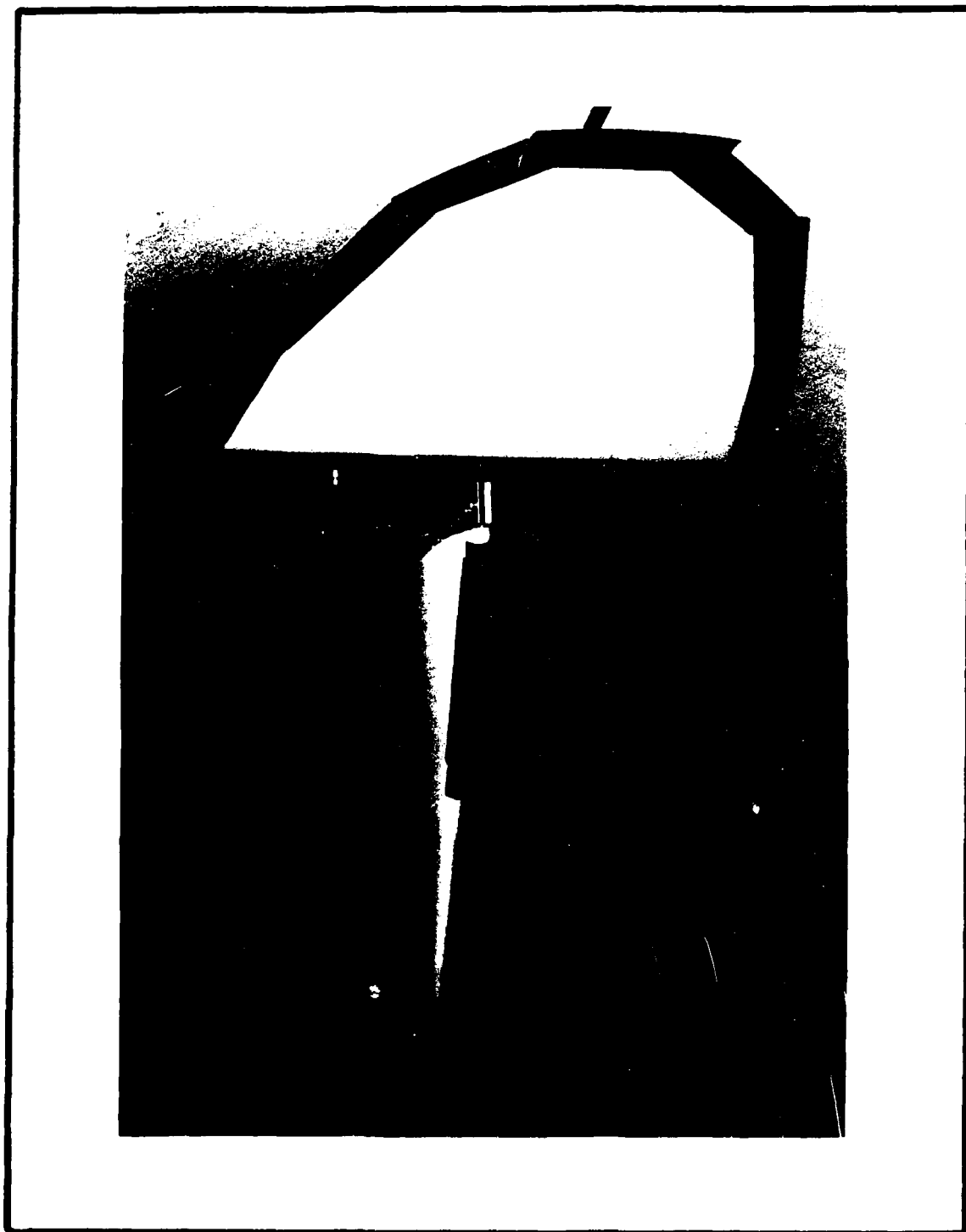


Figure 18. Lead Tape Application and Ramp

VI. Experimental Procedure

Data Collection

Balance strain gage data was read as micro-strain using a balance-indicator unit. These readings were normalized to the strain read at the maximum speed attained with the wing model mounted at the test angle of attack with no control surface deflection. The true lift force on the wing was not required for data reduction. Atmospheric and wind tunnel parameters were available from standard apparatus on the site for calculation of true tunnel airspeed from the equivalent airspeed provided by static pressure taps in the tunnel walls.

A video camera was used to record model deformation through a port below and slightly downstream of the test section and a port in the side of the test section.

Wind Tunnel Corrections

Corrections to the wind tunnel data for tunnel effects were limited to those that influenced lift force measurements only and to those that would effect the validity of tunnel velocity readings. The true lift force on the wing was not critical, only the magnitude of change in the lift curves between each wing configuration. Using this criteria, only solid blockage effects were felt to be significant. Rae and Pope (12:365) provide a simple means for calculating the tunnel velocity solid blockage correction, e_{sb} , that is

$$e_{sb} = KV_m/CA^{3/2} \quad (140)$$

where $K = 0.9$ for a three dimensional wing model, C is the test section cross-sectional area, and V_m is the model volume. For the five foot diameter tunnel and an estimated model volume of 0.95 cubic feet, the solid blockage correction is 4.4%. The corrected tunnel velocity (V_c) is then simply

$$V_c = V + 0.044V \quad (141)$$

Ground Vibration Test

Flutter clearance for the wind tunnel models was accomplished using the CWINGF computer code (18). To validate the frequencies produced in the flutter analysis of the wind tunnel models, a ground vibration test (GVT) is necessary. For the low speeds produced in this experiment, only the first four to five modes were of interest. Limited frequency data was collected on the flat plates prior to covering. Details of this experiment are presented in Appendix C.

Testing Scheme

The Case 3 model was tested first in the wind tunnel followed by the Case 1 model. Tests were performed at 0 and 5 deg angles of attack and 0, 5, and 10 deg deflection angles of the three lateral control surfaces (see Table VII). Controls were always deflected in the same sense as the AOA to produce positive camber.

Each model at each angle-of-attack was initially run with zero control deflection from zero tunnel velocity to 160 mph equivalent airspeed. This velocity sweep produced a lift curve when the balance-measured strains were plotted against the corrected tunnel velocities. Sweeps were made with pauses each 5-10 psf of dynamic pressure to record

TABLE VII
Testing Schedule

velocity sweeps 0 - 160 mph at each condition

Case	AOA (deg)	control deflections (deg)	
1	0	flap	0, 5, 10
		aileron	" "
		flaperon	" "
	5	flap	0, 5, 10
		aileron	" "
		flaperon	" "
	10	flap	0, 5, 10
		aileron	" "
		flaperon	" "
2	-	not run	
3	0	flap	0, 5, 10
		aileron	" "
		flaperon	" "
	5	flap	0, 5, 10
		aileron	" "
		flaperon	" "
	10	flap	0, 5, 10
		aileron	" "
		flaperon	" "

data. During these pauses an excitation was applied by tugging on a wire attached to the tip of the wing. This was intended to excite any flutter modes present at that speed or to observe the degree of damping present. Velocity sweeps were then repeated with controls deflected and this data plotted against the zero-deflection lift curve for the same angle of attack. Reversal speed was determined at the speed at where the control-deflected curve crossed the zero-deflection lift curve. Incrementally higher control deflections were run to verify this speed, however flow separation was expected to cause a slight offset at the reversal point.

VII. Results and Discussion

Static Analysis

Windtunnel test results are presented in Figures 19-24 and in Table VIII. Velocities shown are subject to an error of plus or minus 2 mph. Success was obtained in producing well defined lift curves for the wing at zero AOA and control deflections up to 10 deg. The non-zero lift curves at zero AOA and neutral controls is attributed to a slight rotation of the model from the tunnel centerline due to a small tolerance error in construction of the installation.

Figure 22-23 show that at 5 deg AOA little additional lift was produced for the Case 1 wing with the deflection of the control surfaces. The pronounced rounding of these curves suggest that flow separation and a near-stall condition may have occurred. The flaperon at 10 deg deflection test conditions was tested again with tufts on the wing to assist in flow visualization. This test indicated that regions of separated flow were occurring from $1/4$ to $1/2$ the chord of the wing in the outer half of the span. Flow appeared to re-attach after the $1/2$ chord line and stay attached over the control surfaces. Due to this condition, the 5 deg AOA test points were not repeated with the wind tunnel model.

Tip deflections were approximated visually by sighting through the port in the bottom of the tunnel. Deflections at the tip were up to 1 inch from neutral and up to 8 deg of twist for the 10 deg deflection case. The twisting increased with the deflection.

AD-A188 855

DESIGN OF AN AEROELASTIC COMPOSITE WING WIND TUNNEL
MODEL(U) AIR FORCE INST OF TECH WRIGHT-PATTERSON AFB OH
SCHOOL OF ENGINEERING W J NORTON DEC 87

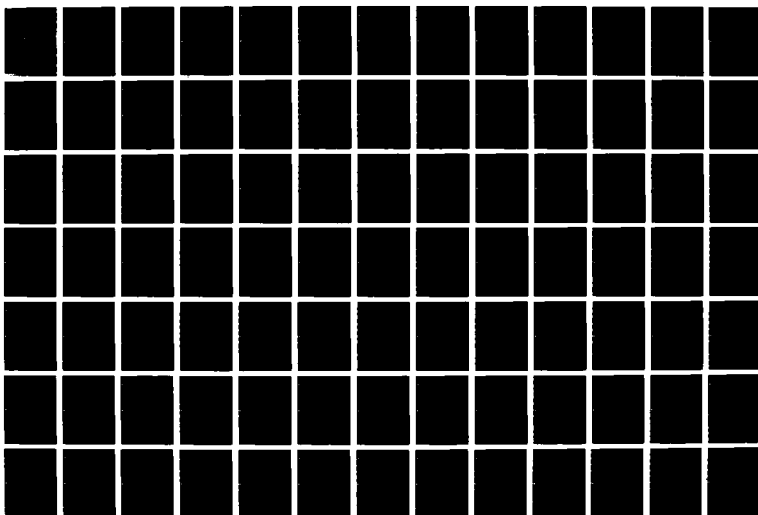
2/3

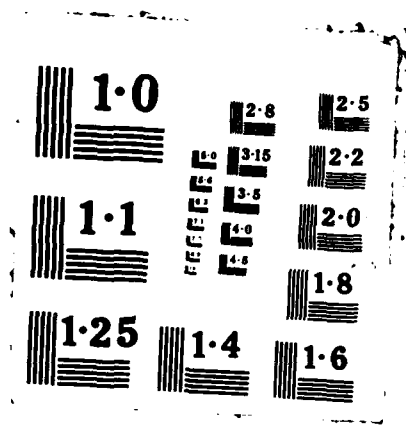
UNCLASSIFIED

AFIT/GAE/AA/87D-15

F/G 1/3

NL





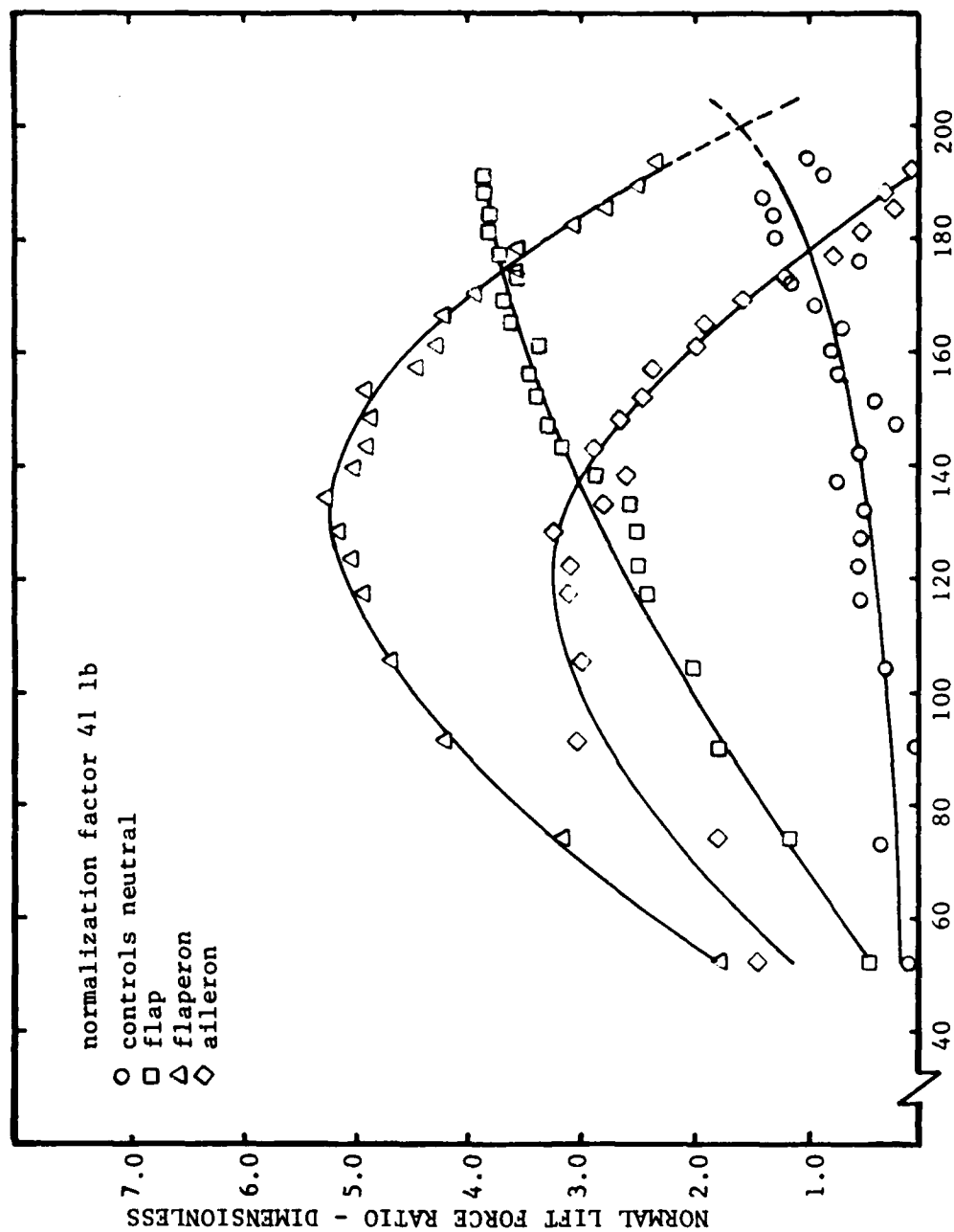


Figure 19. Case 3 Lift Curves - 0° AOA and 5° δ

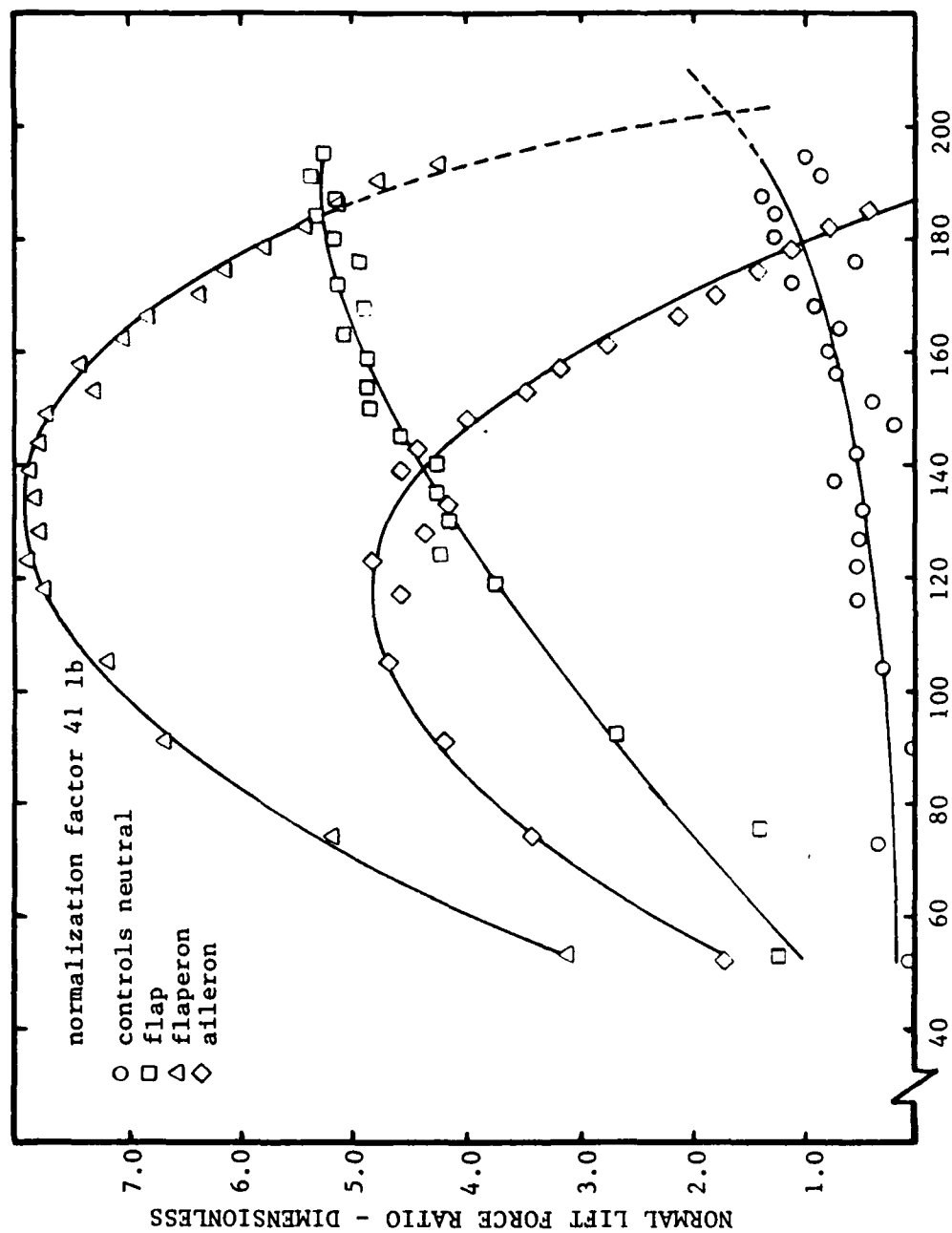


Figure 20. Case 3 Lift Curves - 0° AOA and 10° δ

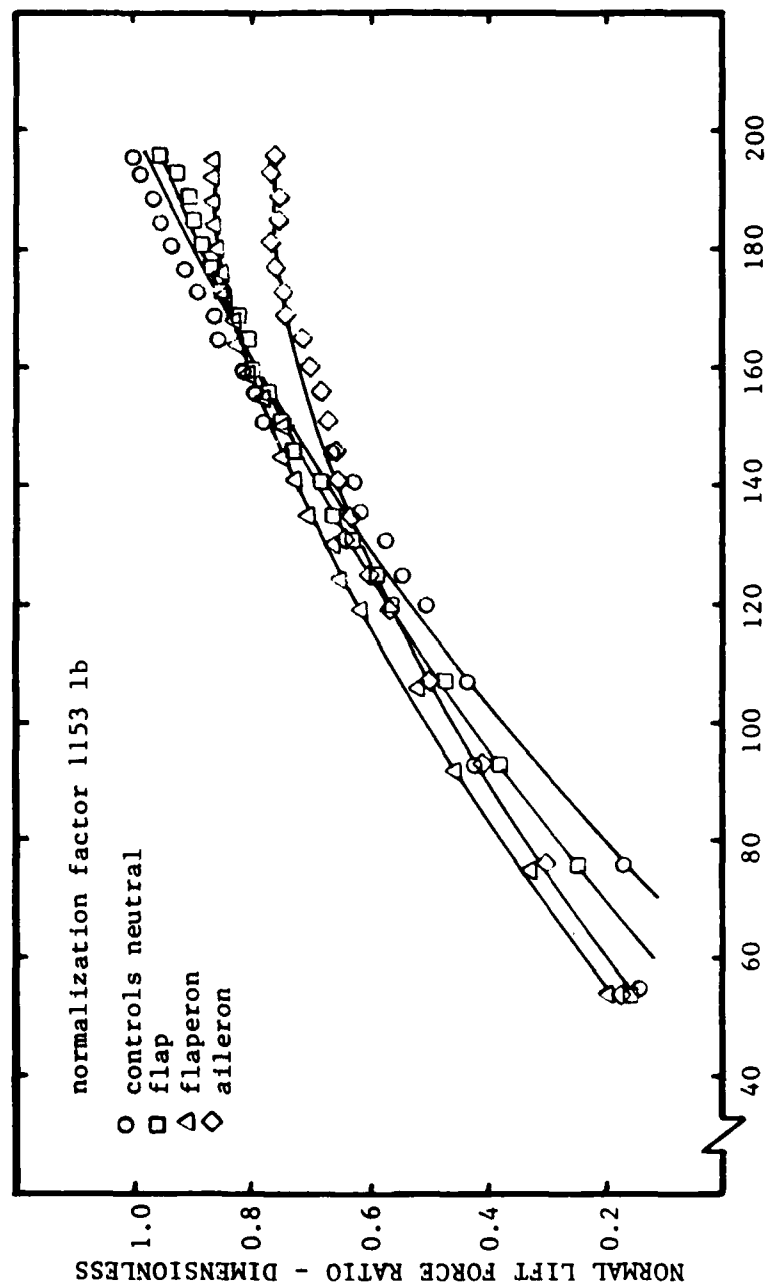


Figure 21. Case 3 Lift Curves - 5° AOA and 5° δ

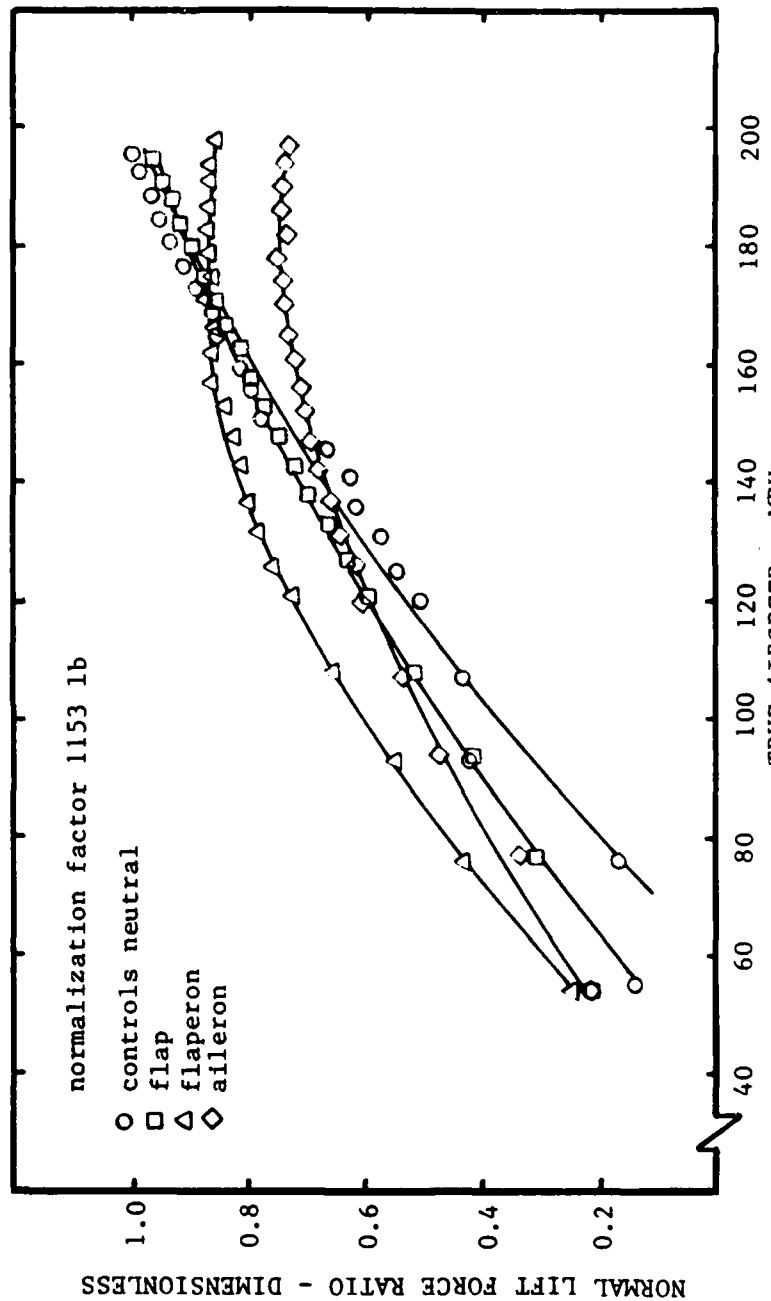


Figure 22. Case 3 Lift Curves - 5° AOA and $10^\circ \delta$

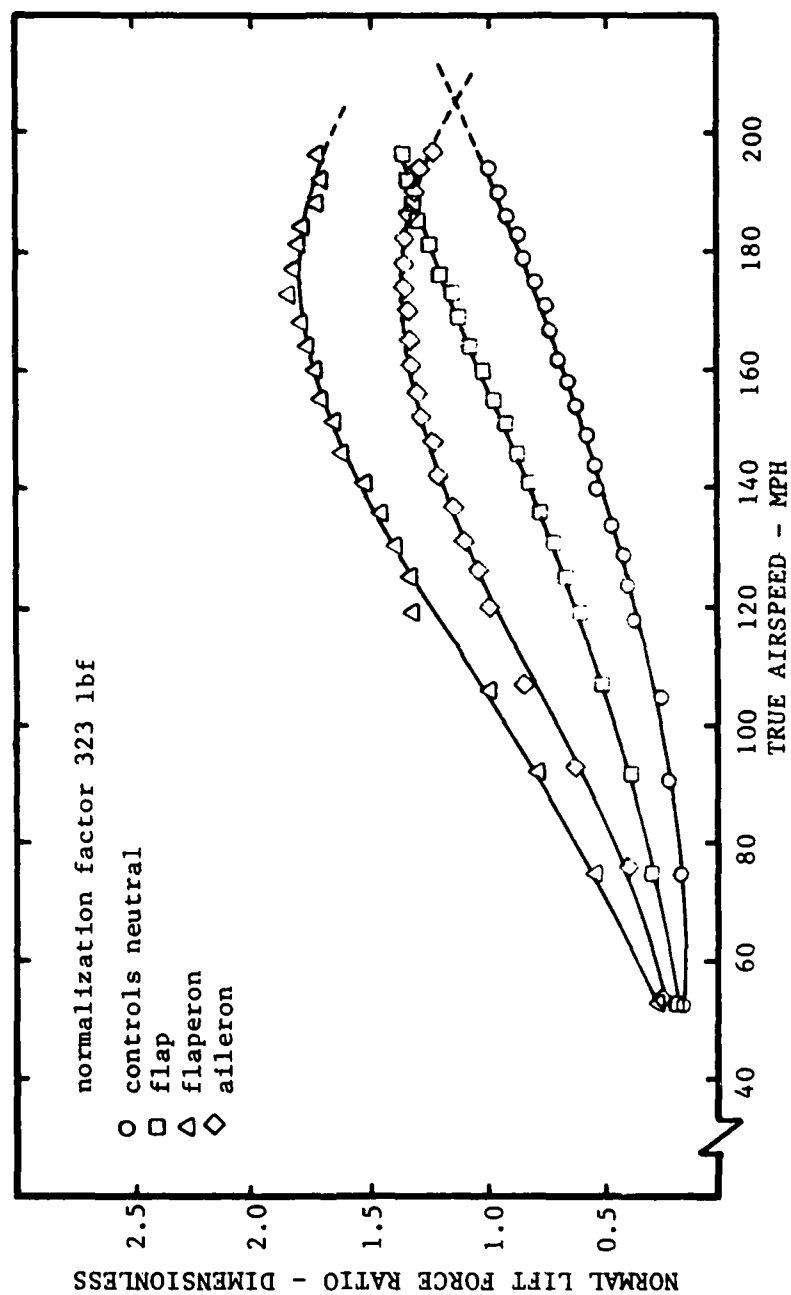


Figure 23. Case 1 Lift Curves - 0° AOA and 5° δ

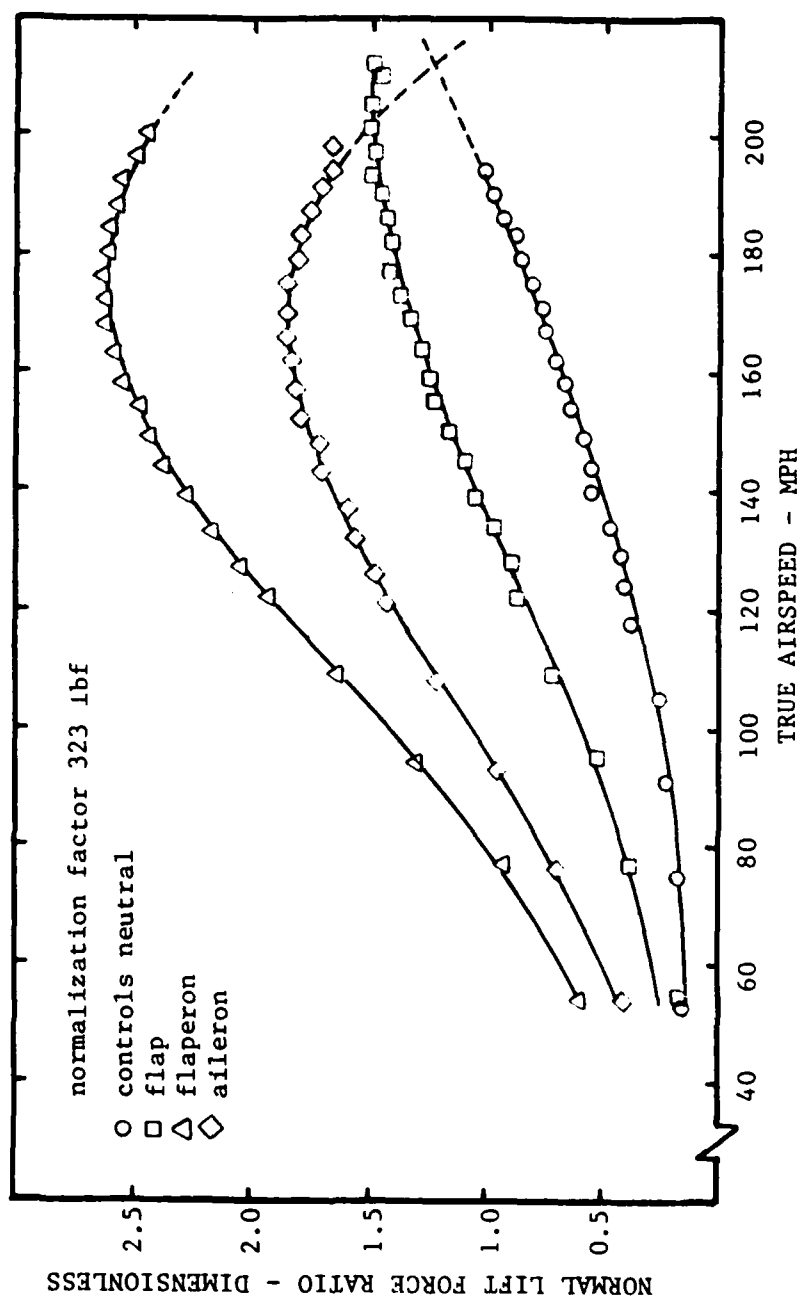


Figure 24. Case 1 Lift Curves - 0° AOA and 10° δ

Table IX
Results Comparison

(all speeds mph)

Control Configuration	Case	V_R	
		Predicted	Measured
Aileron	1	118	208
	2	111	-
	3	108	179
Flaperon	1	109	> 220
	2	104	-
	3	103	201
Flap	1	89	> 230
	2	86	-
	3	92	> 240

deg control deflections. The 5 deg AOA tests produced bending up to 16 inches and twist up to 8 deg at the 5 deg control deflection condition, and up to 20 inches of deflection and 20 deg of torsion for the 10 deg deflection case. Most of the deformation occurred within the first 75 mph. Test normal lift forces measured by the balance may be obtained by use of the normalization factor provided on the lift curve figures. No effort was made to correct these lifts for tunnel effects or other losses.

Tests at 10 deg AOA produced tip bending on the order of 24 inches. This proved to be too severe for the foam adhesive and debonding was experienced. Loads on the order of 1600 pounds on the model were measured, with loads on the individual beam arms exceeding those for which they were calibrated prior to the tunnel tests. Due to these extreme deformations and the unreliability of the strain-to-load conversions, no further tests were conducted at 10 deg AOA.

Reversals occurred as reason would dictate with the tip control surface (aileron) reversing at lower airspeeds than the flaperon, and the flaperon reversing at lower speeds than the root control surface (flap). This is the opposite of the predicted results given in Figure 11 and Table VIII. Further investigation of these results are reproduced in Table IX. The phenomenon is not a result of using composites, but is rather a planform effect. Only the straight wings showed the expected trend of reversal speed increasing as the aileron was moved inboard. Predicted reversal speeds and the differences between them for each case were the same order of magnitude as those shown experimentally and showed the same trend with forward rotation of the laminate. The cause

TABLE IX

Reversal Investigation

(Layup 1, Case 1, 6 panel control surface, 1000 ft PA)

(all speeds MPH)

Planform	V_D	Aileron Position		
		Root	Midspan	Tip
	V_D	V_R	V_R	V_R
swept, tapered	161	97	107	118
swept, tapered (metal)	156	83	94	106
unswept, tapered	122	95	106	121
unswept, straight	97	87	86	81
swept, straight	118	89	86	79

aileron span and wing area constant for all cases

of this error is believed to lie in the nature of the structural influence formulations.

The data indicates that the Case 1 control surfaces reverse at higher airspeeds than Case 3 surfaces. This is not what one would expect because the Case 1 laminate is assumed to be less torsionally stiff since fewer of its fibers are rotated ahead of the elastic axis. Examining the example static analysis results provided in Appendix B shows that the EI parameter for Case 1 is greater than that for Case 3 and the GJ parameter is less than Case 3. However, the bending-torsion coupling parameter K is the most telling for such predictions. This enforces the conclusion that it is difficult to predict composite wing behavior intuitively.

While the error in predicting the static characteristics of the wing are probably due to the analysis method employed, other sources of error are present. Analysis sensitivity to common minor variations in the material properties of the composite is a source of prediction error. Another contributor is the added stiffness of the model covering. Other sources of error may be possible roll-up of the control surfaces and small bending of the attachment brackets. Differing flow separation from the individual model configurations also introduces error. The large model deflections under load may violate the assumption of small deflections to the extent of invalidating the linearized equations.

The COMPSTAT listing and input guide provided in Appendix B permits the separation of the structural box beam portion of the wing from the aerodynamic planform, the later including control surfaces which add

only negligibly to the structural characteristics of the wing. This option was used for the final calculation of the predicted characteristics compared with tunnel results but is not reflected in other predictions presented elsewhere in this thesis. Comparisons with these other predictions indicated that the separation of the two planforms will change divergence and reversal speeds from 4-9%, generally reducing the latter.

Divergence of the Case 1 model was predicted to occur at 174 mph. The model was tested up to 212 mph true airspeed with no divergence evident. Divergence calculations have been common for several decades and failure to predict this event is a fundamental failure of the methods used. This again points to the possible use of an inappropriate structural model.

Examples of other results produced by the static analysis are provided in Appendix B. Some of these results also appear to be suspect. Many of the lift curve slopes computed are very high and the torsional deformations much lower than those observed in the wind tunnel and in one case showing a leading edge up deflection.

Dynamic Analysis

As a means of verifying the predicted elasticity of the composite plates and as a tunnel fit check, the Case 2 bare plate was installed in the tunnel at zero degrees angle-of-attack, flap at zero degrees deflection, and aileron at 10 degrees deflection, prior to productive covered model testing. Excitation was made by pulling on a length of safety wire tied to the outboard aileron attachment bracket and then releasing it.

About 4 overshoots of the tip in response to the excitation was seen initially. This reduced to a deadbeat response at 100 mph. Beginning at about 80 mph, a slight tremor at the tip of the model became evident, attributed to tunnel turbulence. As the tunnel velocity was increased to 110 mph equivalent airspeed the wing plate fluttered violently, with bending as much as 24 inches either side of centerline. No damage was done to the tunnel, mount, or the model.

The flutter was later repeated with neutral controls and the flutter was sustained at approximately 4 inches of tip deflection either side of neutral beginning at approximately 85 mph equivalent airspeed. By painting the edge of the plate white and using a strobe lamp, the bending frequency was determined to be 10.0 Hz. A grid pattern chalked onto the plate assisted in visualizing the flutter mode (see Figure 25).

This test demonstrated that the composite plate could deform under airloads to the extent that control reversal was likely. The flutter event served as a caution for further testing but did not establish a flutter speed as the actual final test conditions with the covered models were not the same.

During the initial wind tunnel velocity sweep of the Case 3 model with foam airfoil covering at zero degrees AOA and zero control deflections, a flutter was experienced at approximately 101-103 mph equivalent airspeed. Unlike the flat plate flutter, this oscillation was characterized by a tip deflection of only 2-3 inches each side of neutral. The flutter mode appeared to be dominated by bending with some torsional deformation. This may indicate that the foam supplies additional damping.

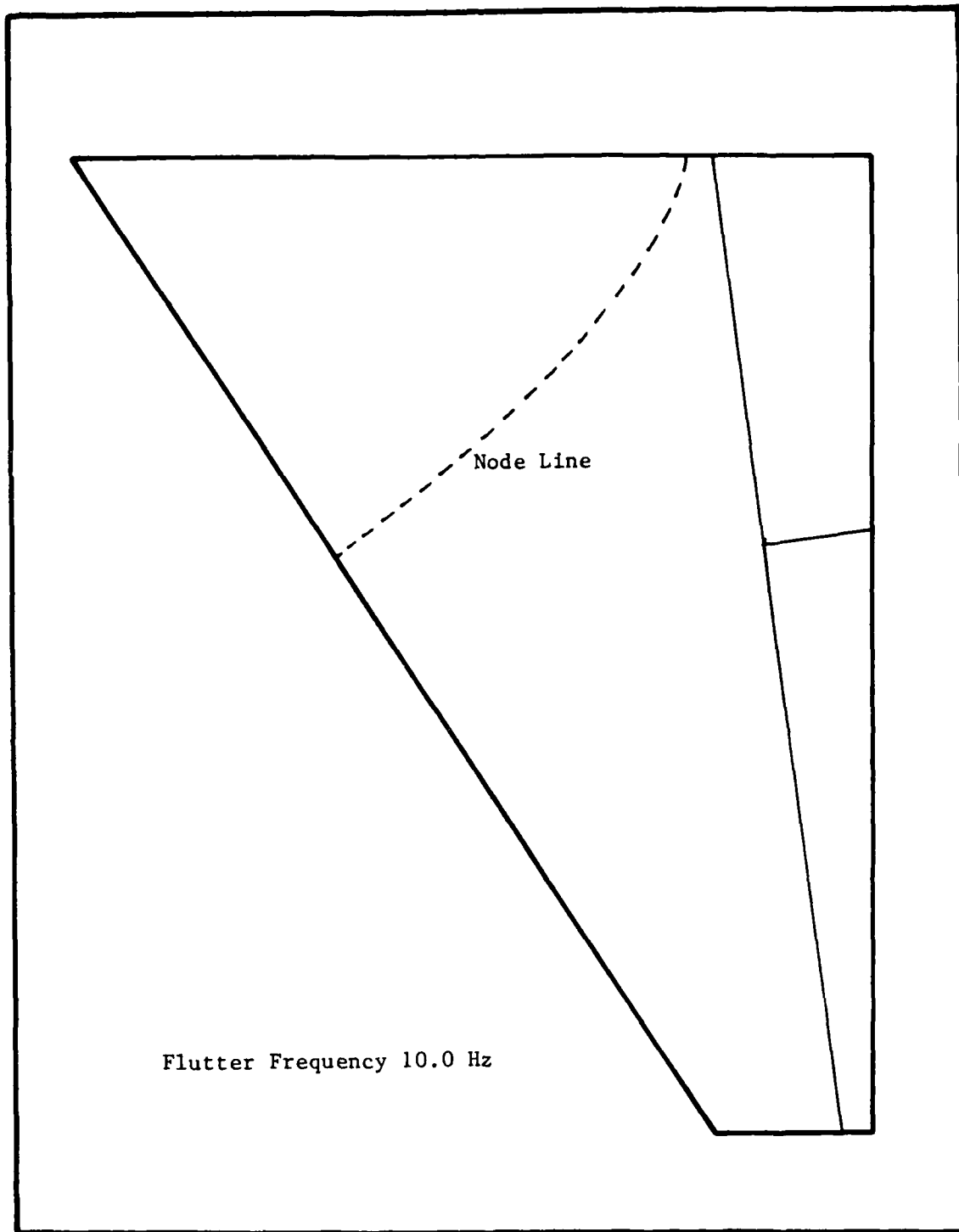


Figure 25. Case 2 Plate Flutter Mode

These unanticipated flutter events (the test envelope having been cleared with CWINGF) required remedy before productive testing could be accomplished. From examination of the GVT modal results (Appendix C) indicates that the flutter mode occurred by a coupling of the first torsion and second bending modes. These modes have very close frequencies. The flutter mode shown in Figure 25 supports this conclusion although the frequency measured with the stobe does not. To separate these frequencies, a relatively the easy solution is to attach additional mass near the leading edge of the model. This biases the center of gravity forward of the elastic axis. This tends to reduce the torsional frequency. Adding tip mass would reduce the bending frequency and only move the modes closer together.

To adjust the mass distribution, 1.0 lbs of lead tape, 1/10 of the plate weight, was fixed to the leading edge of the wing laid in the spanwise direction (Figure 18). The tape was tapered between the 10% and 35% chord lines. This raised the flutter speed to approximately 170-172 mph equivalent airspeed where flutter was again encountered. This speed was satisfactory to allow productive testing. The flutter was easily stopped with the excitation wire before the magnitude of the oscillations exceeded 8-9 inches either side of neutral. All subsequent tests were limited to 160 mph equivalent airspeed to avoid this flutter.

The Case 3 model was tested prior to the Case 1 wing. The lead tape treatment was applied to the Case 1 model prior to any unaltered flutter investigation, and then subjected to the same speed constraints as the Case 1 model in order to avoid damaging the model prior to collection of the necessary static data. When all static data had been collected, the

flutter speed of the Case 1 model with the lead tape treatment was found to be approximately 175 mph equivalent airspeed. Near this speed damping was extremely light with the final flutter oscillation excited with the wire. Turbulence alone was insufficient to excite the flutter. The test was performed with the flap at 10 deg and the aileron at 0 deg deflection. The flutter speed of the Case 1 model without the tape was beyond 175 mph but could not be determined due to the speed limit of the wind tunnel.

The flutter of the wing models appears to involve control surface interactions. Flutter of the flat plate showed heavy flaperon motion. It is possible that attachment plate deformation, composite deformation around the attachments, and deformation of the control surfaces themselves are contributors if not the primary source of the flutter.

The covered models produced the same response to turbulence as described for the flat plate.

Optimization

Examples of the form of the objective function and constraints are presented with optimization results in Table X. It is immediately evident that ADS will disregard symmetry of the ply orientations about the midplane of the plate. This may be enforced by proper selection of design variables. However, ADS often rotated the plies only a few degrees from the starting layup that had to be supplied which was symmetric. Occasionally only a few layers were changed in the input layup. As a consequence of these factors, a nearly symmetric layup may result. As with any optimization method, the risk exists that only a local minimum will be found, as demonstrated in Table XA. ADS is

Table XA

Example Optimization Results

attempting to match results of Case 1
with layup for Case 3 ailerons (see Table VI)
(all speeds mph)

Initial Layup	Final Layup
110.00	75.39
110.00	72.56
110.00	70.33
110.00	69.13
110.00	69.55
110.00	70.55
110.00	76.99
110.00	84.37
65.00	68.35
155.00	168.52
65.00	66.14
155.00	179.97
65.00	173.71
155.00	38.23
65.00	176.41
155.00	2.48
155.00	2.65
65.00	174.70
155.00	0.00
65.00	179.70
155.00	166.68
65.00	69.32
155.00	160.10
65.00	69.32
110.00	106.37
110.00	106.79
110.00	107.10
110.00	107.87
110.00	108.23
110.00	109.24
110.00	108.79
110.00	109.54

Objective: $V_R = 118.0$

Constraints: $1.2V_R \leq V_D$
 $V_D \leq 175$

Results: $V_R = 125$
 $V_D = 161$

Was Seeking: $V_R = 118$
 $V_D = 161$

Comments: Case 1 results would have
been achieved by rotating plies aft
20 deg. Failed to find optimum.

8 Iterations
214 Function Evaluations

Example Optimization Results

Initial Layup	Final Layup
1	1
2	2
3	3
4	4
5	5
6	6
7	7
8	8
9	9
10	10
11	11
12	12
13	13
14	14
15	15
16	16
17	17
18	18
19	19
20	20
21	21
22	22
23	23
24	24
25	25
26	26
27	27
28	28
29	29
30	30
31	31
32	32
33	33
34	34
35	35
36	36
37	37
38	38
39	39
40	40
41	41
42	42
43	43
44	44
45	45
46	46
47	47
48	48
49	49
50	50
51	51
52	52
53	53
54	54
55	55
56	56
57	57
58	58
59	59
60	60
61	61
62	62
63	63
64	64
65	65
66	66
67	67
68	68
69	69
70	70
71	71
72	72
73	73
74	74
75	75
76	76
77	77
78	78
79	79
80	80
81	81
82	82
83	83
84	84
85	85
86	86
87	87
88	88
89	89
90	90
91	91
92	92
93	93
94	94
95	95
96	96
97	97
98	98
99	99
100	100

```

Objective:      VR1 = 100

Constraints:    VR1 + 10 ≤ VR2
                VR2 + 10 ≤ VR3
                1.2VR1 ≤ VD1
                1.2VR2 ≤ VD2
                1.2VR3 ≤ VD3
                VD1 ≤ 175
                VD2 ≤ 175
                VD3 ≤ 175

Results:        VR1 = 109
                VR1 = 108
                VR3 = 108
                VD1 = 4102
                VD2 = 6158
                VD3 = 32002

```

1 Iterations
32 Function Evaluations

Table XC

Example Optimization Results

Single 24 Ply Case, Ailerons
(all speeds mph)

Initial Layup	Final Layup
110.00	97.98
110.00	104.20
110.00	107.83
110.00	67.65
110.00	74.13
110.00	78.23
65.00	0.23
155.00	179.98
65.00	165.85
155.00	179.96
65.00	179.95
155.00	146.08
155.00	137.33
65.00	179.47
155.00	179.96
65.00	163.44
155.00	179.97
65.00	1.17
110.00	75.02
110.00	70.61
110.00	72.34
110.00	82.91
110.00	97.76
110.00	106.83

Objective: $V_D = 175.0$

Constraints: $1.2V_R \leq V_D$
 $V_R \geq 25$
 $V_D \leq 175$

Results: $V_R = 86$
 $V_D = 173$

Comments: Superior to 32 ply case.
 V_D in objective and constraint
created no difficulty.

6 Iterations
254 Function Evaluations

Table XD

Example Optimization Results

24 Plies
3 Rotations of +10 deg, Ailerons,
(all speeds mph)

Initial Layup	Final Layup
------------------	----------------

110.00	103.93
110.00	106.30
110.00	107.81
110.00	110.82
110.00	111.07
110.00	111.54
65.00	73.12
155.00	163.72
65.00	85.33
155.00	163.73
65.00	105.15
155.00	100.87
155.00	100.89
65.00	105.15
155.00	163.73
65.00	85.33
155.00	163.73
65.00	72.13
110.00	111.32
110.00	111.07
110.00	110.81
110.00	103.62
110.00	104.77
110.00	105.63

Objective: $V_{D1} = 175$

Constraints: $V_{R1} - 10 \geq V_{R2}$
 $V_{R2} - 10 \geq V_{R3}$
 $1.2V_{R1} \leq V_{D1}$
 $1.2V_{R3} \leq V_{D2}$
 $1.2V_{R3} \leq V_{D3}$
 $V_{R1} \leq 25$
 $V_{R2} \leq 25$
 $V_{R3} \leq 25$
 $V_{D2} \leq 175$
 $V_{D3} \leq 175$

Results: $V_{R1} = 69$
 $V_{R2} = 74$
 $V_{R3} = 82$
 $V_{D1} = 1808$
 $V_{D2} = 210$
 $V_{D3} = 87$

Comments: Poor match to objective
and V_D constraints. Only minor
rotations from initial layup.

40 Iterations
147 Function Evaluations

Table XE

Example Optimization Results

24 Plies
3 Rotations of -10 deg, Ailerons,
(all speeds mph)

Initial Layup	Final Layup
------------------	----------------

110.00	168.34
110.00	81.51
110.00	11.24
110.00	57.78
110.00	165.18
110.00	69.65
65.00	8.29
155.00	0.02
65.00	16.32
155.00	158.46
65.00	168.78
155.00	18.36
155.00	12.14
65.00	11.92
155.00	173.97
65.00	5.99
155.00	30.65
65.00	8.79
110.00	9.79
110.00	169.24
110.00	50.35
110.00	174.92
110.00	172.39
110.00	173.42

Objective: $V_{D1} = 175$

Constraints: $V_{R1} + 10 \leq V_{R2}$
 $V_{R2} + 10 \leq V_{R3}$
 $1.2V_{R1} \leq V_{D1}$
 $1.2V_{R3} \leq V_{D2}$
 $1.2V_{R3} \leq V_{D3}$

Results: $V_{R1} = 90$
 $V_{R2} = 87$
 $V_{R3} = 96$
 $V_{D1} = 178$
 $V_{D2} = 106$
 $V_{D3} = 151$

Comments: Best results. Would have
made excellent cases for tunnel models.

30 Iterations
299 Function Evaluations

clearly sensitive to the choice of objective, constraints, and the initial values of the design variables. For this reason it is advisable to cast the problem in several forms to improve the chance of locating the global minimum.

COMPSTAT was designed as a program that would run quickly and thus entail little cost for computer resources. This makes these routines ideal for optimization studies. However, the addition of ADS considerably alters this feature. For the three rotation cases shown in Table X, as much as 45 seconds of processor time was required.

The use of automated design techniques as a minimization operation is shown to be practical. The risk of arriving at only a local minimum has been demonstrated, however considerable designer effort is eliminated for beneficial insight into trends. The results provided in Table III show that the wind tunnel models used in the test could have been built about a 24 ply laminate with better results than the 32 ply plates dictated by the need to limit variables for manual design iterations.

Several of the design parameters were used as the objective function. However, the most important aspects of the design lay in the constraints, and it was found that these were often given unknown weighting. This required casting the problem in slightly different forms of the objective and constraints to find the several minimums near the desired result. ADS added considerable computation time to the analysis.

After many optimizations it must be concluded that differences in reversal speeds of 10 mph or more cannot be achieved with moderate

laminate rotations of less than 20 deg for the tunnel speed range, planform, and composite used in this design. Designing a model to demonstrate both control reversal and divergence within the speeds dictated by the AFIT 5 ft tunnel was also extremely difficult, and found to be possible for only one of the three rotation cases. These limitations appear to present a critical obstacle to future efforts of the kind presented in this thesis.

Model Fabrication

Surface finish on the wind tunnel models were not as smooth as desired. The bond of the foam to the composite plate was not as dependable as required. Initial tunnel runs resulted in varying degrees of foam/plate separations. This problem was overcome with a combination of epoxy applied to the trailing edge of the foam and tape between foam gores and the control surfaces (also serving to deal this gap) applied in a manner that would add no stiffness to the model. Without this treatment the gores tended to migrate slightly on the plate under the varying bending and twisting conditions. However, the construction method has been demonstrated to be sound, adding very little stiffness to the laminate structure.

Instrumentation

The bifurcated strain gage balance was not as sensitive as desired. Measuring loads by this means also introduced undesired hysteresis, especially at the low end of the strain range.

Wind Tunnel Installation

The use of a fairing to cover the balance/mount fixture proved impractical as designed. The fairing was designed to be installed with tape alone and this was insufficient to restrain it under loads.

A ramp at the forward end of the tunnel attachment plate was used for one test only to see if it significantly influenced the lift curves. Results indicate that its benefits are negligible.

IX. Suggestions and Recommendations

Static Analysis

Considerable work remains in order to explain the difficulties discussed in the previous section and to remedy them. The use of other structural models for the computation of the stiffness matrix is the first logical step for such a task. A substitution of plate theory for the beam theory used in this thesis is recommended. The experimental results presented offer the necessary data for comparison and validation of any future analysis.

The prediction of bending deformation is recommended as an important addition to the coding provided. This would permit tunnel wall clearance checks and may influence model fabrication options. This would also permit the evaluation of the validity of the assumption of small deformations for equation linearization. A carefully conducted plate load/deformation test to verify predicted influence coefficients is also recommended for future investigation. A reliable method should be found for predicting the additional stiffness contributed by the model cover material and include it in the static analysis. Additionally, evaluation of the rigidity of the tunnel mounting system would allow possible changes to the boundary conditions of the analysis.

Only the minimum necessary data was obtained with the wind tunnel models owing to the press of time, and much remains that could be done with them. Employing a tunnel with a greater velocity range that would

permit the determination of the flap and flaperon reversal speeds and perhaps divergence speeds is recommended for future studies.

Dynamic Analysis

Future investigators must apply more effort to flutter prediction. This is often a complex and costly effort, however the simple, inexpensive methods applied in this thesis gave inadequate results. The use of more sophisticated codes to provide more than one answer to the problem is the desired approach. The addition of the dynamic characteristic of the tunnel mounting system to the analysis may improve the flutter computation.

Only a superficial GVT was performed on the composite plates. A GVT of the completed tunnel models is advised in an effort to determine the effect of the covering material on the dynamic characteristics of the structure. This data would then be available for future dynamic analyses.

The models provide an ideal flutter investigation tool with the potential for much data to be collected from them. The use of a full flutter data collection system will provide information that can then be used to validate dynamic analysis results. By placing strain gages on the composite plates, deformed shape data can be collected in an effort to determine the true nature of the flutter phenomenon experienced during the wind tunnel tests.

Optimization

Further ADS runs can be made with a modified COMPSTAT to provide more flexibility in design variable and bounds. Many more design

variables may be added to the optimization. Iteration on the number of plies would save much time and effort. Other ADS optimization methods can be investigated to see which provides the best minimization for the nature of the design problem. Changing the weighting of the constraints may also assist in improving the minimization.

Model Fabrication

While the fabrication techniques demonstrated in the test effort were largely successful, the difficulties explained in the last section illustrate the need for more investigation in this area. Time spent in experimenting with different foams, adhesives, and skin materials is recommended with the need for low stiffness to be paramount. Every effort should be made to ensure high workability, smooth surface finish, and a durable model.

In the future, care should be taken in selection of the model wing section to avoid the flow separation problem encountered in this test. Section thickness, leading edge radius, and stall characteristics should be considered in this selection. As it is possible that the control surface attachment method may have permitted enough surface deflection to influence or even cause the flutter, other methods should be investigated. It is important that any method not add appreciable stiffness to the model.

Instrumentation

A more sensitive balance coupled to automated data collection and reduction equipment would significantly improve this aspect of the test. The sensitivity of the balance can be improved by milling the attachment

bars to create a thinner neck to which new strain gages can be attached. Calibration by a means that would permit higher loads while retaining the required accuracies would permit future tests to be run to higher angles of attack where greater normal wing loads will occur. A means for measuring tip bending and torsional deflections at the wing tip at a minimum would be a useful addition to the instrumentation package.

Wind Tunnel Installation

It is highly recommended that future research with the equipment constructed for this thesis research include a root fairing to cover the balance and mount. This is common testing practice. To do this, a fairing rigid enough to withstand airloads but adding nothing to the stiffness of the mount must be designed. The use of the ramp (Figure 18) is also advisable to reduce tunnel blockage.

Appendix A: Aeroelastic Subroutines

The analysis methods presented in this thesis have been used in the preparation of a family of mutually interactive aeroelastic subroutines that may be used in operator fashion. Many of the subroutines have been adapted from the Weisshaar CWINGS program.

The subroutines have been prepared using the FORTRAN 77 programming language. The subroutines are highly documented in the form of comments to assist the reader in tracing the sources of the algorithms used. The reader is referred to the listings provided for the input parameters and their units. A consistency in units has been maintained throughout to serve only as a guide for user adaption.

Each subroutine is identified, its purpose stated, and other relevant data provided on a page which serves to separate individual subroutine. This page is followed by a listing of the subroutine, an IO program, a sample input, and a sample output listing, in that order. Sample inputs and outputs are provided to assist the user in "debugging" the subroutine if manually programmed. The IO program for each subroutine is provided so that the subroutines may be used with a general main program. These IO programs may be combined in the creation of a main driver program such as that provided in Appendix B. The IO listings provided follow examples provided throughout the thesis for the experimental models as much as possible.

AERO1

This subroutine determines the aerodynamic influence coefficient matrix by the Weissinger L-method. This method produces bound vortices that are parallel to a line normal to the root chord.

SUBROUTINE AERO1

```

c this subroutine determines the aerodynamic influence coefficient
c (AIC) matrix using modified Weissinger L-method (see NACA TN 3030)

      DIMENSION XV(20),SS(20,20)

      COMMON/A1/C(20),E(20),H(20),X(20),Y(20),AIC(20,20),A0,SYM,NP

c      NP = number of panels in semi-span
c      A0 = 2-D lift-curve slope of section (same for all panels)
c      SYM = +1.0 for symmetric load distribution
c           -1.0 for anti-symmetric distribution
c      C = aerodynamic chord at center of panel (in.)
c      E = distance from reference axis to aerodynamic center at middle
c          of panel along aerodynamic chord (in.)
c      H = width of panel (in.)
c      X = x-axis intercept of panel midchord and reference axis (in.)
c      Y = as in X but for y-axis

      DO 10 I=1,NP
c x-axis distance to quarter-chord
10  XV(I)=X(I)-E(I)

c horseshoe vortex at quarter-chord
c control point at 3/4-chord

c I - panel of interest
      DO 30 I=1,NP

c J - all other panels in wing
      DO 20 J=1,NP

c following equations from page 38 of NACA TN 3030
c working left semi-span

      ARG=(XV(I)+C(I)/2.0-XV(J))**2

c for left semi-span (positive y-coordinates)
      ARG1=SQRT(ARG+(Y(I)-Y(J)+H(J)/2.0)**2)

      ARG2=SQRT(ARG+(Y(I)-Y(J)-H(J)/2.0)**2)

c for right semi-span (negative y-coordinates)
      ARG3=SQRT(ARG+(Y(I)+Y(J)+H(J)/2.0)**2)

      ARG4=SQRT(ARG+(Y(I)+Y(J)-H(J)/2.0)**2)

c left semi-span
      SINPHL=(XV(I)+C(I)/2.0-XV(J))/ARG1
      COSPHL=(Y(I)-Y(J)+H(J)/2.0)/ARG1
      SINTHL=(XV(I)+C(I)/2.0-XV(J))/ARG2
      COSTHL=(Y(I)-Y(J)-H(J)/2.0)/ARG2

c right semi-span
      SINPHR=(XV(I)+C(I)/2.0-XV(J))/ARG3
      COSPHR=(Y(I)+Y(J)+H(J)/2.0)/ARG3
      SINTHR=(XV(I)+C(I)/2.0-XV(J))/ARG4
      COSTHR=(Y(I)+Y(J)-H(J)/2.0)/ARG4

```

```

c eqn A38 of NACA TN 3030
  S1=(1.0+SINPHL)/COSPHL-(1.0+SINTHL)/COSTHL
  S2=(1.0+SINPHR)/COSPHR
  S3=(1.0+SINTHR)/COSTHR

  SXIJ=XV(I)+C(I)/2.0-XV(J)

  SS(I,J)=(S1+SYM*S2-SYM*S3)/SXIJ

c elements of S on the principal diagonal must be positive
c and all other elements must be negative
c (see page 39 of NACA TN 3030)

20 AIC(I,J)=SS(I,J)/(4*A0)

30 CONTINUE

  RETURN
  END

```

PROGRAM AIR1

```

c sample run for subroutine AERO
c present limit twenty semi-span panels

  COMMON/A1/C(20),E(20),H(20),X(20),Y(20),AIC(20,20),A0,SYM,NP

  READ (5,*) NP,A0,SYM
  DO 10 I=1,NP
10 READ (5,*) X(I),Y(I),H(I),E(I),C(I)

  CALL AERO1

  WRITE (6,*) ((AIC(I,J),J=1,NP),I=1,NP)

  END

```

Sample IO program for AERO1

10 6.2832 -1.0

14.22	42.75	4.5	1.866	9.0
12.72	38.25	4.5	2.657	12.0
11.23	33.75	4.5	3.447	15.0
9.73	29.25	4.5	4.237	18.0
8.23	24.75	4.5	5.028	21.0
6.74	20.25	4.5	5.818	24.0
5.24	15.75	4.5	6.609	27.0
3.74	11.25	4.5	7.399	30.0
2.25	6.75	4.5	8.189	33.0
0.75	2.25	4.5	8.980	36.0

Sample input for AER01

7.493575662E-02	-2.207770012E-02	-4.036562052E-03	-1.629635692E-03
-8.562540752E-04	-5.085912999E-04	-3.182469809E-04	-1.972675964E-04
-1.091690065E-04	-3.539172394E-05	-2.020356990E-02	7.317339629E-02
-2.247067727E-02	-4.141298123E-03	-1.661071205E-03	-8.598566055E-04
-4.967279965E-04	-2.933849755E-04	-1.578825468E-04	-5.052157212E-05
-3.096980974E-03	-2.137309872E-02	7.233631611E-02	-2.272206917E-02
-4.214351997E-03	-1.676499262E-03	-8.484872524E-04	-4.653002543E-04
-2.402672690E-04	-7.543955871E-05	-1.137384330E-03	-3.406218952E-03
-2.202968486E-02	7.188423723E-02	-2.287900262E-02	-4.254736472E-03
-1.668253681E-03	-8.079487598E-04	-3.911017266E-04	-1.193181306E-04
-5.638469593E-04	-1.232464565E-03	-3.644940909E-03	-2.242304757E-02
7.162672281E-02	-2.296584472E-02	-4.255419597E-03	-1.614855370E-03
-6.997816381E-04	-2.037926461E-04	-3.207823902E-04	-5.958434194E-04
-1.310992986E-03	-3.819882171E-03	-2.265670523E-02	7.149238139E-02
-2.298180945E-02	-4.182030447E-03	-1.447876566E-03	-3.879829019E-04
-1.930659637E-04	-3.264052793E-04	-6.154816365E-04	-1.363929594E-03
-3.925033379E-03	-2.276484482E-02	7.147631794E-02	-2.286832035E-02
-3.902055323E-03	-8.733025170E-04	-1.151612669E-04	-1.839817996E-04
-3.179474152E-04	-6.120262551E-04	-1.372177736E-03	-3.937773407E-03
-2.272049151E-02	7.168762386E-02	-2.234138362E-02	-2.666509477E-03
-6.120362377E-05	-9.462537855E-05	-1.557991345E-04	-2.783817472E-04
-5.536786048E-04	-1.275789808E-03	-3.743516048E-03	-2.225594409E-02
7.286139578E-02	-1.883693598E-02	-1.895710375E-05	-2.885574031E-05
-4.648166941E-05	-8.038555825E-05	-1.520892547E-04	-3.228292044E-04
-8.024551207E-04	-2.610717667E-03	-1.881437749E-02	9.432584047E-02

Sample output for AER01

CAILRN

This subroutine calculates the change in a composite wing angle of attack from a one radian change in aileron deflection on the left semi-span.

SUBROUTINE CAILRN

c this subroutine calculates the change in a composite wing AOA
c resulting from a one radian change in aileron deflection
c left wing only

DIMENSION COSMAT(20),SINMAT(20),ALPHAD(20),AALPHA(20)
DIMENSION EP(20,20),EI0(20,20),EI3(20,20),EE(20,20)

COMMON/C1/NP,Q,CM(20),CMDEL(20),SHAPE(20),SWEEP(20)
COMMON/C2/H(20),EI(20),GJ(20),AK(20),C(20),DALPHA(20)

c NP = number of spanwise panels in wing semi-span
c Q = dynamic pressure for flight condition (psi)
c SHAPE = aileron segment deflection normalized to largest value
c and negative, example:
c -1.0 if deflects same amount
c -0.5 if deflects half as much
c 0.0 if no deflection
c CM = partial derivative of section lift coefficient wrt
c control deflection divided by the partial wrt AOA
c CMDEL = partial derivative of pitching moment wrt control deflection
c of aileron segment on panel
c H = y-axis width of panel (in.)
c C = aerodynamic chord at middle of panel (in.)
c SWEEP = sweep of structural reference axis of panel (deg)
c EI = bending stiffness of wing box beam (psi)
c GJ = torsional stiffness of wing box beam (psi)
c AK = K, bending-torsion coupling parameter

DO 10 I=1,NP
c change to radians
SWP=SWEEP(I)*ACOS(-1.0)/180.0
c diagonal terms of eqns B23 and B24 of NACA TN 3030
COSMAT(I)=COS(SWP)
10 SINMAT(I)=SIN(SWP)

c initializing matrices
DO 30 I=1,NP
DO 20 J=1,NP
EE(I,J)=0.0
EI0(I,J)=0.0
20 EP(I,J)=0.0
30 CONTINUE

NPM1=NP-1

c constructing [I0] matrix, page 88 of NACA TN 3030
c upper triangular terms
DO 50 I=1,NPM1
II=I+1
DO 40 J=II,NP
40 EI0(I,J)=1.0
50 CONTINUE
c diagonal terms
DO 60 I=1,NP
60 EI0(I,I)=0.500

c [I3] of page 88 of NACA TN 3030 is just transpose of [I0]
DO 80 I=1,NP

```

DO 70 J=1,NP
70 EI3(I,J)=EI0(J,I)
80 CONTINUE

c eqn F6 of NACA TN 3030
c derived from eqn F6 of NACA TN 3030
DO 90 I=1,NP
  EE(I,I)=H(I)*SINMAT(I)*SINMAT(I)/(COSMAT(I)*EI(I))
  EE(I,I)=EE(I,I)-2*H(I)*SINMAT(I)*AK(I)/(EI(I)*GJ(I))
  EE(I,I)=EE(I,I)+H(I)*COSMAT(I)/GJ(I)

c FAC = (1 - kg) where k = K/EI and g = K/GJ
c page 7 of AFFDL-TR-79-3087
  FAC=1.0-(AK(I)**2)/(EI(I)*GJ(I))
90 EE(I,I)=EE(I,I)/FAC

c pre-multiply by [I0]
DO 120 I=1,NP
DO 110 J=1,NP
  SUM1=0.0
DO 100 K=1,NP
100 SUM1=SUM1+EI0(I,K)*EE(K,J)
110 EP(I,J)=SUM1
120 CONTINUE

c post-multiply by [I3]
DO 150 I=1,NP
DO 140 J=1,NP
  SUM1=0.0
DO 130 K=1,NP
130 SUM1=SUM1+EP(I,K)*EI3(K,J)
140 EE(I,J)=SUM1
150 CONTINUE

DO 170 I=1,NP
DO 160 J=1,NP
160 EE(I,J)=EE(I,J)*H(J)*(C(J)**2)
170 CONTINUE

DO 190 I=1,NP
  SUM1=0.0
DO 180 J=1,NP
180 SUM1=SUM1+EE(I,J)*CMDEL(J)*SHAPE(J)

c ALPHAD is change in AOA due to change in section pitching moment
c from twist produced by one radian aileron deflection
c eqn C-8 of AFFDL-TR-79-3087
190 ALPHAD(I)=Q*SUM1

c AALPHA is the apparent change in AOA of wing section due to one radian
c aileron deflection (change in chamber of mean chord line)
c eqn 39 from AFFDL-TR-3087
DO 200 I=1,NP
  AALPHA(I)=SHAPE(I)*CM(I)

c DALPHA is the total AOA change due to one rad. change in aileron deflection
c eqn 39 from AFFDL-TR-79-3087
200 DALPHA(I)=ALPHAD(I)+AALPHA(I)

```

```
RETURN  
END
```

PROGRAM CLN

```
c sample run for subroutine CAILRN  
c present limit twenty semi-span panels  
  
COMMON/C1/NP,Q,CM(20),CMDEL(20),SHAPE(20),SWEEP(20)  
COMMON/C2/H(20),EI(20),GJ(20),AK(20),C(20),DALPHA(20)  
  
READ (5,*) NP,Q  
DO 10 I=1,NP  
READ (5,*) C(I),H(I),EI(I),GJ(I),AK(I)  
10 READ (5,*) SWEEP(I),CM(I),CMDEL(I),SHAPE(I)  
  
WRITE (6,*) "CAILRN RESULTS"  
WRITE (6,*)  
WRITE (6,*) "PANEL", " ", "DALPHA"  
  
CALL CAILRN  
  
DO 20 I=1,NP  
20 WRITE (6,*) I,DALPHA(I)  
  
END
```

Sample IO program for CAILRN

10	.1724			
9.0	4.5	.49355E+05	.16017E+05	.58220E+03
18.4	0.5854	-0.64	-1.0	
12.0	4.5	.70260E+05	.22801E+05	.82879E+03
18.4	0.5854	-0.64	-1.0	
15.0	4.5	.91165E+05	.29584E+05	.10754E+04
18.4	0.5854	-0.64	-1.0	
18.0	4.5	.11207E+06	.36368E+05	.13220E+04
18.4	0.5854	-0.64	-1.0	
21.0	4.5	.13297E+06	.43152E+05	.15686E+04
18.4	0.5854	-0.64	-1.0	
24.0	4.5	.15388E+06	.49936E+05	.18152E+04
18.4	0.5854	-0.64	-1.0	
27.0	4.5	.17478E+06	.56720E+05	.20618E+04
18.4	0.5854	-0.64	0.0	
30.0	4.5	.19569E+06	.63504E+05	.23084E+04
18.4	0.5854	-0.64	0.0	
33.0	4.5	.21659E+06	.70288E+05	.25550E+04
18.4	0.5854	-0.64	0.0	
36.0	4.5	.23750E+06	.77072E+05	.28016E+04
18.4	0.5854	-0.64	0.0	

Sample input for CAILRN

CAILRN RESULTS

PANEL	DALPHA
1	-1.539785266E-01
2	-1.640512347E-01
3	-1.838048398E-01
4	-2.145894468E-01
5	-2.580627203E-01
6	-3.160042167E-01
7	2.021546811E-01
8	1.369802803E-01
9	7.845127583E-02
10	2.533532120E-02

Sample output for CAILRN

CDIVRG

This subroutine calculates the divergence speed for a composite wing using an empirical approach.

SUBROUTINE CDIVRG

c this subroutine calculates the divergence dynamic pressure (psi)
c and divergence speed (mph) for a composite wing

COMMON/CD/RHO,AO,SWEEP,RL,TR,C,EI,GJ,AK,E,AR,QDIV,VDIV

c RHO = air density at flight condition (lbf*sec**2/ft**4)
c AO = 2-dimensional section lift-curve slope for section, same
c full span
c SWEEP = sweep of wing reference axis, positive aft (deg.)
c RL = length of semi-span along reference axis (in.)
c TR = taper ratio of semi-span
c C = root chord perpendicular to reference axis (in.)
c EI = bending stiffness, at root if tapered wing (psi)
c GJ = torsional stiffness, at root if tapered wing (psi)
c AK = K, bending-torsion coupling parameter, at root if
c tapered wing
c E = y-axis distance between reference axis and aerodynamic
c center, at root if tapered wing (in.)
c AR = semi-span aspect ratio

NDV=0

c conversion to radians
SWP=SWEEP*ACOS(-1.0)/180.0
c eqns B-55 and B-56 of AFFDL-TR-78-116
c composite nondimensional bending coupling parameter
AKR=K/EI
c composite nondimensional torsion coupling parameter
GR=K/GJ

ARG1=(GJ/EI)*(RL/E)

c correction of 2-D lift-curve slope for planform effects
c eqn 4a of NACA TN 1680
AOC=AO*AR/(AR+4*COS(SWP))
ARG2=C*(RL**3)*AOC*(COS(SWP)**2)

c check for taper
IF (TR.LT.1.0) GO TO 10

c for constant chord, untapered wing
ARG3=2.47*(1-AKR*GR)/ARG2
ARG4=0.39*(TAN(SWP)-GR)

c divergence dynamic pressure (psi), no taper
c eqn C-18 of AFFDL-TR-78-116
QDIV=ARG3*EI/((1-AK*TAN(SWP))/ARG1-ARG4)

GO TO 20

c for tapered wing

10 ARG3=GJ*(RL/E)/ARG2

c linearized approximation for table on page 55 of
c AFFDL-TR-78-116
RK1=(6.1301-TR)/2.0801

```

      RK2=(2.8149-TR)/4.4114
      ARG4=RK1*(1-AKR*GR)
      ARG5=RK2*ARG1*(TAN(SWP)-GR)
c   divergence dynamic pressure (psi), tapered wing
c   eqn C-30 of AFFDL-TR-78-116
      QDIV=ARG3*ARG4/((1-AKR*TAN(SWP))-ARG5)
c   conversion to inches
      20 RHO=RHO/(12**4)
c   divergence speed (in/sec)**2
      VDIV=2.0*QDIV/RHO
c   test for no divergence (negative divergence velocity)
      IF (VDIV.LT.0.0) NDV=1
      IF (VDIV.LT.0.0) GO TO 30
c   conversion to feet
      VDIV=SQRT(VDIV)/12.0
c   conversion to mph
      VDIV=(3600.0*VDIV/5280.0)
30  RETURN
    END

```

PROGRAM CDV

```

c   sample run for subroutine CDIVRG
      COMMON/CD/RHO,A0,SWEEP,RL,TR,C,EI,GJ,AK,E,AR,QDIV,VDIV
      READ (5,*) RHO,A0,SWEEP,RL,TR
      READ (5,*) C,EI,GJ,AK,E,AR
      CALL CDIVRG
      IF (NDV.GT.0) WRITE (6,*) "THIS WING WILL NOT DIVERGE"
      IF (NDV.GT.0) GO TO 10
      WRITE (6,*) "DIVERGENCE DYNAMIC PRESSURE (PSI) = ",QDIV
      WRITE (6,*)
      WRITE (6,*) "DIVERGENCE SPEED (MPH) = ",VDIV
10  END

```

Sample IO program for CDIVRG

0.002308 6.28 18.4 47.4 0.2
36.13 248000. 80460. 2925. 9.375 4.0

Sample input for CDIVRG

DIVERGENCE DYNAMIC PRESSURE (PSI) = 1.535565704E-01

DIVERGENCE SPEED (MPH) = 9.438024902E+01

Sample output for CDIVRG

CFLEX

This subroutine calculates the flexibility matrix for the left semi-span of a composite box beam wing.

SUBROUTINE CFLEX

c this subroutine determines the composite wing flexibility matrix
c [S], left wing only

DIMENSION D(20),F(20),U(20,20),M(20,20),T(20,20)
DIMENSION TRANS1(20),TRANS2(20),TRANS3(20),V(20,20)
DIMENSION COSMAT(20),SINMAT(20),FAC(20),R1(20,20),R2(20,20)

COMMON/F1/S(20,20),X(20),Y(20),H(20),E(20),SWEEP(20)
COMMON/F2/EI(20),GJ(20),AK(20),NP

REAL M

c NP = number of panels in semi-span
c X = x-axis intercept of panel midchord and reference axis (in.)
c Y = as in X but for y-axis
c H = width of panel along y-axis (in.)
c E = x-axis distance from reference axis to
c aerodynamic center of panel (in.)
c SWEEP = sweep of reference axis on panel from y-axis
c positive aft (deg)
c EI = bending stiffness of box beam (psi)
c GJ = torsional stiffness of box beam (psi)
c AK = K, bending-torsion coupling parameter of box beam

NPM1=NP-1

DO 10 I=1,NPM1
c elements of matrices below
D(I)=Y(I)-Y(I+1)
10 F(I)=X(I)-X(I+1)

DO 20 I=1,NP
c conversion to radians
SWP=SWEEP(I)*ACOS(-1.0)/180.0
c NACA TN 3030 eqn B23 and B24, diagonal terms only (nonzero)
COSMAT(I)=COS(SWP)
20 SINMAT(I)=SIN(SWP)

c initializing matrices
DO 40 I=1,NP
DO 30 J=1,NP
U(I,J)=0.0
R1(I,J)=0.0
30 R2(I,J)=0.0
40 CONTINUE

c nonzero elements of C (see below)
DO 70 I=2,NP
IM1=I-1
DO 60 J=1,IM1
FSUM=0.0
DSUM=0.0
DO 50 K=J,IM1
DSUM=DSUM+D(K)
50 FSUM=FSUM+F(K)

c TN 3030 eqn B26 and B27
R1(I,J)=DSUM*COSMAT(I)

```

      R2(I,J)=DSUM*SINMAT(I)
c   eqn B25 from NACA TN 3030
    60 U(I,J)=E(J)-FSUM
    70 CONTINUE

c   diagonal terms
    DO 80 I=1,NP
      R1(I,I)=H(I)/(8.0*COSMAT(I))-E(I)*SINMAT(I)/2.0
    80 R2(I,I)=E(I)*COSMAT(I)/2.0

c   initializing
    DO 100 I=1,NP
      DO 90 J=1,NP
        M(I,J)=0.0
    90 T(I,J)=0.0
    100 CONTINUE

c   TN 3030 eqn B34 and B35
c   diagonal terms
    DO 110 I=1,NP
      M(I,I)=-SINMAT(I)/2.0
    110 T(I,I)=COSMAT(I)/2.0
    DO 130 I=1,NPM1
c   off-diagonal terms
      IP1=I+1
      DO 120 J=IP1,NP
        M(I,J)=-SINMAT(J)
    120 T(I,J)=COSMAT(J)
    130 CONTINUE

c   ***** MUST PROVIDE THE STRUCTURAL PROPERTIES EI,GJ,K *****

    DO 140 I=1,NP
c   from AFFDL-TR-79-3087 k=K/EI and g=K/GJ
c   FAC is (1 - kg) term
    140 FAC(I)=1.0-(AK(I)**2)/(EI(I)*GJ(I))

c   following is eqn A-16 from AFFDL-TR-79-3087
c   (refer to eqn B-37 from NACA TN 3030)

    DO 150 I=1,NP
      TRANS1(I)=H(I)/COSMAT(I)/(EI(I)*FAC(I))
      TRANS2(I)=H(I)/COSMAT(I)/(GJ(I)*FAC(I))
    150 TRANS3(I)=H(I)*(AK(I)/GJ(I))/(EI(I)*FAC(I))/COSMAT(I)

    DO 170 I=1,NP
      DO 160 J=1,NP
        A=(R1(I,J)-SINMAT(I)*U(I,J))*H(J)
        B=(R2(I,J)+COSMAT(I)*U(I,J))*H(J)
        U(I,J)=TRANS1(I)*A
        V(I,J)=TRANS2(I)*B
        R1(I,J)=TRANS3(I)*A
    160 R2(I,J)=TRANS3(I)*B
    170 CONTINUE

    DO 200 I=1,NP
      DO 190 J=1,NP
        SUM1=0.0
        SUM2=0.0
    DO 180 K=1,NP

```



```

      SUM1=SUM1+M(I,K)*(U(K,J)+R2(K,J))
180 SUM2=SUM2+T(I,K)*(R1(K,J)+V(K,J))

c  flexibility matrix
190 S(I,J)=SUM1+SUM2
200 CONTINUE

      RETURN
      END

```

```

      PROGRAM CF

c  sample run for subroutine CFLEX
c  present limit twenty semi-span panels

      COMMON/F1/S(20,20),X(20),Y(20),H(20),E(20),SWEEP(20)
      COMMON/F2/EI(20),GJ(20),AK(20),NP

      READ (5,*) NP
      DO 10 I=1,NP
      READ (5,*) X(I),Y(I),H(I),E(I),SWEEP(I)
10 READ (5,*) EI(I),GJ(I),AK(I)

      CALL CFLEX

      WRITE (6,*) ((S(I,J),J=1,NP),I=1,NP)

      END

```

Sample IO program for CFLEX

10

14.22	42.75	4.5	1.866	18.4
49355.	16017.		582.20	
12.72	38.25	4.5	2.657	18.4
70260.	22801.		828.79	
11.23	33.75	4.5	3.447	18.4
91165.	29584.		1075.4	
9.73	29.25	4.5	4.237	18.4
112070.	36368.		1322.0	
8.23	24.75	4.5	5.028	18.4
132970.	43152.		1568.6	
6.74	20.25	4.5	5.818	18.4
153880.	49936.		1815.2	
5.24	15.75	4.5	6.609	18.4
174780.	56720.		2061.8	
3.74	11.25	4.5	7.399	18.4
195690.	63504.		2308.4	
2.25	6.75	4.5	8.189	18.4
216590.	70288.		2555.0	
0.75	2.25	4.5	8.980	18.4
237500.	77072.		2801.6	

Sample input for CFLEX

5.491133779E-04	4.016366787E-03	5.804807879E-03	6.779769436E-03
7.069502957E-03	6.762558594E-03	5.973002873E-03	4.742434714E-03
3.113932675E-03	1.136320876E-03	-5.951775238E-04	3.465960734E-03
5.804807879E-03	6.779769436E-03	7.069502957E-03	6.762558594E-03
5.973002873E-03	4.742434714E-03	3.113932675E-03	1.136320876E-03
-1.512221526E-03	2.181915566E-03	5.248665810E-03	6.779769436E-03
7.069502957E-03	6.762558594E-03	5.973002873E-03	4.742434714E-03
3.113932675E-03	1.136320876E-03	-1.950709615E-03	9.793248028E-04
3.883810714E-03	6.220048293E-03	7.069502957E-03	6.762558594E-03
5.973002873E-03	4.742434714E-03	3.113932675E-03	1.136320876E-03
-2.075510565E-03	2.228990197E-04	2.501267474E-03	4.797854926E-03
6.507211830E-03	6.762558594E-03	5.973002873E-03	4.742434714E-03
3.113932675E-03	1.136320876E-03	-1.981792506E-03	-2.218801528E-04
1.522687031E-03	3.281203797E-03	5.041116383E-03	6.198494695E-03
5.973002873E-03	4.742434714E-03	3.113932675E-03	1.136320876E-03
-1.726213144E-03	-4.356959835E-04	8.435694035E-04	2.133063274E-03
3.423580434E-03	4.702845123E-03	5.407503806E-03	4.742434714E-03
3.113932675E-03	1.136320876E-03	-1.343934564E-03	-4.694792442E-04
3.973522689E-04	1.271114685E-03	2.145570237E-03	3.012401052E-03
3.886856604E-03	4.175885580E-03	3.113932675E-03	1.136320876E-03
-8.622845635E-04	-3.614670131E-04	1.349840313E-04	6.354047218E-04
1.136222272E-03	1.632672967E-03	2.133490983E-03	2.633911557E-03
2.546535106E-03	1.136320876E-03	-2.998266136E-04	-1.380913891E-04
2.223375486E-05	1.838408934E-04	3.455760889E-04	5.059011746E-04
6.676365156E-04	8.292436250E-04	9.895686526E-04	5.681604380E-04

Sample output for CFLEX

CSTRUC

This subroutine determines the material properties (EI , GJ , K) for a composite box beam representation of a wing. It has been formulated to permit the most general structure; nonlinear planform taper and nonlinear spanwise thickness taper. All plies in the laminate must be of the same composite material.

Three examples are provided; a linearly tapered wing with constant spanwise thickness, a nonlinearly tapered wing with constant spanwise thickness, and a nonlinearly tapered planform with a nonlinearly tapered spanwise thickness, in that order.

SUBROUTINE CSTRUC

```

c determines material properties for a composite box beam (wing)
c EI, GJ, and K
c for a linearly tapered or general planform
c and a constant thickness or tapered thickness (linear or nonlinear)
c assumes laminate all of same composite material

      DIMENSION BETA(60),DELTA(60),T(60),NR(60)

      COMMON/C1/EI(20),GJ(20),AK(20),SSPAN,CSR,SWEEPR,TAPER,Y(20),NR(60)
      COMMON/C2/E1,E2,P12,G12,DR,N,NV,NP,NLIN,NTAP,M
      COMMON/C3/ZNL(60),ZNU(60),THETA(60),CS(20)

c      EI = panel bending stiffness (psi)
c      GJ = panel torsional stiffness (psi)
c      AK = K, panel bending-torsion coupling parameter
c      E1 = modulus of elasticity along axis 1 of material (psi)
c      E2 = modulus of elasticity along axis 2 of material (psi)
c      P12 = Poisson's ratio for 1-2 axes
c      G12 = shear modulus for 1-2 axes (psi)
c      N = number of plies in box beam laminate
c           (at root for spanwise thickness taper)
c      NV = number of variable plies
c      NP = number of panels in wing semi-span
c      DR = incremental rotation of variable plies (positive fwd, rad)
c      ZNL = distance from mid-plane of box beam to lower surface of
c            ply, positive up (in.)
c      ZNU = as for ZNU but for upper surface of ply
c      THETA = initial orientation of ply (rad.) measured from
c             structural root, positive forward
c      NOTE: for ZNU,ZNL & THETA, input variable plies first
c      TAPER = taper ratio
c      SSPAN = semi-span (in.)
c      SWEEPR = reference chord sweep at root (deg)
c      CSR = structural root chord, perpendicular to reference axis (in.)
c      CS = structural root chord (perpendicular to reference axis) at middle
c           of each panel (in.), panel 1 (one) is at wing tip
c      NLIN = 0, not a linearly tapered planform
c            = 1, linearly tapered planform
c      NTAP = 0, nonlinearly tapered spanwise thickness
c            = 1, constant spanwise thickness (constant properties)
c            = 4, linearly tapered spanwise thickness
c              (linearly tapered planform only)
c      NR = ply numbers to be removed from panel
c      NOTE: for NR, numbered as they are input, remove only outside plies

c      defining pi
c      PI=ACOS(-1.)

c      Poisson's ratio for 2-1 axes
c      eqn 2.26 in MECHANICS OF COMPOSITE MATERIALS by Jones
c      P21=P12*E2/E1

c      eqn 2.61 of JONES
c      Q11=E1/(1.0-P12*P21)
c      Q22=E2/(1.0-P12*P21)
c      Q12=P21*Q22
c      Q66=G12

```

```

c eqn 2.94 of JONES
  U1=(3.0*Q11+3.0*Q22+2.0*Q12+4.0*Q66)/8.0
  U2=(Q11-Q22)/2.0
  U3=(Q11+Q22-2.0*Q12-4.0*Q66)/8.0
  U4=(Q11+Q22+6.0*Q12-4.0*Q66)/8.0
  U5=(Q11+Q22-2.0*Q12+4.0*Q66)/8.0

c check for input error
  IF ((NLIN.EQ.0).AND.(NTAP.EQ.4)) GO TO 10
  GO TO 20

10 WRITE (6,*) "INPUT ERROR, NLIN=0 & NTAP=4 NOT PERMITTED"
  GO TO 140

c following for all but case of nonlinear planform taper
c and nonlinear thickness taper
20 IF ((NLIN.EQ.0).AND.(NTAP.EQ.0)) GO TO 40

  DO 30 I=1,N

c ply thickness
  T(I)=ZNU(I)-ZNL(I)

c eqns A-26 and A-27 of AFFDL-TR-78-116
c area moment of inertia of ply with unit width
  BETA(I)=(T(I)**3+3.0*T(I)*ZNL(I)**2+3.0*ZNL(I)*T(I)**2)/3.0
c first moment of area about the mid plane
30 DELTA(I)=T(I)*(ZNU(I)+ZNL(I))/2.0

  GO TO 70

40 DO 60 I=1,N
c removing plies
  DO 50 J=1,N
50 IF (I.EQ.NR(J)) GO TO 60

c ply thickness
c T(I)=ZNU(I)-ZNL(I)

c eqns A-26 and A-27 of AFFDL-TR-78-116
c area moment of inertia of ply with unit width
  BETA(I)=(T(I)**3+3.0*T(I)*ZNL(I)**2+3.0*ZNL(I)*T(I)**2)/3.0
c first moment of area above about the mid plane
  DELTA(I)=T(I)*(ZNU(I)+ZNL(I))/2.0
60 CONTINUE

c initialization
70 S1=0.0
  S2=0.0
  S3=0.0
  S4=0.0
  S5=0.0
  S6=0.0

c following for nonvariable plies only
  IF (NV.GE.N) GO TO 90
  NFIX=NV+1

  DO 80 I=NFIX,N
  D1=THETA(I)

```

```

      D12=2.0*D1
      D14=4.0*D1

c   eqns 2.93 of JONES
      BQ22=U1-U2*COS(D12)+U3*COS(D14)
      BQ26=.5*U2*SIN(D12)-U3*SIN(D14)
      BQ66=U5-U3*COS(D14)

c   summations for later use
      S1=S1+BQ22*BETA(I)
      S2=S2+BQ22*DELTA(I)
      S3=S3+BQ22*T(I)
      S4=S4+BQ26*BETA(I)
      S5=S5+BQ26*DELTA(I)
      80 S6=S6+BQ66*BETA(I)

c   redefining summation from nonvariable plies
      90 SQ22B=S1
      SQ22D=S2
      SQ22T=S3
      SQ26B=S4
      SQ26D=S5
      SQ66B=S6

c   following for variable plies only
      IF (NV.LE.0) GO TO 110

c   summation now for all plies
      DO 100 I=1,NV

c   rotating variable plies
      D1=DR+THETA(I)
      D12=2.0*D1
      D14=4.0*D1

c   eqns 2.93 of JONES
      BQ22=U1-U2*COS(D12)+U3*COS(D14)
      BQ26=.5*U2*SIN(D12)-U3*SIN(D14)
      BQ66=U5-U3*COS(D14)

c   from eqns A-28 through A-34 of AFFDL-TR-78-116 without constants
      SQ22B=SQ22B+BQ22*BETA(I)
      SQ22D=SQ22D+BQ22*DELTA(I)
      SQ22T=SQ22T+BQ22*T(I)
      SQ26B=SQ26B+BQ26*BETA(I)
      SQ26D=SQ26D+BQ26*DELTA(I)
      100 SQ66B=SQ66B+BQ66*BETA(I)

c   following for all but case of nonlinear planform taper
c   and nonlinear thickness taper
      110 IF ((NLIN.EQ.0).AND.(NTAP.EQ.0)) GO TO 130

      IF (NLIN.EQ.1) CC=CSR

      SWPR=SWEEPR*PI/180.0

c   this portion of subroutine is run for each laminate rotation case

c   for each panel
      DO 120 I=1,NP

```

```

      IF ((NLIN.EQ.0).AND.(NTAP.EQ.1)) CC=CS(I)

c   eqn B-26 of AFFDL-TR-78-116 (see also NACA TO 1680 page 18)
c   rotating y-axis to align with reference axis and
      IF (NLIN.EQ.1) F=1.0-(Y(I)/SSPAN)*(1.0-TAPER)/COS(SWPR)

      IF ((NLIN.EQ.0).AND.(NTAP.EQ.1)) F=1.0

c   material properties for this laminate
c   eqn 8 and eqns B-60 through B-62 of AFFDL-TR-78-116
      EI(I)=(CC*(SQ22B-(SQ22D**2)/SQ22T))*F*NTAP
      GJ(I)=(CC*(4*SQ66B-((2*SQ26D)**2)/SQ22T))*F*NTAP
120  AK(I)=(CC*2*(SQ26B-SQ22D*SQ26D/SQ22T))*F*NTAP

      GO TO 140

c   this portion of the subroutine is run once for each panel

c   following for nonlinear planform taper and thickness taper
c   must input CS and NPR for each NCASE

c   redefining for function
130  CC=CS(M)

c   material properties for this laminate
c   eqn 8 and eqns B-60 through B-62 of AFFDL-TR-78-116
      EI(M)=CC*(SQ22B-(SQ22D**2)/SQ22T)
      GJ(M)=CC*(4*SQ66B-((2*SQ26D)**2)/SQ22T)
      AK(M)=CC*2*(SQ26B-SQ22D*SQ26D/SQ22T)

140  RETURN
      END

```

PROGRAM CST

```

c sample run for subroutine CSTRUC
c present limit twenty semi-span panels and sixty composite plies

COMMON/C1/EI(20),GJ(20),AK(20),SSPAN,CSR,SWEEPR,TAPER,Y(20),NR(60)
COMMON/C2/E1,E2,P12,G12,DR,N,NV,NP,NLIN,NTAP,M
COMMON/C3/ZNL(60),ZNU(60),THETA(60),CS(20)

c defining pi
PI=ACOS(-1.)

READ (5,*) E1,E2,P12,G12

READ (5,*) N,NV,NP,NCASE,NLIN,NTAP,DDEL

DO 10 I=1,N
READ (5,*) ZNL(I),ZNU(I),THETA(I)
IF (I.EQ.1) THETA1=THETA(I)
c change to radians
10 THETA(I)=THETA(I)*PI/180.0

c read only if linear planform taper
IF (NLIN.EQ.0) GO TO 30

READ (5,*) SSPAN,CSR,SWEEPR,TAPER

DO 20 I=1,NP
20 READ (5,*) Y(I)

GO TO 50

c read only if non-linear planform taper but constant thickness
30 IF ((NLIN.EQ.0).AND.(NTAP.EQ.0)) GO TO 50
DO 40 I=1,NP
40 READ (5,*) CS(I)

50 WRITE (6,*) "          THE FIRST ",NV," PLIES WILL BE VARIED"
WRITE (6,*)
WRITE (6,*)

D=0.0

c for each rotation case
DO 110 L=1,NCASE

c converting ply rotation to radians
DR=D*PI/180.0

DD=D+THETA1

WRITE (6,*) "FIRST VARIABLE PLY ORIENTATION = ",DD
WRITE (6,*)
WRITE (6,120)

IF ((NLIN.EQ.0).AND.(NTAP.EQ.0)) GO TO 70

CALL CSTRUC

DO 60 I=1,NP

```



```

60 WRITE (6,130) I,EI(I),GJ(I),AK(I)

GO TO 110

c read only if non-linear planform taper and non-linear thickness taper
c read plies to be removed (numbered as entered above, remove outside)
70 DO 100 M=1,NP
c initializing for each panel
DO 80 J=1,N
80 NR(J)=0.0
c input from tip inboard
READ (5,*) CS(M),NPR
IF (NPR.EQ.0) GO TO 90
READ (5,*) (NR(I),I=1,NPR)

90 CALL CSTRUC

100 WRITE (6,130) M,EI(M),GJ(M),AK(M)

c increment laminate rotation for each case
110 D=D+DDEL

120 FORMAT (4X,5HPANEL5X,5HEI(I),7X,5HGJ(I),8X,4HK(I)/
112X,8H1b-in**2,4X,8H1b-in**2,8X,1H-/)
130 FORMAT (5X,I2,2X,3E12.5//)

END

```

Sample IO program for CSTRUC

18844000.	1468000.	.260	910000.
32 32 10	02 1 1	10.0	
0.07875	0.084		90.0
0.0735	0.07875		90.0
0.06825	0.0735		90.0
0.063	0.06825		90.0
0.05775	0.063		90.0
0.0525	0.05775		90.0
0.04725	0.0525		90.0
0.042	0.04725		90.0
0.03675	0.042		45.0
0.0315	0.03675		135.0
0.02625	0.0315		45.0
0.021	0.02625		135.0
0.01575	0.021		45.0
0.0105	0.01575		135.0
0.00525	0.0105		45.0
0.0	0.00525		135.0
-0.00525	0.0		135.0
-0.0105	-0.00525		45.0
-0.01575	-0.0105		135.0
-0.021	-0.01575		45.0
-0.02625	-0.021		135.0
-0.0315	-0.02625		45.0
-0.03675	-0.0315		135.0
-0.042	-0.03675		45.0
-0.04725	-0.042		90.0
-0.0525	-0.04725		90.0
-0.05775	-0.0525		90.0
-0.063	-0.05775		90.0
-0.06825	-0.063		90.0
-0.0735	-0.06825		90.0
-0.07875	-0.0735		90.0
-0.084	-0.07875		90.0
45.0	36.13	18.4	0.2
42.75			
38.25			
33.75			
29.25			
24.75			
20.25			
15.75			
11.25			
6.75			
2.25			

Sample input for CSTRUC

THE FIRST 32 PLIES WILL BE VARIED

FIRST VARIABLE PLY ORIENTATION = 9.000000000E+01

PANEL	EI(I) lb-in**2	GJ(I) lb-in**2	K(I) -
1	.49355E+05	.16017E+05	.58220E+03
2	.70260E+05	.22800E+05	.82879E+03
3	.91165E+05	.29584E+05	.10754E+04
4	.11207E+06	.36368E+05	.13220E+04
5	.13297E+06	.43152E+05	.15686E+04
6	.15388E+06	.49936E+05	.18152E+04
7	.17478E+06	.56720E+05	.20618E+04
8	.19569E+06	.63504E+05	.23084E+04
9	.21659E+06	.70288E+05	.25550E+04
10	.23750E+06	.77072E+05	.28016E+04

FIRST VARIABLE PLY ORIENTATION = 1.000000000E+02

PANEL	EI(I) lb-in**2	GJ(I) lb-in**2	K(I) -
1	.47248E+05	.19998E+05	-.12356E+05
2	.67261E+05	.28468E+05	-.17590E+05
3	.87273E+05	.36939E+05	-.22824E+05
4	.10729E+06	.45409E+05	-.28057E+05
5	.12730E+06	.53879E+05	-.33291E+05
6	.14731E+06	.62350E+05	-.38525E+05

7	.16732E+06	.70820E+05	-.43758E+05
8	.18733E+06	.79290E+05	-.48992E+05
9	.20735E+06	.87761E+05	-.54226E+05
10	.22736E+06	.96231E+05	-.59459E+05

Sample output for CSTRUC

18844000.	1468000.	.280	910000.
32 32 10	02 0 1 10.0		
0.07875	0.084		90.0
0.0735	0.07875		90.0
0.06825	0.0735		90.0
0.063	0.06825		90.0
0.05775	0.063		90.0
0.0525	0.05775		90.0
0.04725	0.0525		90.0
0.042	0.04725		90.0
0.03675	0.042		45.0
0.0315	0.03675		135.0
0.02625	0.0315		45.0
0.021	0.02625		135.0
0.01575	0.021		45.0
0.0105	0.01575		135.0
0.00525	0.0105		45.0
0.0	0.00525		135.0
-0.00525	0.0		135.0
-0.0105	-0.00525		45.0
-0.01575	-0.0105		135.0
-0.021	-0.01575		45.0
-0.02625	-0.021		135.0
-0.0315	-0.02625		45.0
-0.03675	-0.0315		135.0
-0.042	-0.03675		45.0
-0.04725	-0.042		90.0
-0.0525	-0.04725		90.0
-0.05775	-0.0525		90.0
-0.063	-0.05775		90.0
-0.06825	-0.063		90.0
-0.0735	-0.06825		90.0
-0.07875	-0.0735		90.0
-0.084	-0.07875		90.0
7.19			
10.24			
13.28			
16.33			
19.38			
22.42			
25.47			
28.51			
31.56			
34.61			

Sample input for CSTRUC

THE FIRST 32 PLIES WILL BE VARIED

FIRST VARIABLE PLY ORIENTATION - 9.000000000E+01

PANEL	EI(I) lb-in**2	GJ(I) lb-in**2	K(I) -
1	.49343E+05	.16013E+05	.58206E+03
2	.70275E+05	.22805E+05	.82896E+03
3	.91137E+05	.29575E+05	.10751E+04
4	.11207E+06	.36368E+05	.13220E+04
5	.13300E+06	.43161E+05	.15689E+04
6	.15386E+06	.49931E+05	.18150E+04
7	.17479E+06	.56723E+05	.20619E+04
8	.19566E+06	.63494E+05	.23080E+04
9	.21659E+06	.70286E+05	.25549E+04
10	.23752E+06	.77079E+05	.28018E+04

FIRST VARIABLE PLY ORIENTATION - 1.000000000E+02

PANEL	EI(I) lb-in**2	GJ(I) lb-in**2	K(I) -
1	.47237E+05	.19993E+05	-.12353E+05
2	.67274E+05	.28474E+05	-.17594E+05
3	.87247E+05	.36927E+05	-.22817E+05
4	.10728E+06	.45409E+05	-.28057E+05
5	.12732E+06	.53890E+05	-.33297E+05
6	.14729E+06	.62343E+05	-.38521E+05

7 .16733E+06 .70824E+05 -.43761E+05
8 .18730E+06 .79277E+05 -.48984E+05
9 .20734E+06 .87758E+05 -.54224E+05
10 .22738E+06 .96239E+05 -.59465E+05

Sample output for CSTRUC

18844000.	1468000.	.280	910000.
32 32 10	02 0 0	10.0	
0.07875	0.084		90.0
0.0735	0.07875		90.0
0.06825	0.0735		90.0
0.063	0.06825		90.0
0.05775	0.063		90.0
0.0525	0.05775		90.0
0.04725	0.0525		90.0
0.042	0.04725		90.0
0.03675	0.042		45.0
0.0315	0.03675		135.0
0.02625	0.0315		45.0
0.021	0.02625		135.0
0.01575	0.021		45.0
0.0105	0.01575		135.0
0.00525	0.0105		45.0
0.0	0.00525		135.0
-0.00525	0.0		135.0
-0.0105	-0.00525		45.0
-0.01575	-0.0105		135.0
-0.021	-0.01575		45.0
-0.02625	-0.021		135.0
-0.0315	-0.02625		45.0
-0.03675	-0.0315		135.0
-0.042	-0.03675		45.0
-0.04725	-0.042		90.0
-0.0525	-0.04725		90.0
-0.05775	-0.0525		90.0
-0.063	-0.05775		90.0
-0.06825	-0.063		90.0
-0.0735	-0.06825		90.0
-0.07875	-0.0735		90.0
-0.084	-0.07875		90.0
7.19	18		
1 2 3 4 5 6 7 8 9 24 25 26 27 28 29 30 31 32			
10.24	16		
1 2 3 4 5 6 7 8 25 26 27 28 29 30 31 32			
13.28	14		
1 2 3 4 5 6 7 26 27 28 29 30 31 32			
16.33	12		
1 2 3 4 5 6 27 28 29 30 31 32			
19.38	10		
1 2 3 4 5 28 29 30 31 32			
22.42	8		
1 2 3 4 29 30 31 32			
25.47	6		
1 2 3 30 31 32			
28.51	4		
1 2 31 32			
31.56	2		
1 32			
34.61	0		
7.19	18		
1 2 3 4 5 6 7 8 9 24 25 26 27 28 29 30 31 32			
10.24	16		
1 2 3 4 5 6 7 8 25 26 27 28 29 30 31 32			
13.28	14		
1 2 3 4 5 6 7 26 27 28 29 30 31 32			
16.33	12		

	1	2	3	4	5	6	27	28	29	30	31	32
19.38					10							
	1	2	3	4	5	28	29	30	31	32		
22.42				8								
	1	2	3	4	29	30	31	32				
25.47				6								
	1	2	3	30	31	32						
28.51				4								
	1	2	31	32								
31.56			2									
	1	32										
34.61			0									

Sample input for CSTRUC

THE FIRST 32 PLIES WILL BE VARIED

FIRST VARIABLE PLY ORIENTATION = 9.000000000E+01

PANEL	EI(I) lb-in**2	GJ(I) lb-in**2	K(I) -
1	.14812E+04	.46653E+04	-.44261E+03
2	.31489E+04	.99181E+04	.82897E+03
3	.93546E+04	.13874E+05	.10751E+04
4	.19597E+05	.18615E+05	.13220E+04
5	.34990E+05	.24344E+05	.15689E+04
6	.56759E+05	.31288E+05	.18150E+04
7	.86329E+05	.39739E+05	.20619E+04
8	.12516E+06	.49959E+05	.23080E+04
9	.17497E+06	.62296E+05	.25549E+04
10	.23752E+06	.77079E+05	.28018E+04

FIRST VARIABLE PLY ORIENTATION = 1.000000000E+02

PANEL	EI(I) lb-in**2	GJ(I) lb-in**2	K(I) -
1	.14409E+04	.42209E+04	.19462E+03
2	.36687E+04	.89732E+04	.20769E+04
3	.97522E+04	.13168E+05	.11490E+04
4	.19662E+05	.18544E+05	-.95911E+03
5	.34452E+05	.25416E+05	-.45765E+04
6	.55282E+05	.34133E+05	-.10065E+05

7	.83505E+05	.45123E+05	-.17837E+05
8	.12050E+06	.58796E+05	-.28324E+05
9	.16791E+06	.75667E+05	-.42028E+05
10	.22738E+06	.96239E+05	-.59465E+05

Sample output for CSTRUC

DEFLCT

This subroutine calculates the torsional deflected shape of a box beam wing given the distributed lift and the torsion flexibility matrix.

SUBROUTINE DEFLCT

c this subroutine calculates the semi-span panels
c torsional (deg) and bending (in.) deflections
c leading edge up and plung up positive

COMMON/DF/NP,Q,H(20),C(20),ZAOA(20),S(20,20),SLOPE(20),SAOA(20)

c NP = number of spanwise panels in semi-span
c Q = dynamic pressure (psi)
c H = y-axis width of panel (in.)
c C = x-axis length of aerodynamic chord line of panel (in.)
c ZAOA = incidence from zero-lift line, includes jugged twist (deg)

c ***** MUST SUPPLY THE TORSION AND BENDING STIFFNESS MATRICES [C] *****

c ***** MUST SUPPLY THE FLEXIBLE LIFT DISTRIBUTION PER UNIT SPAN *****

SUM=0.0

DO 20 I=1,NP

DO 10 J=1,NP

10 SUM=SUM+S(I,J)*SLOPE(J)*Q*H(J)*C(J)/ZAOA(J)

c torsional deformation in degrees, eqn 30 of AFFDL-TR-79-3087

20 SAOA(I)=SUM/(2*ACOS(-1.0))

RETURN

END

PROGRAM DEF

c sample run for subroutine DEFLCT
c present limit twenty semi-span panels

```
COMMON/DF/NP,Q,H(20),C(20),ZAOA(20),S(20,20),SLOPE(20),SAOA(20)

READ (5,*) NP,Q
DO 10 I=1,NP
10 READ (5,*) ZAOA(I),H(I),C(I)
DO 20 I=1,NP
20 READ (5,*) SLOPE(I)
READ (5,*) ((S(I,J),J=1,NP),I=1,NP)

CALL DEFLCT

WRITE (6,*) "PANEL TORSIONAL DEFLECTIONS (deg)"
WRITE (6,*) " POSITIVE LEADING EDGE UP"
WRITE (6,*)
WRITE (6,*) "PANEL 1 IS OUTBOARD"
WRITE (6,*)

DO 30 I=1,NP
30 WRITE (6,*) I,SAOA(I)

END
```

Sample IO program for DEFLCT

10 0.1724

1.0 4.5 9.0
1.0 4.5 12.0
1.0 4.5 15.0
1.0 4.5 18.0
1.0 4.5 21.0
1.0 4.5 24.0
1.0 4.5 27.0
1.0 4.5 30.0
1.0 4.5 33.0
1.0 4.5 36.0

1.320819187E+01
1.851183891E+01
2.194256210E+01
2.430217361E+01
2.584784126E+01
2.671536827E+01
2.701198578E+01
2.685069847E+01
2.637708092E+01
2.582395935E+01

5.491133779E-04	4.016366787E-03	5.804807879E-03	6.779769436E-03
7.069502957E-03	6.762558594E-03	5.973002873E-03	4.742434714E-03
3.113932675E-03	1.136320876E-03	-5.951775238E-04	3.465960734E-03
5.804807879E-03	6.779769436E-03	7.069502957E-03	6.762558594E-03
5.973002873E-03	4.742434714E-03	3.113932675E-03	1.136320876E-03
-1.512221526E-03	2.181915566E-03	5.248665810E-03	6.779769436E-03
7.069502957E-03	6.762558594E-03	5.973002873E-03	4.742434714E-03
3.113932675E-03	1.136320876E-03	-1.950709615E-03	9.793248028E-04
3.883810714E-03	6.220048293E-03	7.069502957E-03	6.762558594E-03
5.973002873E-03	4.742434714E-03	3.113932675E-03	1.136320876E-03
-2.075510565E-03	2.228990197E-04	2.501267474E-03	4.797854926E-03
6.507211830E-03	6.762558594E-03	5.973002873E-03	4.742434714E-03
3.113932675E-03	1.136320876E-03	-1.981792506E-03	-2.218801528E-04
1.522687031E-03	3.281203797E-03	5.041116383E-03	6.198494695E-03
5.973002873E-03	4.742434714E-03	3.113932675E-03	1.136320876E-03
-1.726213144E-03	-4.356959835E-04	8.435694035E-04	2.133063274E-03
3.423580434E-03	4.702845123E-03	5.407503806E-03	4.742434714E-03
3.113932675E-03	1.136320876E-03	-1.343934564E-03	-4.694792442E-04
3.973522689E-04	1.271114685E-03	2.145570237E-03	3.012401052E-03
3.886856604E-03	4.175885580E-03	3.113932675E-03	1.136320876E-03
-8.622845635E-04	-3.614670131E-04	1.349840313E-04	6.354047218E-04
1.136222272E-03	1.632672967E-03	2.133490983E-03	2.633911557E-03
2.546535106E-03	1.136320876E-03	-2.998266136E-04	-1.380913891E-04
2.223375486E-05	1.838408934E-04	3.455760889E-04	5.059011746E-04
6.676365156E-04	8.292436250E-04	9.895686526E-04	5.681604380E-04

Sample input for DEFLCT

PANEL TORSIONAL DEFLECTIONS (deg)
POSITIVE LEADING EDGE UP

PANEL 1 IS OUTBOARD

1	3.20415616
2	6.37642050
3	9.47740364
4	1.245326519E+01
5	1.523586273E+01
6	1.774303436E+01
7	1.988074112E+01
8	2.154567909E+01
9	2.262653542E+01
10	2.300656319E+01

Sample output for DEFLCT

DIVERG

This subroutine calculates the divergence speed for a wing using matrix methods.

SUBROUTINE DIVERG

```

c this subroutine calculates the divergence dynamic pressure (psi)
c and divergence speed (mph) for a wing

COMMON/D/AIS(20,20),S(20,20),QDIV,VDIV,RHO,NP

REAL LAMBDA(20)

c read in data or provide from another subroutine

c      NP = number of panels in wing semi-span
c      RHO = air density at flight condition (lbf*sec**2/ft**4)

c ***** MUST PROVIDE THE INVERTED SYMMETRICAL AIC MATRIX [AIS] *****
c                AND THE WING FLEXIBILITY MATRIX [S]

      DO 30 I=1,NP
      DO 20 J=1,NP
      SUM1=0.0
      DO 10 K=1,NP
10 SUM=SUM+AIS(I,K)*S(K,J)
20 COMB(I,J)=SUM
30 CONTINUE

c ***** MUST PROVIDE SUBROUTINE TO PERFORM EIGENSTRUCTURE *****
c                DECOMPOSITION OF A MATRIX

c eigenvalues in {LAMBDA}, use only real parts if complex
      QDIV=LAMBDA(1)

      DO 40 I=1,NP
      FDIV=LAMBDA(I)
c divergence dynamic pressure (q) is the inverse of the largest eigenvalue
40 IF (FDIV.GE.QDIV) QDIV=FDIV

c divergence q (psi)
      QDIV=1.0/QDIV

c divergence speed (in/sec)**2
      VDIV=2.0*QDIV/(RHO/(12**4))

c test for no divergence (negative divergence velocity)
      IF (VDIV.LT.0.0) VDIV=0.0

c conversion to feet
      VDIV=SQRT(VDIV)/12.0
c conversion to mph
      VDIV=(3600.0*VDIV/5280.0)

      RETURN
      END

```

PROGRAM DIV

```
c sample run for subroutine DIVERG
c present limit twenty semi-span panels

COMMON/D/AIS(20,20),S(20,20),QDIV,VDIV,RHO,NP

READ (5,*) NP,RHO

READ (5,*) ((AIS(I,J),J=1,NP),I=1,NP)
READ (5,*) ((S(I,J),J=1,NP),I=1,NP)

CALL DIVERG

IF (VDIV.LE.0.0) WRITE (6,*) "THIS WING WILL NOT DIVERGE"

WRITE (6,*) "DIVERGENCE DYNAMIC PRESSURE (PSI) = ",QDIV
WRITE (6,*)
WRITE (6,*) "DIVERGENCE SPEED (MPH) = ",VDIV

END
```

Sample IO program for DIVERG

10 0.002308

1.522857380E+01	5.96310043	3.82033515	2.87379861	2.36041355
2.05599952	1.87082624	1.76191103	1.70555520	1.68618894
1.807481766E+01	7.97303772	5.39460516	4.19999790	3.54103684
3.15424109	2.92951870	2.81190491	2.76885939	3.14245343
1.979629707E+01	9.40200710	6.62955093	5.31964207	4.60114527
4.19573450	3.98382759	3.90300393	2.18809867	4.66872692
2.117912865E+01	1.065380573E+01	7.79299164	6.44328308	5.72700071
5.35961246	5.21623898	1.68967009	3.39996672	5.92095947
1.023863792E+01	2.245115471E+01	1.188621807E+01	9.01604748	7.69819355
7.05599117	6.80469275	1.39890170	2.70968294	4.48244715
1.150020123E+01	2.375194168E+01	1.322908020E+01	1.043674183E+01	
9.24757767	8.79599571	1.21933305	2.30112791	3.68471789
8.34255409	1.286012268E+01	2.523128319E+01	1.485822678E+01	
1.228022766E+01	1.140461731E+01	1.10676730	2.05220938	3.21712255
4.74516201	6.81793594	9.76934624	1.450068855E+01	2.713015938E+01
1.711086273E+01	1.506569862E+01	1.03905964	1.90560842	2.94873929
4.28035450	6.02116299	8.35450459	1.162740707E+01	1.677473831E+01
2.999795723E+01	2.095891380E+01	1.00545573	1.83426082	2.82081747
4.06414938	5.66253471	7.75183964	1.055162239E+01	1.448704529E+01
2.069534683E+01	3.609405136E+01			
5.459655076E-04	3.998301458E-03	5.810947623E-03	6.778999232E-03	
7.061231881E-03	6.766046397E-03	5.972181447E-03	4.739457741E-03	
3.114864230E-03	1.136294100E-03	-5.997680128E-04	3.447986674E-03	
5.810947623E-03	6.778999232E-03	7.061231881E-03	6.766046397E-03	
5.972181447E-03	4.739457741E-03	3.114864230E-03	1.136294100E-03	
-1.516926568E-03	2.166524995E-03	5.254826043E-03	6.778999232E-03	
7.061231881E-03	6.766046397E-03	5.972181447E-03	4.739457741E-03	
3.114864230E-03	1.136294100E-03	-1.953933388E-03	9.676259942E-04	
3.889188170E-03	6.219237577E-03	7.061231881E-03	6.766046397E-03	
5.972181447E-03	4.739457741E-03	3.114864230E-03	1.136294100E-03	
-2.079066355E-03	2.126973122E-04	2.504463308E-03	4.796230234E-03	
6.498973817E-03	6.766046397E-03	5.972181447E-03	4.739457741E-03	
3.114864230E-03	1.136294100E-03	-1.984966919E-03	-2.301395871E-04	
1.524688676E-03	3.279517172E-03	5.034342408E-03	6.201970857E-03	
5.972181447E-03	4.739457741E-03	3.114864230E-03	1.136294100E-03	
-1.728197094E-03	-4.414077848E-04	8.453819901E-04	2.132172463E-03	
3.418960609E-03	4.705751780E-03	5.406722426E-03	4.739457741E-03	
3.114864230E-03	1.136294100E-03	-1.345874392E-03	-4.739435390E-04	
3.979874309E-04	1.269918866E-03	2.141848905E-03	3.013780806E-03	
3.885711078E-03	4.172910936E-03	3.114864230E-03	1.136294100E-03	
-8.636832354E-04	-3.643112723E-04	1.350609818E-04	6.344335852E-04	
1.133804792E-03	1.633177511E-03	2.132549649E-03	2.631921787E-03	
2.547440352E-03	1.136294100E-03	-3.001438454E-04	-1.388749224E-04	
2.239414607E-05	1.836632728E-04	3.449319920E-04	5.062012351E-04	
6.674702163E-04	8.287391975E-04	9.900082368E-04	5.681470502E-04	

Sample input for DIVERG

DIVERGENCE DYNAMIC PRESSURE (PSI) - 4.492255151E-01

DIVERGENCE SPEED (MPH) - 1.614281006E+02

Sample output for DIVERG

FLEXROL

This subroutine calculates the aileron effectiveness or helix angle, the location of the center of pressure, and the coefficient of lift divided by the wing incidence for a rigid wing. The inverted anti-symmetric aerodynamic influence coefficient matrix (see AERO1) must be provided. The flexibility matrix (see CFLEX or MFLEX) and the total angle of attack due to aileron deflection (see CAILRN and MAILRN) must be provided.

SUBROUTINE FLEXROL

c this subroutine calculates the aileron effectiveness (helix angle),
c the location of the center of pressure, and the coefficient of lift
c divided by wing incidence (rad.) for a flexible wing

DIMENSION SF(20),XV(20),B(20,20),BI(20,20),FCON(20),FROLL(20)
DIMENSION A(20,20)

COMMON/FR1/AS(20,20),AA(20,20),S(20,20),DALPHA(20),FLIFT,PB2V
COMMON/FR2/XCP,YCP,X(20),Y(20),E(20),H(20),SHAPE(20),CM(20),FL
COMMON/FR3/CMDEL(20),C(20),SLOPE(20),SSPAN,AREA,Q,NP,ZAOA(20)

c NP = number of spanwise panels in semi-span
c AREA = planform area of wing (sq in.)
c SSPAN = semi-span of wing (in.)
c ZAOA = panel incidence from zero-lift line, includes jugged twist
c X = x-axis intercept of panel midchord & reference axis (in.)
c Y = as in X but for y-axis
c E = x-axis distance between panel aerodynamic center and structural
c reference axis (in.)
c H = y-axis width of panel (in.)
c C = x-axis length of aerodynamic chord line of panel (in.)
c Q = dynamic pressure (psi)
c CM = partial derivative of the section lift coefficient wrt
c control deflection divided by the partial wrt AOA
c CMDEL = partial derivative of the section pitching moment
c wrt control deflection
c SHAPE = aileron segment deflection normalized to largest value
c and negative, example:
c -1.0 if segments deflects same amount
c -0.5 if deflects half as much

DO 10 I=1,NP
c XV is x-axis distance to the quarter-chord of panel
10 XV(I)=X(I)-E(I)

NCT=0

c **** MUST PROVIDE THE ANTI-SYMMETRIC AIC MATRIX [AA] ****
c first time through

c **** MUST PROVIDE THE SYMMETRIC AIC MATRIX [AS] ****
c second time through

1000 DO 30 I=1,NP
DO 20 J=1,NP
IF (NCT.LE.0) A(I,J)=AA(I,J)
20 IF (NCT.GT.0) A(I,J)=AS(I,J)
30 CONTINUE

c eqn 32 of AFFDL-TR-79-3087
DO 50 I=1,NP
DO 40 J=1,NP

c **** MUST PROVIDE THE FLEXIBILITY MATRIX [S] ****

40 B(I,J)=A(I,J)/Q-S(I,J)
50 CONTINUE

```

c **** MUST NOW PROVIDE MEANS TO INVERT [B] for [BI] ****
      DO 70 I=1,NP
      SUM=0.0

c following equations for left wing only
      DO 60 K=1,NP
c eqn 34 of AFFDL-TR-79-3087
      60 SUM=SUM+BI(I,K)

c SF is the lift per unit span per rad. of wing incidence
      70 SF(I)=SUM

      SUM1=0.0
      SUM2=0.0
      SUM3=0.0

c following for eqn 38 of AFFDL-TR-79-3087 for wing
      DO 80 I=1,NP
      SUM1=SUM1+SF(I)*XV(I)*H(I)
      SUM2=SUM2+SF(I)*Y(I)*H(I)
      80 SUM3=SUM3+SF(I)*H(I)

c FLIFT is the coefficient of lift divided by q*AREA*AOA
c CL alpha, eqn 38 of AFFDL-TR-79-3087
      FLIFT = SUM3/(Q*AREA)

c cartesian coordinates of center of pressure, non-rotated axis
      XCP=SUM1/SUM3
      YCP=SUM2/SUM3

      DO 100 I=1,NP
      SUM1=0.0
      SUM2=0.0

      DO 90 K=1,NP
c equation 44 from AFFDL-TR-79-3087
c denominator
      SUM1=SUM1+BI(I,K)*Y(K)/SSPAN

c *** MUST PROVIDE TOTAL AOA DUE TO AILERON DEFLECTION [DALPHA] ***
c numerator
      90 SUM2=SUM2+BI(I,K)*DALPHA(K)

c contribution from roll itself
      FROLL(I)=SUM1
c contribution from control deflection
      100 FCON(I)=SUM2

      SUM1=0.0
      SUM2=0.0

      DO 110 I=1,NP
c roll-in-damping, apparent AOA change due to the rolling moment
c eqn 41 of AFFDL-TR-79-3087
      SUM1=SUM1+FROLL(I)*Y(I)*H(I)
c effect of apparent AOA change due to the roll
c eqn 44 of AFFDL-TR-79-3087
      110 SUM2=SUM2+FCON(I)*Y(I)*H(I)

```

```

      DO 120 I=1,NP
c   panel lift per unit span divided by C*Q*AOA, CL alpha
      SLOPE(I)=SF(I)/(Q*H(I)*C(I))
c   total flexible wing lift on semi-span (lbf)
      120 FL=FL+SLOPE(I)*Q*H(I)*C(I)/ZAOA(I)

c   PB/2V is the wing aileron effectiveness (helix angle)
c   no good first time through, must use anti-symmetric [AIC]
      IF (NCT.LE.0) PB2V=-SUM2/SUM1

      IF (NCT.GT.0) GO TO 130
      NCT=NCT+1
      GO TO 1000

130 RETURN
      END

```


PROGRAM FLEX

c sample run for subroutine FLEXROL
c present limit twenty semi-span panels

```

COMMON/FR1/AS(20,20),AA(20,20),S(20,20),DALPHA(20),FLIFT,PB2V
COMMON/FR2/XCP,YCP,X(20),Y(20),E(20),H(20),SHAPE(20),CM(20),FL
COMMON/FR3/CMDEL(20),C(20),SLOPE(20),SSPAN,AREA,Q,NP,ZAOA(20)

READ (5,*) NP,SSPAN,AREA,Q
DO 10 I=1,NP
  READ (5,*) X(I),Y(I),H(I),E(I),C(I)
  READ (5,*) ZAOA(I),SHAPE(I),CM(I),CMDEL(I)
10 READ (5,*) DALPHA(I)

  READ (5,*) ((S(I,J),J=1,NP),I=1,NP)
  READ (5,*) ((AS(I,J),J=1,NP),I=1,NP)
  READ (5,*) ((AA(I,J),J=1,NP),I=1,NP)

CALL FLEXROL

WRITE (6,*) "FLEXIBLE WING RESULTS"
WRITE (6,*)
WRITE (6,*) "Pb/2V = ",PB2V
WRITE (6,*)
WRITE (6,*) "CENTER OF PRESSURE LOCATION (inches)   X = ",XCP
WRITE (6,*) "                                           Y = ",YCP
WRITE (6,*)
WRITE (6,*) "CL alpha = ",FLIFT
WRITE (6,*)
WRITE (6,*) "TOTAL LIFT ON SEMI-SPAN (lbf) = ",FL
WRITE (6,20)

DO 30 I=1,NP
30 WRITE (6,*) I,SLOPE(I)

20 FORMAT (/33HPANEL LIFT PER UNIT SPAN (LBF/IN)
1/19HPANEL 1 IS OUTBOARD/)

END

```

Sample IO program for FLEXROL

10 45.0 1012.5 0.1724

14.22 42.75 4.5 1.866 9.0
 1.0 -1.0 0.5854 -0.64
 -.1540

12.72 38.25 4.5 2.657 12.0
 1.0 -1.0 0.5854 -0.64
 -.1641

11.23 33.75 4.5 3.447 15.0
 1.0 -1.0 0.5854 -0.64
 -.1838

9.73 29.25 4.5 4.237 18.0
 1.0 -1.0 0.5854 -0.64
 -.2146

8.23 24.75 4.5 5.028 21.0
 1.0 -1.0 0.5854 -0.64
 -.2581

6.74 20.25 4.5 5.818 24.0
 1.0 -1.0 0.5854 -0.64
 -.3160

5.24 15.75 4.5 6.609 27.0
 1.0 0.0 0.0 0.0
 .2022

3.74 11.25 4.5 7.399 30.0
 1.0 0.0 0.0 0.0
 .1370

2.25 6.75 4.5 8.189 33.0
 1.0 0.0 0.0 0.0
 .0785

0.75 2.25 4.5 8.980 36.0
 1.0 0.0 0.0 0.0
 .0253

5.459655076E-04	3.998301458E-03	5.810947623E-03	6.778999232E-03
7.061231881E-03	6.766046397E-03	5.972181447E-03	4.739457741E-03
3.114864230E-03	1.136294100E-03	-5.997680128E-04	3.447986674E-03
5.810947623E-03	6.778999232E-03	7.061231881E-03	6.766046397E-03
5.972181447E-03	4.739457741E-03	3.114864230E-03	1.136294100E-03
-1.516926568E-03	2.166524995E-03	5.254826043E-03	6.778999232E-03
7.061231881E-03	6.766046397E-03	5.972181447E-03	4.739457741E-03
3.114864230E-03	1.136294100E-03	-1.953933388E-03	9.676259942E-04
3.889188170E-03	6.219237577E-03	7.061231881E-03	6.766046397E-03
5.972181447E-03	4.739457741E-03	3.114864230E-03	1.136294100E-03
-2.079066355E-03	2.126973122E-04	2.504463308E-03	4.796230234E-03
6.498973817E-03	6.766046397E-03	5.972181447E-03	4.739457741E-03
3.114864230E-03	1.136294100E-03	-1.984966919E-03	-2.301395871E-04
1.524688676E-03	3.279517172E-03	5.034342408E-03	6.201970857E-03
5.972181447E-03	4.739457741E-03	3.114864230E-03	1.136294100E-03
-1.728197094E-03	-4.414077848E-04	8.453819901E-04	2.132172463E-03
3.418960609E-03	4.705751780E-03	5.406722426E-03	4.739457741E-03
3.114864230E-03	1.136294100E-03	-1.345874392E-03	-4.739435390E-04
3.979874309E-04	1.269918866E-03	2.141848905E-03	3.013780806E-03
3.885711078E-03	4.172910936E-03	3.114864230E-03	1.136294100E-03
-8.636832354E-04	-3.643112723E-04	1.350609818E-04	6.344335852E-04
1.133804792E-03	1.633177511E-03	2.132549649E-03	2.631921787E-03
2.547440352E-03	1.136294100E-03	-3.001438454E-04	-1.388749224E-04
2.239414607E-05	1.836632728E-04	3.449319920E-04	5.062012351E-04
6.674702163E-04	8.287391975E-04	9.900082368E-04	5.681470502E-04
7.488431782E-02	-2.213571034E-02	-4.105357453E-03	-1.709607313E-03

-9.505109047E-04	-6.211501313E-04	-4.542543320E-04	-3.640271316E-04
-3.169882402E-04	-2.991427900E-04	-2.026449889E-02	7.310753316E-02
-2.254936099E-02	-4.232498351E-03	-1.769537688E-03	-9.910688968E-04
-6.576376036E-04	-4.941440420E-04	-4.132204922E-04	-3.824108280E-04
-3.159705782E-03	-2.144304849E-02	7.224911451E-02	-2.282596938E-02
-4.340040497E-03	-1.831214526E-03	-1.041683601E-03	-7.114530308E-04
-5.611407105E-04	-5.048694438E-04	-1.208507689E-03	-3.489161376E-03
-2.213056944E-02	7.176364958E-02	-2.302692458E-02	-4.440150689E-03
-1.904600882E-03	-1.116692321E-03	-8.058168460E-04	-6.948831142E-04
-6.441903533E-04	-1.327946549E-03	-3.761260305E-03	-2.256543562E-02
7.144998759E-02	-2.319225296E-02	-4.551127553E-03	-2.013115445E-03
-1.255175099E-03	-1.011421205E-03	-4.118355573E-04	-7.054977468E-04
-1.445620786E-03	-3.987679724E-03	-2.287047543E-02	7.121116668E-02
-2.336172760E-02	-4.714160692E-03	-2.226935467E-03	-1.593833440E-03
-2.974603558E-04	-4.540551163E-04	-7.748492062E-04	-1.567144762E-03
-4.190979991E-03	-2.312541381E-02	7.097027451E-02	-2.361375093E-02
-5.066295154E-03	-2.841468900E-03	-2.358799975E-04	-3.341944830E-04
-5.093278596E-04	-8.624911425E-04	-1.710914192E-03	-4.415410105E-03
-2.342718095E-02	7.057461888E-02	-2.424692363E-02	-6.361118052E-03
-2.023099660E-04	-2.737941395E-04	-3.898006398E-04	-5.945017911E-04
-9.990828112E-04	-1.937676920E-03	-4.794762004E-03	-2.407972515E-02
6.926412880E-02	-2.783496864E-02	-1.860412158E-04	-2.462229168E-04
-3.392344515E-04	-4.921636428E-04	-7.643046556E-04	-1.301029930E-03
-2.521812217E-03	-6.071793847E-03	-2.766152285E-02	4.769547656E-02
7.493592799E-02	-2.207652479E-02	-4.036894534E-03	-1.629674225E-03
-8.562180446E-04	-5.086301244E-04	-3.182522196E-04	-1.972638274E-04
-1.091756567E-04	-3.539262252E-05	-2.020737715E-02	7.317356765E-02
-2.247230336E-02	-4.141625483E-03	-1.661106711E-03	-8.599693538E-04
-4.967618152E-04	-2.933932119E-04	-1.578995143E-04	-5.052468987E-05
-3.096119268E-03	-2.136890590E-02	7.233648747E-02	-2.272174507E-02
-4.214034881E-03	-1.676527201E-03	-8.484622231E-04	-4.652725765E-04
-2.402731334E-04	-7.543923857E-05	-1.137308544E-03	-3.405324416E-03
-2.203054412E-02	7.188440114E-02	-2.287869528E-02	-4.254896659E-03
-1.668259036E-03	-8.079282125E-04	-3.911212552E-04	-1.193196222E-04
-5.639339215E-04	-1.232395065E-03	-3.645892255E-03	-2.242389135E-02
7.162687927E-02	-2.296640165E-02	-4.255543929E-03	-1.614875277E-03
-6.998337340E-04	-2.038015082E-04	-3.206946130E-04	-5.955939414E-04
-1.310929772E-03	-3.819461213E-03	-2.265570126E-02	7.149253786E-02
-2.298168652E-02	-4.181896336E-03	-1.447890070E-03	-3.879787691E-04
-1.930344588E-04	-3.263350227E-04	-6.155532319E-04	-1.363928546E-03
-3.924718592E-03	-2.276524901E-02	7.147648931E-02	-2.286828309E-02
-3.902131226E-03	-8.733080467E-04	-1.151710312E-04	-1.839625475E-04
-3.180191270E-04	-6.120912149E-04	-1.372133847E-03	-3.938189708E-03
-2.272072062E-02	7.168778777E-02	-2.234158292E-02	-2.666530665E-03
-6.119107275E-05	-9.458554268E-05	-1.557856158E-04	-2.783295058E-04
-5.535153905E-04	-1.275758259E-03	-3.743321169E-03	-2.225571312E-02
7.286155969E-02	-1.883696206E-02	-1.895726200E-05	-2.885164577E-05
-4.648292452E-05	-8.038311353E-05	-1.520627993E-04	-3.228549322E-04
-8.024410927E-04	-2.610660391E-03	-1.881445944E-02	9.432605654E-02

Sample input for FLEXROL

FLEXIBLE WING RESULTS

Pb/2V = 1.407640129E-01

CENTER OF PRESSURE LOCATION (inches) X = -3.70381021
Y = 1.116182232E+01

CL alpha = -1.870626068E+02

TOTAL LIFT ON SEMI-SPAN (lbf) = 2.975453906E+04

PANEL LIFT PER UNIT SPAN (LBF/IN)
PANEL 1 IS OUTBOARD

1	1.143178567E-01
2	4.805943668E-01
3	4.774543643E-01
4	3.827359378E-01
5	2.355925441E-01
6	5.075030029E-02
7	4.451088607E-02
8	-3.115916138E+02
9	-2.292837352E-01
10	-7.230437398E-01

Sample output for FLEXROL

FLUTR

This program performs simple flutter computations using the dynamic subroutines presented in this Appendix. No example is output is provided for this program.

PROGRAM FLUTR

c sample run for program FLUTR
c present limit 40 DOF/panels combinations

COMMON/FL1/N,VI,VE,RHO,OHMT,RNF(40),EVECT(40,40),MOD(20,20)
COMMON/FL2/RM(20,20),RK(20,20),A(20,20),OHM(20),V,XA(20),SC(20)
COMMON/FL3/RMS(20),OHMH(20),OHMA(20),RA(20),AH(20),OOHM

COMPLEX A

c N - number of DOFs multiplied by number of nodes,
dimension of square operator matrices
c VE - final velocity for analysis (mph)
c VI - velocity increment (mph)
c RHO - air density (lbf sec**2/ft**4)
c OHMT - tolerance on frequency match
c SC - section semi-chord (in.)
c AH - a sub h, distance of elastic axis from section mid-chords
c RMS - section mass per unit length
c OHMH - omega h, uncoupled natural frequency of bending
(rad/sec)
c OHMA - as above but for torsion

READ (5,*) N,NM
READ (5,*) VE,VI,RHO,OHMT
DO 10 I=1,N
READ (5,*) SC(I),AH(I),XA(I),RA(I)
10 READ (5,*) RMS(I),OHMH(I),OHMA(I)

c write header
IF (NM.EQ.1) WRITE (6,*) " VG-METHOD RESULTS"
IF (NM.EQ.2) WRITE (6,*) " K-METHOD RESULTS"
IF (NM.EQ.3) WRITE (6,*) " PK-METHOD RESULTS"
WRITE (6,*)

IF (NM.EQ.1) CALL VGFLUTR
IF (NM.EQ.2) CALL KFLUTR
IF (NM.EQ.3) CALL PKFLUTR

DO 20 I=1,N

c conversion to Hertz
RNF(J)=RNF(J)/(2*ACOS(-1.0))
WRITE (6,*) " NATURAL FREQUENCY (Hz) ",J," = ",RNF(J)
WRITE (6,*)

WRITE (6,*) " MODE ",J," = "
DO 30 J=1,N
30 WRITE (6,*) " ",EVECT(I,J)
20 WRITE (6,*)

END

FUNG

This subroutine calculates tri-diagonal inertia, stiffness and unsteady aerodynamic operators using simple two-dimensional theory.

SUBROUTINE FUNG

c this subroutine creates tri-diagonal operator matrices
c by equations from FUNG p. 217, 2-dimensional, incompressible

DIMENSION RMU(20)

COMMON/O1/RM(20,20),RK(20,20),A(20,20),N,RHO,OOHM,V,XA(20),SC(20)
COMMON/O2/RMS(20),OHMH(20),OHMA(20),RA(20),AH(20)

COMPLEX A,C,CF1,CF2

c N - number of nodes in semi-span
c RHO - air density (lbf sec**2/ft**4)
c XA - x alpha, (S/mb), distance of section center of mass from
c elastic axis in percent semi-chord, positive aft
c RA - r alpha, (sqrt[I alpha/mb**2]), radius of gyration of
c section about elastic axis in percent semi-chords
c SC - section semi-chord (in.)
c AH - a sub h, distance of elastic axis from section mid-chord
c in percent semi-chord, positive aft
c RMS - section mass per unit length
c OHMH - omega h, uncoupled natural frequency of bending (rad/sec)
c OHMA - as above but for torsion (rad/sec)
c OOHM - frequency of case being investigated (rad.)
c V - velocity of case being investigated (mph)
c NOTE: enter node data from tip inboard

c defining pi
PI=ACOS(-1.0)

c conversion to inches
V=V*12*5280/360
RHO=RHO/(12**4)

c ***** MASS *****

NN=1.0

DO 20 I=1,N

c for tri-diagonalization
IF(I.EQ.1) GO TO 10
NN=NN+2

c mass ratio
10 RMU(I)=RMS(I)/(PI*RHO*SC(I)**2)

RM(NN,NN)=-RMU(I)
RM(NN,NN+1)=-RMU(I)*XA(I)
RM(NN+1,NN)=RM(NN,NN+1)
20 RM(NN+1,NN+1)=-RMU(I)*RA(I)**2

c ***** STIFFNESS *****

NN=1.0

c setting up stability determinant
DO 40 I=1,N


```

c   for tri-diagonalization
      IF(I.EQ.1) GO TO 30
      NN=NN+2

      30 RK(NN,NN)=RMU(I)*(OHMH(I)**2)
      40 RK(NN+1,NN+1)=RA(I)*RMU(I)*(OHMA(I)**2)

c       **** AERODYNAMICS ****

      IF (V.EQ.0.0) GO TO 70

      NN=1.0

      DO 60 I=1,N

c   for tri-diagonalization
      IF(I.EQ.1) GO TO 50
      NN=NN+2

c   reduced frequency
      50 RKK=OOHM*SC(I)/V

c   C is Theodorsen function (k less than 0.5)
      CF1=CMPLX(1,-0.0455/RKK)
      CF2=CMPLX(1,-0.3/RKK)
      C=1-(0.165/CF1)-(0.335/CF2)

      A(NN,NN)=CMPLX(-1.0,2*C/RKK)
      A(NN,NN+1)=CMPLX(AH(I)+2*C/(RKK**2),1/RKK+2*C*(0.5-AH(I))/RKK)
      A(NN+1,NN)=CMPLX(AH(I),-2*C*(0.5+AH(I))/RKK)
      A(NN+1,NN+1)=-(AH(I)**2)-1/8+2*C*(0.5+AH(I))*(0.5-AH(I))/RKK
      A(NN+1,NN+1)=A(NN+1,NN+1)+CMPLX(0,-2*C*(0.5+AH(I))/(RKK**2))
      60 A(NN+1,NN+1)=A(NN+1,NN+1)+CMPLX(0,(0.5-AH(I))/RKK)

      70 RETURN
      END

```

PROGRAM FG

c sample run for subroutine FUNG
c present limit ten semi-span nodes

COMMON/O1/RM(20,20),RK(20,20),A(20,20),N,RHO,OOHM,V,XA(20),SC(20)
COMMON/O2/RMS(20),OHMH(20),OHMA(20),RA(20),AH(20)

COMPLEX A

READ (5,*) N,RHO,OOHM,V
DO 10 I=1,N
READ (5,*) SC(I),AH(I),XA(I),RA(I)
10 READ (5,*) RMS(I),OHMH(I),OHMA(I)

CALL FUNG

NN=2*N

WRITE (6,*) ((RM(I,J),J=1,NN),I=1,NN)
WRITE (6,*)
WRITE (6,*) ((RK(I,J),J=1,NN),I=1,NN)
WRITE (6,*)
WRITE (6,*) ((A(I,J),J=1,NN),I=1,NN)

END

Sample IO Program for FUNG

GEOM

This subroutine calculates a number of planform parameters often required in the other subroutines herein provided.

SUBROUTINE GEOM

c this subroutine determines general parameters for a
c linearly tapered planform

COMMON/G1/CR,ER,SSPAN,TAPER,AREA,SWEEPR,CSR,NP
COMMON/G2/H(20),X(20),Y(20),C(20),CS(20),E(20),SWEEP(20)

c NP = number of panels in semi-span
c CR = wing root aerodynamic chord (in.)
c CSR = approximate structural chord at panel center (in.)
c ER = distance between reference axis and aerodynamic
c center at wing root, measured streamwise (in.)
c SSPAN = semi-span measured perpendicular to centerline (in.)
c SWEEPR = sweep of reference axis from Y-axis, positive aft (deg)
c at root
c TAPER = taper ratio

c dividing wing into equal width panels
AH=SSPAN/NP

DO 10 I=1,NP
c sweep of reference axis for panel
SWEEP(I)=SWEEPR
c panel widths
H(I)=AH

c change to radians
SD=SWEEPR*ACOS(-1.0)/180.0

c intercept of panel midchord and reference axis
c linear taper planform
Y(I)=(NP-I)*AH+AH/2.0
X(I)=Y(I)*TAN(SD)

c eqn B-58 of AFFDL-TR-78-116
c linear taper planform
F=1.0-(Y(I)/SSPAN)*(1.0-TAPER)
c aerodynamic chord at center of panel (linear taper)
C(I)=CR*F

F=1.0-(Y(I)/SSPAN)*(1.0-TAPER)/COS(SD)
c structural chord at panel center (linear planform taper)
CS(I)=CSR*F
c distance from reference axis to a.c. (same ratio as root)
E(I)=ER*F

10 SUM=SUM+H(I)*C(I)

c planform area as determined from sum of rectangular panels
AREA=SUM

RETURN
END

PROGRAM GM

```
c sample run for subroutine GEOM
c present limit twenty semi-span panels

COMMON/G1/CR,ER,SSPAN,TAPER,AREA,SWEEPR,CSR,NP
COMMON/G2/H(20),X(20),Y(20),C(20),CS(20),E(20),SWEEP(20)

READ (5,*) NP,CR,CSR,ER
READ (5,*) SSPAN,SWEEPR,TAPER

WRITE (6,20)

CALL GEOM

DO 10 I=1,NP
10 WRITE (6,30) I,X(I),Y(I),C(I),CS(I),H(I),E(I),SWEEP(I)

WRITE (6,*) "SEMI-SPAN PLANFORM AREA (SQ. INCHES) = ",AREA

20 FORMAT (31X,16HALL UNITS INCHES,/,5HPANEL,4X,4HX(I),6X,4HY(I)
1,6X,4HC(I),6X,5HCS(I),6X,4HH(I),6X,4HE(I),4X,6HSWP(I),/)
30 FORMAT (2X,12,7(1X,F9.2),/)
```

END

Sample IO program for GEOM

10 37.5 36.13 9.375
45.0 18.4 0.2

Sample input for GEOM

ALL UNITS INCHES							
PANEL	X(I)	Y(I)	C(I)	CS(I)	H(I)	E(I)	SWP(I)
1	14.22	42.75	9.00	7.19	4.50	1.87	18.40
2	12.72	38.25	12.00	10.24	4.50	2.66	18.40
3	11.23	33.75	15.00	13.28	4.50	3.45	18.40
4	9.73	29.25	18.00	16.33	4.50	4.24	18.40
5	8.23	24.75	21.00	19.38	4.50	5.03	18.40
6	6.74	20.25	24.00	22.42	4.50	5.82	18.40
7	5.24	15.75	27.00	25.47	4.50	6.61	18.40
8	3.74	11.25	30.00	28.51	4.50	7.40	18.40
9	2.25	6.75	33.00	31.56	4.50	8.19	18.40
10	.75	2.25	36.00	34.61	4.50	8.98	18.40

HALF-SPAN AREA = 1012.5000 SEMI-SPAN = 45.0000

Sample output for GEOM

KFLUTR

This subroutine performs iterative flutter computations given the aeroelastic operators using the k-method. No IO program or sample is appropriate for this subroutine.

SUBROUTINE KFLUTR

c this program performs simple flutter computations by the K-method
c assumes no free-body modes in operators

DIMENSION RM(40,40),RK(40,40),A(40,40),RKI(40,40),OHM(40)

COMMON/FL2/N,RC,VS,VI,VE,OHMT,RNF(40),EVECT(40,40)

COMPLEX A,RMAT(40,40),RLAMBDA(40)

c N - number of DOFs multiplied by number of nodes,
c dimension of square operator matrices
c RC - root aerodynamic chord (in.)
c VS - starting velocity (mph), greater than zero
c VE - final velocity for analysis (mph)
c VI - velocity increment (mph)
c OHMT - tolerance on frequency for match

c *** PROVIDE DATA AND SUBROUTINES TO CALCULATE OPERATORS ***
c INERTIA [RM], STRUCTURE [RK], AND AERODYNAMIC [A]

CALL STRUC
CALL MASS

c *** PROVIDE MEANS FOR INVERTING [RK] FOR [RKI] ***

CALL NFREQ

c *** PRODUCES ARRAY OF NATURAL FREQUENCIES [RNF] ***
c AND MATRIX OF NATURAL MODES IN DESCENDING ORDER [EVECT]

c top of velocity loop
DO 90 I=VS,VE,VI

c velocity
V=I

c top of mode loop
DO 80 J=1,N

MODE=J

c using natural frequency as initial guess
IF (V.EQ.VS) OHM(MODE)=RNF(MODE)

c top of frequency loop, 10000 iterations permitted
DO 60 KK=1,10000

c reduced frequency, k
RKK=RC*OHM(MODE)/(2*V)

c [A] expecting k as principal variable
CALL AERO

c replace operators with modal form
CALL MODAL

DO 20 L=1,N
DO 10 K=1,N

10 RMAT(L,K)=(1/OHM(MODE))*A(L,K)-RM(L,K)


```

20 CONTINUE
c premultiply by inverse of [RK]
    DO 50 L=1,N
    DO 40 K=1,N
    SUM=0.0
    DO 30 M=1,N
    30 SUM=SUM+RKI(L,M)*RMAT(M,K)
    40 RMAT(L,K)=SUM
    50 CONTINUE

c *** PROVIDE MEANS FOR PERFORMING AN EIGENVALUE DECOMPOSITION ***
c      ON COMPLEX MATRIX [RMAT]

c {RLAMBDA} is array of eigenvalues in descending order
c each has form (1/ohm**2 + i g/ohm**2)

    OHML=SQRT(1/REAL(RLAMBDA(MODE)))
    DIF=ABS(OHML-OHM(MODE))

c check for suitable match of frequency
    IF (DIF.LE.OHMT) GO TO 70

    60 OHM(MODE)=OHML

    WRITE (6,*) "(NO CONVERGENCE FOR MODE ",MODE," )"
    GO TO 80

c solving for structural damping
    70 G=AIMAG(RLAMBDA(MODE))/REAL(RLAMBDA(MODE))

    WRITE (6,*) "Mode ",J,"    Vel. (MPH) = ",V,"    g = ",G,
    1"    freq. = ",OHM(MODE)

    80 CONTINUE

    90 CONTINUE

    RETURN
    END

```

PROGRAM K

```
c sample input program for subroutine KFLUTR
c present limit 40 DOF/panels combinations

COMMON/FL2/N,RC,VS,VI,VE,OHMT,RNF(40),EVECT(40,40)

READ (5,*) N,RC
READ (5,*) VS,VE,VI,OHMT

c write header
WRITE (6,*) "                K-METHOD RESULTS"
WRITE (6,*)

CALL KFLUTR

DO 10 I=1,N
WRITE (6,*) "    NATURAL FREQUENCY ",J," = ",RNF(J)
WRITE (6,*)

WRITE (6,*) "    EIGENVECTOR ",J," = "
DO 20 J=1,N
20 WRITE (6,*) "                ",EVECT(I,J)
10 WRITE (6,*)

END
```

Sample IO program for KFLUTR

MAILRN

This subroutine performs the same task as CAILRN but for a metallic wing.

SUBROUTINE MAILRN

c this subroutine calculates the change in a metallic wing AOA
c resulting from a one radian change in aileron deflection
c left wing only

DIMENSION COSMAT(20),SINMAT(20),ALPHAD(20),AALPHA(20)
DIMENSION EP(20,20),EI0(20,20),EI3(20,20)

COMMON/M1/NP,Q,CM(20),CMDEL(20),SHAPE(20),SWEEP(20)
COMMON/M2/H(20),EI(20),GJ(20),C(20),E(20,20),DALPHA(20)

c NP = number of spanwise panels in wing semi-span
c Q = dynamic pressure for flight condition (psi)
c SHAPE = deflection of aileron segment on panel, negative
c and normalized to that with the greatest deflection
c -1.0 if deflects same amount
c -0.5 if deflects half as much
c CM = partial derivative of section lift coefficient wrt
c control deflection divided by the partial wrt AOA
c CMDEL = partial derivative of pitching moment wrt control deflection
c of aileron segment on panel
c H = y-axis width of panel (in.)
c C = aerodynamic chord at middle of panel (in.)
c SWEEP = sweep of structural reference axis of panel (deg)
c EI = bending stiffness of wing box beam (psi)
c GJ = torsional stiffness of wing box beam (psi)

DO 10 I=1,NP
c change to radians
SWP=SWEEP(I)*ACOS(-1.0)/180.0
c diagonal terms of eqns B23 and B24 of NACA TN 3030
COSMAT(I)=COS(SWP)
10 SINMAT(I)=SIN(SWP)

c initializing matrices
DO 30 I=1,NP
DO 20 J=1,NP
E(I,J)=0.0
EI0(I,J)=0.0
20 EP(I,J)=0.0
30 CONTINUE

NPM1=NP-1

c constructing [I0] matrix, page 88 of NACA TN 3030
c upper triangular terms
DO 50 I=1,NPM1
II=I+1
DO 40 J=II,NP
40 EI0(I,J)=1.0
50 CONTINUE
c diagonal terms
DO 60 I=1,NP
60 EI0(I,I)=0.500

c [I3] of page 88 of NACA TN 3030 is just transpose of [I0]
DO 80 I=1,NP
DO 70 J=1,NP
70 EI3(I,J)=EI0(J,I)

AD-A188 855

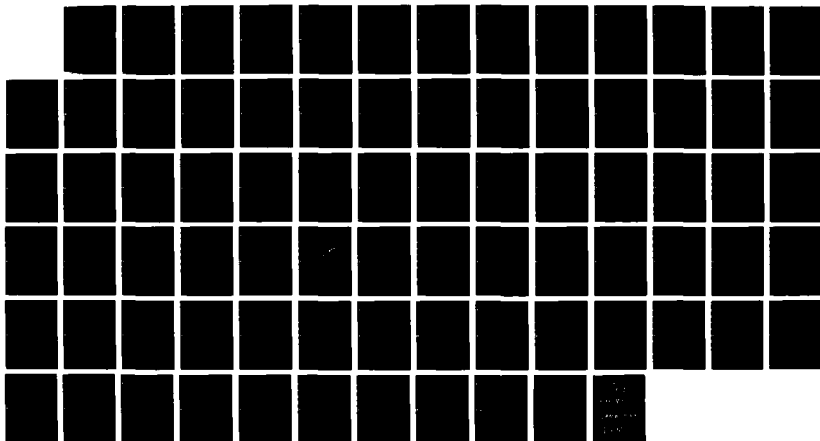
DESIGN OF AN AEROELASTIC COMPOSITE WING WIND TUNNEL
MODEL(U) AIR FORCE INST OF TECH WRIGHT-PATTERSON AFB OH
SCHOOL OF ENGINEERING W J NORTON DEC 87
AFIT/GAE/AA/87D-15

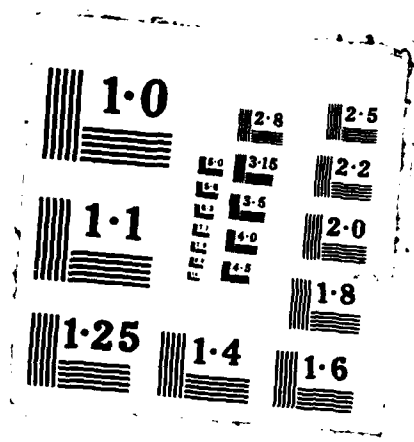
3/3

UNCLASSIFIED

F/G 1/3

NL





```

80 CONTINUE

c eqn F6 of NACA TN 3030
DO 90 I=1,NP
  E(I,I)=H(I)*SINMAT(I)*SINMAT(I)/(COSMAT(I)*EI(I))
90 E(I,I)=E(I,I)+H(I)*COSMAT(I)/GJ(I)

c pre-multiply by [I0]
DO 120 I=1,NP
  DO 110 J=1,NP
    SUM1=0.0
    DO 100 K=1,NP
      100 SUM1=SUM1+EIO(I,K)*E(K,J)
    110 EP(I,J)=SUM1
  120 CONTINUE

c post-multiply by [I3]
DO 150 I=1,NP
  DO 140 J=1,NP
    SUM1=0.0
    DO 130 K=1,NP
      130 SUM1=SUM1+EP(I,K)*EI3(K,J)
    140 E(I,J)=SUM1
  150 CONTINUE

  DO 170 I=1,NP
    DO 160 J=1,NP
      160 E(I,J)=E(I,J)*H(J)*(C(J)**2)
    170 CONTINUE

  DO 190 I=1,NP
    SUM1=0.0
    DO 180 J=1,NP
      180 SUM1=SUM1+E(I,J)*CMDEL(J)*SHAPE(J)

c ALPHAD is change in AOA due to change in section pitching moment
c from twist produced by one radian aileron deflection
c eqn C-8 of AFFDL-TR-79-3087
190 ALPHAD(I)=Q*SUM1

c AALPHA is the apparent change in AOA of wing section due to one radian
c aileron deflection (change in chamber of mean chord line)
c eqn 39 from AFFDL-TR-3087
DO 200 I=1,NP
  AALPHA(I)=SHAPE(I)*CM(I)

c DALPHA is the total AOA change due to one rad. change in aileron deflection
c eqn 39 from AFFDL-TR-79-3087
200 DALPHA(I)=ALPHAD(I)+AALPHA(I)

RETURN
END

```

PROGRAM MLN

c sample run for subroutine MAILRN
c present limit twenty semi-span panels

```
COMMON/M1/NP,Q,CM(20),CMDEL(20),SHAPE(20),SWEEP(20)
COMMON/M2/H(20),EI(20),GJ(20),C(20),E(20,20),DALPHA(20)

READ (5,*) NP,Q
DO 10 I=1,NP
READ (5,*) C(I),H(I),EI(I),GJ(I)
10 READ (5,*) SWEEP(I),CM(I),CMDEL(I),SHAPE(I)

WRITE (6,*) "MAILRN RESULTS"
WRITE (6,*)
WRITE (6,*) "PANEL", "      ", "DALPHA"

CALL MAILRN

DO 20 I=1,NP
20 WRITE (6,*) I,DALPHA(I)

END
```

Sample IO program for MAILRN

10	.1724		
9.0	4.5	.17478E+06	.56720E+05
18.4	0.5854	-0.64	-1.0
12.0	4.5	.17478E+06	.56720E+05
18.4	0.5854	-0.64	-1.0
15.0	4.5	.17478E+06	.56720E+05
18.4	0.5854	-0.64	-1.0
18.0	4.5	.17478E+06	.56720E+05
18.4	0.5854	-0.64	-1.0
21.0	4.5	.17478E+06	.56720E+05
18.4	0.5854	-0.64	-1.0
24.0	4.5	.17478E+06	.56720E+05
18.4	0.5854	-0.64	-1.0
27.0	4.5	.17478E+06	.56720E+05
18.4	0.5854	-0.64	-1.0
30.0	4.5	.17478E+06	.56720E+05
18.4	0.5854	-0.64	-1.0
33.0	4.5	.17478E+06	.56720E+05
18.4	0.5854	-0.64	-1.0
36.0	4.5	.17478E+06	.56720E+05
18.4	0.5854	-0.64	-1.0

Sample input for MAILRN

MAILRN RESULTS

PANEL	DALPHA
1	1.064244509E-01
2	1.026782990E-01
3	9.318208694E-02
4	7.479965687E-02
5	4.369765520E-02
6	-4.654288292E-03
7	-7.548326254E-02
8	-1.747136116E-01
9	-3.089663982E-01
10	-4.855598211E-01

Sample output for MAILRN

MDIVRG

This subroutine performs the same task as CDIVRG but for a metallic wing.

SUBROUTINE MDIVRG

c this subroutine calculates the divergence dynamic pressure (psi)
c and divergence speed (mph) for a metallic wing

COMMON/MD/QDIV,VDIV,RHO,A0,SWEEP,RL,TR,C,EI,GJ,E,AR

c RHO = air density at flight condition (lbf*sec**2/ft**4)
c A0 = 2-dimensional section lift-curve slope for section,
c same full span
c SWEEP = sweep of wing reference axis, positive aft (deg.)
c RL = length of semi-span along reference axis (in.)
c TR = taper ratio of semi-span
c C = root chord perpendicular to reference axis (in.)
c EI = bending stiffness, at root if tapered wing (psi)
c GJ = torsional stiffness, at root if tapered wing (psi)
c E = y-axis distance between reference axis and aerodynamic
c center, at root if tapered wing (in.)
c AR = semi-span aspect ratio

NDV=0

c conversion to radians
SWP=SWEEP*ACOS(-1.0)/180.0

ARG1=(GJ/C)*(RL/E)

c correction of 2-D lift-curve slope for planform effects

c eqn 4a of NACA TN 1680
AOC=A0*AR/(AR+4*COS(SWP))
ARG2=C*(RL**3)*AOC*(COS(SWP)**2)

ARG3=ARG1/ARG2

c linearized approximation for table on page 55 of

c AFFDL-TR-78-116
RK1=(6.1301-TR)/2.0801
RK2=(2.8149-TR)/4.4114

c divergence dynamic pressure (psi)
c eqn 7 of NACA TN 1680
QDIV=ARG3*RK1/(1-RK2*ARG1*TAN(SWP)/EI)

c conversion to inches
RHO=RHO/(12**4)
c divergence speed (in/sec)**2
VDIV=2.0*QDIV/RHO

c test for no divergence (negative divergence velocity)
IF (VDIV.LT.0.0) NDV=1
IF (VDIV.LT.0.0) GO TO 10

c conversion to feet
VDIV=SQRT(VDIV)/12.0
c conversion to mph
VDIV=(3600.0*VDIV/5280.0)

10 RETURN
END

```

PROGRAM MDV
c sample run for subroutine MDIVRG
COMMON/MD/QDIV,VDIV,RHO,A0,SWEEP,RL,TR,C,EI,GJ,E,AR
READ (5,*) RHO,A0,SWEEP,RL,TR
READ (5,*) C,EI,GJ,E,AR
CALL MDIVRG
IF (NDV.GT.0) WRITE (6,*) "THIS WING WILL NOT DIVERGE"
WRITE (6,*) "DIVERGENCE DYNAMIC PRESSURE (PSI) = ",QDIV
WRITE (6,*)
WRITE (6,*) "DIVERGENCE SPEED (MPH) = ",VDIV
END

```

Sample IO program for MDIVRG

0.002308 6.28 18.4 47.4 0.2
36.13 248000. 80460. 9.375 4.0

Sample input for MDIVRG

DIVERGENCE DYNAMIC PRESSURE (PSI) - 2.901382279E-03

DIVERGENCE SPEED (MPH) - 1.297326851E+01

Sample output for MDIVRG

MFLEX

This subroutine performs the same function as CFLEX but for a metallic box beam wing.

SUBROUTINE MFLEX

c this subroutine determines the metallic wing flexibility matrix
c [S], left wing only

```
DIMENSION D(20),F(20),M(20,20),T(20,20),U(20,20)
DIMENSION TRANS1(20),TRANS2(20),A(20,20),B(20,20)
DIMENSION COSMAT(20),SINMAT(20),R1(20,20),R2(20,20)
```

```
COMMON/M1/S(20,20),X(20),Y(20),H(20),E(20),SWEEP(20)
COMMON/M2/NP,EI(20),GJ(20)
```

REAL M

```
c      NP = number of panels in semi-span
c      X = x-axis intercept of panel midchord & reference axis (in.)
c      Y = as in X but for y-axis
c      H = width of panel along y-axis (in.)
c      E = x-axis distance from reference axis to
c          aerodynamic center of panel (in.)
c      SWEEP = sweep of reference axis on panel from y-axis
c              positive aft (deg)
c      EI = bending stiffness of box beam (psi)
c      GJ = torsional stiffness of box beam (psi)
```

NPM1=NP-1

```
      DO 10 I=1,NPM1
c      elements of matrices below
        D(I)=Y(I)-Y(I+1)
      10 F(I)=X(I)-X(I+1)
```

```
      DO 20 I=1,NP
c      conversion to radians
        SWP=SWEEP(I)*ACOS(-1.0)/180.0
c      NACA TN 3030 eqn B23 and B24, diagonal terms only (nonzero)
        COSMAT(I)=COS(SWP)
      20 SINMAT(I)=SIN(SWP)
```

```
c      initializing matrices
      DO 40 I=1,NP
        DO 30 J=1,NP
          U(I,J)=0.0
          R1(I,J)=0.0
        30 R2(I,J)=0.0
      40 CONTINUE
```

```
c      nonzero elements of C (see below)
      DO 70 I=2,NP
        IM1=I-1
        DO 60 J=1,IM1
          FSUM=0.0
          DSUM=0.0
          DO 50 K=J,IM1
            DSUM=DSUM+D(K)
          50 FSUM=FSUM+F(K)
```

```
c      TN 3030 eqn B26 and B27
        R1(I,J)=DSUM*COSMAT(I)
        R2(I,J)=DSUM*SINMAT(I)
```

```

c eqn B25 from NACA TN 3030
60 U(I,J)=E(J)-FSUM
70 CONTINUE
c diagonal terms
DO 80 I=1,NP
R1(I,I)=H(I)/(8.0*COSMAT(I))-E(I)*SINMAT(I)/2.0
80 R2(I,I)=E(I)*COSMAT(I)/2.0
c initializing
DO 100 I=1,NP
DO 90 J=1,NP
M(I,J)=0.0
90 T(I,J)=0.0
100 CONTINUE
c TN 3030 eqn B34 and B35
c diagonal terms
DO 110 I=1,NP
M(I,I)=-SINMAT(I)/2.0
110 T(I,I)=COSMAT(I)/2.0
DO 130 I=1,NPM1
c off-diagonal terms
IP1=I+1
DO 120 J=IP1,NP
M(I,J)=-SINMAT(J)
120 T(I,J)=COSMAT(J)
130 CONTINUE
c ***** MUST PROVIDE THE STRUCTURAL PROPERTIES EI,GJ *****
c following is eqn B-37 from NACA TN 3030
DO 140 I=1,NP
TRANS1(I)=H(I)/COSMAT(I)/EI(I)
140 TRANS2(I)=H(I)/COSMAT(I)/GJ(I)
DO 160 I=1,NP
DO 150 J=1,NP
A(I,J)=(COSMAT(I)*R1(I,J)-SINMAT(I)*U(I,J))*H(J)
150 B(I,J)=(SINMAT(I)*R2(I,J)+COSMAT(I)*U(I,J))*H(J)
160 CONTINUE
DO 190 I=1,NP
DO 180 J=1,NP
SUM1=0.0
SUM2=0.0
DO 170 K=1,NP
SUM1=SUM1+M(I,K)*A(I,J)
170 SUM2=SUM2+T(I,K)*B(I,J)
c flexibility matrix
180 S(I,J)=SUM1+SUM2
190 CONTINUE
RETURN
END

```


PROGRAM MF

```
c sample run for subroutine MFLEX
c present limit twenty semi-span panels

COMMON/M1/S(20,20),X(20),Y(20),H(20),E(20),SWEEP(20)
COMMON/M2/NP,EI(20),GJ(20)

READ (5,*) NP
DO 10 I=1,NP
  READ (5,*) X(I),Y(I),H(I),E(I),SWEEP(I)
10 READ (5,*) EI(I),GJ(I)

CALL MFLEX

WRITE (6,*) ((S(I,J),J=1,NP),I=1,NP)

END
```

Sample IO program for MFLEX

10

14.22	42.75	4.5	1.866	18.4
91165.	29584.			
12.72	38.25	4.5	2.657	18.4
91165.	29584.			
11.23	33.75	4.5	3.447	18.4
91165.	29584.			
9.73	29.25	4.5	4.237	18.4
91165.	29584.			
8.23	24.75	4.5	5.028	18.4
91165.	29584.			
6.74	20.25	4.5	5.818	18.4
91165.	29584.			
5.24	15.75	4.5	6.609	18.4
91165.	29584.			
3.74	11.25	4.5	7.399	18.4
91165.	29584.			
2.25	6.75	4.5	8.189	18.4
91165.	29584.			
0.75	2.25	4.5	8.980	18.4
91165.	29584.			

Sample input for MFLEX

7.51596355	0.000000000E+00	0.000000000E+00	0.000000000E+00	0.000000000E+00
0.000000000E+00	0.000000000E+00	0.000000000E+00	0.000000000E+00	0.000000000E+00
0.000000000E+00	0.000000000E+00	-1.864554596E+01	1.245434570E+01	
0.000000000E+00	0.000000000E+00	0.000000000E+00	0.000000000E+00	0.000000000E+00
0.000000000E+00	0.000000000E+00	0.000000000E+00	0.000000000E+00	0.000000000E+00
-9.554393005E+01	1.058177185E+01	1.603820801E+01	0.000000000E+00	0.000000000E+00
0.000000000E+00	0.000000000E+00	0.000000000E+00	0.000000000E+00	0.000000000E+00
0.000000000E+00	0.000000000E+00	-1.516435852E+02	-5.966799164E+01	
3.198589325E+01	1.827564812E+01	0.000000000E+00	0.000000000E+00	0.000000000E+00
0.000000000E+00	0.000000000E+00	0.000000000E+00	0.000000000E+00	0.000000000E+00
-1.865620880E+02	-1.087365570E+02	-3.118328857E+01	4.661748505E+01	
1.917135239E+01	0.000000000E+00	0.000000000E+00	0.000000000E+00	0.000000000E+00
0.000000000E+00	0.000000000E+00	-2.000968475E+02	-1.364214630E+02	
-7.296876526E+01	-9.31358719	5.436182785E+01	1.871510315E+01	
0.000000000E+00	0.000000000E+00	0.000000000E+00	0.000000000E+00	0.000000000E+00
-1.926979675E+02	-1.431726532E+02	-9.382056427E+01	-4.431097412E+01	
5.21434784	5.456641769E+01	1.691540909E+01	0.000000000E+00	
0.000000000E+00	0.000000000E+00	-1.641178894E+02	-1.287426605E+02	
-9.349117279E+01	-5.812718964E+01	-2.275194931E+01	1.249953079E+01	
4.787477112E+01	1.376546192E+01	0.000000000E+00	0.000000000E+00	
-1.142891388E+02	-9.306398773E+01	-7.191310120E+01	-5.069469833E+01	
-2.946955872E+01	-8.31867027	1.290647411E+01	3.412486267E+01	9.26909351
0.000000000E+00	-4.339167023E+01	-3.631662750E+01	-2.926632690E+01	
-2.219353104E+01	-1.511848450E+01	-8.06818771	-9.931392670E-01	6.07965755
1.312995434E+01	3.42672920			

Sample output for MFLEX

MODAL

This subroutine places the mass, stiffness, and aerodynamic operators into modal form. The sample for this subroutine is taken from Reference 11.

SUBROUTINE MODAL

c this subroutine places the mass, stiffness and aerodynamics
c matrices in modal form

```
DIMENSION MODT(20,20),TEMP1(20,20),TEMP2(20,20),EVECTT(20,20)
DIMENSION TEMP3(20,20),TEMP4(20,20)
```

```
COMMON/CM/N,MOD(20,20),A(20,20),RM(20,20),RK(20,20),EVECT(20,20)
```

```
REAL MOD,MODT
```

c N - order of matrices
c A - unsteady aerodynamics matrix to be placed in modal form,
c original A replaced by modal form
c RM - mass matrix to be placed in modal form,
c original RM replaced by modal form
c RK - stiffness matrix to be placed in modal form,
c original RM replaced by modal form
c EVECT - normalized eigenvector matrix

c transpose of normalized eigenvector matrix

```
DO 20 I=1,N
DO 10 J=1,N
10 EVECTT(I,J)=EVECT(J,I)
20 CONTINUE
```

c pre-multiply by transpose of normalized matrix

```
DO 50 I=1,N
DO 40 J=1,N
SUM1=0.0
DO 30 K=1,N
30 SUM1=SUM1+EVECTT(I,K)*RM(K,J)
40 TEMP1(I,J)=SUM1
50 CONTINUE
```

c post-multiply by normalized matrix

```
DO 80 I=1,N
SUM2=0.0
DO 60 J=1,N
SUM2=SUM2+TEMP1(I,J)*EVECT(J,I)
60 CONTINUE
```

c diagonal terms must equal 1.0

```
RMULT=1/SQRT(SUM2)
DO 70 K=1,N
70 MOD(K,I)=RMULT*EVECT(K,I)
80 CONTINUE
```

c transpose of modal matrix

```
DO 100 I=1,N
DO 90 J=1,N
90 MODT(I,J)=MOD(J,I)
100 CONTINUE
```

c for modal mass matrix ([M] = [I])

c pre-multiply by transpose of modal matrix

```
DO 130 I=1,N
DO 120 J=1,N
SUM3=0.0
DO 110 K=1,N
```

```

110 SUM3=SUM3+MODT(I,K)*RM(K,J)
120 TEMP2(I,J)=SUM3
130 CONTINUE

c post-multiply by modal matrix
  DO 160 I=1,N
  DO 150 J=1,N
  SUM4=0.0
  DO 140 K=1,N
140 SUM4=SUM4+TEMP2(I,K)*MOD(K,J)
c modal matrix
150 RM(I,J)=SUM4
160 CONTINUE

c for modal stiffness matrix (diagonal elements are squares of
c natural frequencies)
c pre-multiply by transpose of modal matrix
  DO 190 I=1,N
  DO 180 J=1,N
  SUM5=0.0
  DO 170 K=1,N
170 SUM5=SUM5+MODT(I,K)*RK(K,J)
180 TEMP3(I,J)=SUM5
190 CONTINUE

c post-multiply by modal matrix
  DO 220 I=1,N
  DO 210 J=1,N
  SUM6=0.0
  DO 200 K=1,N
200 SUM6=SUM6+TEMP3(I,K)*MOD(K,J)
c modal matrix
210 RK(I,J)=SUM6
220 CONTINUE

c for modal aerodynamics matrix
c pre-multiply by transpose of modal matrix
  DO 250 I=1,N
  DO 240 J=1,N
  SUM5=0.0
  DO 230 K=1,N
230 SUM7=SUM7+MODT(I,K)*A(K,J)
240 TEMP4(I,J)=SUM7
250 CONTINUE

c post-multiply by modal matrix
  DO 280 I=1,N
  DO 270 J=1,N
  SUM8=0.0
  DO 260 K=1,N
260 SUM8=SUM8+TEMP4(I,K)*MOD(K,J)
c modal matrix
270 A(I,J)=SUM8
280 CONTINUE

RETURN
END

```

PROGRAM MD

c sample run for subroutine MODAL
c present limit twenty semi-span nodes

COMMON/CM/N,MOD(20,20),A(20,20),RM(20,20),RK(20,20),EVECT(20,20)

REAL MOD

READ (5,*) N
READ (5,*) ((EVECT(I,J),J=1,N),I=1,N)
READ (5,*) ((A(I,J),J=1,N),I=1,N)
READ (5,*) ((RM(I,J),J=1,N),I=1,N)
READ (5,*) ((RK(I,J),J=1,N),I=1,N)

CALL MODAL

WRITE (6,*) ((A(I,J),J=1,N),I=1,N)
WRITE (6,*)
WRITE (6,*) ((RM(I,J),J=1,N),I=1,N)
WRITE (6,*)
WRITE (6,*) ((RK(I,J),J=1,N),I=1,N)

END

Sample IO program for MODAL

3

1.0000	1.0000	1.0000
1.8608	0.2542	-2.1152
2.1617	-0.3407	0.6791

7.4936	-2.2078	-4.0367
-2.0204	7.3173	-2.2471
-3.0970	-2.1373	7.2336

1.	0.	0.
0.	1.	0.
0.	0.	2.

2.	-1.	0.
-1.	3.	-2.
0.	-2.	2.

Sample input for MODAL

2.06189895	-1.37522089	-3.637984395E-01	1.037617207E+01	9.92081356
-3.59587264	3.95323229	6.34809971	3.50999427	

1.00000024	7.808208466E-06	6.020069122E-06	7.808208466E-06	1.00000012
-1.467317343E-04	6.020069122E-06	-1.467317343E-04	9.99999404E-01	

1.391941309E-01	1.043081284E-06	4.842877388E-06	1.013278961E-06	
1.74589849	-4.659593105E-04	4.768371582E-06	-4.659891129E-04	4.11490726

Sample output for MODAL

NFREQ

This subroutine calculates the unforced natural frequencies and normal modes of a system given the stiffness and mass matrices. The sample for this subroutine is taken from Reference 11.

SUBROUTINE NFREQ

c this subroutine calculates the unforced natural frequencies of
c the system (eigenvalues) and the corresponding normalized modes
c eigenvectors)

DIMENSION D(20,20),AA(20,20)

COMMON/CF/N,RM(20,20),RK(20,20),RNF(20),EVECT(20,20)

REAL LAMBDA(20)

c N - number of nodes in semi-span (order of matrix)
c RM - mass matrix
c RK - stiffness matrix

c create dynamical matrix

c ***** MUST PROVIDE MEANS FOR INVERTING [K] *****
c OR JUST READ IN THE FLEXIBILITY MATRIX [AA]

DO 30 I=1,N

DO 20 J=1,N

SUM=0.0

DO 10 K=1,N

c [D]=[K]inv*[M] the dynamical matrix

10 SUM=SUM+AA(I,K)*RM(K,J)

20 D(I,J)=SUM

30 CONTINUE

c solve [D] for eigenvalues

c ***** PROVIDE ROUTINE FOR EIGENSOLUTION *****

DO 40 I=1,N

c [LAMBDA] is array of eigenvalues in descending order

40 RNF(I)=1/SQRT(LAMBDA(I))

c [evect] is matrix of eigenvectors in descending order

c normalizing eigenvector matrix

DO 60 J=1,N

DO 50 I=1,N

IF (I.EQ.1) FIRST=EVECT(1,J)

50 EVECT(I,J)=EVECT(I,J)/FIRST

60 CONTINUE

RETURN

END

```

PROGRAM NF
c sample run for subroutine NFREQ
c present limit twenty semi-span nodes

COMMON/CF/N,RM(20,20),RK(20,20),RNF(20),EVECT(20,20)

READ (5,*) N
READ (5,*) ((RM(I,J),J=1,N),I=1,N)
READ (5,*) ((RK(I,J),J=1,N),I=1,N)

CALL NFREQ

DO 10 I=1,N
IF (RNF(I).EQ.0.00) WRITE (6,*) "RIGID BODY MODE"
10 WRITE (6,*) "NATURAL FREQUENCY ",I," = ",RNF(I)
WRITE (6,*)

DO 30 J=1,N
WRITE (6,*) "EIGENVECTOR ",J," = "
DO 20 I=1,N
20 WRITE (6,*) " ",EVECT(I,J)
30 CONTINUE

END

```

Sample IO program for NFREQ

3

1.	0.	0.
0.	1.	0.
0.	0.	2.
2.	-1.	0.
-1.	3.	-2.
0.	-2.	2.

Sample input for NFREQ

NATURAL FREQUENCY 1 - 3.730872571E-01
NATURAL FREQUENCY 2 - 1.32132459
NATURAL FREQUENCY 3 - 2.02852488

EIGENVECTOR 1 -
1.00000000
1.86080575
2.16170192

EIGENVECTOR 2 -
1.00000000
2.541011870E-01
-3.406651318E-01

EIGENVECTOR 3 -
1.00000000
-2.11490679
6.789628267E-01

Sample output for NFREQ

PKFLUTR

This subroutine performs iterative flutter computations given the aeroelastic operators using the p-k method. No IO program or sample is appropriate for this subroutine.

SUBROUTINE PKFLUTR

c this program performs simple flutter computations by the PK-method
c assumes no free-body modes in operators

DIMENSION RM(40,40),RK(40,40),A(40,40),OHM(40)

COMMON/FL3/N,RC,VS,VI,VE,OHMT,RNF(40),EVECT(40,40)

COMPLEX A,RMAT(40,40),RLAMBDA(40)

c N - number of DOFs multiplied by number of nodes,
c dimension of square operator matrices
c RC - root aerodynamic chord (in.)
c VS - starting velocity (mph), greater than zero
c VE - final velocity for analysis (mph)
c VI - velocity increment (mph)
c OHMT - tolerance on frequency for match

c *** PROVIDE DATA AND SUBROUTINES TO CALCULATE OPERATORS ***
c INERTIA [RM], STRUCTURE [RK], AND AERODYNAMIC [A]

CALL STRUC
CALL MASS

CALL NFREQ
c *** PRODUCES ARRAY OF NATURAL FREQUENCIES [RNF] ***
c AND MATRIX OF NATURAL MODES IN DESCENDING ORDER [EVECT]

c top of velocity loop
DO 60 I=VS,VE,VI

c velocity
V=I

c top of mode loop
DO 50 J=1,N

MODE=J

c using natural frequency as initial guess
IF (V.EQ.VS) OHM(MODE)=RNF(MODE)

c top of frequency loop, 10000 iterations permitted
DO 30 KK=1,10000

c reduced frequency, k
RKK=RC*OHM(MODE)/(2*V)

c [A] expecting k as principal variable
CALL AERO

c replace operators with modal form
CALL MODAL

DO 20 L=1,N
DO 10 K=1,N
10 RMAT(L,K)=RK(L,K)-A(L,K)
20 CONTINUE

```

c *** PROVIDE MEANS FOR PERFORMING AN EIGENVALUE DECOMPOSITION ***
c ON COMPLEX MATRIX [RMAT]

c [RLAMBDA] is array of eigenvalues in descending order
c each has form (ohm + i g*ohm)

      OHML=REAL(RLAMBDA(MODE))

      DIF=ABS(OHML-OHM(MODE))

c check for suitable match of frequency
      IF (DIF.LE.OHMT) GO TO 40

30 OHM(MODE)=OHML

      WRITE (6,*) "(NO CONVERGENCE FOR MODE ",MODE," )"
      GO TO 50

c solving for system damping
40 G=AIMAG(RLAMBDA(MODE))/REAL(RLAMBDA(MODE))

      WRITE (6,*) "Mode ",J," Vel. (MPH) = ",V," g = ",G,
1" freq. = ",OHM(MODE)

50 CONTINUE

60 CONTINUE

      RETURN
      END

```

```

      PROGRAM PK
c  sample input program for subroutine PKFLUTR
c  present limit 40 DOF/panels combinations

      COMMON/FL3,N,RC,VS,VI,VE,OHMT,RNF(40),EVECT(40,40)

      READ (5,*) N,RC
      READ (5,*) VS,VE,VI,OHMT

c  write header
      WRITE (6,*) "                PK-METHOD RESULTS"
      WRITE (6,*)

      CALL PKFLUTR

      DO 10 I=1,N
      WRITE (6,*) "      NATURAL FREQUENCY ",J," = ",RNF(J)
      WRITE (6,*)

      WRITE (6,*) "      EIGENVECTOR ",J," = "
      DO 20 J=1,N
20  WRITE (6,*) "              ",EVECT(I,J)
10  WRITE (6,*)

      END

```

Sample IO program for PKFLUTR

RIGDROL

This subroutine performs the same function as FLEXROL but for a rigid wing. The flexibility matrix and the total angle of attack due to aileron deflection need not be provided.

SUBROUTINE RIGDROL

c this subroutine calculates the aileron effectiveness (helix angle),
c the location of the center of pressure, and the coefficient of lift
c divided by wing incidence (rad.) for a rigid wing

DIMENSION RDAMP(20),RAIL(20),A(20,20),SR(20),XV(20)

COMMON/R1/AREA,SSPAN,RLIFT,RPB2V,XCP,YCP,AIS(20,20),NP
COMMON/R2/X(20),Y(20),C(20),E(20),H(20),SHAPE(20),Q,RL
COMMON/R3/CM(20),CMDEL(20),SLOPE(20),AIA(20,20),ZAOA(20)

c NP = number of spanwise panels in semi-span
c AREA = planform area of wing (sq in.)
c SSPAN = semi-span of wing (in.)
c ZAOA = panel incidence from zero-lift line, includes jugged twist
c Q = free-stream dynamic pressure (psi)
c X = x-axis intercept of panel midchord & reference axis (in.)
c Y = as in X but for y-axis
c C = x-axis lenth of aerodynamic chord line of panel (in.)
c E = x-axis distance between panel aerodynamic center and structural
c reference axis (in.)
c H = y-axis width of panel (in.)
c CM = partial derivative of the section lift coefficient wrt
c control deflection divided by the partial wrt AOA
c CMDEL = partial derivative of the section pitching moment
c wrt control deflection
c SHAPE = aileron segment deflection normalized to largest value
c and negative, example:
c -1.0 if segments deflects same amount
c -0.5 if deflects half as much

DO 10 I=1,NP
c XV is x-axis distance to the quarter-chord of panel
10 XV(I)=X(I)-E(I)

NCT=0

c ***** PROVIDE THE INVERTED ANTI-SYMMETRICAL AIC MATRIX [AIA] *****
c first time through

c ***** PROVIDE THE INVERTED SYMMETRICAL AIC MATRIX [AIS] *****
c second time through

100 DO 30 I=1,NP
DO 20 J=1,NP
IF (NCT.LE.0) A(I,J)=AIA(I,J)
20 IF (NCT.GT.0) A(I,J)=AIS(I,J)
30 CONTINUE

c initializing
DO 50 I=1,NP
SUM1=0.0
SUM2=0.0
SUM3=0.0

c following equations for left wing only
DO 40 K=1,NP

c from eqn 34 of AFFDL-TR-79-3087 for rigid wing ([B] = [A])
SUM1=SUM1+A(I,K)

```

c from eqn 41 of AFFDL-TR-79-3087 for rigid wing
  SUM2=SUM2+A(I,K)*Y(K)
c from eqn 39 of AFFDL-TR-79-3087 for rigid wing
40 SUM3=SUM3+A(I,K)*SHAPE(K)*CM(K)

c SR is the lift per unit span per rad. of wing incidence divided by
c the dynamic pressure q
  SR(I)=SUM1

c roll-in-damping or lift opposing rolling moment from apparent AOA change
  RDAMP(I)=SUM2

c lift from apparent AOA change due to one rad. aileron deflection
50 RAIL(I)=SUM3

  SUM=0.0

  DO 60 I=1,NP
60 SUM=SUM+SR(I)*H(I)

c RLIFT is the coefficient of lift divided by q*AREA*AOA
c CL alpha, eqn 38 of AFFDL-TR-79-3087 for rigid wing
  RLIFT=SUM/(Q*AREA)

  SUM3=0.0
  SUM2=0.0
  SUM1=0.0
  SUM4=0.0
  SUM5=0.0

c following for eqn 44 of AFFDL-TR-79-3087 for rigid wing
c [B]=[A] and [E]=0
  DO 70 I=1,NP
    SUM1=SUM1+SR(I)*XV(I)*H(I)
    SUM2=SUM2+SR(I)*Y(I)*H(I)
    SUM3=SUM3+SR(I)*H(I)
    SUM4=SUM4+RDAMP(I)*H(I)*Y(I)
70 SUM5=SUM5+RAIL(I)*H(I)*Y(I)

c cartesian coordinates of center of pressure, non-rotated axis
  XCP=SUM1/SUM3
c (assumed to lie on quarter-chord)
  YCP=SUM2/SUM3

  DO 80 I=1,NP
c panel lift per unit span divided by C*Q*AOA, CL alpha
  SLOPE(I)=SR(I)/(Q*H(I)*C(I))
c total rigid wing lift on semi-span (lbf)
80 RL=RL+SLOPE(I)*Q*H(I)*C(I)/ZAOA(I)

c RPB/2V is the rigid wing aileron effectiveness (helix angle)
c no good first time through, must use anti-symmetric [AIC]
  IF (NCT.LE.0) RPB2V=-SUM5/(SUM4/SSPAN)

  IF (NCT.GT.0) GO TO 90
  NCT=1
  GO TO 100

90 RETURN
END

```

PROGRAM RIG

```

c sample run for subroutine RIDGROL
c present limit twenty semi-span panels

COMMON/R1/AREA,SSPAN,RLIFT,RPB2V,XCP,YCP,AIS(20,20),NP
COMMON/R2/X(20),Y(20),C(20),E(20),H(20),SHAPE(20),Q,RL
COMMON/R3/CM(20),CMDEL(20),SLOPE(20),AIA(20,20),ZAOA(20)

READ (5,*) NP,Q,SSPAN,AREA
DO 10 I=1,NP
READ (5,*) X(I),Y(I),H(I),E(I),C(I)
10 READ (5,*) ZAOA(I),SHAPE(I),CM(I),CMDEL(I)

READ (5,*) ((AIA(M,N),N=1,NP),M=1,NP)
READ (5,*) ((AIS(M,N),N=1,NP),M=1,NP)

CALL RIGDROL

WRITE (6,*) "RIGID WING RESULTS"
WRITE (6,*)
WRITE (6,*) "Pb/2V = ",RPB2V
WRITE (6,*)
WRITE (6,*) "CENTER OF PRESSURE LOCATION (inches)    X = ",XCP
WRITE (6,*) "                                           Y = ",YCP
WRITE (6,*)
WRITE (6,*) "CL alpha = ",RLIFT
WRITE (6,*)
WRITE (6,*) "TOTAL LIFT ON SEMI-SPAN (lbf) = ",RL
WRITE (6,20)

DO 30 I=1,NP
WRITE (6,*) 1,SLOPE(I)
30 CONTINUE

20 FORMAT (/33HPANEL LIFT PER UNIT SPAN (lbf/in)
1/19HPANEL 1 IS OUTBOARD/)

END

```

Sample IO program for RIGDROL

10 .1724 45.0 1012.5

14.22	42.75	4.5	1.866	9.00
1.0	-1.0	0.5854	-0.64	
12.72	38.25	4.5	2.657	12.0
1.0	-1.0	0.5854	-0.64	
11.23	33.75	4.5	3.447	15.0
1.0	-1.0	0.5854	-0.64	
9.73	29.25	4.5	4.237	18.0
1.0	-1.0	0.5854	-0.64	
8.23	24.75	4.5	5.028	21.0
1.0	-1.0	0.5854	-0.64	
6.74	20.25	4.5	5.818	24.0
1.0	-1.0	0.5854	-0.64	
5.24	15.75	4.5	6.609	27.0
1.0	0.0	0.0	0.0	
3.74	11.25	4.5	7.399	30.0
1.0	0.0	0.0	0.0	
2.25	6.75	4.5	8.189	33.0
1.0	0.0	0.0	0.0	
0.75	2.25	4.5	8.980	36.0
1.0	0.0	0.0	0.0	

1.509504795E+01	5.73390913	3.48990107	2.42930818	1.78549194
1.33152413	9.752132893E-01	6.714459658E-01	3.951042891E-01	
1.308466047E-01	5.19806242	1.771542358E+01	7.45260477	4.69136143
3.28613472	2.38382387	1.71628881	1.16904998	6.835322976E-01
2.256794274E-01	2.86450267	6.97287941	1.909598732E+01	8.45105934
5.38750124	3.73845124	2.62520599	1.76178288	1.02131355
3.358560205E-01	1.83893025	4.06110573	8.05369186	1.996614075E+01
9.06076145	5.75315189	3.87828088	2.54590464	1.45814145
4.768725634E-01	1.26493430	2.65693283	4.82835197	8.73858166
2.046922302E+01	9.33213806	5.78209400	3.65660071	2.05561686
6.668341160E-01	8.926386833E-01	1.81893468	3.16474676	5.28559446
9.07884789	2.060920715E+01	9.21843147	5.37993860	2.92605567
9.366811514E-01	6.241097450E-01	1.24725080	2.11532426	3.40066576
5.41666031	9.03147793	2.030063248E+01	8.57571793	4.32574940
1.34998214	4.134300947E-01	8.159627318E-01	1.36240053	2.14122369
3.30258894	5.12547445	8.45479679	1.932588387E+01	7.06468630
2.06804013	2.359407842E-01	4.621981680E-01	7.647440434E-01	1.18952620
1.80147088	2.71625233	4.18732119	7.00693607	1.712791824E+01
3.67482018	7.650993764E-02	1.493618190E-01	2.461101413E-01	
3.808220029E-01	5.726240277E-01	8.538046479E-01	1.28810740	2.03329325
3.66406035	1.140818214E+01			

1.522857380E+01	5.96310043	3.82033515	2.87379861	2.36041355
2.05599952	1.87082624	1.76191103	1.70555520	1.68618894
1.807481766E+01	7.97303772	5.39460516	4.19999790	3.54103684
3.15424109	2.92951870	2.81190491	2.76885939	3.14245343
1.979629707E+01	9.40200710	6.62955093	5.31964207	4.60114527
4.19573450	3.98382759	3.90300393	2.18809867	4.66872692
2.117912865E+01	1.065380573E+01	7.79299164	6.44328308	5.72700071
5.35961246	5.21623898	1.68967009	3.39996672	5.92095947
1.023863792E+01	2.245115471E+01	1.188621807E+01	9.01604748	7.69819355
7.05599117	6.80469275	1.39890170	2.70968294	4.48244715
1.150020123E+01	2.375194168E+01	1.322908020E+01	1.043674183E+01	
9.24757767	8.79599571	1.21933305	2.30112791	3.68471789
8.34255409	1.286012268E+01	2.523128319E+01	1.485822678E+01	
1.228022766E+01	1.140461731E+01	1.10676730	2.05220938	3.21712255
4.74516201	6.81793594	9.76934624	1.450068855E+01	2.713015938E+01

Sample input for RIGDROL

1	5.63242245
2	6.04264164
3	5.88019848
4	5.59788942
5	5.28864479
6	4.97651196
7	4.66740799
8	4.36177492
9	4.05870152
10	3.75838327

205

VGFLUTR

This subroutine performs iterative flutter computations given the aeroelastic operators using the V-g method. No IO program or sample is appropriate for this subroutine.

SUBROUTINE VGFLUTR

c this program performs simple flutter computations by the VG-method
c assumes no free-body modes in operators

DIMENSION RM(40,40),RK(40,40),A(40,40),RKI(40,40),OHM(40)

COMMON/FL1/N,VI,VE,OHMT,RNF(40),EVECT(40,40)

COMPLEX A,RMAT(40,40),RLAMBDA(40)

c N - number of DOFs multiplied by number of nodes,
c dimension of square operator matrices
c VE - final velocity for analysis (mph)
c VI - velocity increment (mph)
c OHMT - tolerance on frequency for match

c *** PROVIDE DATA AND SUBROUTINES TO CALCULATE OPERATORS ***
c INERTIA [RM], STRUCTURE [RK], AND AERODYNAMIC [A]

CALL STRUC
CALL MASS

c *** PROVIDE MEANS FOR INVERTING [RK] FOR [RKI] ***

CALL NFREQ

c *** PRODUCES ARRAY OF NATURAL FREQUENCIES [RNF] ***
c AND MATRIX OF NATURAL MODES IN DESCENDING ORDER [EVECT]

c top of velocity loop
DO 90 I=0,VE,VI

c velocity
V=I

c top of mode loop
DO 80 J=1,N

MODE=J

c using natural frequency as initial guess
IF (V.EQ.0.0) OHM(MODE)=RNF(MODE)

c top of frequency loop, 10000 iterations permitted
DO 60 KK=1,10000

CALL AERO

c replace operators with modal form
CALL MODAL

DO 20 L=1,N

DO 10 K=1,N

10 RMAT(L,K)=(1/OHM(MODE))*A(L,K)-RM(L,K)

20 CONTINUE

c premultiply by inverse of [RK]

DO 50 L=1,N

DO 40 K=1,N

```

        SUM=0.0
        DO 30 M=1,N
30      SUM=SUM+RKI(L,M)*RMAT(M,K)
40      RMAT(L,K)=SUM
50      CONTINUE

c  ***  PROVIDE MEANS FOR PERFORMING AN EIGENVALUE DECOMPOSITION  ***
c      ON COMPLEX MATRIX [RMAT]

c  {RLAMBDA} is array of eigenvalues in descending order
c  each has form (1/ohm**2 + i g/ohm**2)

        OHML=SQRT(1/REAL(RLAMBDA(MODE)))

        DIF=ABS(OHML-OHM(MODE))

c  check for suitable match of frequency
        IF (DIF.LE.OHMT) GO TO 70

c  solving for new frequency and damping
60      OHM(MODE)=OHML

        WRITE (6,*) "(NO CONVERGENCE FOR MODE ",MODE," )"
        GO TO 80

c  solving for structural damping
70      G=AIMAG(RLAMBDA(MODE))/REAL(RLAMBDA(MODE))

        WRITE (6,*) "Mode ",J,"   Vel. (MPH) = ",V,"   g = ",G,
1"   freq. = ",OHM(MODE)

80      CONTINUE

90      CONTINUE

        RETURN
        END

```


PROGRAM VG

```
c sample input program for subroutine VGFLUTR
c present limit 40 DOF/panels combinations

COMMON/FL1/N,VI,VE,OHMT,RNF(40),EVECT(40,40)

READ (5,*) N
READ (5,*) VE,VI,OHMT

c write header
WRITE (6,*) "                VG-METHOD RESULTS"
WRITE (6,*)

CALL VGFLUTR

DO 10 I=1,N
WRITE (6,*) "    NATURAL FREQUENCY ",J," = ",RNF(J)
WRITE (6,*)

WRITE (6,*) "    EIGENVECTOR ",J," = "
DO 20 J=1,N
20 WRITE (6,*) "                ",EVECT(I,J)
10 WRITE (6,*)

END
```

Sample IO program for VGFLUTR

Appendix B: Sample Statics Program

The listing and users manual for the static aeroelastic computer program COMPSTAT (Composite Static) is here provided. This program serves as an example of a driver or main program for the series of subroutines provided elsewhere in this report. This program was used for the optimization exercise described in the body of this report and is provided here primarily for illustrative purposes, although it may be adapted to the specific uses of the reader. The input follows the convention established within the body of this report. It essentially performs the same tasks as Dr. Weisshaar's CWINGS program but also determines the reversal speed, the total wing lift, and the torsional deflected shape. It permits a nonuniform spanwise thickness distribution of the composite, wing incidence plus washout or washin, and separation of the box beam from the control surfaces of the overall aerodynamic planform. Total semi-span lift and torsional deflections are also calculated.

CARD 1:

Header card, reproduced in the print-out to identify the run

CARD 2:

N	= number of composite plies, at root if tapered thickness
NV	= number of plies to have orientation changed

NP = number of spanwise panels in the semi-span, should be greater than 7 for accuracy

NCASE = number of laminate rotation variations to be analyzed

NLIN = 0 - nonlinearly tapered planform
 = 1 - linearly tapered planform

NTAP = 0 - nonlinearly tapered spanwise laminate thickness
 = 1 - constant spanwise laminate thickness
 = 4 - fourth order spanwise laminate thickness

NSTR = 0 - box beam and aerodynamic planform treated sa same
 = 1 - box beam parameters input separate from aerodynamic planform

CARD 3:

DDEL = fiber angle increment for each NCASE (deg)

A0 = section lift-curve slope, constant full span

CARD 4:

VQ = velocity at which analysis will be done (mph)

RHO = freestream air density ($\text{lbf-s}^2/\text{ft}^4$)

ITER = 0 - iterate velocity for reversal speed search
 = other than 0 - no velocity iteration

Card 5 is read if ITER = 0

CARD 5:

VQI = velocity increment added to VQ (mph)

ITN = number of velocity iterations to be performed

CARD 6:

CR = aerodynamic chord at wing root (in.)

CSR = structural chord at wing root (in.)

ER = distance between a.c. and reference axis, measured parallel to flow, positive forward (in.)

CARD 7:

SSPAN = wing semi-span perpendicular to root (in.)

SWEEPR = sweep of reference axis at root, positive aft (deg), measured perpendicular to root

TAPER = wing taper ratio

Card 8 is read if NSTR = 1

CCSR = box beam structural root chord (in.)

CSWEEPR = box beam reference axis sweep angle (deg.)

CARD 9:

E1 = modulus of elasticity along axis 1 of material (psi)

E2 = modulus of elasticity along axis 2 of material (psi)

P12 = Poisson's ratio of material

G12 = shear modulus of material (psi)

Input next data in order for each panel, from the tip inboard.

CARD 10:

ZAOA = panel incidence from section zero-lift AOA (deg)

CM = $c_{l\delta} / c_{l\alpha}$ for panel

CMDEL = $c_{m\delta}$ for panel

SHAPE = aileron segment deflection normalized to largest value and negative, example: -1.0 if deflects same amount, -0.5 if deflects half as much, 0.0 if no aileron on panel

There will be N or card 11, numbered as input. Input variable plies first.

CARD 11:

ZNL = distance from mid plane of box beam to lower surface of ply, positive up
ZNU = as in ZNL but for ply upper surface
THETA = initial ply orientation as measured from the structural root, positive forward

Cards 12-13 are used if NLIN=0 and NTAP=0. There will be NP of Card 12.

CARD 12:

NPR = number of plies to be removed from panel

There will be NPR of card 13.

CARD 13:

NR = number of the ply to be removed, remove only outer plies

PROGRAM COMPSTAT

c main program for running composite static subroutines

```
COMMON/C1/CR,ER,SSPAN,TAPER,AREA,SWEEPR,CSR,NP
COMMON/C2/H(20),X(20),Y(20),C(20),CS(20),E(20),SWEEP(20)
COMMON/C3/EI(20),GJ(20),AK(20),NR(60),SHAPE(20)
COMMON/C4/E1,E2,P12,G12,DR,N,NV,NLIN,NTAP,SAOA(20)
COMMON/C5/ZNL(60),ZNU(60),THETA(60),S(20,20),MM
COMMON/C6/SPAN,RLIFT,RPB2V,XCP,YCP,AIS(20,20)
COMMON/C7/CM(20),CMDEL(20),SLOPE(20),AIA(20,20)
COMMON/C8/AS(20,20),AA(20,20),DALPHA(20),FLIFT,PB2V
COMMON/C9/QDIV,VDIV,RHO,AIC(20,20),A0,SYM,Q,RL,FL,ZAOA(20)
```

CHARACTER*4 HEADER(18)

c defining PI

PI=ACOS(-1.0)

```
READ (5,890) HEADER
READ (5,*) N,NV,NP,NCASE,NLIN,NTAP,NSTR
READ (5,*) DDEL,A0
READ (5,*) VQ,RHO,ITER
IF (ITER.EQ.0) READ (5,*) VQI,ITN
READ (5,*) CR,CSR,ER
READ (5,*) SSPAN,SWEEPR,TAPER
IF (NSTR.EQ.1) READ (5,*) CCSR,CSWEEPR
```

c use full planform values for aero calculations

```
IF (NSTR.EQ.1) CSRS=CSR
IF (NSTR.EQ.1) SWEEPRS=SWEEPR
READ (5,*) E1,E2,P12,G12
```

c input aileron data from tip inboard

```
DO 10 I=1,NP
10 READ (5,*) ZAOA(I),CM(I),CMDEL(I),SHAPE(I)
DO 20 I=1,N
20 READ (5,*) ZNL(I),ZNU(I),THETA(I)
```

c conversion to ft/sec

V=(VQ/3600)*5280

c conversion to psi

Q=(RHO/(12**4))*0.5*(V*12.)**2

c copy of input

```
WRITE (6,890) HEADER
WRITE (6,*)
WRITE (6,*)
WRITE (6,*) "TEST CONDITIONS:"
WRITE (6,*) "    INITIAL VELOCITY (mph) = ",VQ
WRITE (6,*) "    VELOCITY INCREMENT (mph) = ",VQI
WRITE (6,*) "    NUMBER OF VELOCITY INCREMENTS = ",ITN
WRITE (6,*) "    TEST DYNAMIC PRESSURE (psi) = ",Q
WRITE (6,*) "    AIR DENSITY (lbf s**2/ft**4) = ",RHO
WRITE (6,*)
WRITE (6,*) "INPUT CONSTANTS:"
WRITE (6,*) "    NUMBER OF SEMI-SPAN PANELS = ",NP
WRITE (6,*) "    NUMBER OF PLYS TO BE ROTATED = ",NV
WRITE (6,*) "    VARIABLE PLY ROTATION ANGLE (degrees) = ",DDEL
WRITE (6,*)
WRITE (6,*) "WING PARAMETERS:"
WRITE (6,*) "    2-D LIFT CURVE SLOPE OF SECTION = ",A0
```

```

WRITE (6,*) "    ROOT A.C. & STRUCTURAL AXIS OFFSET (inches) = ",ER
WRITE (6,*)
WRITE (6,*) "AILERON DATA:"
WRITE (6,900)
DO 30 I=1,NP
30 WRITE (6,910) I,ZAOA(I),SHAPE(I),CM(I),CMDEL(I)
WRITE (6,*)
WRITE (6,*) "MATERIAL PROPERTIES:"
WRITE (6,*) "    E1 (psi) = ",E1
WRITE (6,*) "    E2 (psi) = ",E2
WRITE (6,*) "    P12 = ",P12
WRITE (6,*) "    G12 (psi) = ",G12
WRITE (6,*)
WRITE (6,*) "COMPOSITE LAYUP:"
IF (NTAP.EQ.0) WRITE (6,*) "    NONLINEARLY TAPERED SPANWISE
1 LAYUP THICKNESS"
IF (NTAP.EQ.1) WRITE (6,*) "    CONSTANT SPANWISE LAYUP THICKNESS"
IF (NTAP.EQ.4) WRITE (6,*) "    LINEARLY TAPERED SPANWISE LAYUP
1 THICKNESS"
WRITE (6,920)
DO 40 I=1,N
IF (I.EQ.1) THETA1=THETA(I)
40 WRITE (6,910) I,ZNL(I),ZNU(I),THETA(I)

DO 50 I=1,N
50 THETA(I)=THETA(I)*PI/180.0

WRITE (6,*)
WRITE (6,*) "PLANFORM DATA:"
WRITE (6,*) "    ROOT CHORD (INCHES) = ",CR
WRITE (6,*) "    ROOT STRUCTURAL CHORD (inches) = ",CSR
WRITE (6,*) "    ROOT STRUCTURAL CHORD SWEEP (degrees) = ",SWEEP
WRITE (6,*) "    SEMI-SPAN (inches) = ",SSPAN
WRITE (6,*) "    WING TAPER RATIO = ",TAPER
IF (NSTR.EQ.1) WRITE (6,*) "    BOX BEAM ROOT CHORD (inches) = ",
1CCSR
IF (NSTR.EQ.1) WRITE (6,*) "    BOX BEAM REF. AXIS SWEEP (deg) = ",
1CSWEEP

c calculating geometry parameters
CALL GEOM

WRITE (6,*) "    SEMI-SPAN AREA (in.**2) = ",AREA
IF (NLIN.EQ.1) WRITE (6,*) "    LINEARLY TAPERED PLANFORM"
IF (NLIN.EQ.0) WRITE (6,*) "    NONLINEARLY TAPERED PLANFORM"
c write heading for GEOM printout
WRITE (6,930)

DO 60 I=1,NP
60 WRITE (6,940) I,X(I),Y(I),C(I),CS(I),H(I),E(I),SWEEP(I)

SYM=1.0
c symmetric aero matrix
CALL AERO1
DO 80 I=1,NP
DO 70 J=1,NP
70 AS(I,J)=AIC(I,J)
80 CONTINUE

c MUST PROVIDE MEANS OF INVERTING [AS] FOR [AIS]

```

```

        SYM=-1.0
c  anti-symmetric aero matrix
        CALL AERO1
        DO 100 I=1,NP
        DO 90 J=1,NP
        90 AA(I,J)=AIC(I,J)
        100 CONTINUE

c  MUST PROVIDE MEANS OF INVERTING [AA] FOR [AIA]

c  rigid wing characteristics
        CALL RIGDROL

c  printings only first time through at initial test velocity
        IF (ITC.GT.0) GO TO 120
        WRITE (6,*)
        WRITE (6,*)
        WRITE (6,*) "(ALL VALUES FOLLOWING FOR INITIAL VELOCITY ONLY)"
        WRITE (6,*)
        WRITE (6,*) "          * RIGID WING RESULTS *"
        WRITE (6,*)
        WRITE (6,*) "Pb/2V = ",RPB2V
        WRITE (6,*)
        WRITE (6,*) "CENTER OF PRESSURE LOCATION (inches)    X = ",XCP
        WRITE (6,*) "                                           Y = ",YCP
        WRITE (6,*) "CL alpha = ",RLIFT
        WRITE (6,*)
        WRITE (6,*) "TOTAL LIFT ON SEMI-SPAN (lbf) = ",RL
        WRITE (6,970)

        DO 110 I=1,NP
        WRITE (6,*) I,SLOPE(I)
        110 CONTINUE

        120 D=0.0

c  top of loop for each rotation case
        DO 230 L=1,NCASE

        DR=D*PI/180.0

        DD=D+THETA1

        WRITE (6,*)
        WRITE (6,*) "*****"
        WRITE (6,*)
        WRITE (6,*) "FIRST VARIABLE PLY ORIENTATION = ",DD
        WRITE (6,950)

c  use only structural values for structural calculations
        IF (NSTR.NE.1) GO TO 125
        CSR=CCSR
        SWEEP=CSWEEP
        CALL GEOM

        125 IF ((NLIN.EQ.0).AND.(NTAP.EQ.0)) GO TO 140

c  calculating structural properties

```



```

      CALL CSTRUC

      DO 130 I=1,NP
130  WRITE (6,960) I,EI(I),GJ(I),AK(I)
      GO TO 180

c  read plies to be removed (numbered as entered above, remove outside)
140 DO 170 M=1,NP
c  initializing for each panel
      DO 150 J=1,N
150  NR(J)=0.0
      READ (5,*) NPR
      IF (NPR.EQ.0) GO TO 160
      READ (5,*) (NR(I),I=1,NPR)

c  calculating structural properties
160  CALL CSTRUC

      170  WRITE (6,960) MM,EI(MM),GJ(MM),AK(MM)

c  flexibility matrix
180  CALL CFLEX

c  back to full planform values for deformation calculations
      IF (NSTR.NE.1) GO TO 185
      CSR=CSRS
      SWEEPR=SWEEPRS
      CALL GEOM

c  velocity increment counter
185  ITC=0

c  reversal parameters
      VR=0.0
      VV=VQ

c  top of loop for velocity iterations
c  conversion to ft/sec
500  V=(VV/3600)*5280
c  conversion to psi
      Q=.5*(RHO/(12**4))*(V*12)**2

c  calculate AOA from aileron deflection
      CALL CAILRN

c  flexible wing characteristics
      CALL FLEXROL

      IF (ITC.GT.0) GO TO 210
      WRITE (6,*)
      WRITE (6,*) "          * FLEXIBLE WING RESULTS *"
      WRITE (6,*)
      WRITE (6,*) "Pb/2V = ",PB2V
      WRITE (6,*)
      WRITE (6,*) "CENTER OF PRESSURE LOCATION (inches)  X = ",XCP
      WRITE (6,*) "                                           Y = ",YCP
      WRITE (6,*) "CL alpha = ",FLIFT
      WRITE (6,*)
      WRITE (6,*) "TOTAL LIFT ON SEMI-SPAN (lbf) = ",FL
      WRITE (6,970)

```

```

      DO 200 I=1,NP
200  WRITE (6,*) I,SLOPE(I)
      WRITE (6,*)

c   calculate torlional deformations

      CALL DEFLCT

      WRITE (6,*) "PANEL TORSIONAL DEFLECTIONS (deg)"
      WRITE (6,*) "  POSITIVE LEADING EDGE UP"
      WRITE (6,*)

      DO 205 I=1,NP
205  WRITE (6,*) I,SAOA(I)

      WRITE (6,*)

c   calculate divergence conditions

210  CALL DIVERG

      IF (ITC.GT.0) GO TO 220
      IF (VDIV.LE.0.0) WRITE (6,*) "THIS WING WILL NOT DIVERGE"

      WRITE (6,*) "DIVERGENCE DYNAMIC PRESSURE (psi) = ",QDIV
      WRITE (6,*)
      WRITE (6,*) "DIVERGENCE SPEED (mph) = ",VDIV
      WRITE (6,*)
220  IF ((PB2V.LE.0).AND.(VV.GT.VQ)) WRITE (6,*)
1"REVERSAL SPEED (MPH) = ",VV
      IF ((PB2V.LE.0).AND.(VV.EQ.VQ)) WRITE (6,*)
1"REVERSAL SPEED LESS THAN STARTING VELOCITY"
      IF (PB2V.LE.0) GO TO 230
      VV=VV+VQI
      ITC=ITC+1
      IF ((PB2V.GT.0).AND.(ITC.GT.ITN)) WRITE (6,*)
1"NO REVERSAL WITHIN SPEED RANGE"
      IF (ITC.GT.ITN) GO TO 230
      GO TO 500

c   increment laminate rotation for each case
230  D=D+DDEL

890  FORMAT (18A4)
900  FORMAT (3X,5HPANEL,4X,4HZAOA,6X,5HSHAPE,7X,2HCM,6X,
15HCMDEL)
910  FORMAT (5X,I2,4(1X,F9.4))
920  FORMAT (3X,5HLAYER,6X,3HZNL,7X,3HZNU,4X,5HTHETA)
930  FORMAT (31X,18H(all units inches)/22X,
136H(X,Y panel center on reference axis)/3X,5HPANEL,5X,1HX,9X,
21HY,9X,1HC,8X,2HCS,9X,1HH,9X,1HE,6X,8HSWP(DEG))
940  FORMAT (4X,I2,7(1X,F9.2))
950  FORMAT (/ ,4X,5HPANEL7X,2HEI,9X,2HGJ,11X,1HK/
112X,8Hlb-in**2,4X,8Hlb-in**2,8X,1H-)
960  FORMAT (5X,I2,2X,3E12.5)
970  FORMAT (/ ,2X,14HPANEL CL alpha/19HPANEL 1 IS OUTBOARD/)

      END

```

A sample input for COMPSTAT is provided following. The input is that used to produce some of the data presented in the body of this report. Details of the derivation of some of this input are given below.

$$C_{l\alpha} = 6.28 \text{ (} 2\pi \text{, symmetric airfoil)}$$

$$C_{l\delta} = 3.7 \text{ (Figure 26)}$$

(c_f is percent chord of control surface)

$$C_{m\delta} = -0.64$$

from the equation provided in Reference 7

$$C_{m\delta} = -2\pi c_f (1 - c_f/c)^3/c \quad (142)$$

$$CM = 0.5892 \quad CMDEL = -0.64$$

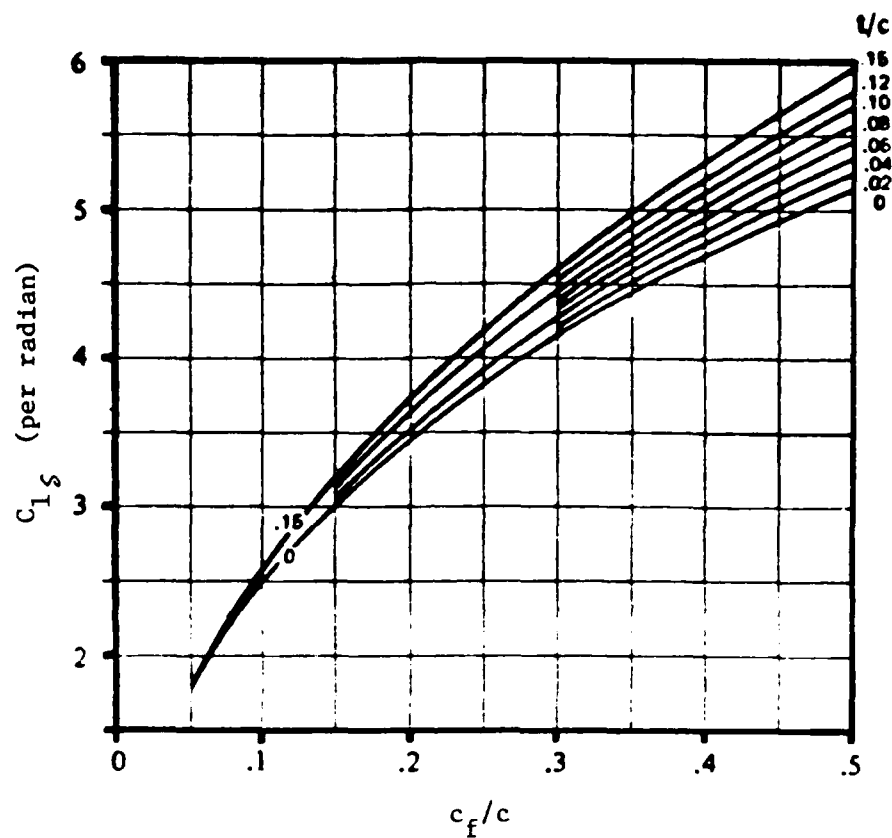


Figure 26. Theoretical Lift Effectiveness for Plain Flap
(from Reference 8)

A sample output for the COMPSTAT program corresponding to the input deck is provided in the following pages. These result are those presented within the body of this report.

SAMPLE RUN FOR PROGRAM COMPSTAT

32 32 10 3 1 1 1

10.0 6.2832
100.0 0.002308 0
1.0 100

37.5 36.13 9.375 18.75
45.0 18.4 0.2

28.25 21.5

18844000. 1468000. .280 910000.

5.0	0.5854	-0.64	-1.0
5.0	0.5854	-0.64	-1.0
5.0	0.5854	-0.64	-1.0
5.0	0.5854	-0.64	-1.0
5.0	0.5854	-0.64	-1.0
5.0	0.5854	-0.64	-1.0
5.0	0.5854	-0.64	0.0
5.0	0.5854	-0.64	0.0
5.0	0.5854	-0.64	0.0
5.0	0.5854	-0.64	0.0

0.07875	0.084	90.0
0.0735	0.07875	90.0
0.06825	0.0735	90.0
0.063	0.06825	90.0
0.05775	0.063	90.0
0.0525	0.05775	90.0
0.04725	0.0525	90.0
0.042	0.04725	90.0
0.03675	0.042	45.0
0.0315	0.03675	135.0
0.02625	0.0315	45.0
0.021	0.02625	135.0
0.01575	0.021	45.0
0.0105	0.01575	135.0
0.00525	0.0105	45.0
0.0	0.00525	135.0
-0.00525	0.0	135.0
-0.0105	-0.00525	45.0
-0.01575	-0.0105	135.0
-0.021	-0.01575	45.0
-0.02625	-0.021	135.0
-0.0315	-0.02625	45.0
-0.03675	-0.0315	135.0
-0.042	-0.03675	45.0
-0.04725	-0.042	90.0
-0.0525	-0.04725	90.0
-0.05775	-0.0525	90.0
-0.063	-0.05775	90.0
-0.06825	-0.063	90.0
-0.0735	-0.06825	90.0
-0.07875	-0.0735	90.0
-0.084	-0.07875	90.0

Sample input for COMPSTAT

SAMPLE RUN FOR PROGRAM COMPSTAT

TEST CONDITIONS:

INITIAL VELOCITY (mph) = 1.000000000E+02
 VELOCITY INCREMENT (mph) = 1.00000000
 NUMBER OF VELOCITY INCREMENTS = 100
 TEST DYNAMIC PRESSURE (psi) = 1.723876595E-01
 AIR DENSITY (lbf s**2/ft**4) = 2.308000112E-03

INPUT CONSTANTS:

NUMBER OF SEMI-SPAN PANELS = 10
 NUMBER OF PLYS TO BE ROTATED = 32
 VARIABLE PLY ROTATION ANGLE (degrees) = 1.000000000E+01

WING PARAMETERS:

2-D LIFT CURVE SLOPE OF SECTION = 6.28319979
 ROOT A.C. & STRUCTURAL AXIS OFFSET (inches) = 9.37500000

AILERON DATA:

PANEL	ZAOA	SHAPE	CM	CMDEL
1	5.0000	-1.0000	.5854	-.6400
2	5.0000	-1.0000	.5854	-.6400
3	5.0000	-1.0000	.5854	-.6400
4	5.0000	-1.0000	.5854	-.6400
5	5.0000	-1.0000	.5854	-.6400
6	5.0000	-1.0000	.5854	-.6400
7	5.0000	.0000	.5854	-.6400
8	5.0000	.0000	.5854	-.6400
9	5.0000	.0000	.5854	-.6400
10	5.0000	.0000	.5854	-.6400

MATERIAL PROPERTIES:

E1 (psi) = 1.884400000E+07
 E2 (psi) = 1.468000000E+06
 P12 = 2.800000012E-01
 G12 (psi) = 9.100000000E+05

COMPOSITE LAYUP:

LAYER	CONSTANT	SPANWISE	LAYUP	THICKNESS
	ZNL	ZNU	THETA	
1	.0787	.0840	90.0000	
2	.0735	.0787	90.0000	
3	.0683	.0735	90.0000	
4	.0630	.0683	90.0000	
5	.0578	.0630	90.0000	
6	.0525	.0578	90.0000	
7	.0472	.0525	90.0000	
8	.0420	.0472	90.0000	
9	.0367	.0420	45.0000	
10	.0315	.0367	135.0000	
11	.0262	.0315	45.0000	
12	.0210	.0262	135.0000	
13	.0158	.0210	45.0000	
14	.0105	.0158	135.0000	
15	.0052	.0105	45.0000	
16	.0000	.0052	135.0000	
17	-.0052	.0000	135.0000	
18	-.0105	-.0052	45.0000	
19	-.0158	-.0105	135.0000	

20	-.0210	-.0158	45.0000
21	-.0262	-.0210	135.0000
22	-.0315	-.0262	45.0000
23	-.0367	-.0315	135.0000
24	-.0420	-.0367	45.0000
25	-.0472	-.0420	90.0000
26	-.0525	-.0472	90.0000
27	-.0578	-.0525	90.0000
28	-.0630	-.0578	90.0000
29	-.0683	-.0630	90.0000
30	-.0735	-.0683	90.0000
31	-.0787	-.0735	90.0000
32	-.0840	-.0787	90.0000

PLANFORM DATA:

ROOT CHORD (INCHES) = 3.750000000E+01
 ROOT STRUCTURAL CHORD (inches) = 3.613000107E+01
 ROOT STRUCTURAL CHORD SWEEP (degrees) = 1.839999962E+01
 SEMI-SPAN (inches) = 4.500000000E+01
 WING TAPER RATIO = 2.000000030E-01
 BOX BEAM ROOT CHORD (inches) = 2.825000000E+01
 BOX BEAM REF. AXIS SWEEP (deg) = 2.150000000E+01
 SEMI-SPAN AREA (in.**2) = 1.012500000E+03
 LINEARLY TAPERED PLANFORM

(all units inches)

PANEL	X	Y	C	CS	H	E	SWP(DEG)
1	14.22	42.75	9.00	7.19	4.50	1.87	18.40
2	12.72	38.25	12.00	10.24	4.50	2.66	18.40
3	11.23	33.75	15.00	13.28	4.50	3.45	18.40
4	9.73	29.25	18.00	16.33	4.50	4.24	18.40
5	8.23	24.75	21.00	19.38	4.50	5.03	18.40
6	6.74	20.25	24.00	22.42	4.50	5.82	18.40
7	5.24	15.75	27.00	25.47	4.50	6.61	18.40
8	3.74	11.25	30.00	28.51	4.50	7.40	18.40
9	2.25	6.75	33.00	31.56	4.50	8.19	18.40
10	.75	2.25	36.00	34.61	4.50	8.98	18.40

(ALL VALUES FOLLOWING FOR INITIAL VELOCITY ONLY)

* RIGID WING RESULTS *

Pb/2V = 7.593737841E-01

CENTER OF PRESSURE LOCATION (inches) X = 4.685883224E-01
 Y = 1.936562538E+01

CL alpha = 2.137715340E+01

TOTAL LIFT ON SEMI-SPAN (lbf) = 2.600272217E+02

PANEL CL alpha
 PANEL 1 IS OUTBOARD

1	5.63283920
2	6.04308939
3	5.88063383
4	5.59830379
5	5.28903675

6 4.97688055
 7 4.66775370
 8 4.36209822
 9 4.05900240
 10 3.75866151

FIRST VARIABLE PLY ORIENTATION - 9.000000000E+01

PANEL	EI lb-in**2	GJ lb-in**2	K -
1	.35461E+05	.11719E+05	.41888E+03
2	.52108E+05	.17220E+05	.61552E+03
3	.68755E+05	.22721E+05	.81216E+03
4	.85402E+05	.28222E+05	.10088E+04
5	.10205E+06	.33723E+05	.12054E+04
6	.11870E+06	.39224E+05	.14021E+04
7	.13534E+06	.44725E+05	.15987E+04
8	.15199E+06	.50226E+05	.17953E+04
9	.16864E+06	.55727E+05	.19920E+04
10	.18528E+06	.61228E+05	.21886E+04

* FLEXIBLE WING RESULTS *

Pb/2V - 6.531494111E-02

CENTER OF PRESSURE LOCATION (inches) X - 1.13275003
 Y - 2.067225456E+01

CL alpha - 2.10867143

TOTAL LIFT ON SEMI-SPAN (lbf) - 7.149621582E+01

PANEL CL alpha
 PANEL 1 IS OUTBOARD

1 1.98852074
 2 2.08585072
 3 1.97293186
 4 1.81573761
 5 1.65025866
 6 1.48767102
 7 1.33277619
 8 1.18872142
 9 1.05883360
 10 9.485813379E-01

PANEL TORSIONAL DEFLECTIONS (deg)
 POSITIVE LEADING EDGE UP

1 4.022011906E-02
 2 7.944701612E-02
 3 1.168501452E-01
 4 1.515954584E-01
 5 1.828642488E-01
 6 2.098727375E-01
 7 2.318922579E-01
 8 2.482672185E-01
 9 2.584269345E-01
 10 2.618871629E-01

DIVERGENCE DYNAMIC PRESSURE (psi) = 4.427346289E-01

DIVERGENCE SPEED (mph) = 1.602576141E+02

REVERSAL SPEED (MPH) = 1.050000000E+02

FIRST VARIABLE PLY ORIENTATION = 1.000000000E+02

PANEL	EI lb-in**2	GJ lb-in**2	K -
1	.33911E+05	.14720E+05	-.90781E+04
2	.49830E+05	.21630E+05	-.13340E+05
3	.65750E+05	.28540E+05	-.17601E+05
4	.81669E+05	.35450E+05	-.21863E+05
5	.97588E+05	.42360E+05	-.26125E+05
6	.11351E+06	.49270E+05	-.30386E+05
7	.12943E+06	.56180E+05	-.34648E+05
8	.14535E+06	.63090E+05	-.38909E+05
9	.16126E+06	.70000E+05	-.43171E+05
10	.17718E+06	.76910E+05	-.47433E+05

* FLEXIBLE WING RESULTS *

Pb/2V = -4.143407568E-02

CENTER OF PRESSURE LOCATION (inches)	X =	3.489552736E-01
	Y =	1.913026619E-01

CL alpha = 6.401095390E-01

TOTAL LIFT ON SEMI-SPAN (lbf) = 5.033717957E+02

PANEL CL alpha
PANEL 1 IS OUTBOARD

1	8.288786411E-01
2	8.866006732E-01
3	8.611028790E-01
4	8.200795054E-01
5	7.774482369E-01
6	7.365571856E-01
7	6.977873445E-01
8	6.604267955E-01
9	6.231769323E-01
10	5.841282010E-01

PANEL TORSIONAL DEFLECTIONS (deg)
POSITIVE LEADING EDGE UP

1	-4.646832589E-03
2	-9.582110681E-03
3	-1.484933961E-02
4	-2.036479674E-02
5	-2.595181204E-02
6	-3.136026859E-02
7	-3.627770767E-02
8	-4.033524171E-02
9	-4.310931265E-02

10 -4.411911219E-02

DIVERGENCE DYNAMIC PRESSURE (psi) - 2.882335281E+01

DIVERGENCE SPEED (mph) - 1.293061401E+03

REVERSAL SPEED LESS THAN STARTING VELOCITY

FIRST VARIABLE PLY ORIENTATION - 1.100000000E+02

PANEL	EI lb-in**2	GJ lb-in**2	K -
1	.29422E+05	.22320E+05	-.16048E+05
2	.43233E+05	.32797E+05	-.23582E+05
3	.57045E+05	.43275E+05	-.31115E+05
4	.70857E+05	.53753E+05	-.38649E+05
5	.84668E+05	.64230E+05	-.46183E+05
6	.98480E+05	.74708E+05	-.53716E+05
7	.11229E+06	.85186E+05	-.61250E+05
8	.12610E+06	.95664E+05	-.68784E+05
9	.13991E+06	.10614E+06	-.76317E+05
10	.15373E+06	.11662E+06	-.83851E+05

* FLEXIBLE WING RESULTS *

Pb/2V - -1.098326221E-01

CENTER OF PRESSURE LOCATION (inches) X - -3.124650717E-01
Y - 1.782903290E+01

CL alpha - 3.189558983E-01

TOTAL LIFT ON SEMI-SPAN (lbf) - 5.303195801E+02

PANEL CL alpha
PANEL 1 IS OUTBOARD

1	4.749123752E-01
2	5.200316310E-01
3	5.204787254E-01
4	5.140408278E-01
5	5.080339909E-01
6	5.035698414E-01
7	4.998199344E-01
8	4.949915111E-01
9	4.863912165E-01
10	4.697191417E-01

PANEL TORSIONAL DEFLECTIONS (deg)
POSITIVE LEADING EDGE UP

1	-1.826104894E-02
2	-3.659510985E-02
3	-5.482691899E-02
4	-7.262137532E-02
5	-8.952312917E-02
6	-1.049788967E-01
7	-1.183499768E-01
8	-1.289179921E-01

9 -1.358843893E-01
10 -1.383622438E-01

DIVERGENCE DYNAMIC PRESSURE (psi) - 3.664583130E+02

DIVERGENCE SPEED (mph) - 4.610618164E+03

REVERSAL SPEED LESS THAN STARTING VELOCITY

Sample output for COMPSTAT

Appendix C: Dynamic Data

Ground Vibration Test Results

The GVT was performed on the bare plates suspended in the wind tunnel in the same manner as they would be for an actual "wind-on" data run. The GVT was conducted using the sine-dwell method. The excitation point and reference accelerometer were placed at different locations depending upon the mode sought. A roving accelerometer was used to locate node lines. Accelerometers were applied to the plate with double-sided tape.

Results of the GVT are presented in Figures 27-29 and summarized in Table XI. Figures for the first bending mode are not shown because, by definition, the node line always occurs at the root and a figure would be uninteresting. Dotted lines indicate node lines. Shaker and reference accelerometer locations are indicated.

The damping given in Table XI is the viscous damping factor for the first bending mode. This was derived from a trace of vibration decay for this mode using the log decrement technique (11:30-31). The viscous damping factor is defined as

$$\zeta = \delta / (4\pi^2 + \delta^2)^{1/2} \quad (143)$$

where

$$\delta = (1/j)\ln(x_1/x_{j+1}) \quad (144)$$

and x_1 is the magnitude of one trace oscillation, peak-to-peak, and x_{j+1}

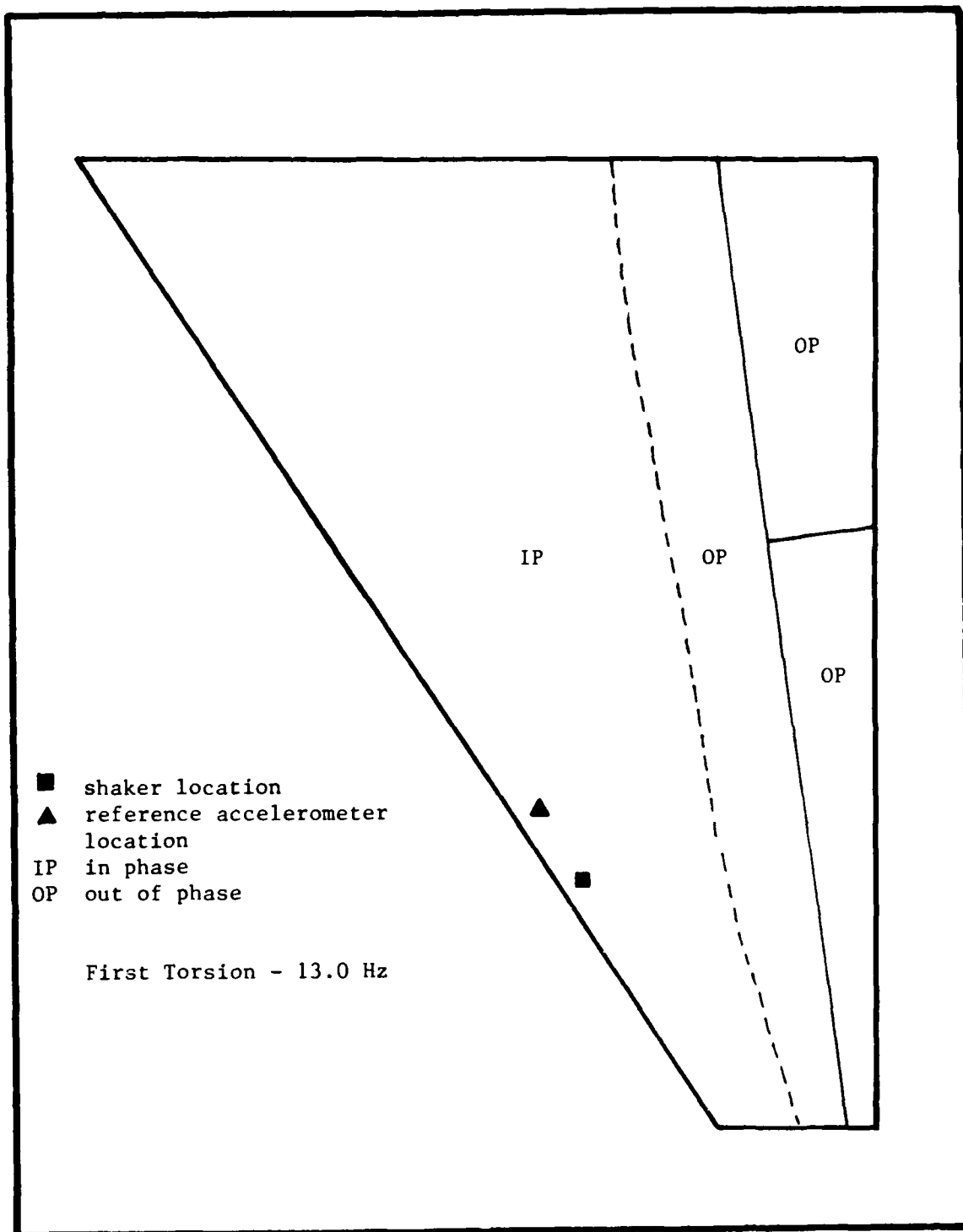


Figure 27A. Case 1 GVT Results

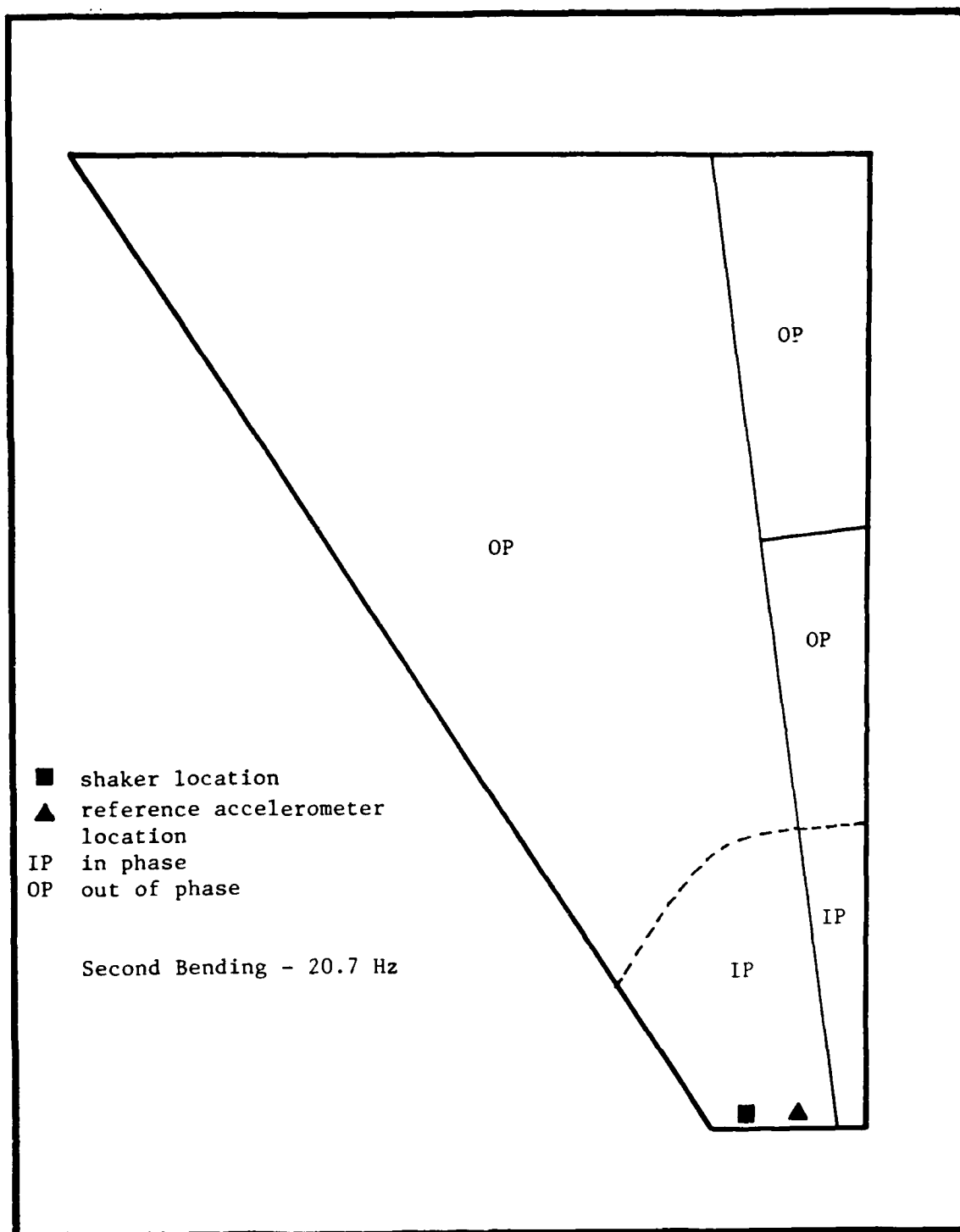


Figure 27B. Case 1 GVT Results

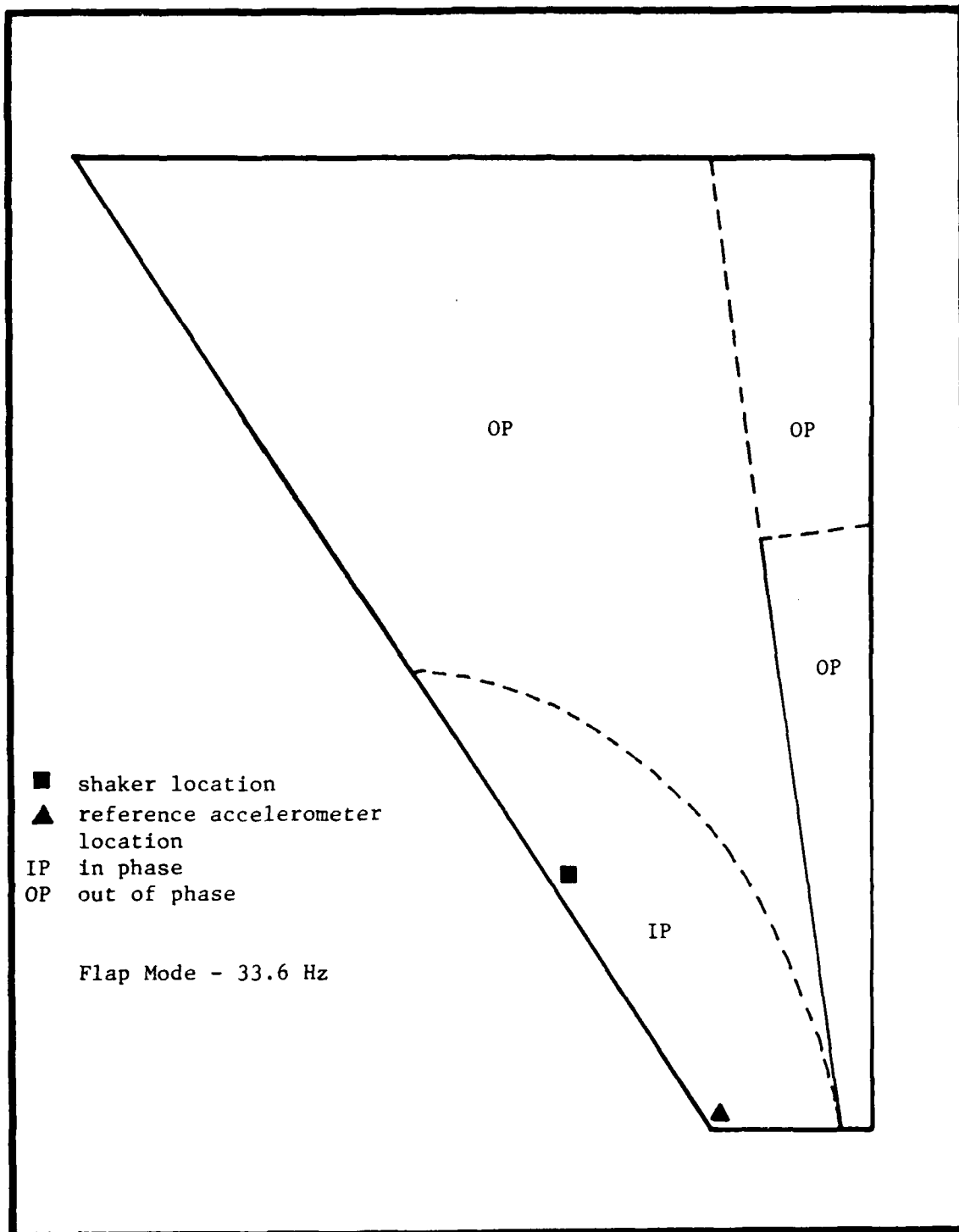


Figure 27C. Case 1 GVT Results

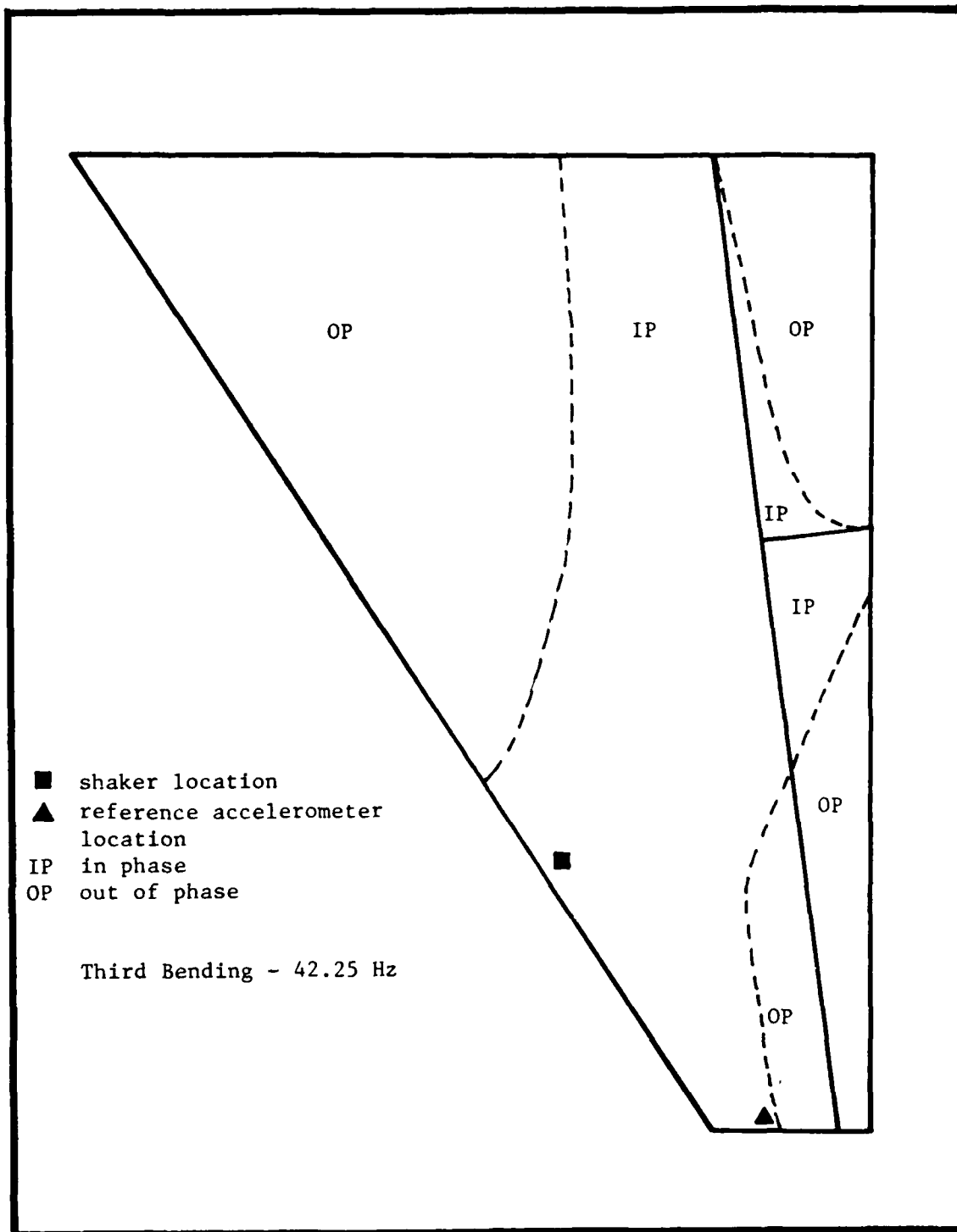


Figure 27D. Case 1 GVT Results

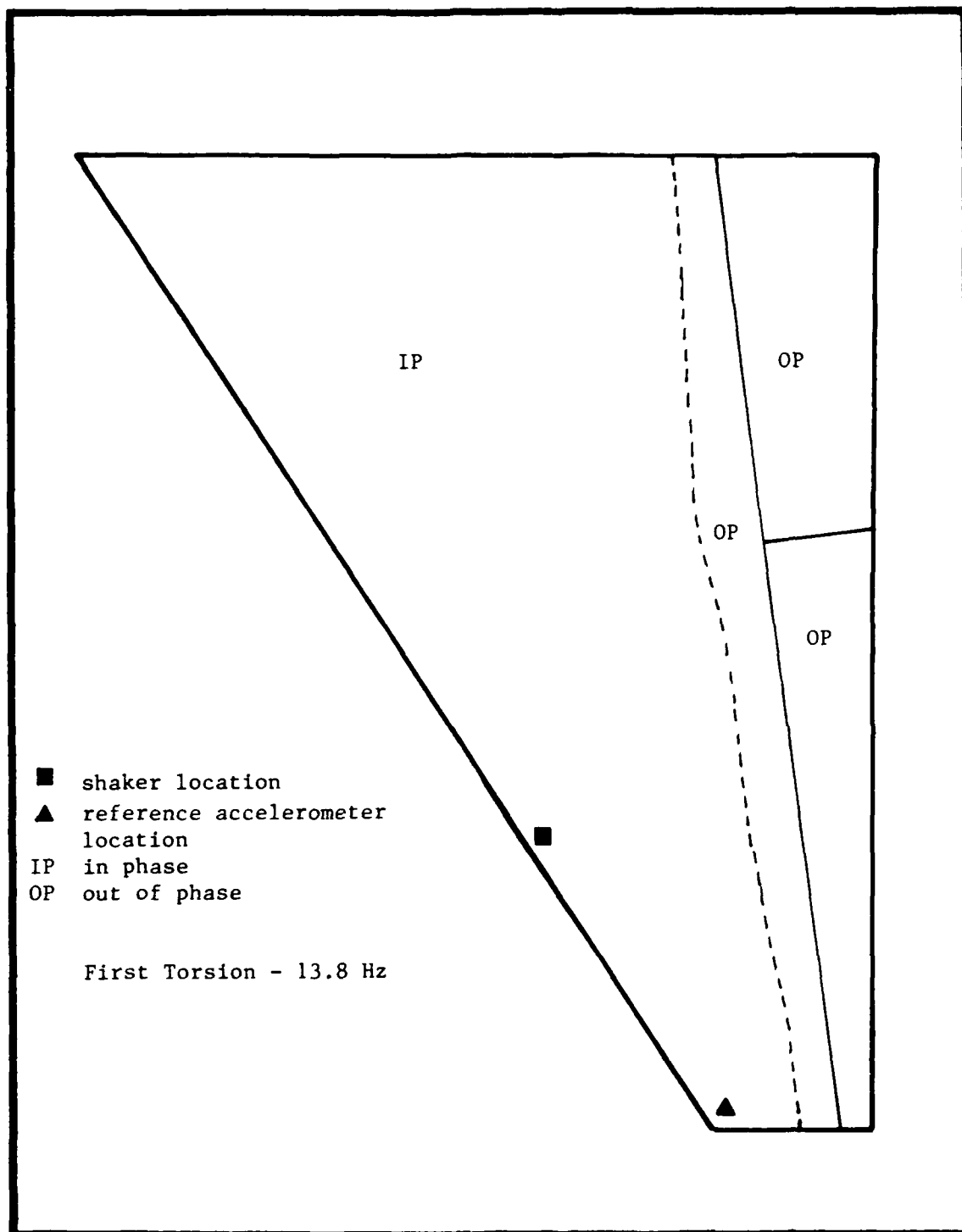


Figure 28A. Case 2 GVT Results

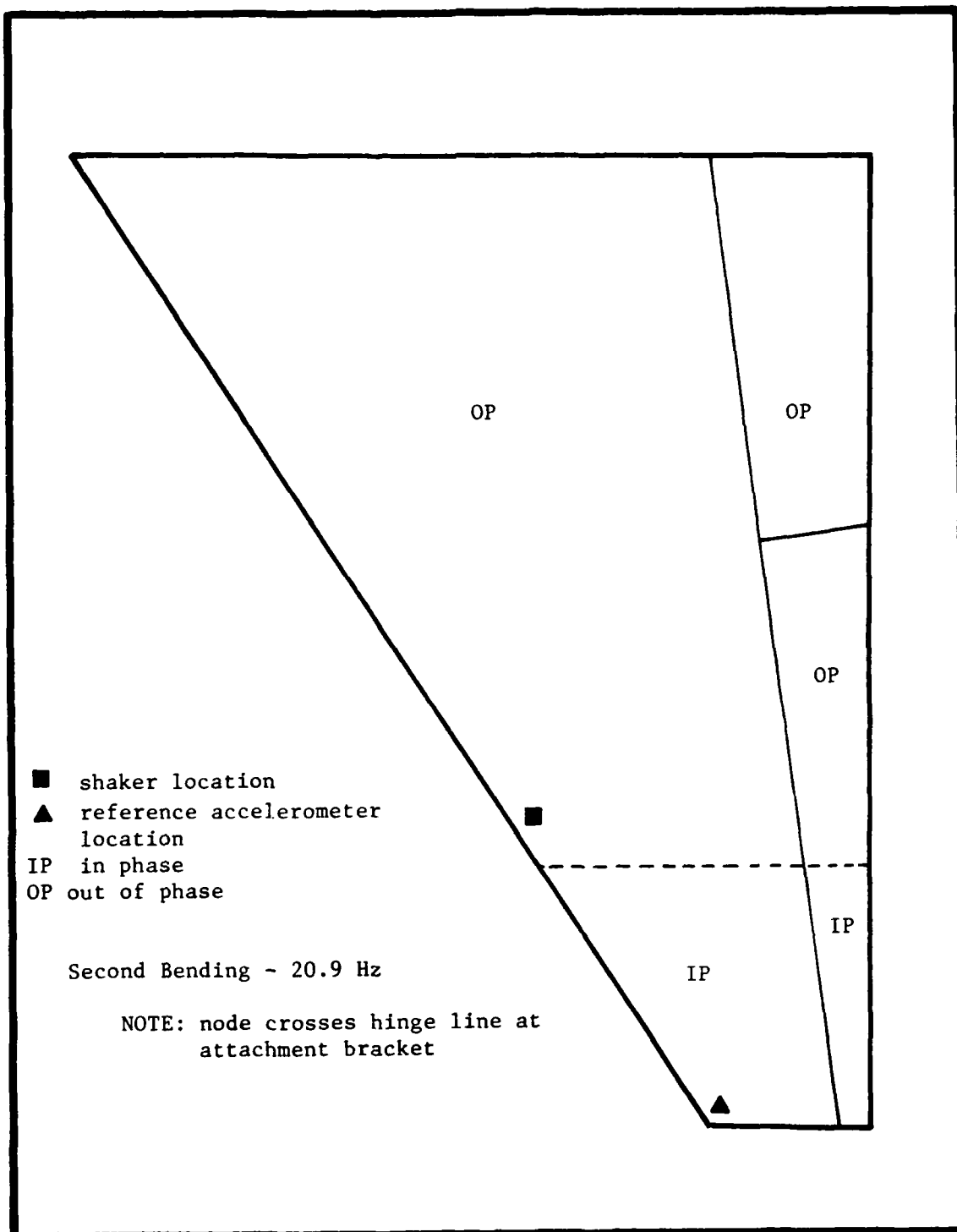


Figure 28B. Case 2 GVT Results

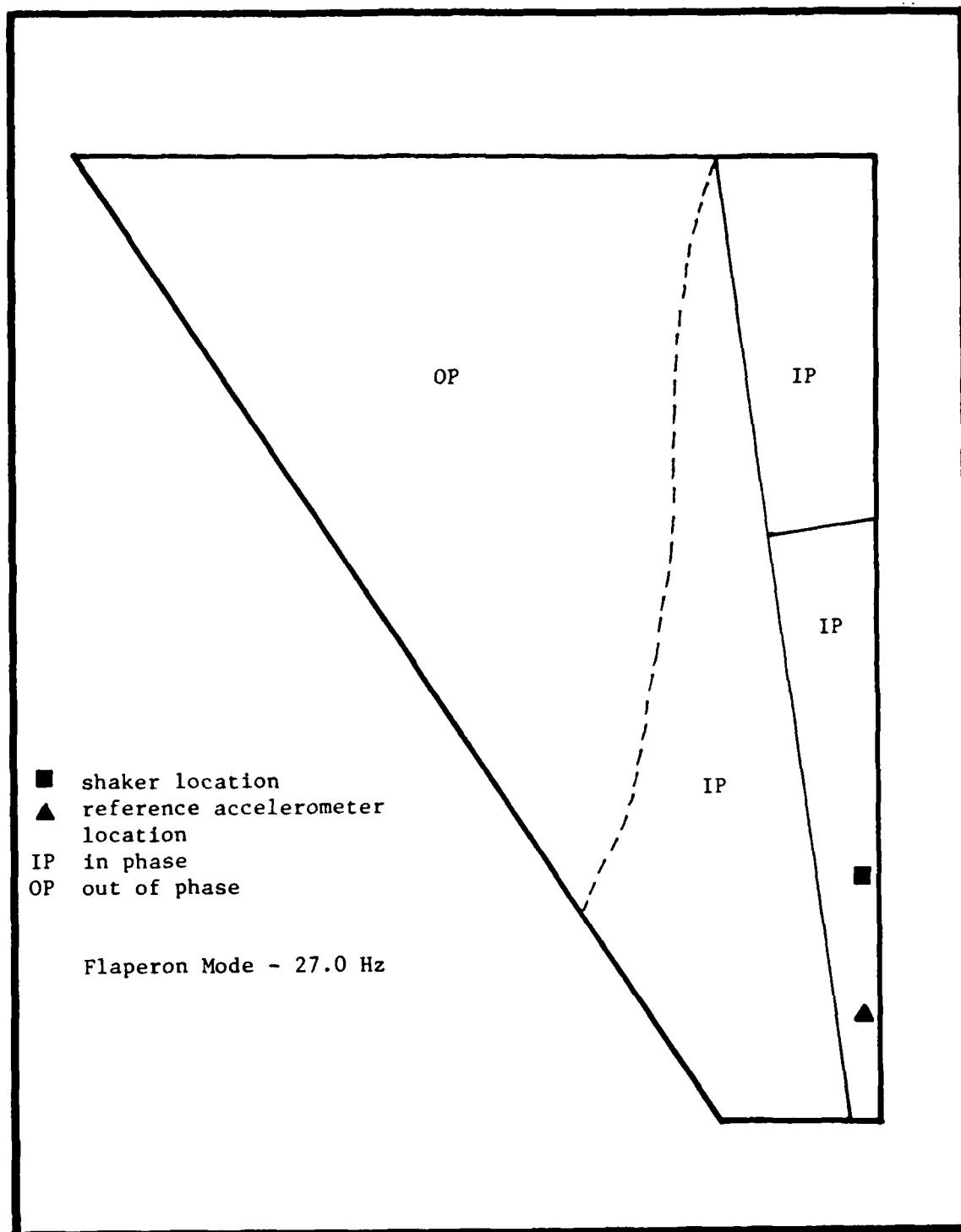


Figure 28C. Case 2 GVT Results

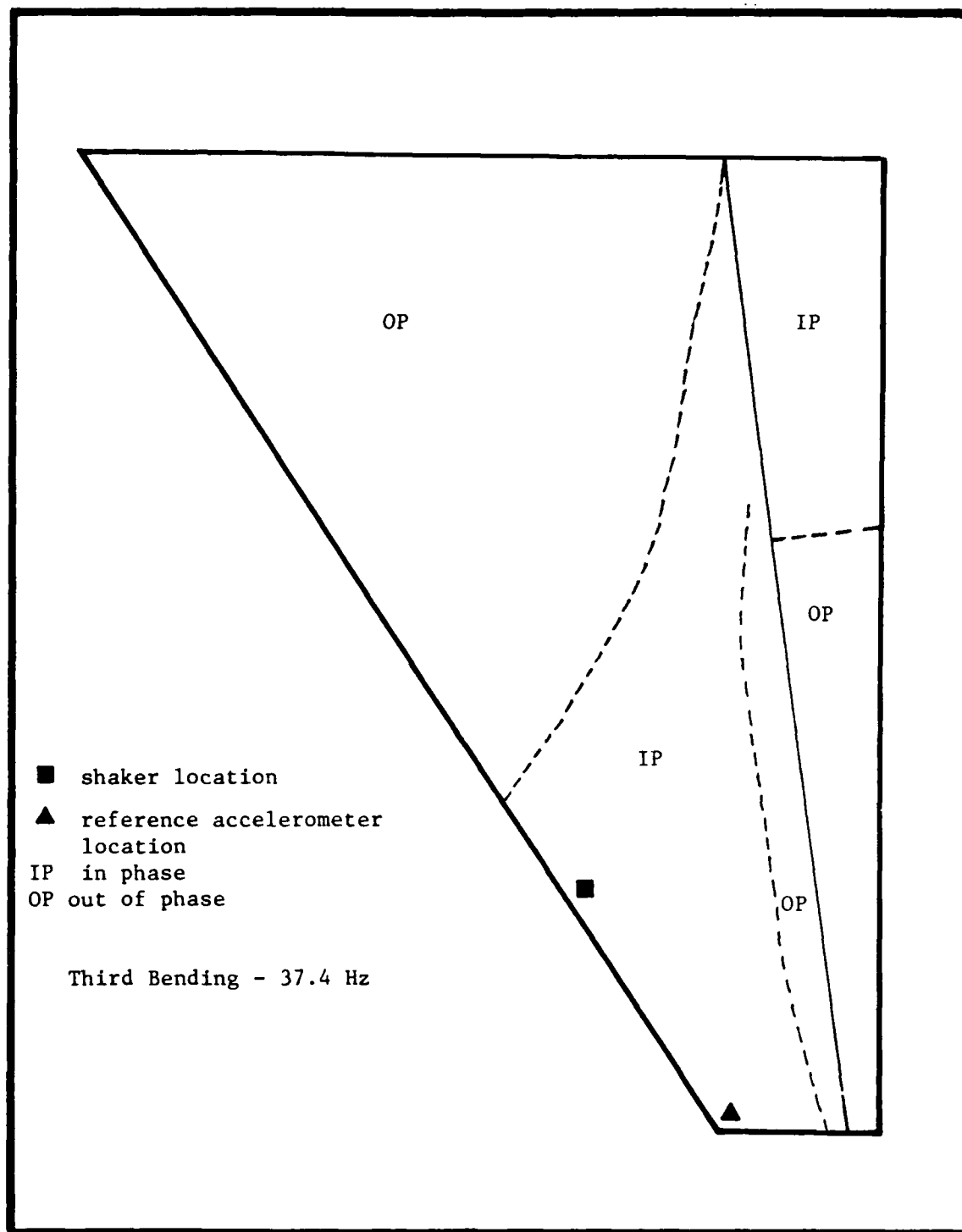


Figure 28D. Case 2 GVT Results

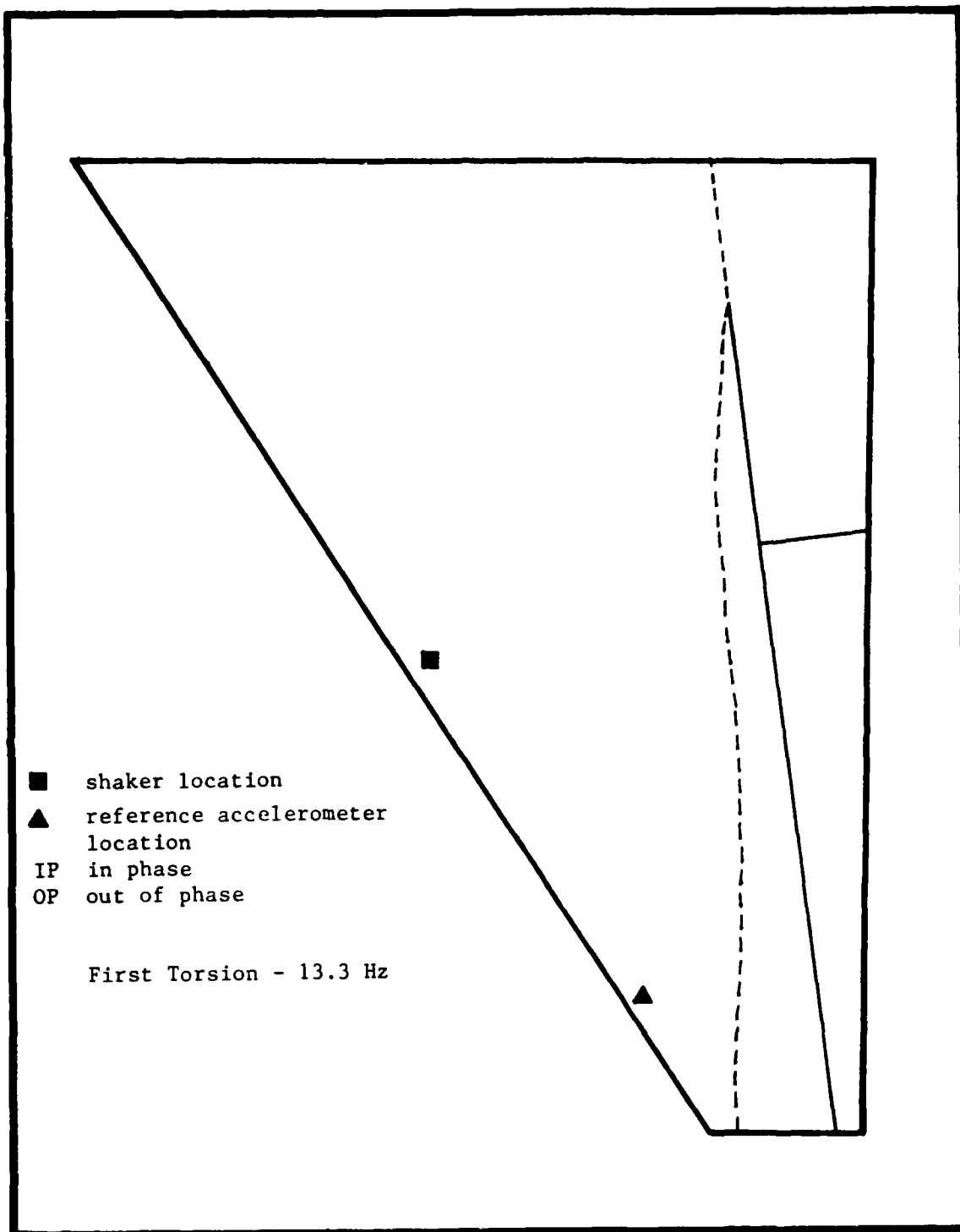


Figure 29A. Case 3 GVT Results

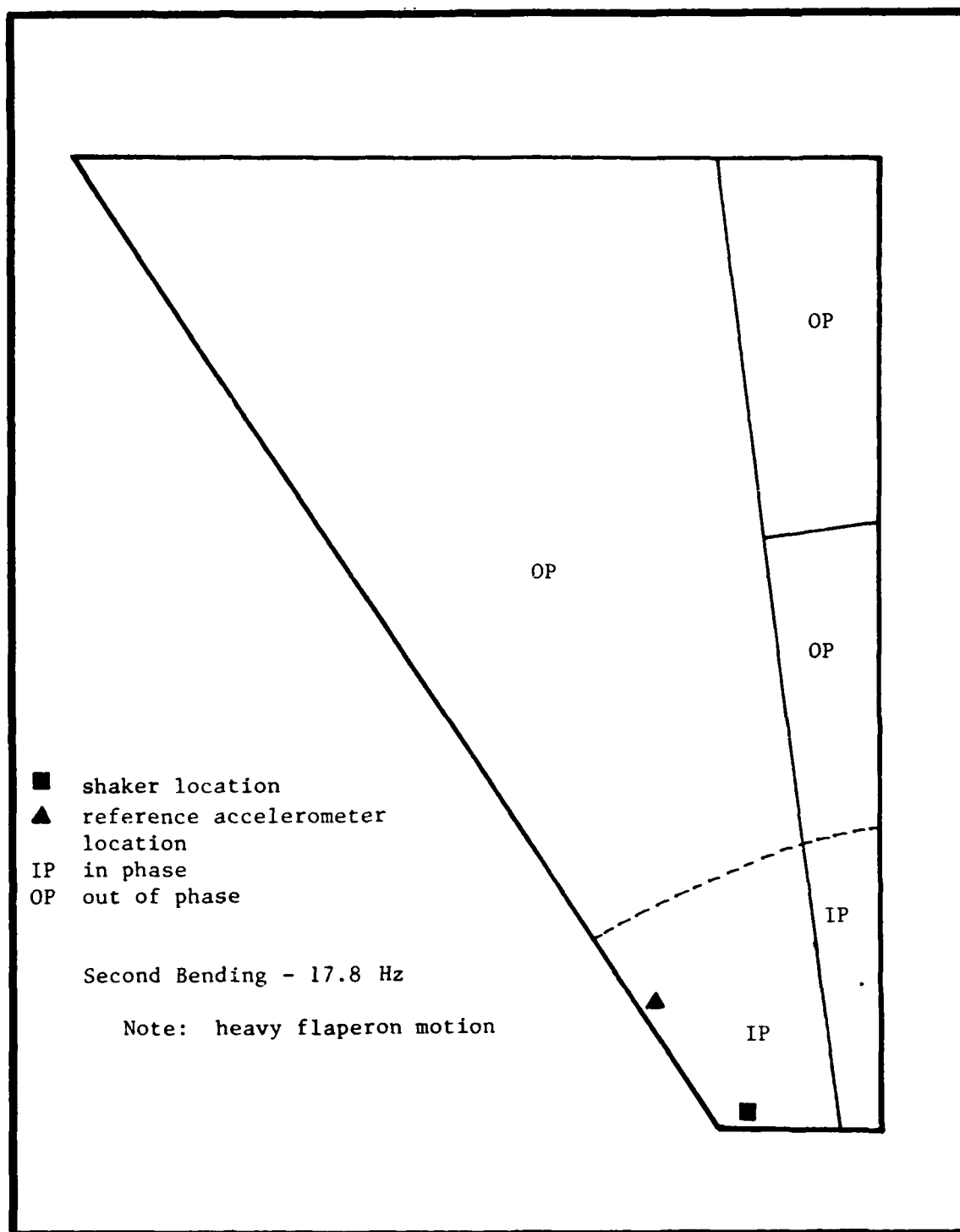


Figure 29B. Case 3 GVT Results

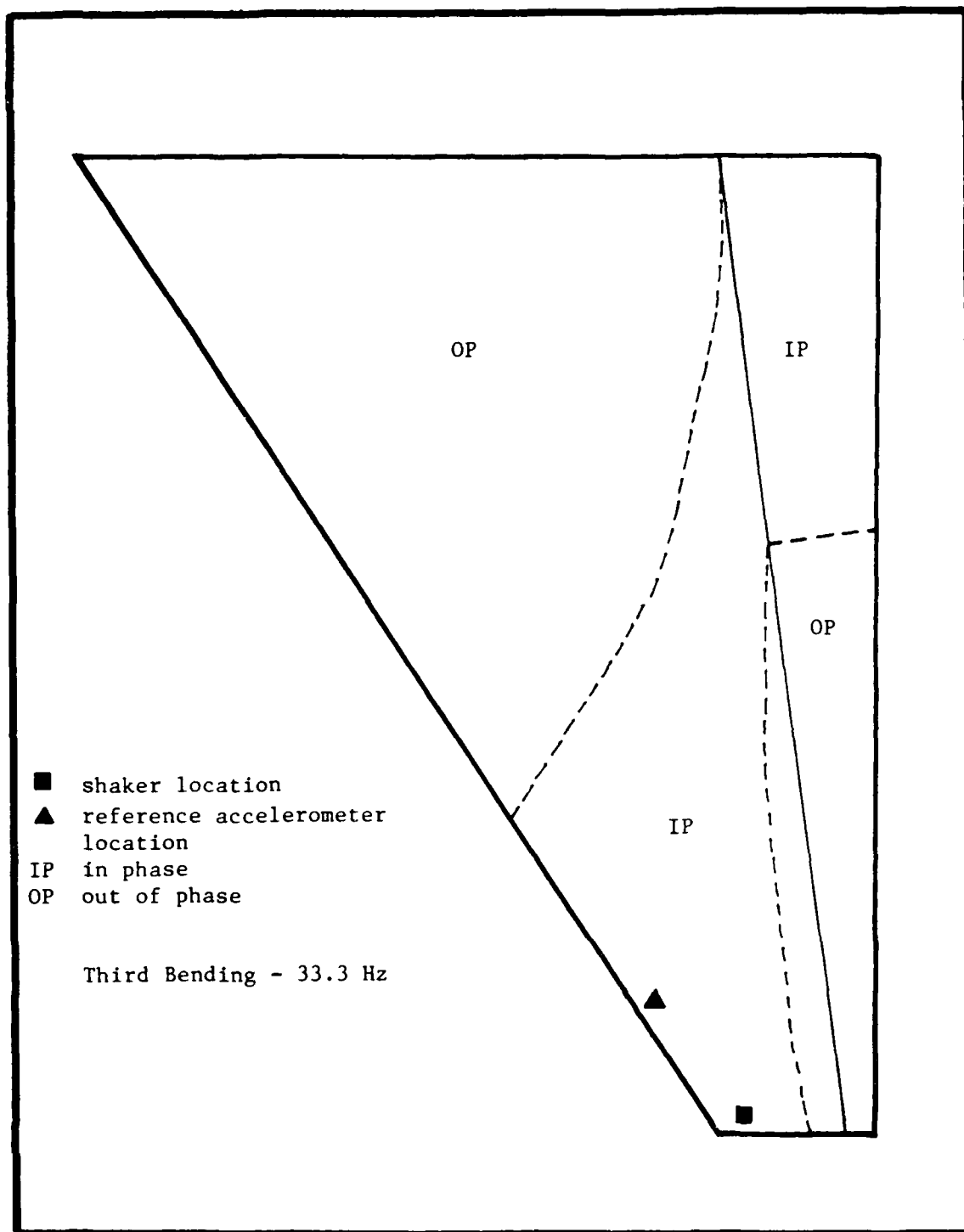


Figure 29C. Case 3 GVT Results

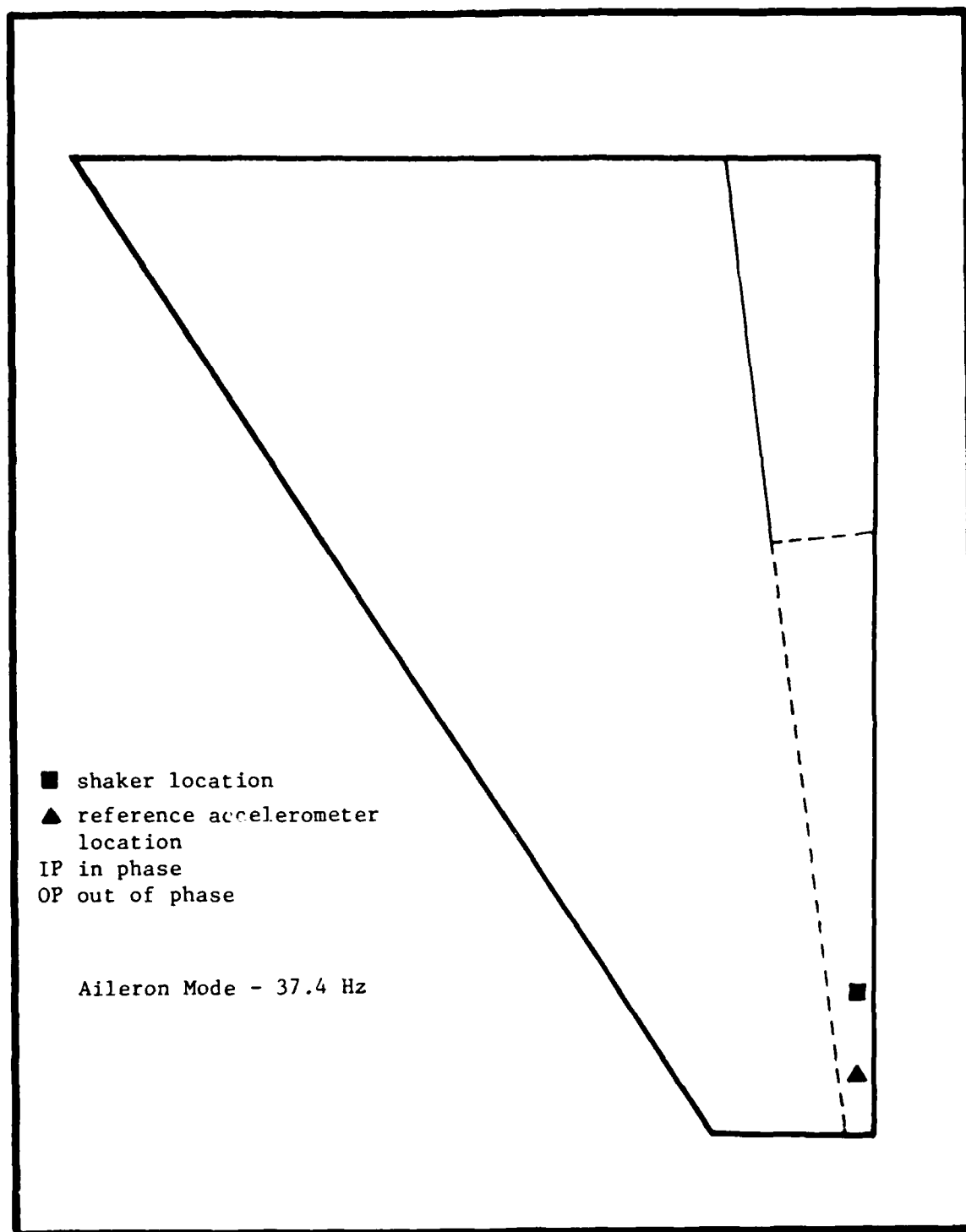


Figure 29D. Case 3 GVT Results

Table XI
Ground Vibration Test Results

Mode	Natural Frequencies (Hz)		
	Case 1	Case 2	Case 3
1st Bending	4.5	4.3	3.7
1st Torsion	13.9	13.8	13.3
2nd Bending	17.8	20.9	17.8
3rd Bending	42.25	37.4	33.3
Aileron	-	27.0	37.4
Flap	33.6	-	-
Damping Factor	-	0.0082	0.0246

the magnitude of another j peaks away. ζ is related to the natural frequency (ω_n) and damping factor by the expression

$$\zeta = C_f / 2m\omega_n \quad (145)$$

The exponential decay of the structure's oscillation is due to viscous damping, where the exponent is a linear function of ζ . Therefore, ζ is a measure of the structure's damping.

Derivation of Dynamic Parameters

The dynamic parameters used in program CWINGF have been derived by simplified methods that are outlined here.

section center of gravity assumed to be at midchord
square of the panel radius of gyration about the elastic axis
has been approximated to be $c^2/12$
the mass per unit length of the covering material on each
plate panel has been approximated with the following
equation

$$m_i = 0.078(2.0)c_i^2h_i \quad (146)$$

where 2.0 is the density of the material in lbm/ft^3

CWINGF Results

The following parameters were used in the input deck for Dr. Weisshaar's CWINGF flutter analysis program. Only those that cannot be deduced from other portions of this report are included.

100 lbm = one half of fuselage mass

9999 lfm in² = one half of fuselage pitching moment of

inertia about fuselage center of gravity

0.0 in. = offset of reference axis at root and fuselage center

0.0 in. = offset of reference axis at root and aircraft c.g.

2733300 psi = fuselage bending stiffness

5466600 psi = fuselage torsion stiffness

Frequency and divergence data produced by the CWINGF program using beam theory are provided in Table XII for both the covered and uncovered composite plates. Comparison with the GVT (Table XI) and static analysis results show poor correlation. This comparison is uncertain in that the modes are not identified. This poor correlation casts doubt on the flutter computation results which predicted flutter-free operation to 300 mph. The reduction of the frequencies with the addition of the mass contributed by the foam covering is as expected.

Table XII

CWINGF Flutter Analysis Results

(V_D in mph)

Mode	Natural Frequencies (Hz)					
	Uncovered			Covered		
	Case 1	Case 2	Case 3	Case 1	Case 2	Case 3
1	5.8	5.1	4.1	4.4	3.8	3.0
2	10.8	12.3	15.2	7.4	8.5	10.4
3	25.1	21.3	17.4	16.6	14.8	12.5
4	27.5	32.2	34.8	20.2	22.1	23.1
5	40.5	39.7	40.5	27.8	27.7	28.7
V _D	267	3248	*	268	1645	*

* divergence impossible

Appendix D: Material Properties

Material Properties

The material properties of the AS4-3501-6 composite used in the analysis of the test plates are given below.

$$E_1 = 18844000 \text{ psi}$$

$$E_2 = 1468000 \text{ psi}$$

$$\mu_{12} = 0.28$$

$$G_{12} = 910000 \text{ psi}$$

$$\text{ply thickness} = 0.00525 \text{ inches}$$

$$\text{material density} = 0.059 \text{ lbm/in}^3$$

Tensile Test Results

As explained in Section V, special samples of the composite material were subjected to laboratory tests to more precisely determine the material properties. These results were used for the final comparison of test to predicted aeroelastic response. These properties are provided below.

$$E_1 = 18100000 \text{ psi}$$

$$E_2 = 1650000 \text{ psi}$$

$$\mu_{12} = 0.30$$

$$G_{12} = 740000 \text{ psi}$$

$$\text{ply thickness} = 0.00522 \text{ inches}$$

When composite plies are stacked with the fibers parallel, a "nesting" of the fibers occur. When the thickness of a laminate is divided by the number of plies for such a stacking arrangement, a smaller ply thickness will result than for a similar procedure for a laminate with crossed plies.

Bibliography

1. Bertin, J.J. and Smith, M.L., Aerodynamics for Engineers, Prentice-Hall, 1979.
2. Bisplinghoff, R.L., Ashley, H. and Halfman, R.L., Aeroelasticity, Addison-Wesley, 1955.
3. Bisplinghoff, R.L. and Ashley, H., Principles of Aeroelasticity, Dover Publications, 1975.
4. Diederich, F.W. and Budiansky, B., Divergence of Swept Wings, Naca TN 1680, August 1948.
5. Fung, Y.C., An Introduction to the theory of Aeroelasticity, John Wiley & Sons, Inc., 1955.
6. Gray, W.L. and Shenk, K.M., A Method for Calculating the Subsonic Steady-State Loading on an Airplane with a Wing of Arbitrary Planform and Stiffness, NACA TN 3030, December 1953.
7. Hoak, D.E., et al, USAF Stability and Control DATCOM, Revised April 1978, Flight Controls Division, Air Force Flight Dynamics Laboratory.
8. Hoak, D.E., et al, USAF Stability and Control DATCOM, Revised October 1960, Flight Controls Division, Air Force Flight Dynamics Laboratory.
9. Housner, J.M. and Stein, M., Flutter Analysis of Swept-Wing Subsonic Aircraft with Parameter Studies of Composite Wings, NASA TN D-7539, September 1974.
10. Jones, R.M., Mechanics of Composite Materials, McGraw-Hill Book Co., 1975.
11. Meirovitch, L., Elements of Vibration Analysis, McGraw-Hill Book Co., 1986.
12. Rae, W.H., Jr. and Pope, A., Low-Speed Wind Tunnel Testing, John Wiley & Sons, 1984.
13. Sherrer, V., Hertz, T. and Shirk, Michael, A Demonstration of the Principle of Aeroelastic Tailoring Applied to Forward Swept Wings, AFWAL-TR-3066, January 1982.

14. Vanderplaats, G.N., ADS-A Fortran Program for Automated Design Synthesis, NASA Contractor Report 172460, Naval Postgraduate School, Monterey, October 1984.

15. Weisshaar, Terrence A., Aeroelastic Stability and Performance Characteristics of Aircraft with Advanced Composite Sweptforward Wing Structures, FFDL-TR-78-116, September 1978.

16. Weisshaar, Terrence A., Forward Swept Wing Static Aeroelasticity, FFDL-TR-79-3087, June 1979.

17. Weisshaar, Terrence A., The Influence of Aeroelasticity on Swept Composite Wings, Vol. 1 and Vol. 2, AFWAL-TR-80-3137, November 1980.

18. Weisshaar, Terrence A. and Foist, Brian L., Aeroelastic Tailoring of Aircraft Subject to Body Freedom Flutter, AFWAL-TR-83-3123, November 1983.

Vita

Captain William J. Norton was born on 6 February 1959 in Oakland, California. After graduating from High School in 1977, he commenced his college studies at California State Polytechnic University, Pomona. While at the University, he conducted a grant-supported study for the Ames Research Center, NASA, and served as a co-op student at the Air Force Flight Test Center (AFFTC), and the MX Missile Civil Engineering Office. In 1982 he received a Bachelor of Science degree in Aerospace Engineering and was granted a commission in the US Air Force. His initial assignment was to Aeronautical Systems Division (ASD), Wright-Patterson AFB, Ohio. His first duties were to act as the ASD engineering representative during the Dual Role Fighter flight test program at AFFTC. In the summer of 1983 he began working as a flight test engineer at the 4950th Test Wing. His flight test experience includes performance, flying qualities, structural evaluation, and aircraft subsystems. He entered the Air Force Institute of Technology in 1986.

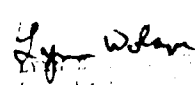
Permanent address: 460 E. Dayton-Y.S. #75
Fairborn, Ohio, 45324


UNCLASSIFIED

SECURITY CLASSIFICATION OF THIS PAGE

REPORT DOCUMENTATION PAGE

Form Approved
OMB No. 0704-0188

1a. REPORT SECURITY CLASSIFICATION UNCLASSIFIED			1b. RESTRICTIVE MARKINGS		
2a. SECURITY CLASSIFICATION AUTHORITY			3. DISTRIBUTION/AVAILABILITY OF REPORT Approved for public release, distribution unlimited		
2b. DECLASSIFICATION/DOWNGRADING SCHEDULE					
4. PERFORMING ORGANIZATION REPORT NUMBER(S) AFIT/GAE/AA/87D-15			5. MONITORING ORGANIZATION REPORT NUMBER(S)		
6a. NAME OF PERFORMING ORGANIZATION School of Engineering	6b. OFFICE SYMBOL (if applicable) AFIT/ENY	7a. NAME OF MONITORING ORGANIZATION			
6c. ADDRESS (City, State, and ZIP Code) Air Force Institute of Technology (AU) Wright-Patterson AFB, Ohio 45433-6583		7b. ADDRESS (City, State, and ZIP Code)			
8a. NAME OF FUNDING/SPONSORING ORGANIZATION Wright Aeronautical Laboratory	8b. OFFICE SYMBOL (if applicable) FIBR	9. PROCUREMENT INSTRUMENT IDENTIFICATION NUMBER			
8c. ADDRESS (City, State, and ZIP Code) Wright-Patterson AFB, Ohio 45433		10. SOURCE OF FUNDING NUMBERS			
		PROGRAM ELEMENT NO.	PROJECT NO.	TASK NO.	WORK UNIT ACCESSION NO.
11. TITLE (Include Security Classification) DESIGN OF AN AEROELASTIC COMPOSITE WING WIND TUNNEL MODEL					
12. PERSONAL AUTHOR(S) William J. Norton, Capt, USAF					
13a. TYPE OF REPORT MS Thesis	13b. TIME COVERED FROM _____ TO _____	14. DATE OF REPORT (Year, Month, Day) 1987 December		15. PAGE COUNT 267	
16. SUPPLEMENTARY NOTATION					
17. COSATI CODES			18. SUBJECT TERMS (Continue on reverse if necessary and identify by block number)		
FIELD	GROUP	SUB-GROUP			
01	01		Composites, Aileron Reversal, Aileron Effectiveness Divergence, Flutter, Aeroelasticity, Optimization Wind Tunnel ←		
19. ABSTRACT (Continue on reverse if necessary and identify by block number)					
Thesis Advisor: Lanson J. Hudson, Major, USAF Instructor of Aeronautical Engineering					
<div style="text-align: right;">  31 Dec 87 Lanson J. Hudson, Major, USAF Air Force Institute of Technology (AFIT) Wright-Patterson AFB OH 45433 </div>					
20. DISTRIBUTION/AVAILABILITY OF ABSTRACT <input checked="" type="checkbox"/> UNCLASSIFIED/UNLIMITED <input type="checkbox"/> SAME AS RPT. <input type="checkbox"/> DTIC USERS			21. ABSTRACT SECURITY CLASSIFICATION UNCLASSIFIED		
22a. NAME OF RESPONSIBLE INDIVIDUAL Lanson J. Hudson, Major, USAF			22b. TELEPHONE (Include Area Code) (513) 255-3708		22c. OFFICE SYMBOL AFIT/ENY



The USAF planned to participate in a parametric study investigating the effects of composite lamina fiber orientation on control reversal for various wing/fin configurations. Only recently have complete wings, stabilizers, and control surfaces been fabricated from this material and a careful parametric study of aeroelastic effects has not been undertaken. In support of this effort, this thesis involved testing a single aft-swept wing planform with full and partial span trailing edge lateral control surfaces in a subsonic wind tunnel and comparing the results with predictions rendered from simple computer modeling. Three identical planform and composite laminate plates were tested but with the entire laminate rotated to different angles relative to the elastic axis. The composite plates were covered with foam and fabric to create a symmetric airfoil. The entire design methodology and construction techniques employed are presented. The research includes computer subroutines for initial design and prediction of the aeroelastic characteristics of each proposed configuration in terms of deformed shape, control reversal, divergence, and flutter.

Raymond

END

FILMED

MARCH, 19 88

DTIC